Tryptophan Metabolism and its Relationship with Central Nervous System Parameters in People Living With HIV

Michael Roger Keegan

Department of Infectious Diseases

Faculty of Medicine

Imperial College London

A thesis submitted for the degree of Doctor of Philosophy at

Imperial College London

2018

“Got a mind full of questions and a teacher in my soul.”

Eddie Vedder, ‘Guaranteed’

“Knowledge is hassle.”

Karl Pilkington

ACKNOWLEDGEMENTS

This work is dedicated to the memory of my dad, one of the cleverest chaps I have ever met. As I get older and (hopefully) a little wiser, I think I understand him more and more. He was a true teacher and a role model. And to my lovely mum, who inspired me to work in medicine to help people and who inspires me to be kind every day.

This work is also dedicated to Riley and Nathan, my awesome little boys. You make me proud every single day and inspire me to be a better man.

To John Pottage, Eric Le Fevre and Andrew Clark, thank you for believing in this scruffy dude and for all of the support, guidance, encouragement and funding. I really appreciate what you have done for me. A big thank you also goes to Katy Hayward, Katie Lipscombe, Gillian Kenwood, Kris Webb, David Shepherd, Mary Kerr, Andrew Benzie, Jim Demarest, Martin Gartland, Wendy Snowden, David Butcher, Carol House (for the near endless supply of useful references), Richard Stroder, Romina Quercia and Adam Stubbs at ViiV Healthcare Ltd. for all of the advice and cheerleading. It is an immense pleasure and honour to work with such talented, good-hearted people.

A special and very big thank you to Robert Cuffe for his advice regarding the statistical analyses for the clinical studies.

A massive thank you to my tutors Alan Winston, Adriano Boasso and Peter Keleher, as well as Myra McClure. Your patience, guidance, enthusiasm, fun approach and blood (in some cases) have been immeasurable. It has been absolutely fantastic to learn from and you have helped me grow as a research scientist. I hope that we can continue to collaborate in the future.

A special thank you to Scott Letendre and Ron Ellis for your generosity in sharing your teams' data with me and allowing me to work on the CHARTER study. A big thank you also to Jennifer Iudicello and Seetharamaiah Chittripol for your help.

A debt of gratitude goes to Dietmar Fuchs and his team for their support in analyzing samples.

I am especially grateful to Mark Nelson and Chris Higgs for agreeing to let me join their study team and to learn from them.

To David Leather, Mike Lim, Daren Thorborn and Nick Fitch for helping me get started in this field and for simultaneously being the best and the most appalling role models a guy could have. Thanks for taking the time to teach me, chaps! Some of it, I never wanted to know…

To my wife Tash, whom I married during the last year of this PhD. You had a real experience of the natural drama of a PhD student with all of its highs and lows… and did not run away. Despite many ruined weekends and evenings, you have always provided moral support, counseling, encouragement, threats, food, laughs and jokes throughout. I could not have done this without you.

To Chris Colebrook, Matt Keenan, Spencer Komodromou, Justin Crane and Barry Critchell for inspiring me to work hard at something I love.

Thank you to David Ryan and everyone at Watford Freestyle Kickboxing for helping me develop my mental strength and discipline over many years. 'Dig deep, finish strong' has never been more relevant!

This thesis was written up in some glorious places – in the French Quarter of New Orleans, a beach in Malta, the bay area of Vancouver, the British Library and, of course, good ol' Watford Town, particularly the LP Café (thanks for playing the tunes and keeping the coffee flowing!).

And finally, the biggest thank you goes to all of the people who gave their time and biological samples for this work. We never met, but you were in my thoughts throughout the last seven years. Thank you.

DECLARATION OF ORIGINALITY

I, Michael Keegan, declare that the work presented in this thesis is my own and that there appropriate I have acknowledged any contribution by other persons. Information derived from published work has been clearly indicated in the test and in the list of references.

COPYRIGHT DECLARATION

ABSTRACT

HIV-1 enters the central nervous system (CNS) during the early stages of HIV-infection and has been associated with neurological and neuropsychiatric effects, including major depressive disorder and cognitive impairment. However, a clear picture of their neuropathogenesis remains elusive and is thought to be multifactorial in nature. A possible contributing mechanism is immune-mediated degradation of tryptophan (TRP) via the kynurenine (KYN) pathway, resulting in decreased production of serotonin and production of neuroactive KYN pathway catabolites. TRP metabolism has been shown to be disturbed throughout the course of infection in people living with HIV (PLWH) and initiation of antiretroviral therapy has been shown significantly, but incompletely, to reduce its degradation. I aimed to establish whether TRP metabolism, as measured by kynurenine/tryptophan (KYN/TRP) ratios, a marker of indoleamine 2,3-dioxygenase (IDO) enzyme activity, is increased in the presence of the HIV-1 virus or antiretroviral agents and whether increased TRP metabolism is associated with poorer cognitive performance and increased rates of depression in PLWH.

In *in vitro* experiments, no significant effect was observed on TRP metabolism following acute exposure of human peripheral blood mononuclear cells and hepatocyte, astrocyte and microglial cell lines to a range of different antiretroviral agents, both individually and in clinically-relevant combinations, at supratherapeutic and clinically-relevant concentrations.

In a cross-sectional analysis of archived cerebrospinal fluid and plasma samples from PLWH, the inflammatory markers (tumour necrosis factor-α) TNF-α and neopterin (NEO) were associated with increased KYN production, suggesting ongoing immune activation. Lower KYN/TRP ratios in plasma were associated with cognitive impairment and depression in virologically-suppressed subjects, suggesting that KYN catabolites may have a net neuroprotective effect in this population. This was supported by a prospective clinical study in which increased KYN concentrations were associated with decreases in CNS toxicities in subjects following switch from efavirenz to dolutegravir. This observation may be confounded by the inherent neurotoxicity of efavirenz and a possible drug interaction between efavirenz and the tryptophan 2,3-dioxygenase (TDO) enzyme that mediates TRP metabolism in the liver. In contrast, a second prospective clinical study found that KYN/TRP ratios negatively

correlated with modest changes in cognitive function, suggesting that KYN metabolites have a net neurotoxic effect in PLWH.

In conclusion, these data demonstrate an ongoing disturbance in TRP metabolism in virologically-suppressed PLWH that is mediated by residual immune activation and choice of antiretroviral agents.

TABLE OF CONTENTS

LIST OF FIGURES

LIST OF TABLES

ABBREVIATIONS

3TC	Lamivudine
ABC	Abacavir
AIDS	Acquired Immune Deficiency Syndrome
ANI	Asymptomatic Neurocognitive Impairment
ART	Antiretroviral Therapy
ARV	Antiretroviral
ATV	Atazanavir
AZT	Zidovudine
BBB	Blood-Brain Barrier
BH_4	Tetrahydrobiopterin
BHIVA	British HIV Association
BIC	Bictegravir
c	Cobcistat
CCL	Chemokine Ligand
CCR	CC-Chemokine Receptor
CD	Cluster of Differentiation
CDC	Centers for Disease Control
CI	Cognitive Impairment
CMV	Cytomegalovirus
CNS	Central Nervous System
CSF	Cerebrospinal Fluid
d4T	Stavudine
ddC	Zalcitabine
ddI	Didanosine
DLV	Delavirdine
DNA	Deoxyribonucleic Acid
DRV	Darunavir
DTG	Dolutegravir
EBV	Epstein Barr Virus
EFV	Efavirenz
Env	Envelope

ETV	Etravirine
EVG	Elvitegravir
FPV	Fosamprenavir
FTC	Emtricitabine
Gag	Group specific antigen
GALT	Gut-Associated Lymph Tissue
GDS	Global Deficit Score
GTO-CH1	Guanosine-Triphosphate-Cyclohydrolase-1
HAD	HIV-Associated Dementia
HAND	HIV-Associated Neurocognitive Disorder
HIV	Human Immunodeficiency Virus
HLA	Human Leukocyte Antigen
HTLV	Human T-Lymphotropic Virus
IDO	Indoleamine 2,3-Dioxygenase
IDV	Indinavir
IFN	Interferon
IL	Interleukin
INI	Integrase Inhibitor
INSTI	Integrase Strand Transfer Inhibitor
KYN	Kynurenine
LAV	Lymphadenopathy-Associated Virus
LPS	Lipopolysaccharide
LPV	Lopinavir
MND	Mild Neurocognitive Disorder
MVC	Maraviroc
MRS	Magnetic Resonance Spectroscopy
NAD+	Nicotinamide Adenine Dinucleotide
Nef	Negative factor
NFV	Nelfinavir
NEO	Neopterin
NNRTI	Non-Nucleoside Reverse Transcriptase Inhibitor
NRTI	Nucleoside Reverse Transcriptase Inhibitor
NVP	Nevirapine
PAH	Phenylalanine-Hydroxylase

PCNSL	Primary Central Nervous System Lymphoma
PCP	*Pneumocystis Carinii/Jirovecii* Pneumonia
PHE	Phenylalanine
PI	Protease Inhibitor
PLWH	People Living With HIV
PML	Progressive Multifocal Leukoencephalopathy
Pol	Polymerase
RAL	Raltegravir
Rev	Regulator of virion
RNA	Ribonucleic Acid
ROS	Reactive Oxygen Species
RPV	Rilpivirine
RTV or r	Ritonavir
SIV	Simian Immunodeficiency Virus
SQV	Saquinavir
T-20	Enfuvirtide
TAF	Tenofovir Alafenamide
Tat	Trans-activation of transcription
TDF	Tenofovir Disoproxil Fumarate
TDO	Tryptophan 2,3-Dioxygenase
TNF-α	Tumour Necrosis Factor-Alpha
TPH	Tryptophan-Hydroxylase
TPV	Tipranavir
TRP	Tryptophan
TYR	Tyrosine
Vif	Viral infectivity factor
Vpu	Viral protein u
Vpr	Viral protein r

1 INTRODUCTION

1.1 Aims and Hypotheses

1.1.1 Aims

The aim of this PhD is to determine whether chronic immune activation in people living with HIV leads to alterations in tryptophan (TRP) metabolism and whether these are associated with cognitive impairment and depressed mood.

1.1.2 Hypotheses

The hypotheses for these research projects are:

TRP metabolism is increased in the presence of the HIV-1 virus or antiretroviral agents.

Increased TRP metabolism is associated with poorer cognitive performance and increased rates of depression in people living with HIV.

1.2 The Origin of AIDS

On the 5th June 1981, five cases of a rare lung infection, *Pneumocystis carinii* pneumonia (PCP, now known as *Pneumocystis jirovecii* pneumonia), were reported in previously healthy young men in Los Angeles, California (1, 2). PCP had only previously been observed in people with severe impairment of their immune system, such as those receiving chemotherapy. Their case histories, however, suggested a "cellular-immune dysfunction related to a common exposure that predisposes individuals to opportunistic infections." A few weeks later, 26 cases of PCP and Kaposi's sarcoma, a rare and aggressive cancer, were reported in gay men from New York and California, prompting enormous media attention (3). New cases were soon reported in other groups, including intravenous drug users, haemophiliacs and heterosexual men and women. By September of 1982, the Centers for Disease Control and Prevention (CDC) had recorded a total of 593 cases of severe immune deficiency, 243 of whom had died (4). This

new condition was named Acquired Immune Deficiency Syndrome (AIDS), though the cause was not yet known.

In 1983, two independent groups of researchers in France and the United States of America announced the discovery of previously unknown retroviruses in the same issue of the journal *Science* (5, 6). The French team, led by Luc Montagnier, named their virus 'Lymphadenopathy-Associated Virus' (LAV), and the US team, led by Robert Gallo, named theirs the 'Human T-Lymphotropic Virus (HTLV)-III'. Both groups suggested that their retrovirus was the cause of AIDS. LAV and HTLV-III were subsequently found to be the same virus and, in 1986, the International Committee on the Taxonomy of Viruses renamed it the Human Immunodeficiency Virus (HIV) (7).

Soon after the identification of AIDS, outbreaks of severe infections and wasting were observed in Asian rhesus macaques kept in US-maintained primate colonies. A retrovirus similar to HIV was found in these animals and termed simian immunodeficiency virus (SIV) (8). Retroviruses are so-named because they transcribe ribonucleic acid (RNA) into deoxyribonucleic acid (DNA), which is then integrated into the host cell DNA genome. This is the reverse of the normal process (i.e. DNA transcribed into RNA), hence their name. The process of reverse transcription by the viral enzyme reverse transcriptase is detailed in Figure 1.1 (Section 1.3 provides more detail on the structural biology of the virus itself).

Retroviruses are further subdivided into 'lentiviruses' (i.e. HIV and SIV), 'oncoviruses' (i.e. HTLV-1) and the non-pathogenic 'spumaviruses'. SIVs are retroviruses that infect apes and monkeys. Indeed, SIV is something of a misnomer as most non-human primates who become naturally infected tolerate their species-specific SIV infections very well without developing immune deficiency despite detectable viral loads; disease (i.e immune deficiency) is only evident following cross-species transmission of viruses, for example from sooty mangabeys to rhesus macaques (9). Following the discovery of SIV, a second HIV virus was discovered in AIDS patients from West Africa, which was more closely related to the SIV virus than it was the first HIV virus. It became known as HIV-2 (9).

Figure 1.1. Conversion of the Single-Stranded RNA Genome of a Retrovirus into Double-Stranded DNA by Reverse Transcription

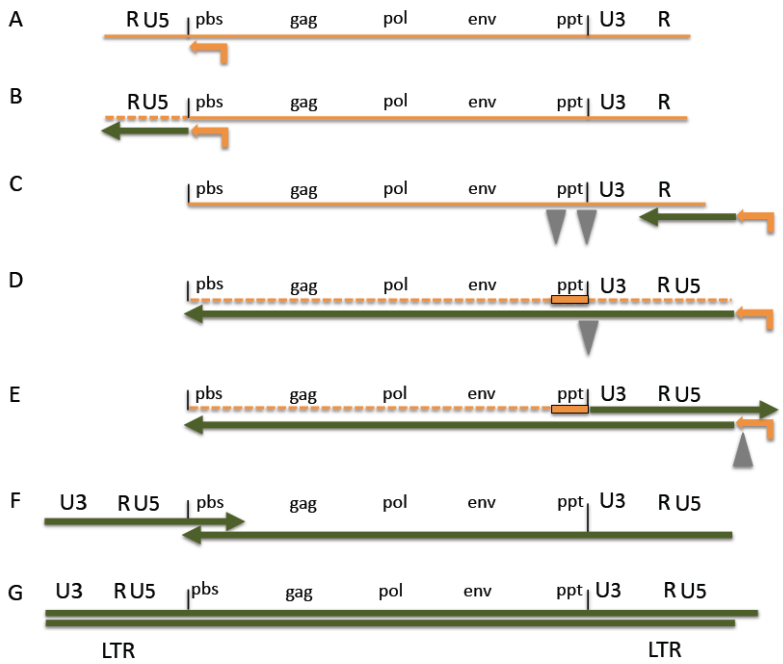

Footnote: The positions of the R, U5 and U3 regions of the long-terminal repeats (LTRs), the polypurine tract (ppt), and the primer-binding site (PBS) are indicated. (A) The RNA genome (displayed in orange) has a transfer ribonucleic acid (tRNA) primer base paired at the 5' end. (B) Reverse transcriptase (RT) initiates reverse transcription, which generates minus-strand DNA (displayed in green). (C) The minus-strand DNA is transferred between the R sequences at both ends of the genome, which allows minus-strand DNA synthesis to continue (D). This is accompanied by RNA degradation by the enzyme ribonuclease H (RNase H). (E) An RNase H-resistant ppt adjacent to the U3 region serves as the primer for the synthesis of plus-strand DNA. (F) The tRNA primer is removed and plus-strand DNA transfer occurs. (G) Plus and minus DNA strand synthesis is complete (10).

Adapted from Hu W-S and Hughes SH. Cold Spring Harb Perspect Med 2012 (10).

The origin of HIV has been traced back to Africa, with the current HIV-1 pandemic dating back to the early 1900's (11, 12). The construction of two large railroads in what is now known as the Democratic Republic of Congo provided a fertile ground for the transmission and amplification of the virus. Between 1885 and 1908, this area of Central Africa was known as the *Etat Independant du Congo* (Independent State of the Congo), which was part of the Kingdom of Belgium under the rule of Leopold II. The exploration and exploitation of this region by the ruling administration was hampered by a poor transport infrastructure and so, between 1890 and 1898, the Matadi-Leopoldville Railway was constructed. Later, in 1921, at the same time as this railway was being expanded, the *Societe de Construction des Batignolles* was contracted to construct the *Chemin de fer Congo-Ocean* Railway between the bustling townships of Brazzaville on the Congo River and Pointe-Noire on the coast. The railroads are situated approximately 100 kilometres apart, each stretching over 500 kilometres in length across a dense and hilly equatorial rain forest. More than 125,000 forced-labour workers were recruited from southern Chad and the Central African Republic. Working conditions were appalling with inadequate food, medicine and housing, resulting in the deaths of between 15,000 to 23,000 workers. The current HIV pandemic is thought to be the result of at least twelve cross-species transmission events of SIV from non-human primates to humans via a process called zoonosis. Epidemiologic data suggest that the first transmissions were to injured hunters who were killing and butchering primates to feed the railroad workers (11). Evidence suggests that HIV was crucially amplified via needle-sharing during the implementation of Jamot's doctrine[a] for the treatment of African trypanosomiasis (sleeping sickness), a disease that was sweeping the work camps at the time (11).

[a] Jamot's doctrine involved testing and treating whole villages and work camps for African trypanosomiasis using whatever medications were available to hand.

Figure 1.2. The Molecular Phylogeny of Primate Immunodeficiency Viruses

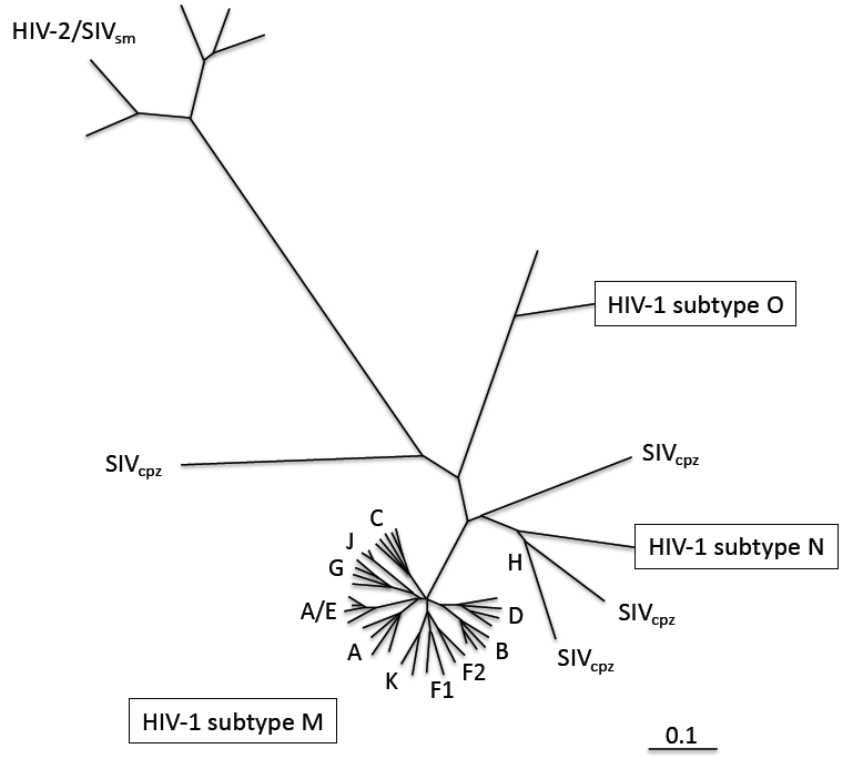

Footnote: A phylogenetic tree of primate immunodeficiency viruses estimated using an alignment of the envelope gene (gp160). HIV is classified into two major subtypes, HIV-1 and HIV-2. HIV-1 is co-segregating with chimpanzee SIV strains and HIV-2 is co-segregating with sooty mangabey SIV strains, indicating zoonotic origins. The scale bar (i.e. 0.1) indicates 10% nucleotide sequence divergence (13).

Key: sm, sooty mangabey; cpz, chimpanzee.

Adapted from Hoy JF, *et al*. HIV Management in Australasia: A Guide for Clinical Care. 2009 (13).

As of 2017, four groups of HIV-1 have been identified: main (M); outlier (O); non-M, non-O (N); and P. Group M is further divided into 11 subtypes (A1, A2, B, C, D, F1, F2, G, H, J and K) and 88 circulating recombinant forms (14). The nucleotide sequences of each of the subtypes differ by about 20% (i.e. they have approximately 80% homology). Evidence from phylogenetic analyses is conclusive and demonstrates that groups M and N originated from SIV viruses found in a sub-group of chimpanzees called *Pan troglodytes troglodytes* (Figure 1.2)(13). Groups O and P are believed to have originated from SIV viruses from Lowland gorillas (*Gorilla gorilla gorilla)*(11), though data suggests that gorillas may have been intermediate hosts between chimpanzees and humans (12). HIV-2 has eight subtypes, A to H, with only one circulating recombinant form found to-date (Figure 1.2). Only subtypes A and B have been shown to spread between humans, while subtypes C to H represent individual human infection cases. HIV-2 originated from SIV in Sooty Mangabey monkeys (*Cercocebus atys atys*). Using molecular clock dating techniques, it has been estimated that the times of the most recent common ancestor for SIV in chimpanzees and Sooty Mangabeys are the years 1492 (1266-1685) and 1809 (1729-1875), respectively, indicating that SIV may have infected these hosts for only a few hundred years before giving rise to HIV (12).

The spread of HIV from Africa to Haiti and, onwards, to the US is well-documented (11). Since the early 1900's, the virus has spread across the globe and more than 70 million people have been infected, approximately half of whom have died of HIV-related causes (15). Due to innate differences in transmission rates and virulence, HIV-1 group M became responsible for the vast majority of infections globally, whilst other groups of HIV-1 and HIV-2 remain primarily confined to Africa with stable or declining numbers of infections (9). Table 1.1 details the global distribution of the two HIV viruses and their various subtypes as of 2015.

Given that the current pandemic is overwhelmingly driven by HIV-1 infections, this body of work focuses on this virus. HIV-2, whilst very important, is not covered in any further detail.

Table 1.1. Global Distribution of HIV-1 and HIV-2 and Their Subtypes

Virus	Group	Subtype	Distribution
HIV-1	M	A	East Africa, Central Africa, Eastern Europe, Pakistan
		B	North America, Western Europe, Australia, Thailand, China, rare in Central Africa
		C	Southern Africa, Central Africa, India, China, represents 50% of all HIV-1 infections worldwide
		D	East Africa, Central Africa
		CRF01-AE	Thailand, other parts of Asia, Central Africa
		CRF02-AG	West Africa, parts of Central Africa
		All other subtypes and recombinants	Central Africa, various other regions
	O	-	Cameroon and adjacent countries
	N	-	Cameroon
	P	-	Cameroon
HIV-2	A	-	Guinea-Bissau, The Gambia, Senegal
	B	-	Ivory Coast
	C to H	-	Sierra Leone, Liberia, each found in only one human

Key: CRF, circulating recombinant form

Adapted from: Pepin J. The Origin of AIDS. Cambridge University Press. 2011 (11).

1.3 Structural Biology of HIV-1

A diagram of the structure of HIV-1 is shown below (Figure 1.3 A). The virus consists of an outer phospholipid bilayer that expresses two key glycoprotein receptors (gp120 and gp41), a viral core constructed from the p17 matrix protein, and a nucleocapsid made from the p6, p7 and p24 proteins. The nucleocapsid contains two RNA strands and the three enzymes necessary for viral replication - reverse transcriptase, integrase and protease (Figure 1.3 A).

The viral genome is comprised of nine genes: group specific antigen (*gag*), polymerase (*pol*), envelope (*env*), trans-activation of transcription (*tat*), regulator of virion (*rev*), negative factor (*nef*), viral protein r (*vpr*), viral infectivity factor (*vif*), and viral protein u (*vpu*) (Figure 1.3 B) (13, 16, 17). The *gag, pol and env* genes code for the structural proteins of the virus (13): *gag* codes for the matrix protein p17, the capsid protein p24, the nucleocapsid protein p7 and p6,

which binds *vpr* and packages it in the core; *env* codes for the surface envelope glycoprotein gp120 and the transmembrane envelope glycoprotein gp41*;* and *pol* codes for the enzymes reverse transcriptase (p66 and p51), integrase (p32) and protease (p10). *Tat* (p14) and *rev* (p19) are regulatory proteins that code for the activation of transcription of HIV RNA and the post-transcriptional regulation of viral genes, respectively (16). The remaining four genes – *nef* (p17)*, vpr* (p15), *vpu* (*p16)* and *vif* (p23) – are accessory proteins involved in functions that aid viral spread (13): *nef* enhances infectivity by down-regulating CD4 and MHC class I expression; *vpr* enhances nuclear transport of HIV post-entry; *vpu* enhances the release of viral particles; and *vif* suppresses the anti-viral activity of APOBEC3 proteins, which render HIV genomes non-functional.

Figure 1.3 A: Structure of a Mature HIV Virion.

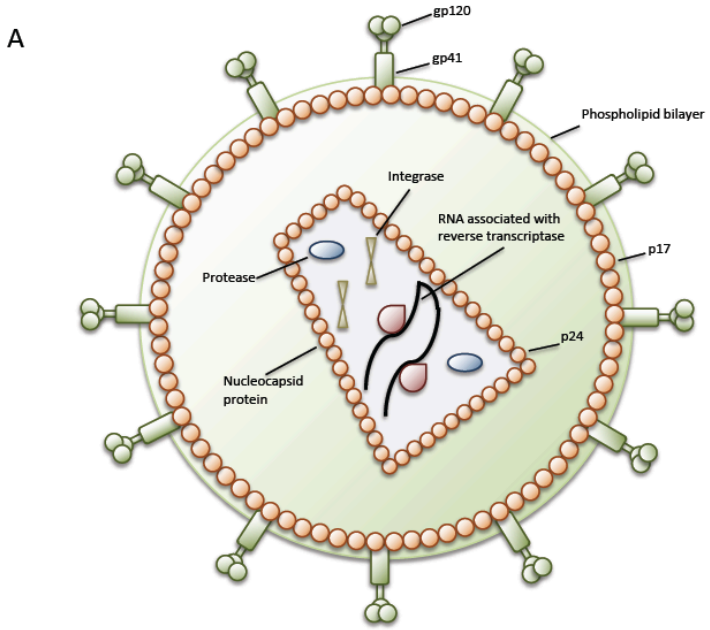

Figure 1.3 B: Structure of the HIV Genome.

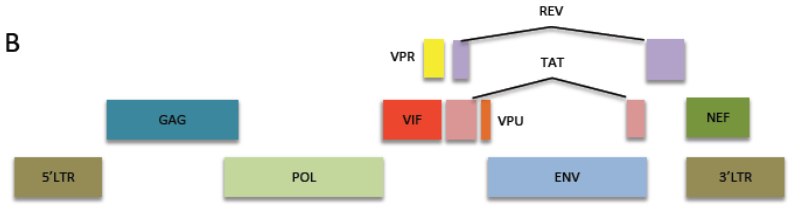

Footnote: (A) HIV virion structure highlighting envelope (gp120, gp41) and structural (gag p17, gag p24) proteins. (B) The single-stranded RNA genome of HIV encodes nine major structural and catalytic proteins.
Adapted from: Barmania F and Pepper MS. *Appl Transl Genom* 2013; and Moore MD and Hu W-S. *AIDS Rev* 2009 (16, 18).

1.4 Viral Transmission and Infection

1.4.1 Viral Transmission

Most, but not all, HIV-1 infections occur by sexual exposure to cell-free HIV-1 virions and/or HIV-1-infected cells contained in the mucosa of the genital or rectal tracts of infected persons (19). These tracts are covered by different types of epithelial barriers, which must be breached by the virus in new hosts for infection to occur. Simple epithelia, such as those found in the endocervix, rectum and intestine, consist of single layers of epithelial cells, separated by tight junctions. Stratified epithelia, such as those found in the vagina, exocervix and anus, are made of multiple layers of epithelial cells in which various immune cells are inserted. HIV-1 crosses simple epithelia by transcytosis, a process whereby the virus is captured by a vesicle on one side of the cell, drawn across it, and ejected on the other side. In stratified epithelia, HIV-1 transmission is believed to involve Langerhans cells, a type of cluster of differentiation 1a (CD1a)-positive dendritic cell, which form a network across this barrier. HIV-1 can enter Langerhans cells using its envelope glycoprotein subunit, gp120, by binding to CD4 receptors, CC-chemokine receptor 5 (CCR5) co-receptors and C-type lectin receptors, such as CD207 (langerin), located on the cell surface. The Langerhans cell captures the virus and passes it to susceptible CD4+ T helper cells and, to a lesser extent, CCR5+ monocytes and macrophages without being productively infected themselves (19). Less is known about transmission of the virus through the male foreskin and urethra. Evidence suggests that epidermal Langerhans cells in the foreskin become infected and migrate to the mucosal surface. There they form conjugates with T helper cells and transfer the virus to them (19). Physical trauma, ulceration or co-existing genital infections make it easier for the virus to breach epithelial barriers (20, 21).

In the same way as Langerhans cells, the entry of HIV-1 into T helper cells and monocytes/macrophages requires the formation of complexes between gp120 and gp41, and the cellular receptor, CD4, as well as a co-receptor, usually either CCR5 or CXCR4 (22, 23). This initiates a cascade of conformational changes that results in the fusion of the viral and host cell membranes and, ultimately, the release of the viral core into the cytoplasm of the cell. Once this has been achieved, the viral reverse transcriptase enzyme converts the single stranded RNA into double-stranded DNA, which is then transported to the host nucleus where the viral integrase enzyme integrates it into the host cell DNA. Viral DNA is then transcribed

into RNA and translated using host cell mechanisms, after which it is cleaved by viral protease into functional viral proteins. The new viral RNA and proteins are assembled at the cell surface where they bud from the cellular membrane (16, 23, 24). This process is displayed in Figure 1.4.

Figure 1.4. Schematic Overview of the HIV-1 Replication Cycle.

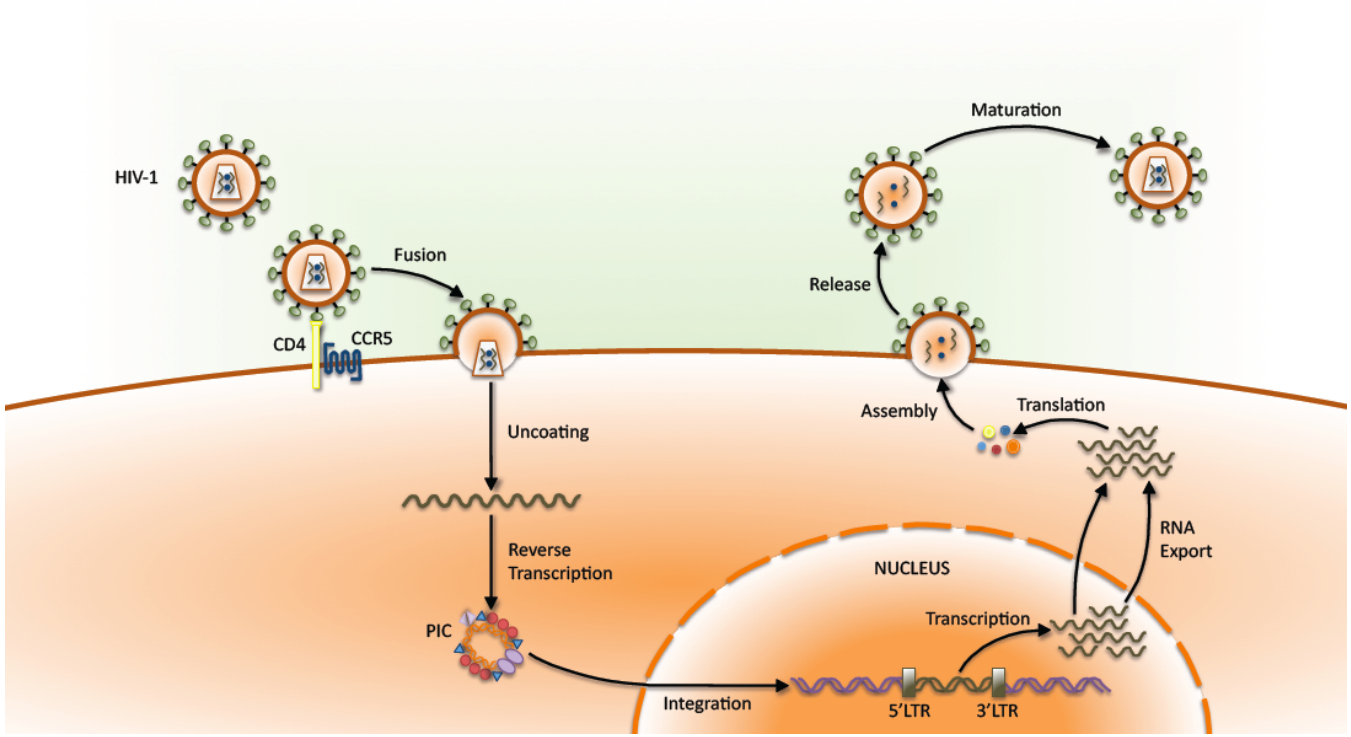

Footnote: The figure illustrates the HIV-1 replication cycle, including viral binding to the CD4 receptor and co-receptor (CCR5); fusion with the host cell surface; uncoating of the viral capsid and subsequent release of viral RNA and proteins; reverse transcription of viral RNA to DNA; formation of the pre-integration complex (PIC); integration of viral DNA into the host cell DNA; transcription and translation of viral DNA to RNA and proteins; translocation of viral RNA and proteins to the cell surface; assembly of new immature virus; viral budding; and finally viral maturation (25).

Key: PIC, pre-integration complex; LTR, long terminal repeat.

Adapted from: Barre-Sinoussi F, *et al*. *Nature Reviews Microbiology* 2013 (25).

1.4.2 HIV-1 Infection

Following transmission, the course of untreated HIV-1 infection is characterised by four distinct clinical stages. The first stage is primary HIV infection, which includes an asymptomatic incubation phase and an acute infection phase during which time the host may experience symptoms that are similar to those of other viral infections, though HIV may not be suspected. Next is a silent latency phase during which the virus replicates and almost always causes progressive destruction of the immune system. Following this is a symptomatic phase during which time the host is more susceptible to opportunistic infections. Left untreated, HIV infection almost always leads to AIDS and, finally, death (26).

1.4.2.1 Primary HIV-1 Infection: Incubation and Acute Infection

In most cases, mucosal HIV infection occurs with a single founder virus. For the first 10 days, known as the 'Eclipse Phase', the virus replicates locally (27). This is aided by innate immune responses, in which additional CD4+ T helper cells are recruited to the area where they can be infected (20). During this time, HIV replication is associated with the activation of a dramatic cytokine cascade, one that exceeds those seen in other viral infections (20, 27, 28). Figure 1.5 (below) shows the proportional scaled fold-change in mean plasma levels of acute-phase proteins, cytokines and chemokines in response to increasing viraemia during the first few weeks of infection (28). There are two initial waves of cytokines: interleukin-15 (IL-15) and interferon-α (IFN-α), followed by tumour necrosis factor-alpha (TNF-α), IL-18 and CXCL-10 (27). The pattern of elevations of these agents is consistent with a response involving sequential activation of plasmacytoid and myeloid dendritic cells, and other adaptive responses. This cascade likely contributes to the control of viral replication either directly or indirectly via the activation of other effector mechanisms (27). The roles of some of these agents in relation to this thesis, specifically IFN-α, IFN-γ and TNF-α, are discussed in further detail later in this chapter.

Figure 1.5. The Cytokine Storm Following HIV-1 Infection.

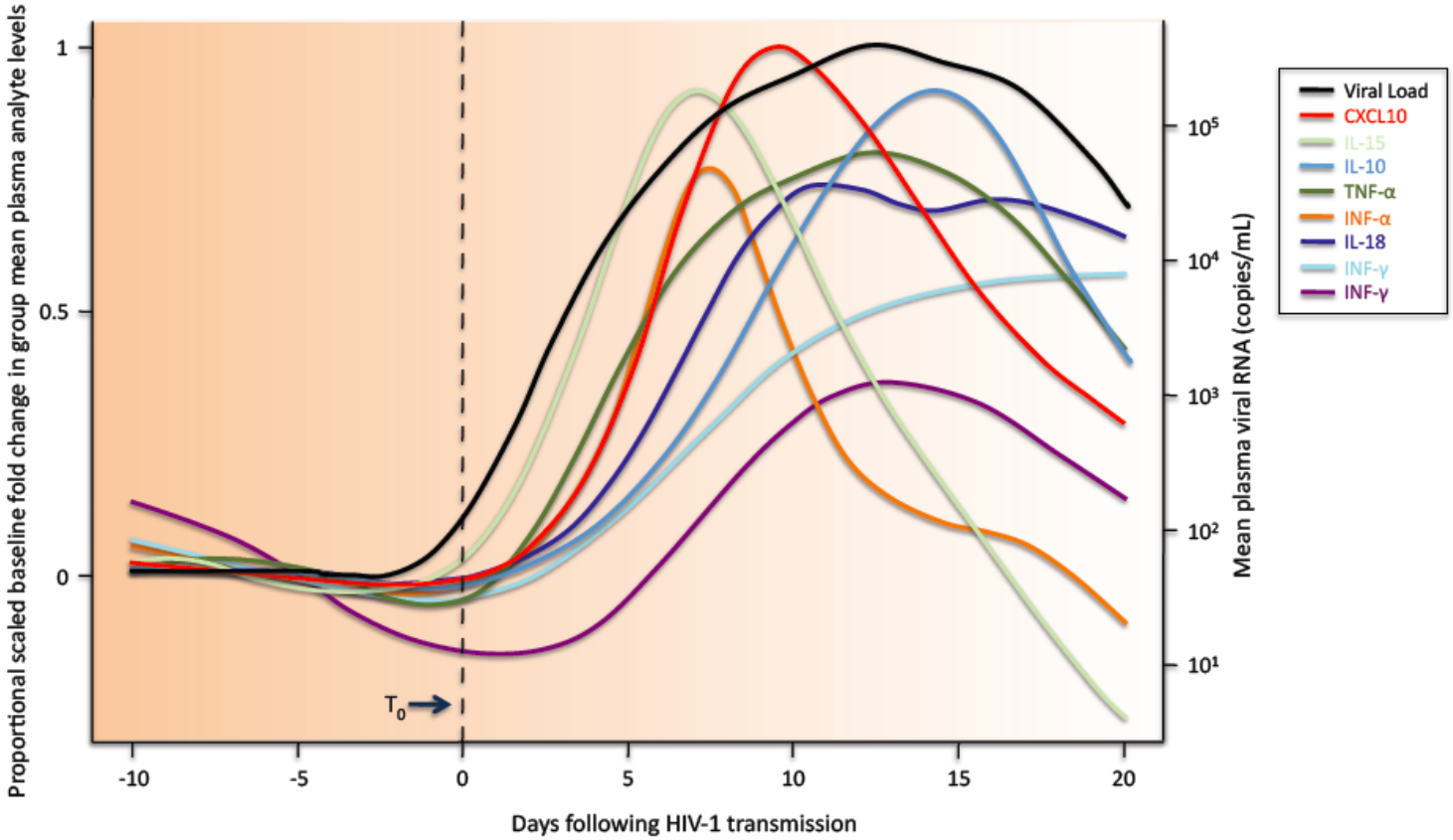

Footnote: The figure shows the scaled proportional fold change relative to baseline over time in plasma levels of selected cytokines and the viral load in subjects with acute HIV infection. Time is plotted in days relative to Time zero (T_0)(27).

Adapted from: Stacey AR, *et al. J Virology* 2009 (27).

Following the Eclipse phase, HIV particles or virus-containing cells reach local lymph nodes, where the infection amplifies and spreads systemically, particularly to gut-associated lymphoid tissue (GALT), which contains large numbers of CD4+ CCR5+ T helper cells (21, 27). Approximately, 20% of GALT T helper cells become infected with HIV-1 and an additional 60% of uninfected T helper cells become activated and apoptose (a process of programmed cell death), leading to a total reduction of approximately 80% of CD4+ T helper cells within the first few weeks of infection. Viral replication in the GALT increases exponentially during this time. At its' peak, at about 21-28 days post-infection, viral loads are usually in excess of one million HIV-1-RNA copies/mm^3 of blood (Figure 1.6) (20). The damage caused to the gut epithelium increases microbial translocation, a process whereby gastrointestinal microflora pass through the intestinal epithelial barrier and the lamina propria into mesenteric lymph nodes and other tissues (29). This further drives systemic immune activation.

1.4.2.2 Chronic Infection

Following the first few weeks, CD8+ T killer cells start to respond and begin to curtail viral replication. The earliest T cell responses are often specific for *Env* and *Nef*, with *Gag*- and *Pol*-specific responses arising later. The cytokine storm recedes in parallel with the decreasing viral loads, likely reducing host pathology caused by elevated immune activation processes (28). Up until this point, the virus is homogeneous to the founder virus. However, following the peak in the CD8+ T killer cell response, there is a rapid selection of mutations in the viral sequence at sites (epitopes) recognized by the CD8+ T killer cells. With these epitopes no longer recognized by the CD8+ T cells, the virus is able to escape the immune response to continue replicating. CD8+ T killer cells eventually target the new mutants but further mutants are selected, which, in turn, also escape the immune response. This pattern continues throughout the course of HIV infection (20).

HIV does not replicate in B cells and they are not depleted during early HIV infection. However, the high viral load, rapid increase in levels of pro-inflammatory factors, and loss of other cell types important to the development of germinal centres leads to dysregulation of the B cell response throughout the course of infection (30).

Figure 1.6. Innate and Adaptive Immune Responses to HIV-1 Infection.

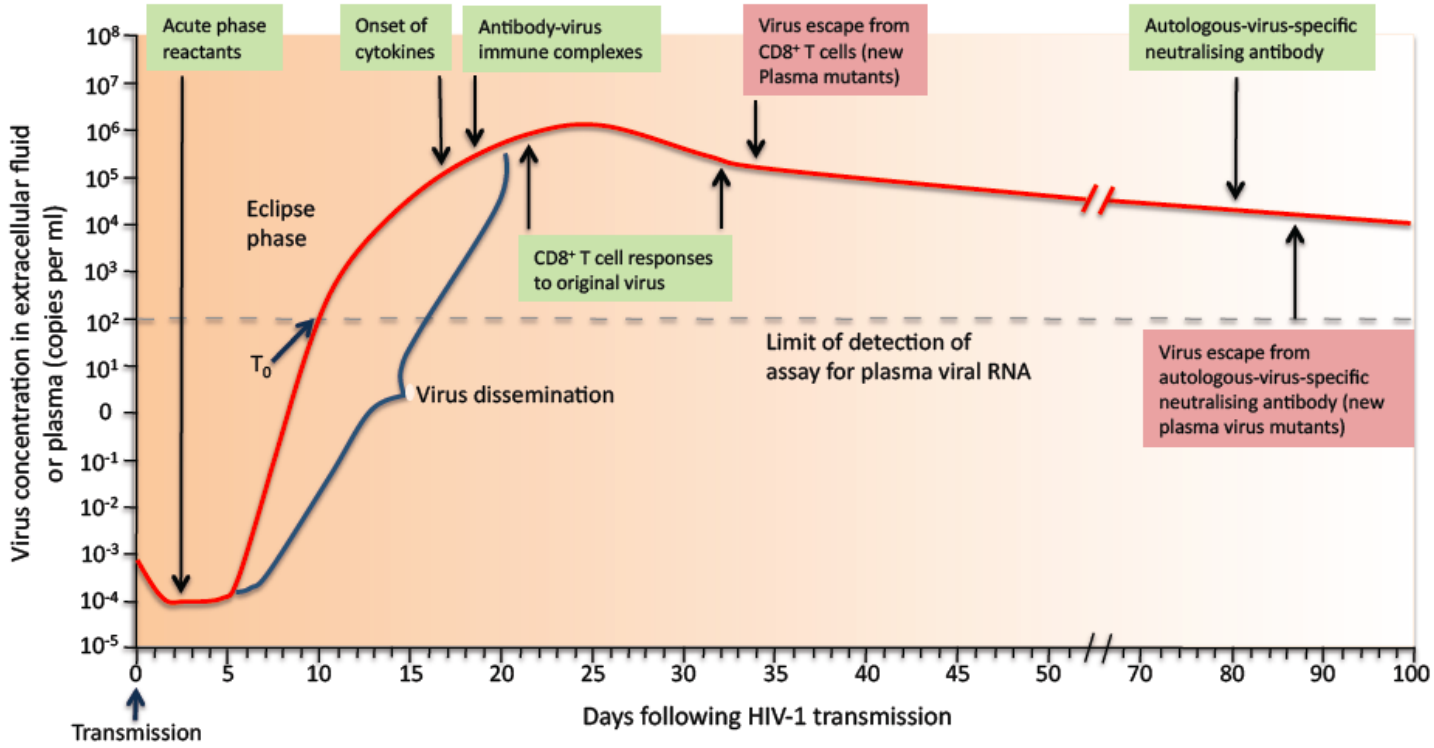

Footnote: The first immune responses to HIV-1 infection are increases in levels of acute-phase proteins in the plasma whilst the virus is restricted to mucosal tissue and lymph nodes. The virus is first detected in plasma by Day 10 (T_0) and is associated with increases in plasma cytokine levels (see also Figure 1.5). Within days, antibody–virus immune complexes are detected. Expansion of HIV-1-specific CD8+ T cell responses commences prior to peak viraemia, followed by detection of gp41-specific antibodies. Viral escape from CD8+ T cell responses can occur rapidly, within 10 days of T cell expansion. Autologous-virus-neutralizing antibodies are detected by day 80. Antibody escape virus mutants emerge in the plasma within the following 7 days (20).
Key: The dotted grey line denotes a plasma viral load of 50 copies/mL.
Adapted from: McMichael AJ, *et al. Nat Rev Immunol* 2010 (20).

Over the next 12-20 weeks the viral load continues to decrease until a stable viral set point is established whereby viral replication and the immune response eventually reach equilibrium (Figure 1.6). The duration of this can last for many years, with the median time to progression to AIDS estimated to be 9.8 years if not receiving ART (31). It appears to be, at least partially, determined by the genetics of the infected individual. People living with HIV (PLWH) with human leukocyte antigen (HLA) types associated with CD8+ T cell recognition of more conserved regions of the HIV-1 virus, such as HLA-B27, HLA-B51, HLA-B*5701, HLA-B*5703 and HLA-B*5801 tend to have better control over the virus, resulting in a lower viral set-point and a slower disease progression. In contrast, HLA-B35 is associated with rapid disease progression (20). Other genetic differences, such as the CCR5-Δ32 mutation in the CCR5 gene, have been shown to influence infection, viral control and disease progression. The CCR5 gene is located on chromosome 3. Individuals with homozygous deletion of the Δ32-region do not express any CCR5 receptors on their cell surface, which confers almost complete protection from CCR5-tropic strains of HIV-1. Heterozygous deletion results in reduced expression of the CCR5 receptor, resulting in elevated resistance to infection and, if infected, a significantly slowed progression to AIDS (by approximately 2 to 3 years) (22, 32, 33).

If left untreated the massive destruction of T helper cells leads to increasingly compromised immune function. The relative inefficiency of CD8+ T cell responses against escape mutants, compared with their comparatively strong response to founder virus, might be a direct consequence of waning T helper cell function. Eventually, CD8+ T cells also become exhausted due to persistent antigen exposure and repeated activation. They lose proliferative capacity and effector functions, ultimately leading to immune collapse and leaving the patient with an increased susceptibility to various opportunistic diseases. The PLWH may experience complications of both infectious and/or non-infectious origin, the nature of which highly correlate with CD4+ T helper cell counts (Table 1.2, below) (34). However, such is the inflammatory nature of HIV and the arising immune dysfunction that even at 'normal' CD4+ cell counts (i.e. >500 cells/mm^3) the risk of death, serious AIDS-related or serious non-AIDS-related events is significantly increased in PLWH (35). The START and TEMPRANO ANRS 12136 studies demonstrated that early initiation of ART resulted in a significant reduction of in the risk of these events even in subjects with >500 CD4+ cells/mm^3 (36, 37).

Table 1.2. Correlations of Complications with CD4+ T Helper Cell Counts.

CD4+ T Cell Count	Infectious Complications	Non-Infectious Complications
>500 cells/mm^3	Acute retroviral syndrome Candidal vaginitis	Persistent generalized lymphadenopathy Guillain-Barré syndrome Myopathy Aseptic meningitis
200-500 cells/mm^3	Pneumococcal and other bacterial pneumonia Pulmonary tuberculosis Herpes zoster Oropharyngeal candidiasis (thrush) Cryptosporidiosis, self-limited Kaposi's sarcoma Oral hairy leukoplakia	Cervical and anal dysplasia Cervical and anal cancer B-cell lymphoma Anaemia Mononeuronal multiplex Idiopathic thrombocytopenic purpura Hodgkin lymphoma Lymphocytic interstitial pneumonitis
<200 cells/mm^3	Pneumocystis pneumonia Disseminated histoplasmosis and coccidioidomycosis Miliary/extrapulmonary tuberculosis Progressive multifocal leukoencephalopathy	Wasting Peripheral neuropathy HIV-associated dementia Cardiomyopathy Vacuolar myelopathy Progressive polyradiculopathy Non-Hodgkin's lymphoma
<100 cells/mm^3	Disseminated herpes simplex Toxoplasmosis Cryptococcosis Cryptosporidiosis, chronic Microsporidiosis Candidal esophagitis	
<50 cells/mm^3	Disseminated cytomegalovirus Disseminated *Mycobacterium avium* complex	Primary central nervous system lymphoma

Adapted from: Hanson DL, *et al. Archives of Internal Medicine* 1995 (34).

The CDC have published a standardized definition for cases of HIV infection (for both HIV-1 and HIV-2) and AIDS (Table 1.3, below) (38, 39). In adults and adolescents (aged ≥13 years), HIV infection is categorized by increasing severity as Stage 1, Stage 2, Stage 3 (AIDS) or as Stage Unknown.

Table 1.3. Surveillance Case Definition for HIV Infection Among Adults and Adolescents (aged ≥13 years).

Stage	Laboratory Evidence	Clinical Evidence
Stage 1	Laboratory confirmation of HIV infection *and* CD4+ T-lymphocyte count of ≥500 cells/µL *or* CD4+ T-lymphocyte percentage of ≥29	None required (but no AIDS-defining condition)
Stage 2	Laboratory confirmation of HIV infection *and* CD4+ T-lymphocyte count of 200-499 cells/µL *or* CD4+ T-lymphocyte percentage of 14-28	None required (but no AIDS-defining condition)
Stage 3 (AIDS)	Laboratory confirmation of HIV infection *and* CD4+ T-lymphocyte count of <200 cells/µL *or* CD4+ T-lymphocyte percentage of <14	*or* documentation of an AIDS-defining condition (with laboratory confirmation of HIV infection)
Stage Unknown	Laboratory confirmation of HIV infection *and* no information on CD4+ T-lymphocyte count or percentage	*and* no information on presence of AIDS-defining conditions

Adapted from: CDC. *MMRW* 2008 (39).

AIDS-defining conditions include, but are not limited to: bacterial infections (multiple or recurrent); candidiasis; cervical cancer; coccidioidomycosis; cryptococcosis; cryptosporidiosis; cytomegalovirus disease; HIV-related encephalopathy; disseminated herpes simplex; histoplasmosis; isosporiasis; Kaposi's sarcoma; lymphoid interstitial pneumonia; lymphoma; *Mycobacterium* infections; *PCP*; pneumonia (recurrent); progressive multifocal leukoencephalopathy; *Salmonella* (recurrent); Toxoplasmosis of brain; HIV-related wasting syndrome. Left untreated, the host usually succumbs to one of these opportunistic conditions (26).

Disease of the CNS is common in HIV, either as a direct consequence of HIV infection or of an indirect result of immune system depletion, which leaves subjects vulnerable to opportunistic pathogens and tumours (40, 41). Common opportunistic infections and malignancies of the CNS during HIV infection are shown in Table 1.4 (below). The prevalence of each condition is somewhat dependent on geographical location and the risk group for HIV exposure (41).

Given that opportunistic infections are not the focus of this PhD, they will not be discussed further.

Table 1.4. Common Opportunistic CNS Infections Encountered During HIV/AIDS in the Pre- and Post-HAART Eras in the Edinburgh Cohort.

Opportunistic Infection	Pre-HAART (n=228)	Post-HAART (n=42)
Cytomegalovirus (CMV) encephalitis	9%	5%
Primary central nervous system lymphomas (PCNSL) driven by Epstein Barr virus (EBV)	6%	7%
Toxoplasmosis	5%	0%
Herpes simplex virus encephalitis	>1%	>1%
Progressive multifocal leukoencephalopathy (PML) (associated with JC virus infection of oligodendrocytes)	3%	3%
Varicella zoster virus encephalitis	>1%	>1%

Adapted from: Anthony IC and Bell JE. *Int Rev Psychiatry* 2008 (41).

1.5 Antiretroviral Therapy

As of 2017, nearly 30 antiretroviral agents targeting four different steps in the HIV-1 replication cycle are approved for administration to PLWH, with more in development. These are detailed in Table 1.5. Two agents, maraviroc (MVC) and enfuvirtide (T-20), block the entry of the virus into new target cells. MVC disrupts the interaction between viral gp120 and the cell co-receptor, CCR5. T-20 prevents the fusion process between the viral and cellular membranes (23, 42). Nucleoside and nucleotide reverse transcriptase inhibitors (N(t)RTIs) and non-nucleoside reverse transcriptase inhibitors (NNRTIs) target the reverse transcription process (Figure 1.1) that converts viral RNA into DNA. N(t)RTIs are analogues of the building blocks of DNA, the purine nucleosides adenosine and guanine, and the pyrimidine nucleosides

cytidine and thymidine, and act as DNA chain terminators (23, 42, 43). NNRTIs are allosteric inhibitors that induce a conformational change in the structure of the reverse transcriptase enzyme, resulting in its inability to pick up nucleoside bases to attach to the growing viral DNA chain (23, 42, 44). Integrase strand transfer inhibitors (INSTIs or INIs), prevent the integrase inhibitor from inserting the viral DNA strand into the host cell genome. Protease inhibitors inhibit the activity of the protease enzyme, thus preventing the maturation of viral particles (23, 42).

ART has unequivocally been shown to provide massive benefit to PLWH by reducing viral loads to undetectable levels (usually at least <50 c/mL in plasma), thus allowing the hosts immune system to reconstitute itself. This also results in dramatic reductions in systemic inflammation and immune activation, which are linked to comorbidities and mortality (35), and allows for a near normal life expectancy.

According to the treatment guidelines of the British HIV Association (BHIVA), the primary aim of antiretroviral therapy (ART) is “the prevention of the mortality and morbidity associated with chronic HIV infection at low cost of drug toxicity” (45). ART usually consists of three fully-active ARVs. For therapy-naïve PLWH who are commencing ART for the first time, a combination containing two NRTIs and either an INI, an NNRTI or a boosted PI is recommended (45-48). The effectiveness and tolerability of ART has improved significantly over time and many of the ARVs are available in fixed-dose combinations, thus reducing the daily pill burden and increasing convenience for PLWH.

Table 1.5. Currently Licensed Antiretroviral Agents.

Class	Sub-Class	Name
Entry inhibitors	CCR5 antagonist	Maraviroc (MVC)
	Fusion inhibitor	Enfuvirtide (T-20)
Nucleoside / Nucleotide Reverse Transcriptase Inhibitors (N(t)RTIs)	Adenosine analogue	Didanosine (ddI)
		Tenofovir, either as tenofovir disoproxil fumarate (TDF) or tenofovir alafenamide (TAF)
	Cytidine analogue	Emtricitabine (FTC)
		Lamivudine (3TC)
		Zalcitabine (ddC)
	Guanosine analogue	Abacavir (ABC)
	Thymidine analogue	Stavudine (d4T)
		Zidovudine (AZT)
Non-Nucleoside Reverse Transcriptase Inhibitors (NNRTIs)	-	Delavirdine (DLV)
		Efavirenz (EFV)
		Etravirine (ETV)
		Nevirapine (NVP)
		Rilpivirine (RPV)
Integrase Inhibitors	Integrase strand transfer inhibitor	Bictegravir (BIC)
		Dolutegravir (DTG)
		Elvitegravir (EVG)
		Raltegravir (RAL)
Protease Inhibitors	-	Atazanavir (ATV)
		Darunavir (DRV)
		Fosamprenavir (FPV)
		Indinavir (IDV)
		Lopinavir (LPV)
		Nelfinavir (NFV)
		Ritonavir (RTV)
		Saquinavir (SQV)
		Tipranavir (TPV)
Pharmacokinetic Enhancers	CYP3A inhibitor	Cobicistat (c)
	Protease Inhibitor	Ritonavir (r)

Two key surrogate biological markers are used in both clinical research and clinical practice to determine the efficacy of treatment. The first is a measure of the viral load in plasma, which is the most important indicator of both the initial and sustained response to ART (47). This is typically measured prior to initiation of therapy, and at regular intervals after starting treatment. It is determined using an *in vitro* reverse transcription-polymerase chain reaction (RT-PCR) assay for the quantitation of HIV-1-RNA. The primers and probe in the Abbott Real*Time* HIV-1 Viral Load assay, a widely used product, target the integrase region of the HIV-1 polymerase gene and can measure viral loads down to 40 copies/mL (1.6 log copies/mL) and up to 10 million copies/mL (7.0 log copies/mL) in plasma, with a specificity of 100% (95% CI, 99.28 to 100%) (49). Systematic reviews have established that sustained decreases in viral loads following the initiation of ART are associated with dramatic reductions in the risk of progression to AIDS or death (47, 50-52). The second key marker is the CD4+ cell count in plasma, which is a surrogate indicator of immune function, and a strong predictor of disease progression and survival (36, 47). Several technologies exist for the determination of CD4+ cell counts and include flow cytometric and non-flow cytometric methods. The WHO recommends that immunofluorescence analysis by flow cytometry using either single- or dual-platform methods as the gold standard (53).

ARV-associated neurotoxicity is discussed in more detail in Section 1.6.2.

1.6 HIV-1 and the Central Nervous System

HIV-1 enters the central nervous system (CNS) during the early stages of HIV-infection (54, 55) and has been associated with neurological and neuropsychiatric effects, including major depressive disorder (MDD) and cognitive impairment (CI). Initial interest in the neurology of HIV infection focused on the opportunistic infections and malignancies that affect the CNS, rather than any direct effect of the virus. However, HIV is now known to be neurovirulent and quickly establishes a persistent infection in the CNS compartment (56).

1.6.1 Crossing the Blood-Brain Barrier

Trafficking of immune cells into the CNS is a cardinal pathological feature of CNS inflammatory diseases and HIV is no exception (57, 58). In HIV, CD14+ CD16+ monocytes are critical to the

neuropathogenesis observed due to their role in the promotion of viral seeding in the CNS. Human monocyte classification is primarily based on the expression of the lipopolysaccharide (LPS) receptor, CD14. Whilst most circulating monocytes express CD14, peripheral monocytes are heterogeneous and have differing sizes, levels of maturation and function. CD16 is an additional monocyte marker that is of interest in HIV's role in the CNS. Mature monocytes expressing both CD14 and CD16 receptors account for approximately 5-10% of the circulating peripheral monocyte population and are particularly susceptible to HIV infection (54). Infected CD14+ CD16+ monocytes have been shown to have a sustained, increased chemotactic response to chemokine ligand 2 (CCL2), also known as monocyte chemoattractant protein-1 (MCP-1), and are preferentially directed to the blood-brain barrier (BBB) by the baseline levels of CCL2 present in the brain (59). Uninfected cells are not primed in this way and so do not respond to these low levels of CCL2. It is thought that infected CD14+ CD16+ monocytes are attracted to the BBB and then cross it via a multi-step process consisting of capture from the circulating blood flow onto the epithelial cells, rolling, firm arrest, intravascular crawling and, ultimately, diapedesis whereby the monocyte is shepherded into the brain in a zipper-like fashion by tight-junction proteins and adhesion molecules, including junctional adhesion molecule-A (JAM-A), activated leukocyte cell adhesion molecule (ALCAM), CD99, and platelet endothelial cell adhesion molecule 1 (PECAM-1) (59). Once the CNS is infected, CCL2 levels become elevated, attracting both infected and uninfected monocytes to the BBB and allowing them to enter the CNS. The virus, therefore, enters the CNS as an integrated provirus inside the monocyte genome, or as a non-integrated circular form. Viral particles capable of infecting other cells are released resulting in neuroinflammation and the creation of a viral reservoir (54, 59). CNS HIV is similar to plasma-derived virus but, over time, it evolves independently into a compartmentalized CNS virus. It becomes more macrophage tropic, allowing it to persist in CNS perivascular macrophages and monocytes despite low levels of CD4+ T cells in the CNS (60).

1.6.2 Introduction to the Neuropathogenesis of HIV Infection

The pathogenesis of HIV-related CNS disease is characterised by leukocyte infiltration, activated microglia, reactive astrogliosis and neuronal loss (particularly in the hippocampus, basal ganglia and cerebral cortex) (Figure 1.7). In the brain, perivascular monocyte-derived macrophages and microglial cells are the main producers of HIV-1 (61-63). Astrocytes have

also been shown to be capable of being infected but they restrict virus production and, instead, serve as reservoirs for the virus. A small number of studies suggest that oligodendrocytes and neurons may also become infected, though this is controversial(55), and the infection may not be productive (60). If neurons are not infected, or are infected in limited numbers, then indirect pathways for neuronal injury and death are implicated. This might be accomplished by the inherent toxicity of secreted viral proteins, the release of inflammatory mediators and neurotoxins by infected macrophages and microglia, and the loss of integrity of compromised blood-brain and blood-cerebrospinal fluid (CSF) barriers that allow toxins into the CNS from plasma (56, 64-67). Chapter 2 provides an overview of the various virological, host response and CNS damage markers that have been investigated in HIV-1 CNS disease.

A significant number of additional pathological mechanisms are thought to contribute to CI in PLWH, including sub-optimal penetration of ART into the CNS reservoir (macrophages, the principal target for HIV within the brain, require far higher concentrations of ARVs to inhibit replication than do T lymphocytes) (68, 69), ARV neurotoxicity, co-morbid mood disorders, hepatitis C co-infection, cerebrovascular disease, psychoactive drug use, genetic factors, ageing, and low educational level (70). Figure 1.8 details the proposed pathological mechanism underlying HIV-associated neurocognitive disorders.

Figure 1.7. Basic Model of HIV-1 Neuropathogenesis.

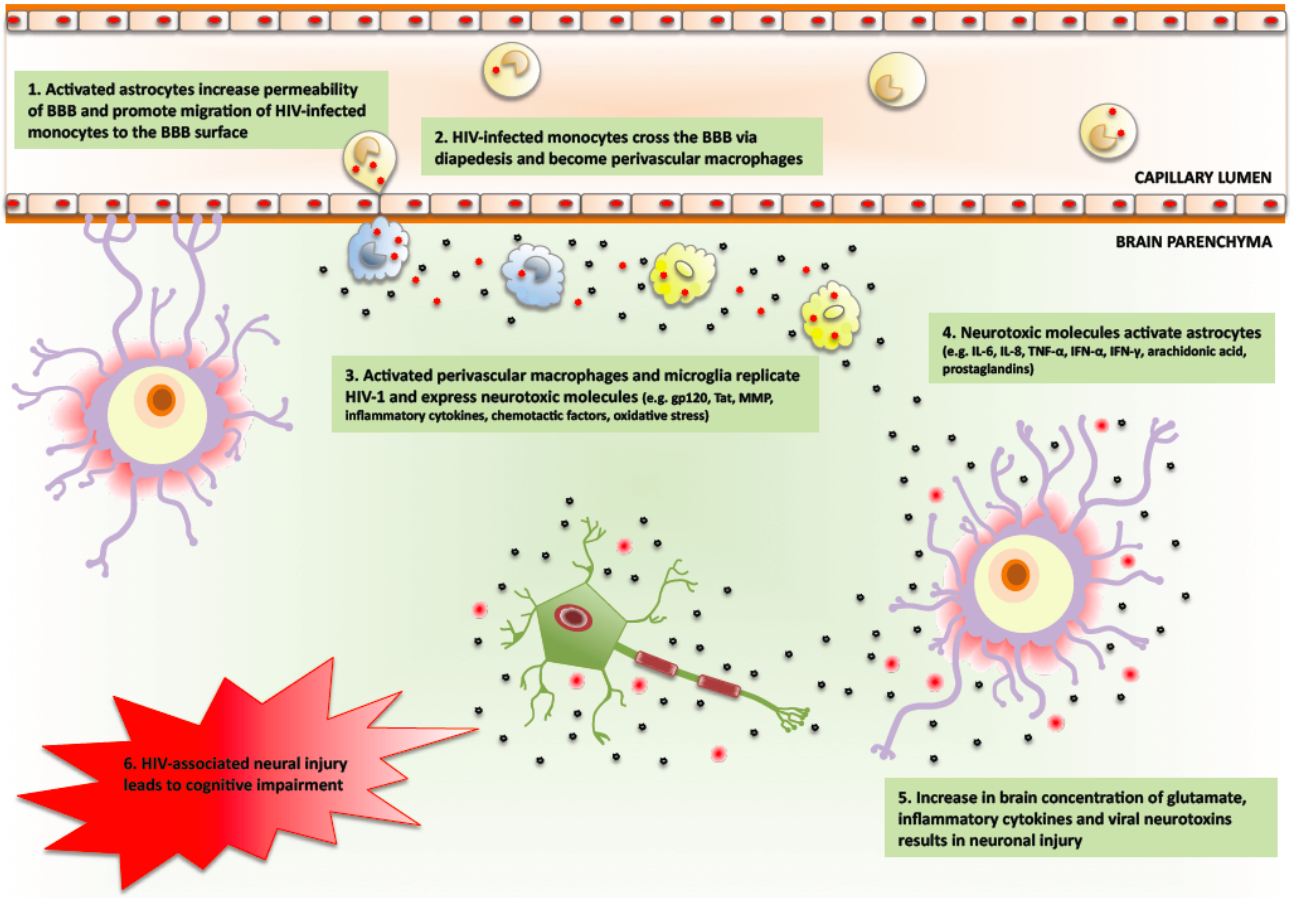

Footnote: The figure illustrates the pathogenesis of HIV-related CNS disease, which is characterised by leukocyte infiltration, activated microglia, reactive astrogliosis and neuronal loss (particularly in the hippocampus, basal ganglia and cerebral cortex) (56, 66, 67).

Adapted from: Kramer-Hammerle S, *et al. Virus Res* 2005; Vazquez-Santiago FJ, *et al. J Neurovirol* 2014; and Letendre SL. *49th ICAAC* 2009, Oral Presentation (55, 66, 67).

Figure 1.8. Overview of Proposed Pathological Mechanisms Underlying HIV-Associated Neurocognitive Disorders.

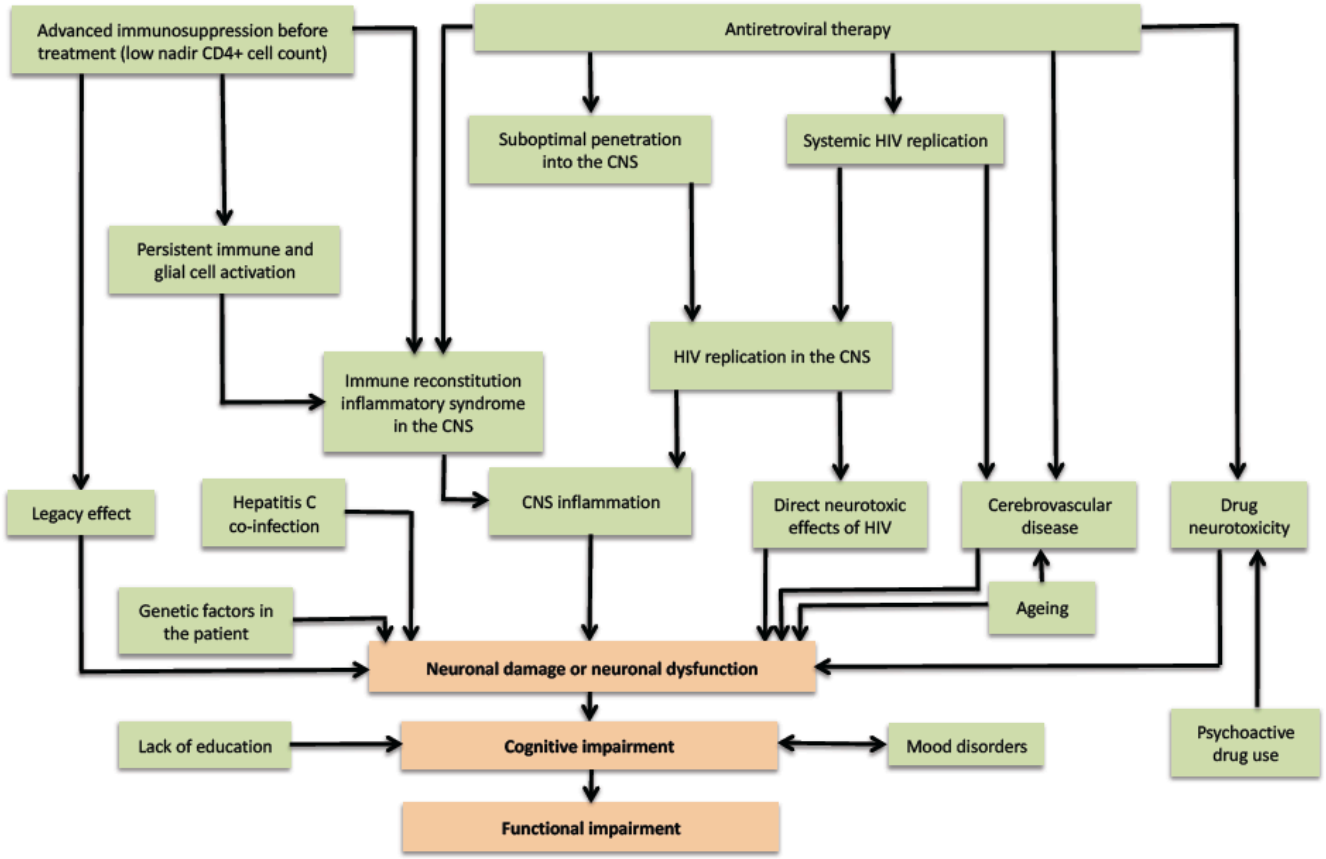

Adapted from: Nightingale S, *et al. Lancet Neurol* 2014 (70).

The advent of antiretroviral therapy has substantially altered the nature and prevalence of HIV-associated CI (71). Much has been made of the penetration of ARV drugs through the BBB and their potential for decreasing viral loads in the CNS compartment and for treating HIV-related CNS disease (72). The ability of these agents to pass into the brain depends on several characteristics, including their protein binding, molecular size, lipophilicity, drug transporters and blood-brain barrier permeability (73). The classification of ARV drugs into either low-, intermediate- or high-CNS-penetrating agents was attempted by Letendre *et al*. based on the physico-chemical properties of drug, their recorded CSF concentrations and their effectiveness in treating CNS disease (72). Using this system, combinations of drugs and their expected CNS penetration could then be ranked according to their individual components. However, this simple ranking system did not consider other drug properties, such as drug interactions at the blood-CNS interface or, indeed, that many ARV agents are associated with CNS toxicities and that combinations of them may be associated with increased neurotoxicity (73).

The pathogeneses of CNS toxicities from ARV agents remain elusive (74). One potential mechanism is direct neuronal toxicity. EFV is a widely-used agent and is associated with CNS clinical toxicities including vivid dreams, insomnia, cognitive impairment, suicidal ideation, and suicide (75). In combination with ABC/3TC, it has been shown to result in reductions in grey matter and cortical volume (76). This has resulted in HIV treatment guidelines moving towards the use of integrase inhibitors in first-line ARV regimens (45-48). Although overt CNS side effects may be less prevalent with the integrase inhibitor class, emerging toxicities are being reported (77, 78).

In a study by Robertson *et al.*, the neurotoxicity of various ARVs was compared using MAP-2 staining in primary cultures of rat neurons. The median toxic doses of ABC, ddI, ETV and NVP leading to significant reductions in neuronal density, as evidenced by the loss of microtubule-associated protein (MAP)-2 staining, fell within the range of concentrations reported in both the plasma and CSF of patients on ARV therapy (79). Dose response curves were calculated and are shown in Figure 1.9, below. The greatest neurotoxicities were associated with ABC, EFV, ETV, NVP and ATV, whilst the lowest were with DRV, FTC, TDF and MVC. These data indicate that ARVs may contribute to microtubule damage in neurons.

Figure 1.9. Antiretroviral Therapy-Induced Neurotoxicity.

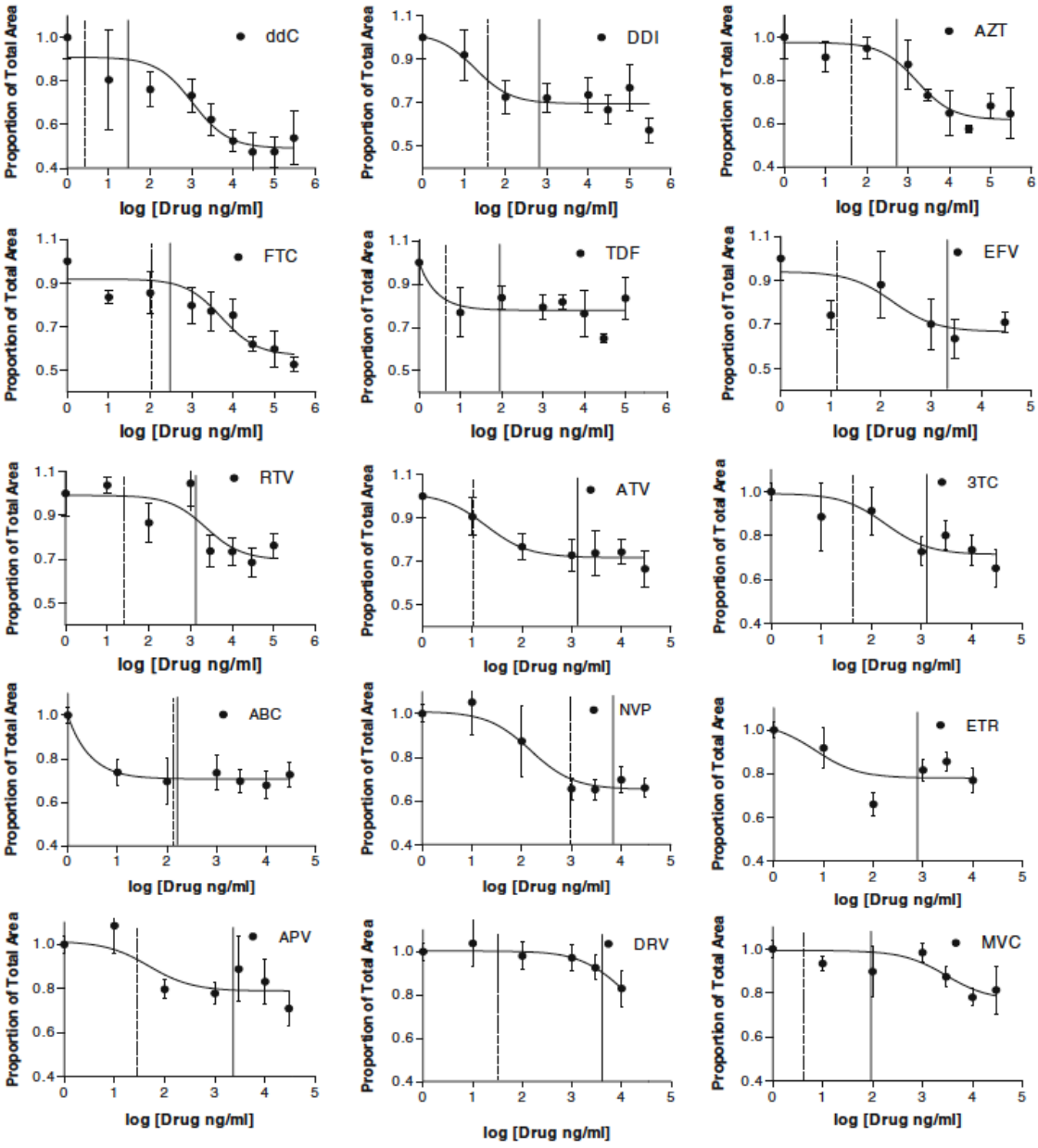

Footnote: The figure shows dose-response curves for damage induced by different antiretroviral agents incubated in neural cultures for 1 week (79). The proportion of total area occupied by MAP-2 stained neurons relative to untreated control cultures is plotted versus the log of the drug concentration (ng/ml).

Key: Solid lines indicate the therapeutic concentration reported in plasma. Dashed lines indicated the reported concentration in CSF.

In other studies, EFV and its major metabolite, 8-hydroxy-efavirenz, have been shown to be toxic in neuron cultures at concentrations found in cerebrospinal fluid (79-83). Other indirect pathways may also result in neurotoxicity.

1.6.3 Cognitive Impairment and Depression in HIV-1

HIV-infection has been associated with neurological and neuropsychiatric effects, including MDD and CI. The reported rates of MDD in people infected with HIV vary from 5% to almost 50% (84, 85). Several factors likely contribute to the development and persistence of MDD during HIV infection (40, 86-89). Untreated depression in people infected with HIV is associated with non-adherence to antiretroviral therapy (ART) (90), poorer performance in tests of cognitive function (91), more rapid progression to AIDS (92), and shorter survival(93).

CI is highly prevalent among HIV-infected individuals. Prior to the advent of ART, CI was reported in approximately 30% of individuals with otherwise asymptomatic HIV infection, and about 50% of individuals with AIDS. This usually presented as a severe motor and cognitive disorder (94). Following the advent of ART, the incidence of the most severe forms of HIV-related CI has decreased dramatically, while the prevalence of less severe forms remains high (95-99), although in a recent study of patients well-controlled on combination ART, rates are lower (96). In the current era, HIV-related CI manifests as milder disturbances of psychomotor speed, processing speed, executive function, or memory (100). Despite being of a milder form, HIV-related CI can still negatively affect daily function, ART adherence, and quality of life (100, 101).

There are three sets of criteria that are commonly used to determine neurocognitive impairment in PLWH. These include the 'Frascati' criteria (102), the global deficit score (GDS)(103), and the multivariate normative comparison (MNC) (104).

The Frascati criteria were proposed by Antinori *et al*. in 2007. Based on the American Academy of Neurology's published diagnostic criteria for neurologic manifestations of HIV infection, which defined two levels of neurologic manifestations of HIV infection, HIV-associated dementia (HAD) and minor cognitive motor disorder (MCMD), these updated criteria recognise the following three conditions: asymptomatic neurocognitive impairment (ANI),

HIV-associated mild neurocognitive disorder (MND), and HAD. Antinori *et al.* define ANI as "performance at least one standard deviation (SD) below the mean of demographically adjusted normative scores in at least two cognitive domains (attention-information processing, language, abstraction-executive, complex perceptual motor skills, memory, including learning and recall, simple motor skills or sensory perceptual abilities)." They specify that at least five cognitive domains are examined. Also, the impairment should not occur solely as part of a delirium or be explained by other comorbidities (102). In addition to the criteria for ANI, MND requires that there also be impairment in everyday functioning. Diagnosis of HAD requires that the individual has acquired moderate-to-severe cognitive impairment defined by a score at least 2 SDs below demographically adjusted normative means in at least two different cognitive areas, marked difficulty in activities of daily living, and should not be related to delirium or other comorbidities (102).

The GDS is an approach that converts demographically corrected standard scores (*T* scores) on individual neuropsychological measures to deficit scores ranging from 0 (no impairment) to 5 (severe impairment). The deficit scores are then averaged to create the GDS measure. This approach has been validated in detecting HIV-associated CI with a cutpoint of $\geq$0.5 indicating CI (104).

The MNC approach is a statistical method that may be seen as a multivariate version of Student's *t*-test for one sample. A complete cognitive profile comprising multiple tests is compared in a single instant with the control sample, rather than comparing each test result separately to its norm. It was specifically designed to control the false-positive rate of multiple individual tests whilst retaining sensitivity and has been validated in HIV-associated CI (104, 105).

Agreement between each of these approaches has been evaluated in a cohort of PLWH (106). Agreement of the MNC with Frascati and GDS was moderate, whilst agreement between Frascati and GDS was good, demonstrating that commonly-used criteria of CI show fair agreement (106).

Throughout this document, the terms HIV-associated CI and HIV-related CNS disease will be used, except when reporting on studies where the condition has been defined according to the AAN or Frascati criteria.

1.7 Interpreting Biomarker Data from HIV-1 Neuropathology Studies

A plethora of data exist regarding the underlying pathological processes of HIV-related CNS disease but the heterogeneity and complexity of the disease, its' treatment, co-morbidities, patient sub-populations, and the resulting complex 'inflammatory soup', hamper their clear interpretation. Various investigative modalities have been employed to elucidate the underlying pathological processes and to tease out biological disease markers that may be of use in the description, determination, measurement and diagnosis of HIV's effect on the CNS and its' function. Therefore, before attempting to provide summaries of the available data, some general principles must first be discussed to allow an understanding of the relative strengths, weaknesses and logistical challenges inherent in such a broad data set.

The term 'biomarker' is a portmanteau of 'biological marker'. Traditionally, it is defined as a biological characteristic that is assessed in lieu of something else. More precise definitions come from the U.S.'s National Institutes of Health (*'a characteristic that is objectively measured and evaluated as an indicator of normal biologic processes, pathogenic processes, or pharmacologic responses to a therapeutic intervention'*)(107) and the International Programme on Chemical Safety (*'any substance, structure, or process that can be measured in the body or its products and influence or predict the incidence of outcome or disease'*) (108). Other definitions exist but, at its' root, a biomarker is merely a measurable surrogate for some associated characteristic or process difficult or undesirable to assess directly.

Biomarkers of disease are typically – though not always – associated with the pathogenic process as either contributors or outcomes and may therefore have the potential to be prognostic or diagnostic. Such biomarkers may also be used as qualitative or quantitative indications of their associated processes and may also indicate the probability of a therapeutic response or adverse event, including its severity. Clinical medicine abounds with biomarkers used for these purposes. HIV medicine has long made use of plasma HIV-1-RNA viral loads and CD4+ cell counts as surrogates of disease prognosis and, thereby, of antiretroviral agent efficacy. Clinical chemistry analytes serve as biomarkers of various clinical diseases and adverse events. Prognostic and diagnostic markers of variable correlation exist for many diseases, and targeted therapies in many disciplines require biomarkers to determine treatment suitability, or indeed unsuitability (for example, the assessment of HLA-B*5701 in HIV to predict the likelihood of a hypersensitivity reaction to abacavir) (109, 110). Regardless

of its purpose, however, an effective biomarker has certain requirements. It must be biologically plausible as a surrogate marker and have acceptable sensitivity and specificity for a particular outcome in the population in which it is measured. A reliable and reproducible assay procedure is essential, as is a clear understanding of the collection, handling and storage factors affecting marker stability or quantification, and how these affect the interpretation of results (111).

Biomarkers can be obtained from various bio-fluids and tissues. However, while blood, urine, tears and saliva can be obtained easily, these liquids are vulnerable to exogenous factors and finding biomarkers that pertain directly to CNS-related events is usually difficult and potentially confounded. By contrast, CSF is more difficult to extract (i.e. via lumbar-puncture), but is potentially a more useful medium since it provides an insight into the brain microenvironment given its close anatomical contact with the brain interstitial fluid, wherein biochemical changes related to CNS disease may be reflected (112). Whilst brain tissue itself remains the gold standard, it is methodologically and ethically difficult to procure and, thus, CSF, along with imaging techniques, serves as a 'practical' gold standard for neurological research.

CSF is produced in the ventricles of the brain and in the subarachnoid space. Its composition is dependent upon many factors, including metabolic production rates in the brain, metabolite concentrations in blood, and transport processes at the blood-CSF, blood-brain and CSF-brain barriers. The total volume of CSF at any given time is approximately 150 mL and, normally, around 500 mL of CSF is produced each day. Thus, there is a high turnover of fluid in this compartment, resulting in a reduction in the concentrations of individual proteins and metabolites as they are flushed out. This is likely to complicate analysis of CSF as molecules of interest may be difficult to detect at these lower concentrations, though background 'noise' would be greatly reduced compared, for example, to plasma where more abundant proteins could mask the presence of less abundant ones (112).

Traditional, targeted, literature- and biological model-based sampling is still a valuable way of assessing markers of interested. Newer technologies, such as proteomics, lipidomics and metabolomics, have enabled the identification and quantitative description of vast numbers of molecules in cellular, tissue and biological fluid compartments in an unbiased manner (113). These techniques mark a new approach more akin to untargeted 'fishing trips', allowing

researchers to view the molecular composition of a diseased fluid in its entirety and to compare it with fluid from normal subjects. Those molecules whose concentrations are different from the comparator can then be researched in more detail. Efforts have been made to characterise the 'normal' human CSF proteome, lipidome and metabolome, thus allowing comparisons to be made with CSF from diseased subjects (112, 114-116). Other modalities include brain-imaging techniques, such as magnetic resonance imaging (MRI), magnetic resonance spectroscopy (MRS), diffusion tensor imaging (DTI), and positron emission tomography (PET), *in vitro* models, and animal models.

When evaluating each of these modalities, it is important to remember that many potential confounding factors exist. CNS injury is not a universal complication of HIV infection and HIV-infected individuals differ in their likelihood of experiencing CI according to several fundamental factors, including ongoing viral replication, CD4+ cell count, inter-individual differences in immune response, legacy effects, cognitive reserve, and possibly disease duration (117). Differences in the integrity of the blood-brain and blood-CSF barriers could result in differing competencies in the exclusion of, potentially toxic, plasma proteins (118, 119). Other factors, such as co-morbidities, duration of ARV therapy, inter-drug variability in CNS penetration, distribution, toxicity and neurologic effectiveness in lowering HIV viral loads, could also confound analyses when evaluating biomarkers (117). Many of the biochemical cascades set in motion by these factors are interdependent and cannot be studied in isolation. Sampling individual markers and trying to generalise the overall pathological process is akin to peering through a keyhole into a room and trying to describe the entire room just from the restricted view on offer - interpreting the significance of any individual biomarker in the context of all the processes that affect it may be impossible. These potential confounding factors must be considered in any interpretation of biomarker data (117, 120). With these caveats in mind, an overview of the investigated biomarkers for HIV-related CNS disease is provided in the following pages.

1.8 Cerebrospinal Fluid and Plasma Biomarkers of HIV-1 Central Nervous System Infection

In their recent reviews, two groups – Brew & Letendre (117) and Schouten *et al.* (121) – describe simple classification systems for biomarkers of HIV-related CI, organising them into three broad categories - those that are virological in origin, host response markers and markers of CNS damage. For the purposes of this review, this framework will be used and added to when describing the results of biomarker research. Table 1.6 (below) provides a summary of the main biomarkers of HIV-1 CNS infection that have been investigated to-date and that are described in this section.

Table 1.6. Potentially Useful Biomarkers of HIV-1 Central Nervous System Infection

Virological Markers
HIV-1-RNA (122-141)
HIV-1-DNA (127, 138, 140, 142)
HIV-1 Subtype (143-146)
HIV-1 Encoded Proteins (147-152)
Dual infection (153)
Host Response Markers
Markers of Inflammation
• Lymphocytes (139, 154-156)
○ Beta-2-microglobulin (β2M) (136, 155, 157-161)
• Monocytes and Macrophages (58)
○ Soluble CD14 (sCD14) (126, 156, 162-164)
○ Soluble CD163 (sCD163) (58, 128, 165, 166)
○ Osteopontin (167)
• Microglia (168)
○ CD40 and Soluble CD40 ligand (sCD40-L) (151)
Cytokines
• Interferons and Interferon-Inducible Proteins
○ Interferon-α (169-172)
○ Interferon-γ (173, 174)
○ Interferon-γ Inducible Protein-10 (IP or CXCL10) (175-179)
• Interleukins (169, 172, 178, 180-188)
• Tumour Necrosis Factor (TNF) Superfamily Proteins

- TNF-α (134, 169, 189, 190)
- Soluble TNF Receptors (sTNFRs) (191-193)
- Fas/TNFRSF6 and Fas-ligand (Fas-L)/TNFFSF6 (194-197)

- Chemokines
  - Monocyte Chemotactic Proteins (59, 172, 188, 198-204)
  - Macrophage Inflammatory Proteins (172, 178, 188, 205)
  - Fractalkine (CX3CL1) (204, 206, 207)
  - Transforming Growth Factor (TGF) (170, 208, 209)

Neopterin (136, 137, 155, 210, 211)

Intercellular Adhesion Molecules

- Intercellular Adhesion Molecule (ICAM)-1 (212-214)
- PrP^c and soluble PrP^c ($sPrP^c$) (215)

Proteases

- Matrix Metalloproteases (MMPs) (216-221)
- Cathepsins and Cystatins (222)
- Urokinase-Type Plasminogen Activator Receptor (uPAR) and soluble receptor (suPAR) (223-225)

microRNA (miRNA) (226)

Vascular Endothelial Growth Factor (VEGF) (227, 228)

Metabolic Abnormalities

- Sphingolipids (229, 230)

Autophagy

- Beclin-1 (231)
- Autophagy-Related Gene (Atg)-5 (231)
- Atg-7 (231)
- Light Chain 3 (LC3)-II (231)

Tryptophan and Kynurenine Metabolites (232-238)

Markers of CNS Tissue Damage

Neuronal Markers

- Cytoskeleton
  - Microtubules and Microtubule-Associated Proteins (MAPs) (239)
  - MAP2 (240)
  - Tau (239, 241-249)
  - Amyloid (243, 244, 250-256)
  - Neurofilament Proteins (NF) (256-261)
- 14-3-3 Protein (262, 263)

- Particularly Interesting Cysteine Histidine-Rich Protein (PINCH) (264)
- N-acetylaspartate (NAA), choline (Cho), myo-inositol (mI), Glutamate and Glutamine (Glx) (265-268)

Macroglia

- Astrocytes
    - S-100β (269-271)
    - Glial Fibrillary Acid Protein (GFAP) (228)
- Endothelial Cells / Blood-Brain Barrier
    - Albumin, Immunoglobulin G and Total Protein (272)

1.8.1 Virological Markers

1.8.1.1 HIV-1-RNA and DNA

Quantitative measurement of HIV-1-RNA can be performed in both plasma and CSF, with detectable viral loads reflecting productive viral replication (CSF HIV-1-RNA measurements are used as a proxy for brain tissue-derived HIV-1) (117, 122). Plasma HIV-1-RNA levels do not appear to be predictive, specific or sensitive as biomarkers of CI in ART-naïve and ART-treated PLWH (117, 122). Rates of CSF HIV-RNA vary, with mean reported prevalence rates of 10% in neurologically asymptomatic subjects and 14% in neurologically symptomatic subjects undergoing CSF examination for clinical reasons (123). A number of studies have demonstrated that greater HIV-1-RNA levels in CSF are associated with CI in ART-naïve populations, however, but that these associations do not appear to be consistent in PLWH receiving suppressive ART (124-140). Indeed, CI has been shown to occur in the absence of elevated HIV-1-RNA levels in the CSF, though this is uncommon (134, 139, 141). Brew and Letendre have proposed a number of possible explanations, including that this may be a residual deficit reflecting permanently damaged brain tissue or possibly that the CI was initiated by HIV-related damage but has subsequently become an independent disorder that is driven by immune activation (117).

In the case of HIV-1-DNA, greater plasma DNA levels are associated with greater immune activation, which may in turn contribute to neurological damage and CI (136, 142). Studies investigating HIV-1-DNA in CSF are lacking, but three small studies suggest that HIV-1-DNA levels in plasma may correlate with an increased risk for HIV-associated CI (127, 138, 140). In one small study in HIV+ treatment-naïve Thai PLWH (N=61), elevated levels of CD14+

monocyte HIV-1-DNA content in plasma correlated with an increased risk for HIV-associated CI (140). In this study, HIV-1-DNA levels also correlated with MRS markers of brain injury and neopterin (NEO) levels. This relationship is further supported by data from another small study of subjects with undetectable viral loads (n=5) showing that HIV-1-DNA levels in circulating CD14+/CD16+ monocyte subsets correlate with diagnoses of HAD (127). Another study in 18 younger patients (aged 22-40 years) and 26 older patients (aged 50-71 years) who were virologically-suppressed showed no difference in HIV-1-DNA levels in CD4+ cells in plasma between the groups (138). Older patients, however, had higher levels of inflammatory markers (sCD163, IL-6, IL-8, CCL2/MCP-1) in CSF and plasma compared to the younger group. Among older patients, higher HIV-1-DNA levels were significantly associated with more severe CI, an association that was not observed in the younger group. Measures of inflammatory markers were not associated with CI in either group. The authors suggest that correlates of CI might differ between younger and older adults (138).

1.8.1.2 HIV-1 Subtypes

Increases in the prevalence and severity of HIV-associated CI have been observed in individuals infected with HIV-1 subtype B versus those with subtype C virus, suggesting that there may be subtype-specific differences in neuropathogenicity (143). In an HIV-related CNS disease mouse model, Rao *et al*. demonstrated that animals infected with subtype B virus performed worse in tests of memory, and were seen to have increased astrogliosis and loss of neuronal network integrity than those with subtype C virus (144). *In vitro* data suggest that the majority of Tat protein in subtype C virus worldwide have a Cys32Ser polymorphism, which leads to it being defective for monocyte chemotaxis, resulting in fewer infected monocyte cells migrating to the brain and, consequently, less neuronal damage (143). In addition to this, in primary monocytes, subtype B Tat has been found to induce greater amounts of pro-inflammatory factors than subtype C Tat, such as TNF, IL-6, CCL2/MCP-1, and indoleamine 2,3-dioxygenase (IDO; an enzyme in the kynurenine pathway that leads to production of neurotoxins, such as quinolinic acid)(145). Subtype B Tat has also been shown to disrupt the integrity of brain microvascular endothelial cells to a greater extent than subtype C Tat (146). These observations clearly warrant investigation of the other subtypes of virus.

1.8.1.3 HIV Encoded Proteins

The HIV encoded proteins gp120, Nef, Tat, gp41, and Vpr are known to be neurotoxic *in vitro* through a variety of mechanisms (117, 147). Both gp120 and Tat have direct toxic effects on neurons, particularly dopaminergic neurons, contribute to the breakdown of the BBB and, by interacting with microglia, monocytes and macrophages, facilitate the release of other neurotoxic mediators, such as TNF-α and glutamate (66, 148-151). In addition to this, gp120 toxicity is enhanced in the presence of morphine and cocaine (150, 152). Tat depolarises neurons through direct interaction with cells membranes and can induce aggregation of neural cultures (148). Gp41 has been shown to induce the activity of matrix metalloproteinases (MMPs) in neuronal cultures, non-specific enzymes that are capable of degrading neuronal synapses and the BBB (148).

1.8.1.4 HIV Dual Infection

In a recent study, dual infection with different strains of HIV-1 in chronically-infected PLWH receiving ART was found to be associated with HIV-associated CI, though a causal association has not yet been identified (153).

1.8.2 Host Response Markers

1.8.2.1 Markers of Inflammation

Lymphocytes

The CD4+ cell count is not a direct marker of HIV-related CNS disease, but it has been found to be a useful indirect marker of the risk of developing CI. In the pre-highly-active antiretroviral (HAART) era, the lower the CD4 count the greater the risk of developing neurological issues. In antiretroviral (ARV)-treated patients, increasing evidence now points to the value of the nadir, rather than the current, CD4+ cell count (117, 139, 154, 155). In one study, CD4 nadir was shown to be positively correlated with fine motor skill impairment, and in another study with memory impairment and non-dominant hand fine motor skills (156).

Beta-2-Microglobulin

Beta-2-microglobulin (β_2M) is a small membrane protein composed of 99 amino acids belonging to the immunoglobulin superfamily. It is the light chain of class I major

histocompatibility complex proteins and is expressed on the surface of all nucleated cells with the exception of neurons and erythrocytes. It is particularly highly expressed on lymphocytes and, thus, serves as a marker of these cells. β_2M plasma concentrations are increased in multiple pathologies and serve as a non-specific marker of inflammatory and lympho-proliferative conditions (157). In HIV, elevated CSF β_2M concentrations correlate well with CNS disease progression with declines in levels following the advent of ART (136, 155, 157, 159-161, 250).

Monocytes & Macrophages

A prominent role for activated monocytes and macrophages in HIV CNS disease has been postulated due, at least in part, to the involvement of monocyte subsets expressing both CD14+ and CD16+ in the promotion of viral seeding in the CNS (see Section 1.6.1 above for a description of monocytes and their role in trafficking HIV into the CNS). A number of studies have demonstrated that, despite virological-suppression with ART, infectious, replication competent virus can still be found in circulating monocytes, thus indicating that monocytes remain a source of viral production, including in the brain (58).

A number of monocyte-associated markers have been assessed with regards to their relation with CI in HIV disease, including soluble CD14 (sCD14), sCD163, CD69, osteopontin and neopterin.

Soluble CD14

The membrane-bound form of CD14 is a glycophosphatidylinositol (GPI)-anchored glycoprotein present on myeloid cells as an inflammatory receptor for lipopolysaccharide (LPS), the expression of which is modulated by proinflammatory factors (273, 274). In addition to this form, two soluble isoforms of CD14 exist that have been shown to play roles in both proinflammatory functions, as well as the prevention of cytokine release and LPS-induced shock (273).

In HIV, elevations in serum sCD14 are associated with HIV disease progression (162). In plasma, sCD14 concentrations are higher in cognitively impaired patients vs. non-cognitively impaired patients receiving ARV therapy (163). In one study, sCD14 was not correlated with overall neuropsychological impairment, but was positively correlated with information processing speed (156). In another study, plasma sCD14 levels, but not LPS or CCL2 levels,

were higher in HIV+ individuals not well-controlled on ART with advanced disease (nadir CD4 counts <300) and impairment in global neurocognitive test scores compared to those without impairment. The authors concluded that plasma sCD14 was a better predictor of impaired global, attention and learning T scores than plasma or CSF viral load, or CD4 count (126). In another study by the same group, plasma and CSF concentrations of sCD14 were found to be increased in subjects with impaired neurocognitive test scores who were receiving ART but had detectable viral loads in plasma (164). The same association was not found to exist in virologically-suppressed subjects.

Soluble CD163

CD163 is a haptoglobin-haemoglobin scavenger receptor expressed by peripheral blood monocytes, perivascular macrophages and microglia (58). It plays a complex role in both down-regulating and up-regulating inflammation by acting as an anti-inflammatory scavenger receptor for the tumour necrosis factor-like weak inducer of apoptosis (TWEAK), as well as an inducer of pro-inflammatory cytokine production in macrophages (165). CD163 expression is altered in a number of diseases, including HIV. Its soluble form, sCD163, is involved in the resolution of inflammation.

In SIV-infected rhesus macaque models, the number of CD14+CD16+ monocytes expressing CD163 in plasma increases relative to viral loads and may be reflective of disease progression (58). CD14+CD16+CD163+ monocytes are capable of repopulating perivascular macrophages within the CNS of SIV-infected macaques (58). CD163 is also highly expressed in macrophages and microglia in the brains of SIV-infected macaques and PLWH (166).

CD163 is also shed in from the cell surface of monocytes and macrophages in its soluble form (sCD163), accumulating in plasma, the levels of which has been shown to positively correlating with monocyte activation and expansion (128, 165).

Plasma levels of sCD163 are increased in virologically-suppressed PLWH with CI, indicating that monocyte and macrophage activation persists despite effective cART (128). sCD163 is significantly elevated in individuals with mild cognitive defects compared to those with those with no impairment and is possibly predictive of impairment over time (128).

Osteopontin

Osteopontin (OPN) is a phosphoylated glycoprotein involved in a diverse range of cellular functions, including adhesion, migration, and the inflammatory responses of macrophages, T-cells and dendritic cells (275) It is a component of the extracellular matrix of many different types of cell and is also found as a soluble cytokine (275).

In HIV, OPN expression is increased on CNS-resident macrophages, microglia, astrocytes and neurons (167). It is found at increased levels in the CSF of PLWH with CI compared with HIV-controls; this increased expression may facilitate the entry of monocytes into the CNS, thereby maintaining the viral reservoir (58, 167). OPN is also expressed on CNS-resident macrophages, microglia, astrocytes and neurons in PLWH (167). It is thought that OPN stimulates HIV replication via an NF-κB-dependent mechanism that acts via OPN receptors (167).

Microglia

Microglia are considered to be the immune cells of the CNS. They comprise approximately 12% of the cells in the CNS but are not uniformly distributed. More microglia are found in grey matter, with the highest concentrations in the hippocampus, olfactory telencephelon, basal ganglia and substantia nigra, where they are located in close vicinity to neurons. In the white matter, microglia are localised between fibre tracts (65).

Microglial activation was found to be increased in the basal ganglia of cognitively aymptomatic PLWH receiving ART, which was associated with poorer performance in tests of verbal learning and memory (168).

CD40 and Soluble CD40 Ligand

CD40 is found on many different cells, including macrophages, dendritic cells, B cells, endothelial cells, smooth muscle cells, astrocytes and microglia. CD40 ligand (CD40-L), also known as CD154, has been shown to synergise with Tat protein, causing elevated TNF-α production by human monocytes and microglia. This occurs via Tat upregulation of CD40 expression on these cells, sensitising them to CD40-L (151). CD40-L also occurs in a soluble, secreted form (sCD40-L) that retains biological activity to bind and activate membrane-bound CD40. Untreated HIV-1 infection is associated with an elevated release of sCD40-L. ARV therapy has been shown to have no effect on sCD40-L (151). Similar to HIV-1 Tat protein, sCD40-L also interacts with the chemokine IL-8 (CXCL8). sCD40-L is integral to the actions

CXCL8, as microglia only secrete it after ligation of surface CD40 with CD40-L. Elevations in plasma and CSF sCD40-L have been found in cognitively impaired PLWH compared with PLWH without cognitive impairment (151).

1.8.2.2 Cytokines

Cytokines are soluble proteins that serve as chemical communicators between cells. They are usually secreted by cells, but some are expressed on the cell surface whilst others are maintained in reservoirs in the extracellular matrix (276). Cytokines combine with surface receptors on target cells that are linked to intracellular signal transduction pathways to modify and coordinate antibody and T cell immune system interactions and reactions. They include monokines, such as interleukin (IL)-1, tumour necrosis factor (TNF), α and β interferons, and colony-stimulating factors, which are produced by macrophages, and lymphokines, such as IL-2 to 6, INF-γ, and granulocyte-macrophage colony-stimulating factors, which are produced by activated T lymphocytes (276). Endothelial cells, fibroblasts, and some other cell types may also synthesise cytokines.

<u>Interferons and Interferon-Inducible Proteins</u>

The interferons are a large family of immunoregulatory cytokines synthesised by T lymphocytes, fibroblasts, and other types of cells following stimulation with viruses, antigens, mitogens, double-stranded DNA or lectins, and facilitate cellular resistance to viral infection by enhancing the ability of macrophages to destroy tumour cells, viruses and bacteria (276). Interferons are categorised into α and β (previously known as Type I interferons), which are antivirals, and γ (previously known as Type II interferon), which is known as immune interferon.

Interferon-α

Interferon-α (IFN-α) is the name given to at least 13 different immunomodulatory glycoproteins synthesised by macrophages and B cells that are able to prevent the replication of viruses, are antiproliferative, and are pyrogenic (276). In the brain, astrocytes and microglia in particular can produce IFN-α. Whilst its primary role may be to protect the brain from viral infections, with prolonged exposure and/or high concentrations, it may injure it.

Several studies have measured IFN-α in HIV disease (169-172) with most of them identifying that higher levels in CSF were associated with HIV-related CNS disease (169-171), and higher CSF HIV-1-RNA levels (170, 171).

Interferon-γ

Interferon-γ (INF-γ) is a glycoprotein that is synthesised by activated CD4 T_H1 cells, CD8 T cells and natural killer cells with antiproliferative and antiviral properties. It is also a powerful activator of mononuclear phagocytes (276). IFN-γ has been shown to be increased in both plasma and CSF during HIV infection, though neither of these studies identified links with neurological disease (173, 174).

Interferon-γ Inducible Protein-10

Interferon-γ Inducible Protein-10 (IP-10 or CXCL10) is a α-chemokine of the CXC family with angiostatic properties that is produced after INF-γ stimulation of endothelial cells, monocytes, macrophages, fibroblasts, keratinocytes and astrocyte (176, 276). It acts on its receptor, CXCR3, to attract activated T cells, NK cells and blood monocytes, and appears to be important in a variety of inflammatory conditions, including HIV (172, 176-179, 191). It has also been shown to be a potent neurotoxin (175).

CXCL10 expression is inducible by HIV Tat and IFN-γ (175) and is elevated in both plasma and CSF, with concentrations in CSF being higher and correlating with CSF viral loads and pleocytosis (176-178). Levels are lower in those receiving fully-suppressive ART (177). It has been suggested that it is produced intrathecally and accumulates in this compartment (176). In Nef-expressing astrocyte and neuronal co-cultures, CXCL10 was shown to be expressed by astrocytes and cause neuronal cell death (179).

<u>Interleukins</u>

Interleukins (IL) are a diverse family of cytokines that are primarily synthesised by leukocytes (276). Several studies have investigated the presence of various ILs in the CSF and plasma of people with chronic HIV-infection. Interpretation of these data are hampered by the inclusion of subjects with various inflammatory CNS co-infections, as well as the use of HIV- control populations, many of which have inflammatory CNS diseases or conditions. However, the

general picture appears to be one of an inflammatory environment characterised by inadequate anti-inflammatory responses to elevated pro-inflammatory cytokines (185).

IL-1 is comprised of two proteins, designated IL-1α and IL-1β, that are produced by activated macrophages and other antigen presenting cells, as well as astrocytes and microglia (180). IL-1 promotes inflammation as an inducer of inducible nitric oxide synthase, the products of which can be highly toxic (181), and also mediates cell proliferation and apoptosis (184). IL-1β is induced by HIV-1 gp120 and gp41 and both IL-1α and IL-1β are found in the CSF of PLWH, though their levels do not correlate with measures of CI (169, 180-183). IL-1α does not appear to be detectable in the plasma of PLWH (169). Two studies have reported that IL-1β is not detectable in plasma (183, 184), but two others report finding elevated plasma levels that correlate with lower volumes in the globus pallidus, putamen, thalamus, hippocampus, amygdala, cortical grey matter and cerebral white matter, and higher ventricular volumes (185, 186). One of these studies also found a correlation between higher IL-1β plasma levels and lower cognitive performance (185).

IL-2 is produced by Type 1 helper T cells (Th1) and activates macrophages. It appears to down-regulate the expression of CD4 and CCR5 in monocytes and macrophages and, therefore, slows the recruitment of new host cells by HIV-1, though it is unclear whether this occurs in the CNS (181). IL-2 is not detectable in the CSF of PLWH (180, 187).

IL-4 is produced by activated T cells and has anti- and pro-inflammatory capacities.[11] Its' function in HIV-related CNS disease is unclear. The elevated expression of IL-4 in CSF may contribute to elevated recruitment of HIV-1 from the blood into brain parenchyma and of CD4-independent infection of myeloid cells within the CNS (181, 182).

IL-5 is synthesised by activated CD4+ lymphocytes and mast cells and is an important growth-factor for B lymphocytes (276). The possible role of IL-5 in HIV-related CNS disease development is unknown and it is not detectable in the CSF of PLWH (178).

IL-6 is a strongly proinflammatory cytokine produced by vascular endothelial cells, mononuclear phagocytes, fibroblasts, activated T lymphocytes and macrophages (181, 276). Studies have reported mixed findings in terms of its' presence in the CSF and plasma of PLWH

(169, 178, 180, 183-186). One study found that higher IL-6 plasma concentrations correlated with lower volumes in the putamen, pallidum, thalamus, hippocampus, amygdala, cortical grey matter and white matter, and higher ventricular volume, but this finding was not replicated in a second study (185). This second study did, however, find that IL-6 levels were negatively correlated with psychomotor speed (185).

IL-7 is a stimulant for B cells and is necessary for the survival of lymphoid cells. High levels of IL-7 in ART-treated patients are linked to therapy failure and progression to NCI (181).

IL-8 is a chemokine of the CXC family that has powerful neutrophil chemotactic properties (172, 185, 188, 276). In HIV, it has been shown to be significantly elevated in both plasma and CSF (184). CSF levels positively correlate with memory performance and higher plasma levels correlate with lower volumes in cerebral white matter and lower cognitive performance (172, 184, 188).

IL-10 acts as an anti-inflammatory molecule by inhibiting the synthesis of other cytokines (such as TNF-α, IL-1β, IL-6 and IL-8), and by inhibiting the activation and function of T cells, monocytes and macrophages (276). It is expressed by CD4+ and CD8+ T cells, monocytes, macrophages and activated B cells. IL-10 has been shown to be elevated in the plasma and CSF of PLWH but does not appear to be specific for NCI (180, 182, 184, 185). Kallianpur *et al.* investigated the ratios of various inflammatory cytokines to IL-10 and found that high ratios of IL-1β/IL-10, IL-6/IL-10 and IL-8/IL-10 were associated with reductions in white matter volumes, and high ratios of IL-1β/IL-10 and IL-8/IL-10 were associated with reductions in thalamus volumes. These ratios were not related to measures of CI, however (185).

IL-15 activates, and is chemotactic for, T-cells and NK-cells. It is not found ubiquitously in the CSF of PLWH, therefore it is presumed that the main source of IL-15 in CSF is the blood (181). IL-15 has been found to be highly expressed in subjects with HIV-related CNS disease compared to neurologically asymptomatic subjects (182).

IL-16, also known as lymphocyte chemoattractant (LCA), is expressed by CD4+ T cells, mast cells and eosinophils as a precursor peptide (pro-IL-16) that requires processing by an enzyme termed ‘caspase-3’ to become active (276). Its’ role includes the suppression of T cell proliferation. IL-16 plasma concentrations have been found to negatively correlate with

volumes in the putamen, pallidum, thalamus, hippocampus, amygdala, cortical grey matter and white matter, and with higher ventricular volume (181).

IL-18 is a strong proinflammatory cytokine produced by macrophages that activates antiviral responses by enhancing IFN-γ levels (276). IL-18 concentrations are significantly elevated in the plasma of PLWH and these increases are correlated with lower volumes in the putamen, pallidum, thalamus, hippocampus, amygdala, cortical grey matter and white matter, with higher ventricular volume, and with worse memory performance (184, 186).

Tumour Necrosis Factor (TNF) Superfamily Proteins

Tumour necrosis factor (TNF) is the prototype of a family of molecules that are involved with immune regulation and inflammation (276). Receptors for TNF and other proteins, such as soluble first apoptosis signal receptor (Fas/TNFRSF6), constitute a super-family of related proteins. TNF-α is a cytotoxic cytokine comprised of 157 amino acid residues. It is produced by monocytes, macrophages, T lymphocytes, B lymphocytes, NK cells, microglia and astrocytes and participates in inflammation, wound healing, remodeling of tissue and the induction of apoptosis (277). Its receptors are tumour necrosis factor receptor 1 (TNFR1 or CD120a) and TNFR2 (or CD120b) (276). These receptors form a heterocomplex that mediates the recruitment of two anti-apoptotic proteins, c-IAP1 and c-IAP2. It has been suggested that these proteins may protect neurons from apoptosis by stimulating antioxidative pathways (276). Fas is a death receptor that initiates apoptosis once its ligand (FasL/TNFSF6) binds to it (276).

In HIV, TNF-α concentrations appear to be elevated in the CSF and plasma of individuals with HIV-related CNS disease compared to that of neurologically asymptomatic PLWH (134, 169, 189). Similarly, expression of TNF-α mRNA is elevated in post-mortem brain tissue samples from individuals with HIV-related CNS disease compared to that of neurologically asymptomatic HIV+ controls (190).

sTNFR1 and sTNFR2 levels appear to be elevated slightly in the CSF of PLWH experiencing neurological problems, but much higher levels are found in those who also have a CNS opportunistic infection, particularly those that are fungal or protozoal in nature (191-193). Plasma levels were not significantly increased.

Three studies have measured levels of sFas and sFasL, and have identified associations between higher levels of sFas in CSF and HIV-related CNS disease (194-196).

Whilst TNF-α (163), sTNFRs and sFas concentrations in plasma and CSF have been shown to decline upon initiation of ARV therapy, they can be still detected (197).

Chemokines

Chemokines (chemotactic cytokines) are molecules that recruit and activate leukocytes and other cells at sites of inflammation. They exhibit both chemoattractant and cytokine properties. There are two types of chemokines: α-chemokines (C-X-C chemokines) that activate neutrophils; and β-chemokines (C-C chemokines) that activate monocytes, lymphocytes, basophils and eosinophils (276).

Monocyte Chemotactic Proteins

Monocyte chemoattractant protein (MCP-1/CCL2) is a β-chemokine, which is believed to be one of the most significant chemokines in inflammatory diseases controlled by mononuclear leukocytes (276). Multiple lines of evidence support the role of MCP-1 in HIV neuropathogenesis. As described in Section 1.6.1, MCP-1 is instrumental in attracting and inducing infected CD14+CD16+ monocytes across the BBB (59). HIV also induces the expression of MCP-1/CCL2 from monocytes, microglia and astrocytes (198, 199). Multiple studies have reported levels of MCP-1 in CSF in HIV-infected individuals, most of which showed that raised levels of MCP-1 were associated with worse outcomes (117, 172, 188, 200-204). MCP-1 levels in CSF appear to be directly related to plasma viral replication (202), with MRS markers of neuronal damage (204), and with neurological disease (172, 203), making this a potentially useful biomarker (202).

Macrophage Inflammatory Proteins

Macrophage inflammatory proteins (MIP)-1α (CCL3), MIP-1β (CCL4) and RANTES are β-chemokines that have roles in monocyte chemotaxis (MIP-1α) and leukocyte chemoattraction (MIP-1β and RANTES), respectively (276). They each bind to CCR5, the most commonly used receptor by HIV for entry into lymphocytes and microglia, and have HIV-suppressive effects, acting synergistically together (117, 276).

Several studies have compared levels of MIP-1-α, MIP-1-β and RANTES in CSF to neurologic outcomes in PLWH (172, 178, 188, 205). Three studies indicate that levels of these chemokines are undetectable in the CSF of PLWH with and without NCI (172, 178, 188). Two of these studies did not provide details on whether patients were receiving ART or not, making interpretation more difficult (178, 188). However, in one study CSF levels of MIP1-β and RANTES were higher in HIV+ subjects with CI, whereas levels of MIP-1α were lower in those with CI, perhaps indicating that higher levels are neuroprotective. In this study, use of ART did not appear to influence CSF chemokine levels (205).

Fractalkine

Fractalkine (CX3CL1) is a chemokine that is expressed in neurons throughout the CNS and appears to be important in reducing neurotoxicity associated with activated microglia (117, 278). Its receptor, CX3CR1, is highly expressed in the CNS by microglia, but also by neurons and astrocytes (206, 278). Microglial cultures and neuron-microglial co-cultures stimulated by LPS produce proinflammatory molecules, upregulate inducible nitric oxide synthase (iNOS), and induce neuron death, the effects of which can be attenuated by the addition of fractalkine (278).

The role of fractalkine in HIV is not clear. Findings indicate that there are non-specific increases in the levels of fractalkine in the CSF of individuals suffering from neurologic disease, perhaps indicating the hosts attempts at neuroprotection (204, 206, 207). However, evidence also suggests that neuronal injury by HIV could induce the production of fractalkine as a distress signal, attracting mononuclear phagocytes to the site of injury, resulting in neuron cell death (206). Therefore, fractalkine could potentially be involved in HIV neuropathogenesis.

Transforming Growth Factor

Transforming growth factors (TGF) are polypeptides produced by virus-transformed cells that induce various cells to alter their phenotypes (276). TGF-α has a powerful stimulatory effect on cell growth. TGF-βs (there are five TGF-βs designated one through five) regulate cell growth and differentiation and have a host of other effects, including the down regulation of T cell and macrophage activation, modulation of pro-inflammatory cytokines and protection against neurotoxicity, indicating a role in reparative processes (209, 276). Exposing astroglial-cortical neuron co-cultures to gp120 results in increases in Ca^{2+} causing the neurons to apoptose. Pre-

treatment of the co-cultures with TGF-β1 was shown to prevent this (209). In clinical samples the picture is less clear; CSF TGF-β1 concentrations were shown to be elevated during mild HIV-related CNS disease (170, 208) and undetectable in severe disease (170), perhaps indicating a differential response that varies with disease severity. The effect of ART is, as yet, unknown.

1.8.2.3 Neopterin

NEO is a product of guanosine triphosphate metabolism, and is mainly produced by activated monocytes, macrophages and microglia following stimulation by INF-γ (276). Increased NEO levels in serum and urine can be found in approximately 80% of PLWH and almost all individuals who have progressed to AIDS. Indeed, increasing NEO levels are an early predictor of disease progression.

CSF concentrations have been shown to correlate with the severity of HIV-related CNS disease, and elevated levels have been associated with an increased risk of developing HIV-related CNS disease, at least in individuals with advanced HIV disease (155, 210). However, high CSF concentrations are also found in PLWH with opportunistic CNS infections such as CMV encephalitis and cryptococcal meningitis (211). CSF NEO levels have been shown to decrease with ARV therapy. However, after two years of virologic suppression only 55% had normal CSF NEO levels and, in another study, at 10 years 83% of subjects had normal CSF levels. These data indicate a persistent low-level intrathecal immune activation, the implications of which are currently unknown (136, 137, 211).

1.8.2.4 Intercellular Adhesion Molecules

Intercellular adhesion molecules (ICAMs) are leukocyte integrin ligands that facilitate the binding of lymphocytes and other leukocytes to various cells, such as antigen-presenting cells and endothelial cells (276).

<u>Intercellular Adhesion Molecule (ICAM)-1</u>

ICAM-1 is a cellular membrane glycoprotein that occurs in multiple cell types, including dendritic cells, cerebral endothelial cells and activated astrocytes. HIV gp120 and pro-inflammatory cytokines, such as IFN-γ, TNF and IL-1, can up-regulate the expression of ICAM-

1 (212, 213). Soluble ICAM-1 (sICAM-1) levels in CSF were found to be modestly elevated in PLWH (213) with greater levels than HIV-negative subjects (214). Greater levels were found in subjects experiencing HIV-related CNS disease.

Protease Resistant Protein, Cellular Form (PrP^c)

PrP^c is the non-pathological cellular isoform of the human prion protein. It is most abundantly expressed in the CNS, where it is found on CNS cells, the BBB and on infiltrating leukocytes. PrP^c localises to the cell membrane, where it is anchored by glycosylphosphatidylinosistol and functions as both an adhesion molecule and transducer of intracellular signaling. It plays a role in physiological processes that are disrupted during HIV-1 infection, including monocyte transmigration across the BBB, macrophage phagocytosis, microglia and leukocyte activationcellular taxis, glutamate metabolism, cellular taxis, neuronal synaptic plasticity, and NMDA receptor-associated calcium signaling (215). It has also been postulated that human prion protein is, amongst many other disparate functions, involved in the maintenance of long-term memory, possibly via hippocampal long-term potentiation (279, 280).

PrP^c levels have been shown to be significantly elevated in both the CNS of PLWH with neurocognitive impairment, and in SIV-infected macaques with encephalitis, with CSF levels correlating with the degree of CNS compromise (215). Soluble PrP^c was shown to mediate neuroinflammation by inducing astrocytes production of CCL2 and IL-6 (215).

1.8.2.5 Proteases

Proteases are enzymes that break the peptide bond that joins amino acids together in proteins (281). Based on their method of catalysis, proteases are classified into six distinct classes, including aspartic, glutamic, metalloproteases, cysteine, serine and threonine (282). The first three classes utilise an activated water molecule as a nucleophile to attack the peptide bond of the substrate, whereas the remaining enzymes use an amino acid residue (Cys, Ser or Thr, respectively) as the nucleophile (282). Several metalloproteases and cysteine proteases have been investigated to elucidate their roles in HIV-related CNS disease because of their roles in the regulation of neuroinflammation, BBB permeability and cell migration (216).

Matrix Metalloproteases (MMPs)

Matrix metalloproteinases (MMPs) are a family of zinc-containing endopeptidases that are part of the innate immune system and important in many pathological processes, including neuroinflammation. MMP activity is elevated in the CSF of PLWH. They have been shown to be capable of cleaving the Tat protein of HIV thus inactivating it and, possibly, preventing it from causing neurotoxicity (217). However, emerging evidence suggests that the non-specific nature of the action of MMPs may also contribute more directly to neuronal injury by enzymatically degrading neuronal synapses and the basal lamina of the BBB, thus making it more permeable and facilitating the migration of leukocytes into the brain (218). In addition to this, MMPs can cleave other host proteins, the products of which can cause neurotoxicity (219).

In a recent study, plasma and CSF levels of MMP-1 (collagenase-1), MMP-2 (gelatinase A), MMP-7 (matrilysin), MMP-9 (gelatinase B) and MMP-10 (stromelysin-2) were measured in a small cohort of recently infected (>1 year) subjects (n=52) and an age-matched control group of HIV- subjects (n=21) (216). Plasma MMP-2 levels were found to be significantly reduced in early HIV infection and correlated with altered white matter integrity and atrophic brain changes. MMP-9 levels were higher in the 27 patients receiving ART compared with the 25 not receiving ART. Only MMP-2 and MMP-9 were detected in the CSF of HIV+ subjects. CSF MMP-2 correlated with white matter integrity and volumetric changes in basal ganglia. CSF MMP-2 and MMP-9 levels correlated highly with psychomotor speed and verbal fluency, respectively.

In other studies, MMP-9 (gellatinase B) has been detected more frequently in PLWH with neurological deficits than asymptomatic or sero-negative controls (220, 221).

Cathepsins and Cystatins

Cathepsins are a group of 15 aspartic, cysteine and serine proteases that are abundant in endosomes of antigen-presenting cells. Cathepsin B is known to play a role in inflammation, intracellular protein degradation and cell death (276). Increased cathepsin B levels were observed in perivascular macrophages from white matter in the brains of individuals with AIDS in the pre-HAART era. Cystatins are a family of cysteine protease inhibitors that are present in the cytosol of many cell types and body fluids. Cystatin B and and cystatin C are the endogenous inhibitors of cathepsin B (222).

In a retrospective study of 63 HIV+ Hispanic women, increased cathepsin B and cystatin B and C levels were found in plasma, with the greatest intracellular expression of cathepsin B and cystatin B in monocytes of women with HAD. Significant increases in cystatin B concentrations in CSF were found in women with dementia compared with neurologically-asymptomatic HIV+ women (222).

Urokinase-Type Plasminogen Activator Receptor

Urokinase-type plasminogen activator (uPA) is a serine protease that is synthesised as an inactive precursor molecule (pro-uPA) that then undergoes proteolytic activation (223). Both pro-uPA and uPA bind to the uPA receptor (uPAR) on the cell surface of neutrophils, mononuclear phagocytes, and activated T lymphocytes. uPA plays a role in the activation, adhesion and migration of these cells. Elevated concentrations of the soluble form of uPAR (suPAR) are observed in the plasma and CSF of PLWH, correlate with HIV-related CNS disease, and decline significantly with ARV therapy (223, 224). Elevated expression of uPAR/uPA in cerebral lesions of HIV-infected patients with opportunistic CNS disease, such as CMV encephalitis, toxoplasmosis, or lymphoma, have also been observed (225).

1.8.2.6 microRNA (miRNA)

MicroRNAs (miRNAs) are small non-coding RNA molecules that down-regulates, or completely suppresses, the expression of one or more genes. Host-encoded miRNAs are able to regulate both host and viral gene expression. In one study, PLWH with HIV-associated CNS disease and those without have shown differentially expressed miRNA profiles in plasma, suggesting that these could be useful biomarkers of HIV-related CNS disease, as well as providing useful insights into the underlying disease mechanisms (226).

1.8.2.7 Vascular Endothelial Growth Factor (VEGF)

Vascular endothelial growth factor (VEGF) is a potent angiogenic agent. When activated by inflammatory cytokines and oxidative stress, it induces angiogenesis, extracellular matrix degradation, has chemotactic effects on leukocytes, and induces a variety of mediators, such as MMPs and adhesion molecules, that are known to contribute to HIV-1 neuropathogenesis (227). In a small study of PLWH with HIV-related CNS disease (n=8) and PLWH without

neurological disorders (n=18), CSF and plasma VEGF levels were determined. Plasma, but not CSF, VEGF levels were shown to be increased in subjects with CNS disease compared to those without. A significant decrease in plasma VEGF concentrations was observed in two subjects that received ART (228).

1.8.2.8 Metabolic Abnormalities

Sphingolipids

Sphingolipids are enriched in the CNS where, in addition to structural roles, they function as regulators of protein scaffolding, and second messengers that shape cellular signaling events. Ceramides are the simplest sphingolipid and can be deacylated to sphingosine, or converted to more complex sphingolipids, such as glycosphingolipids or sphingomyelin. Each of these reactions is bidirectional, and there is evidence that the relative balance of ceramide to these other ceramide-derived lipids can play important roles in regulating cellular events (229).

CSF sphingomyelin:ceramide ratios for acyl chain lengths of C16:0, C18:0, C22:0 and C24:0 have been associated with worse performance on several indices of memory in PLWH. Acyl chain C18:0 was associated with the most striking findings and was consistently associated with performance on multiple tests of memory (229, 230).

1.8.2.9 Autophagy

Autophagy is the natural, orderly degradation and recycling of cellular components. It can be induced in response to nutrient depletion and is a non-apoptotic pathway of programmed cell death (231). In a small post-mortem study of 32 PLWH (12 without evidence of HIV-1 encephalitis or clinical signs of CNS impairment and 20 with histopathological findings of HIV-1 encephalitis) and eight HIV- subjects with no evidence of neuropathology, the autophagic proteins Beclin 1, autophagy-related gene (Atg)-5, Atg-7 and light chain 3 (LC3)-II were found to be significantly increased in the brains of subjects with HIV-1 encephalitis. No increases were observed in the HIV+ group without encephalitis compared with the HIV- control group. These data suggest that dysregulation of autophagy may be important in the pathogenesis of CNS-related HIV disease (231).

1.8.2.10 Tryptophan, Kynurenine and Metabolites of the Kynurenine Pathway

Tryptophan (TRP) is an essential amino acid and acts as a substrate for tryptophan 5-hydroxylase, leading to the production of 5-hydroxytryptophan (serotonin). Under physiological conditions, TRP is also degraded via hepatic metabolism by tryptophan 2,3-dioxygenase (TDO), which is activated when the concentration of tryptophan exceeds the requirements for its metabolic needs. TRP is also catabolised extrahepatically in intestinal, lung, placenta and brain tissues by indoleamine 2,3-dioxygenase (IDO-1), which is inducible by proinflammatory cytokines (232, 233, 283). In the CNS, the cellular localization of IDO-1 has been shown to be primarily in infiltrating macrophages and resident microglial cells. Increasing IDO-1 activity diverts TRP away from serotonin production and results in the production of kynurenine (KYN) and a number of neuroactive catabolites, most of which are either neurotoxic or neuroprotective (232-235, 283). The net result during HIV infection is unclear, but there is potential for neural damage to occur, which could impact cognition and mood (236-238).

TRP, KYN and the KYN pathway are the focus of this PhD. As such, Section 1.9 provides more detail on this pathway.

1.8.3 Markers of CNS Tissue Damage

1.8.3.1 Neuronal Markers

Markers of neuronal damage include structural proteins that are important for cytoskeletal stability and axonal transport. Following neuronal damage, these proteins are released into the intercellular space and from there into the CSF where they can be quantified (284). They include the different proteins of the cytoskeleton, 14-3-3 protein and N-acetyl aspartate (NAA).

<u>Cytoskeleton</u>

With the exception of erythrocytes, all eukaryotic cells contain an organelle known as the cytoskeleton, which provides structure and support. The cytoskeleton organises the functional activities of the cell and serves as an anchoring point for other organelles, as well as serving as tracts by which organelles and other cellular materials can move around. The cytoskeleton of the neuron is comprised of a network of protein structures: microtubules;

neurofilaments; and microfilaments (also known as actin filaments). The effect of HIV-1 on some of these structures has been investigated.

Microtubules and Microtubule-Associated Proteins

Neuronal microtubules are hollow cylindrical tubes formed from protein polymers made up of tubulin sub-units known as 'dimers'. A dimer is a dipolar globular protein that consists of two parts - α-tubulin and β-tubulin, each made of approximately 450 amino acids. Dimers align end to end to form protofilaments, 13 of which join laterally in a helical fashion to form a tube shape (285). Microtubule-associated proteins (MAPs) are proteins that bind to the tubulin subunits of microtubules and regulate their stability. MAP-2 and tau (another type of MAP) link microtubules and neurofilaments, acting as a scaffold that stabilises and facilitates the assembly of microtubules, therefore playing a critical role in the maintenance of neuronal integrity (41, 239). Tau is primarily found in the axon and MAP-2 is found in dendrites.

MAP-2

In a rat model, exposure of embryonic cortical neurons to HIV-1 Tat led to the rapid degradation of MAP-2 and the collapse of cytoskeleton filaments. The mechanism was shown to involve Tat-mediated translocation of cellular proteasomes (proteins that degrade unneeded or damaged proteins by proteolysis) to the site of microtubule filaments resulting in MAP-2 degradation. In the same study, immunohistochemical analysis of brain tissue samples from individuals with HIV encephalitis revealed a significant decrease in MAP-2 and an increase in S20 (a core particle of proteasomes) in cortical neurons (240).

Tau

Tau binding and stabilisation of microtubules is controlled by its phosphorylation state, which fluctuates as part of normal cellular processes. When phosphorylated, tau dissociates from microtubules, making them unstable and preparing them for growth and remodeling. Tau can become hyperphosphorylated, however, leading to the self-assembly and deposition of paired helical tau filaments as neuritic threads, and neurofibrillary pre-tangles and tangles, ultimately resulting in the interruption of axonal transportation, loss of structural integrity of the neuron, and cell death (41, 239).

Tau phosphorylation is strongly positively correlated with the expression of glycogen synthase kinase 3β (GSK-3β), which has been shown to be upregulated by HIV-1 Tat protein *in vitro* (41).

A number of clinical studies have examined the relationship between t-tau, p-tau and HIV-associated CNS disease, nearly all of which indicate that t-tau and p-tau concentrations in CSF are increased in PLWH compared with HIV- controls (239, 241-248, 250). However, drawing firm conclusions from these studies is difficult due to the heterogeneity of the HIV+ populations included and the varied control groups utilised. Most of these studies did not account for the use of ART or included groups of PLWH of which only some were receiving ART and had fully-suppressed viral loads. In addition to this, neurological complications were not homogenous across the studies meaning that they are reporting on differing sub-populations. This was particularly evident in the only study that reported no differences in either t-tau or p-tau concentrations in the CSF of PLWH experiencing neurological complications compared to control groups. In this study, CSF tau concentrations from PLWH with HAD (n=24) were compared with those from patients with lymphoma (n=10), cerebral infarction (n=20) or miscellaneous conditions, such as headache (n=22) (242). The HIV+ group was heterogeneous in terms of ART use (some were receiving ART and some were not receiving any treatment at all) and many of them had co-infections, such as CMV, cryptococcal and toxoplasmosis, and comorbidities. In addition to this, there was no healthy control population. Thus, drawing conclusions from these data is problematic.

Tau disturbance may be a useful marker of HIV-related CNS damage, but additional larger studies in less heterogeneous groups of patients are needed (249).

Amyloid

Amyloid precursor protein (APP) is a ubiquitous, type 1 transmembrane glycoprotein and synaptic adhesion molecule that is concentrated in the synapses of neurons. Its primary function is unknown, though it has been implicated as a regulator of synapse formation and function (286). APP can be processed via two pathways – amyloidogenic and non-amyloidogenic. In the amyloidogenic pathway, APP is cleaved by β-secretase and γ-secretase, resulting in the production of amyloid β (Aβ), 40 or 42 amino peptides (286). A number of *in vitro* and transgenic Alzheimer's disease mouse model studies have suggested that APP overexpression results in the accumulation and aggregation of Aβ, the primary peptide constituent of amyloid plaques in Alzheimer's disease, causing a decrease in both synaptic activity and dendritic spine density (286). Amyloid β42 (Aβ42) aggregation, in particular, has been implicated in Alzheimer's disease. The mechanism of action appears to be related to the

ability of Aβ to aggregate into flexible soluble oligomers that can exist in several forms, including a misfolded form that can induce other Aβ molecules to misfold, leading to a chain reaction. The resulting amyloid plaques are toxic to neurons and may induce misfolding in other proteins, including tau (287). Low CSF levels of Aβ42 and increased levels of t tau and p tau serve as biomarkers of conversion to Alzheimer's disease (288, 289). Aggregation of Aβ42 appears to be the most likely cause for the decreased CSF Aβ42 concentrations with the aggregated state inhibiting it from being transported from brain interstitial fluid to CSF (289).

Similar neuropathologic abnormalities are thought to occur in PLWH. Neuroasymptomatic HIV+ subjects have increased APP, probably related to the action of inflammatory molecules on neurons. IL-1, TNF-α and INF-γ increase the activity of gamma-secretase, which degrades APP to neurotoxic amyloid β fragments, including amyloid-β42 (250). In addition to this, evidence suggests that HIV-1 Tat may inhibit the endonuclease neprolysin, which is responsible for the breakdown of Aβ peptides (250, 251, 290).

In an *in vitro* pilot study, the effects of AZT, 3TC, ABC and IDV (as single agents or in combination) on neuronal Aβ production and clearance by microglial phagocytosis were investigated (252). All of the ARV compounds were shown to increase Aβ1-40, 42 generation in murine N2a cells transfected with the human 'Swedish' mutant form of APP (SweAPP N2a cells), with the combination of ABC, 3TC and IDV exerting the most significant amyloidogenic effects. Microglial phagocytosis was found to be significantly inhibited by all ARV compounds and combinations in N9 microglial cultures (252).

In a clinical study investigating CSF concentrations of Aβ42, no differences were found when comparing neurologically asymptomatic HIV+ subjects, of whom 90% were receiving ART, with healthy controls (253). Two clinical studies of neurologically symptomatic PLWH either failing therapy (243) or not on therapy (244) showed reduced CSF concentrations of Aβ42 compared to healthy controls, with a third study, in PLWH of whom approximately 80% were receiving ART, showing no difference (254). In the two studies that did not show a difference, amyloid deposition itself was also measured using the PET amyloid binding agent N-methyl-[^{11}C]2-(4-methylaminophenyl)-6-hydroxythiazole (^{11}C-PiB) (253, 254). Neither study showed increased amyloid deposition. In another study investigating the presence of amyloid plaques in 97 subjects who died from AIDS-related illnesses, post-mortem analyses of brain biopsies showed

that there was a significantly greater prevalence of plaques in subjects with AIDS compared to age-matched, HIV- controls (29% vs. 13%; p<0.004; n=125) (255).

In a study of ART-naïve subjects with primary HIV infection (n=92), CSF Aβ42 concentrations were found to be greater than in HIV- controls (n=25), though this did not correlate with neuropsychological abnormalities (256). APP concentrations were not found to be significantly different. The authors suggest that the differences observed in Aβ42 concentrations may be due to increased cerebral inflammation in the primary HIV infection group.

Collectively, these data suggest that throughout HIV infection the production and deposition of Aβ may be disturbed.

Neurofilament Proteins

The role of neurofilaments is to maintain the structure of the cell. There are three major neurofilament subunits, the names of which are based upon their molecular mass: neurofilament light (NFL), medium (NFM) and heavy (NFH). The light subunit is the essential component of the neurofilament core and acts as the backbone to which NFM and NFH copolymerise.

Cerebrospinal fluid levels of NFL have been found to be significantly elevated in most PLWH (256-260), but data are conflicted in terms of whether levels are higher in individuals with neurological symptoms compared with those without. In one study, NFL concentrations increased when ARV therapy was interrupted (258). Two studies have shown decreases in NFL to normal levels (<250 ng/L) when commenced on treatment (257, 260).

In a single study, high levels of CSF NFH, protein carbonyls and nityrosine have been found in PLWH who were cognitively normal, suggesting that neuronal injury may occur early in the course of infection. Individuals with a decline in cognitive status also showed an increase in CSF NFH levels but these were not significantly different from those who were neurocognitively normal (261).

No studies have assessed the role of NFM in this setting.

14-3-3 Protein

The 14-3-3 family of adaptor proteins consists of seven isoforms (β, γ, ς, ε, η, θ/τ, and σ) and two phosphorylated isotypes (α and δ) (262). 14-3-3 proteins are abundant in the human brain, comprising approximately 1% of its total protein (291). and play diverse physiological roles interacting with a multitude of substrate proteins during normal development and adulthood. They are also detected in CSF in various neurodegenerative diseases, including multiple sclerosis and Creutzfeldt-Jakob disease (262, 263, 291), with their presence thought to be indicative of neuronal damage.

In HIV, high concentrations of 14-3-3ς, ε and γ isoforms were observed in the CSF of male subjects with AIDS, particularly those with low CD4+ cell counts (262). In addition to this, 14-3-3ς and ε isoform concentrations were found to be elevated 2-fold in brain sections from male subjects with HIV encephalitis (HIVE) and HIV-associated CI compared to HIV- controls (263).

Isoform 14-3-3ε (also known as YWHAE) is of particular interest as the loss of this gene and neighbouring genes in humans leads to Miller-Dieker Syndrome, a severe form of retardation. In addition, mice that lack YWHAE display impaired memory and enhanced anxiety, along with defects in neuronal migration (263). In a small study of HIV+ and HIV- women, individuals who were HIV+ and heterozygous for polymorphisms at the rs4790084/rs1204828 loci, were three times more likely to display reduced cognitive function, to have received an HIV-associated CI diagnosis, and to have less YHWAE protein expressed than homozygotes, suggesting that YWHAE is a potential genetic risk factor for the development of CI (263).

PINCH

Particularly interesting cysteine histidine-rich (PINCH) protein functions as a shuttling protein in Schwann cells after peripheral nerve damage, during repair and remodeling, and in maintaining neuronal polarity. PINCH expression has been found in abundance in the neurons and extracellular matrix of HIV subjects' brains. Interestingly, PINCH patterns of distribution were found to be different in PLWH with CNS disease compared to those without CNS involvement. In addition to this, CSF levels of PINCH were found to be significantly increased in PLWH with and without CNS involvement, though they were found to be lower in neurosymptomatic patients than neuroasymptomatic patients. Thus, variations in CSF levels

of PINCH in PLWH during disease progression may indicate CNS alterations for early neuronal signaling changes in the CNS (264).

N-acetylaspartate, Choline, Myo-Inositol, Creatine and Glx (glutamate + glutamine)

Proton magnetic resonance spectroscopy (^{1}H-MRS) is a non-invasive imaging technique that is capable of quantifying cerebral metabolites associated with different aspects of cell function, including N-acetylaspartate (NAA), choline-containing compounds (Cho), myo-inositol (mI) and creatine (Cr) (292). NAA is synthesised in neurons from the amino acid aspartic acid and acetyl-coenzyme A. It is postulated to play a role in brain fluid balance, as well as being a source of acetate for lipid and myelin synthesis in oligodendrocytes, a precursor for the synthesis of N-acetylaspartylglutamate, and a contributor to energy production in neuronal mitochondria. NAA is used as a sensitive marker of neuronal integrity *in vivo*, with reductions in its concentrations being indicative of damage and, possibly, a reduction in neuronal density (117, 265, 292). Cho is a water-soluble vitamin-like essential nutrient, whilst mI is a simple sugar-alcohol that is believed to be a marker of astrocyte integrity and, possibly, a breakdown product of myelin (292, 293). Cho and mI are indicators of glial proliferation and cellular injury and, as such, their levels increase with neuroinflammation. Cr is a marker of intracellular energy stores and is used as a reference for metabolite levels (292, 294).

Glx is a combination of glutamate, an excitatory neurotransmitter found primarily in glutamatergic neurons, and its stored form, glutamine, which is found within astrocytes. Since glutamate is required for aspartate synthesis within the neuronal mitochondria, decreased levels of Glx may be an early indicator of neuronal metabolism changes induced by this disease (265).

NAA and Glx concentrations are reduced in frontal cortex grey matter and are significantly decreased in subjects with early (n=8) and chronic (n=10) HIV-infection compared to levels measured in healthy controls (n=9). Within the white matter, no difference was observed between subjects during early HIV infection and seronegative controls. Only NAA levels in chronically-infected subjects were reduced from those of controls (265).

In a study investigating the differences between changes in cerebral function and alternative ART regimens, treatment-naïve, HIV-1-infected individuals were randomly allocated to

commence ART with two NRTIs (TDF/FTC) plus either the NNRTI EFV (n=9), the PI ATV/r (n=9), or two additional NRTI's (ABC + AZT; n=12) (266-268). Increases in the NAA/Cr ratio were observed in all anatomical voxels (right frontal white matter, mid-frontal grey matter and the right basal ganglia) from baseline to Week 48. Greater increases were observed in subjects receiving EFV-based ART compared with the other two groups. Interestingly, despite the greater increases in NAA/Cr observed in the EFV group, the NRTI-only group experienced greater improvements in neurocognitive performance compared with both the EFV and ATV/r groups. No significant differences were observed for Cho/Cr or mI/Cr between groups, though a trend toward a greater increase in the mI/Cr ratio in right frontal white matter in patients receiving EFV-based ART compared with those receiving the four NRTIs was observed (266).

1.8.3.2 Macroglia

Astrocytes

S-100β

S-100β is an acidic calcium-binding protein that is most abundantly found in astrocytes. It is also found in small quantities in neurons but not in microglia (269). S-100β plays a role in neural development and maintenance. It is secreted by astrocytes and released from damaged cells into extracellular fluids and blood; as such, it has become a biomarker of CNS damage and blood-brain barrier permeability. High extracellular concentrations of S-100β (i.e. in the micromolar region) may lead to neuronal apoptosis via induction of nitric oxide (270).

In one study, raised levels of S-100β in CSF occurred in PLWH receiving ART with either moderate or severe HAD and predicted a rapid progression to death (269). In another study investigating continued combination ART (n=34) versus simplifying ART to monotherapy with ritonavir-boosted lopinavir (LPV/r; n=31) in virologically-suppressed subjects, CSF S-100β concentrations were found to be significantly elevated in the LPV/r group compared with subjects that remained on combination ART (271). These data indicate that LPV/r monotherapy may elicit an astrocytic response that could be damaging and that this maintenance strategy may be sub-optimal.

Glial fibrillary acid protein (GFAP)

Glial fibrillary acid protein (GFAP) is major structural protein of astrocytes. A single study in PLWH with HAD (n=11) and those without HAD (n=21), and in those with opportunistic CNS diseases (n=13), compared with HIV- controls, indicates that it is not a sensitive marker in HIV-related CNS disease (228).

Endothelial Cells / Blood-Brain Barrier

Albumin, Immunoglobulin G, and Total Protein

Albumin, immunoglobulin G (IgG) and other large proteins are usually excluded from the CNS by an intact BBB. However, when injured, the permeability of the BBB to large molecules increases. Therefore, the presence and concentrations of these molecules in the CSF may reflect BBB damage and provide some measure of that damage (117). In one study, the mean total intrathecal IgG synthesis rate, a measure of intrathecal plasma cell activity, were significantly higher in subjects with HIV-related CNS disease compared with PLWH without neurologic disease (272). In the same study, the mean trans-BBB albumin leakage rate increased significantly in patients with neurologic disease. Total protein, however, does not appear to correlate well with neurologic disease in PLWH (117).

1.9 Tryptophan Metabolism and HIV-1

1.9.1 Tryptophan Metabolism and Inflammatory Disease

Many of the pathological factors and the various virological, host response and CNS damage markers underlying HIV-associated CI have been discussed in the previous sections. This PhD thesis is focused on the role of TRP because the effects exerted by its catabolites on neural tissue, mood and cognition in individuals with immune-related diseases such as HIV-infection is an area of increasing interest.

TRP is an essential amino acid that acts as a precursor for two important biochemical pathways: 1) production of the neurotransmitter 5-hydroxytryptamine (serotonin) by the tetrahydrobiopterin (BH_4)-dependent TRP 5-hydroxylase; and 2) formation of kynurenine (KYN) derivatives and nicotinamide adenine dinucleotide (NAD+), initiated by the heme-dependent enzymes TDO and IDO 1 + 2 (234, 283, 295). TDO activity is highest in the liver,

whereas IDO is absent from the liver in most mammals but is expressed by antigen-presenting cells both systemically and in intestinal, lung, placenta and brain tissue (234, 283).

Under normal physiological conditions, TDO is active only when TRP concentrations exceed the requirements for its need. Evidence suggests that TDO is induced by inflammation that is mediated indirectly by increased glucocorticoid receptor activation (297). IDO is inducible by proinflammatory cytokines, such as IFN-γ and TNF-α, which are increased during inflammatory disease (232, 233, 283). Induction of these enzymes leads to the acceleration of TRP degradation via the KYN pathway (Figure 1.10), resulting in systemic and local TRP depletion and corresponding increases in KYN production, both of which are important mechanisms of antimicrobial resistance to parasites, bacteria and some viruses, including HIV (298). In contrast, it can also lead to immunosuppression by antigen-specific T-cell exhaustion and recruitment of T regulatory cells. In acute infection, this can be advantageous as exaggerated immune responses are prevented, but during chronic infections it suppresses the immune mechanisms that would eradicate the infection (299, 300). In addition to this, recent evidence suggests that the increased KYN impacts the gut mucosa via aryl hydrocarbon receptor, resulting in microbial translocation, which further drives immune activation and IDO expression and creates a self-sustaining feedback loop whereby TRP is depleted and KYN is produced (300).

Inflammatory factors also activate the enzyme guanosine-triphosphate-cyclohydrolase-1 (GTP-CH1), which produces 7,8-dihydroneopterin triphosphate (NH_2PPP), leading to the production of neopterin (NEO) and a reduction in BH_4 production (Figure 1.11). Concomitantly, BH_4 is destroyed by reactive oxygen species (ROS) leading to further reductions. BH_4 plays an instrumental role in the production of the neurotransmitters serotonin, dopamine, adrenaline and noradrenaline. BH_4 deficiency could lead to decreases in the production of dopamine and serotonin, resulting in reduced function of these pathways (234, 298, 301-305).

Figure 1.10. Simplified Diagram of the Kynurenine Pathway.

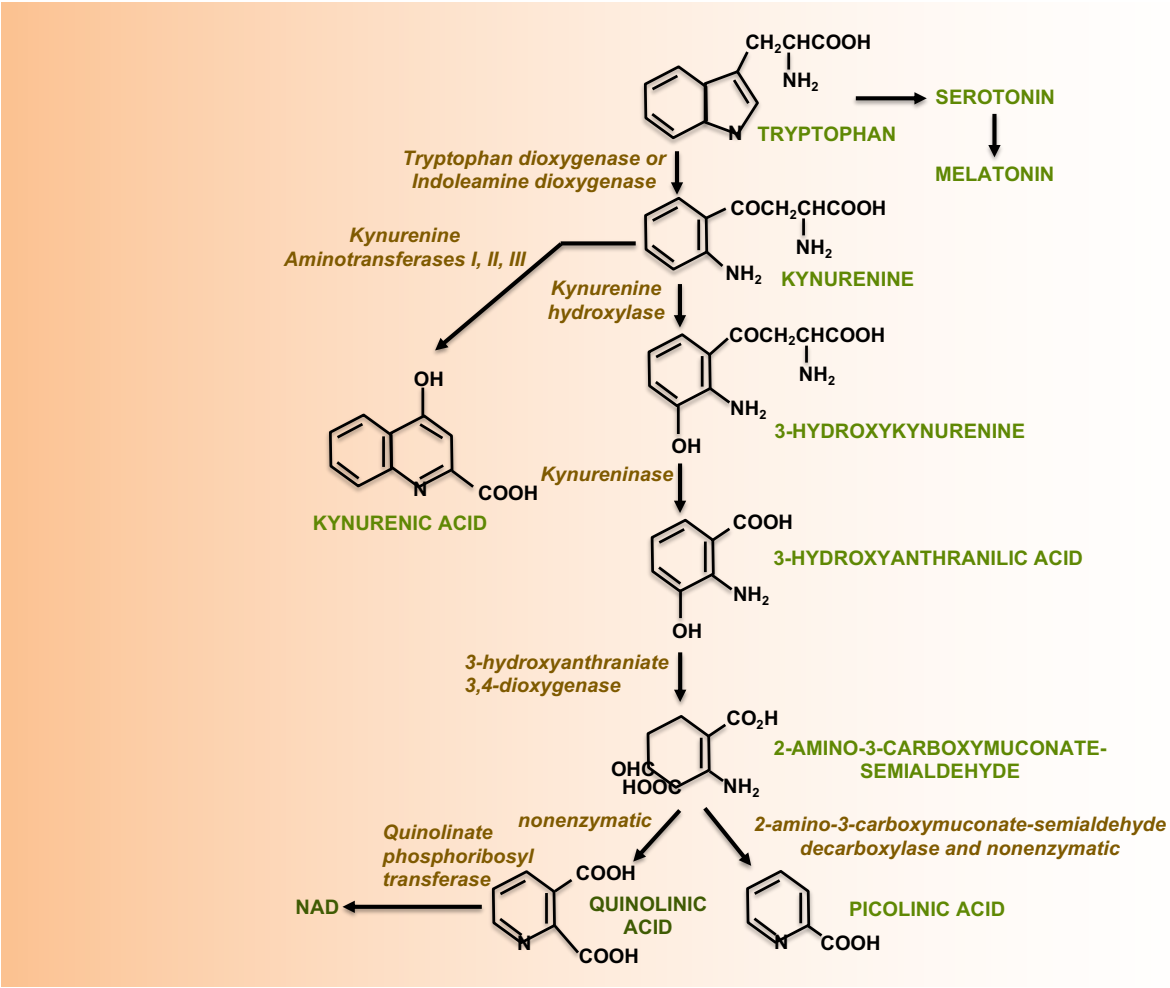

Adapted from Stone TW. *Pharmacological Reviews* 1993 and Guillemin GJ, *et al. J Neuroscience* 2007 (283, 296).

Figure 1.11. Effects of Inflammatory Factors on Indoleamine-2,3-Dioxygenase (IDO) and Guanosine-Triphosphate-Cyclohydrolase-1 (GTP-CH1) Pathways.

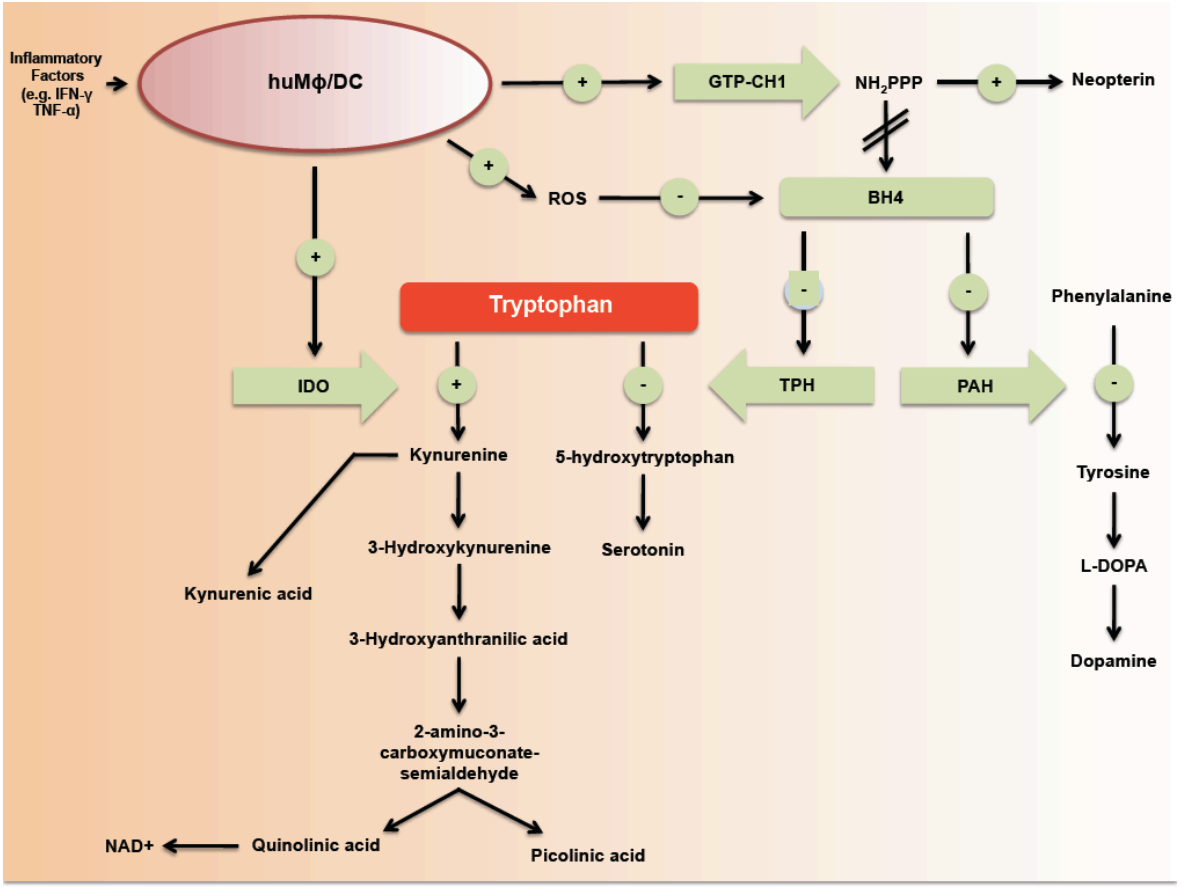

Footnote: The figure illustrates the effects of inflammatory factors on IDO and GTP-CH1 pathways.

Adapted from: Guillemin GJ, *et al. Adv Exp Med Biol* 2003; Stone TW. *Pharmacological Reviews* 1993; and Capuron L. *Biol Psychiatry* 2011; and Murray MF. *The Lancet ID* 2003 (234, 283, 306, 307).

Systemic KYN is further catabolised, resulting in the production of several neuroactive intermediates, some of which can be neurotoxic, such as 3-hydroxykynurenine (3-HK), 3-hydroxyanthranilic acid (3-HAA) and quinolinic acid (QUIN), or neuroprotective, such as kynurenic acid (KYNA), and picolinic acid (PIC) (234-236, 283), KYN and some of its' catabolites, such as QUIN, are able to cross the BBB, where they may be further catabolised by macrophages, microglia, and possibly astrocytes, neurons and BBB epithelial cells (234, 235, 296, 308, 309).

TRP metabolism has been shown to be disturbed throughout the course of HIV-1 infection, despite adequate dietary intake (234). As with other inflammatory conditions, IDO is induced via the proinflammatory mediators IFN-γ and TNF-α in HIV disease. The expression and/or activity of IDO is further induced in monocyte-derived macrophages and plasmacytoid dendritic cells (pDC) by HIV virions and their viral proteins, particularly Nef and Tat (233). The resulting chronic depletion of TRP leads to the suppression of CD4+ T cell, CD8+ T cell, NK cell and B cell proliferation (233, 299, 310), decreased TRP concentrations, increased KYN and QUIN concentrations, and decreased serotonin and intracellular NAD+ concentrations (173, 232, 233, 237, 307). The decrease in serotonin production and increase in neurotoxin production could be of particular importance in the pathogenesis of depression and CI in PLWH (311).

Of the neurotoxic products, QUIN is probably the most important in terms of biological activity and is known to be associated with the neuropathogenesis of Alzheimer's disease, Huntingdon's disease, amyotrophic lateral sclerosis and HIV (312). QUIN is derived from 2-amino-3-carboxymuconatesemialdehyde by non-enzymatic synthesis. Its' neurotoxicity is mediated through several pathways. QUIN is a weak *N*-methly-D-aspartate (NMDA) agonist at normal physiological levels (235). However, during inflammatory disease, when its levels are elevated by several orders of magnitude, it exerts excitotoxic effects via NMDA receptors (313). Braidy *et al.* showed that QUIN acts as a substrate for NAD+ synthesis at very low, physiological, concentrations (<50 nM) in both neurons and astrocytes resulting in a significant increase in intracellular NAD+. However, it was shown to be cytotoxic at greater than physiological concentrations (>150 nM) in both cell types, and this is supported by further work performed in glial cells (312). Other routes of NMDA excitotoxicity include production of reactive oxygen species (ROS), mitochondrial dysfunction and lipid peroxidation (117, 234). Under normal physiological conditions, QUIN is converted to NAD+ by quinolate

phosphoribosyl transferase (QPRT). However, QPRT does not appear to be upregulated during inflammatory disease in the same way as other enzymes, and so QUIN accumulates, causing toxicity. A critical question is whether QPRT is also inducible because this would have the potential to draw down the local QUIN concentrations and interrupt the neurotoxic effects associated with high concentrations of this metabolite (314).

3-HK and 3-HAA are other potentially neurotoxic metabolites of the KYN pathway. Their neurotoxicity is thought to be mediated by increases in hydrogen peroxide concentrations that are presumed to be generated by 3-HK and 3-HAA oxidation (315).

The kynurenine aminotransferases (KAT)-I, -II and -III enzymes are responsible for the synthesis of KYNA from KYN (296). KYNA is a glutamate-receptor antagonist, preferentially blocking the glycine site of the NMDA receptor and, as such, is neuroprotective. In a cell model using neurons stimulated with QUIN, KYNA was shown to significantly reduce excitotoxicity compared to unstimulated control neurons (296).

Like QUIN, PIC is also synthesised from 2-amino-3-carboxymuconatesemialdehyde. It is catabolised by 2-amino-3-carboxymuconatesemialdehyde decarboxylase to 2-aminomuconic semialdehyde with subsequent non-enzymatic conversion to PIC (316). PIC displays antagonistic properties towards the toxic effects of QUIN via an unknown mechanism. It is also known to have antiviral properties but it's levels in HIV infection have not yet been assessed (316, 317).

NAD+ is one of the end products of the KYN pathway and is essential for electron transfer reactions in all living cells. It is synthesized *de novo* from ingested TRP or from ingestion of niacin and is a cofactor for the DNA repair enzyme poly(ADP-ribose) polymerase (PARP) – an essential intracellular enzyme for repair of DNA damage caused by reactive oxygen species (ROS). Excessive activation of PARP causes intracellular NAD+ depletion and contributes to cell death (318). Therefore, it has been proposed that the KYN pathway is a cellular protective pathway as NAD+ is a metabolic goal product (236). Niacin supplementation (in the form of oral nicotinamide) has been shown to be clinically beneficial to HIV-1-infected individuals; specifically, it has been associated with increased CD4 counts, slowed progression to AIDS, and prolonged survival (94). It has also been suggested that circulating niacin could feedback to inhibit excessive TRP oxidation by IDO in the same way as it does with TDO, leading to a

reduction in the concentration of neurotoxic catabolites, such as QUIN (319). This theory remains to be tested, however. Murray *et al*. initiated a very small clinical trial (N=4) that showed that HIV-related serum TRP depletion is reversible using high-dose niacin supplementation in the form of oral nicotinamide. PLWH with decreased TRP levels who were either not receiving ARV's or were stable on ARV therapy for at least three months were given oral nicotinamide 3g daily for two months. Increases in plasma tryptophan levels of 21 - 70% were observed (320). Whilst central TRP levels were not investigated and neurocognitive assessments not performed, this study indicates that it might be possible to correct TRP depletion using a dietary supplement.

1.9.2 Cellular Localisation of the Kynurenine Pathway in the Central Nervous System

In the brain, the cellular localisation of the KYN pathway has been shown to be primarily expressed in infiltrating macrophages and resident microglial cells (234, 235). Astrocytes, neurons and BBB epithelial cells also express the KYN pathway to varying degrees (235, 296, 308, 309).

1.9.2.1 Macrophages and Microglia

Macrophages and microglia express the KYN pathway in its entirety. Infiltrating macrophages have been shown to be the most potent QUIN producers during brain inflammatory diseases, with microglia playing a lesser role (macrophages produce 19 times more QUIN than microglia) (234, 235). This is likely because they produce greater concentrations of IDO when exposed to IFN-γ (macrophages produce three times more IDO than microglia).

1.9.2.2 Astrocytes

Astrocytes do not express kynurenine hydroxylase (KYN(OH)ase) and, therefore, cannot produce 3-HK. However, they are able to produce large amounts of the early KYN pathway metabolites, such as KYN and KYNA, and only minute amounts of the late metabolites QUIN (only when 3-HAA is added) and PIC. Essentially, the pathway is split in half in astrocytes (235, 308).

The lack of KYN(OH)ase in astrocytes could prove to be neuroprotective in the absence of macrophages and/or activated resident microglia by catabolising any synthesised QUIN and by producing KYNA, an antagonist of QUIN. During inflammation, however, they could contribute to neurotoxicity by producing KYN, thus 'unwittingly' providing a substrate for QUIN production to infiltrating activated macrophages and activated microglia (308).

1.9.2.3 Neurons

KYN pathway enzymes are variably expressed in neurons (296). KYN(OH)ase expression tends to be localised to non-pyramidal neurons in the frontal cortex, with only a minority of neurons expressing it. PIC is expressed but QUIN has not been detected. Therefore, the net result of KYN pathway induction in human neurons is predicted to result in neuroprotection, immune regulation and tumour inhibition, rather than neurotoxicity (235, 296).

1.9.2.4 Blood-Brain Barrier Epithelial Cells

The human blood-brain barrier has limited expression of the KYN pathway. Immune stimulation results in the production of various intermediate metabolites that could be further processed by brain-resident monocytic-lineage cells to neurotoxic KYN pathway metabolites, in particular QUIN, thus causing local neurotoxicity (309).

1.9.3 Tryptophan Metabolism and Antiretroviral Therapy

Initiation of ART has been shown to significantly reduce, but not completely reduce, the degradation of TRP (321).

In a small, single arm, prospective study of HIV-1-seropositive subjects without neurological symptoms (N=14), CSF and plasma concentrations of indoleamines and catecholamines were measured prior to treatment with AZT, after 3-14 months treatment, and finally after 14-30 months. TRP concentrations were shown to increase, and NEO concentrations to decrease, significantly in both CSF and plasma following initiation of AZT. No significant changes were observed for serotonin in plasma, 5-hydroxyindoleacetic acid (5-HIAA; the main metabolite of serotonin) in CSF, homovanillic acid (HVA; a metabolite of dopamine) in CSF, or 3-methoxy-4-hydroxyphenylglycol (a metabolite of norepinephrine) in CSF (322).

In another small, single arm, prospective study of PLWH with no signs of neurological disease (N=14), CSF and plasma concentrations of TRP, KYN and NEO were measured prior to treatment with AZT and after 4-14 months of treatment (323). Significant increases in TRP in both CSF and plasma, and significant decreases in NEO in CSF only, were observed following treatment. No changes were observed in KYN concentrations.

In a study of 45 PLWH, plasma TRP and KYN concentrations were measured before and 6 months after initiation of ART (either two NRTIs plus a PI or three NRTIs) and compared with those of HIV- controls (n=not provided) (324). Compared with the healthy control group, the HIV+ subjects presented with lower TRP and greater KYN concentrations, and a greater KYN/TRP ratio, prior to treatment. Following treatment, TRP concentrations increased and KYN concentrations and the KYN/TRP ratio decreased.

CSF QUIN levels have been shown to fall rapidly with ARV treatment (197, 313, 325), probably as a result of a reduction in virus-related immune activation.

There are currently no published data reporting on whether ARV therapy has an effect on TRP metabolism independent of HIV-1.

1.9.4 Tryptophan Metabolism and Mood Disturbance in HIV-1

Several lines of evidence suggest that major depressive disorders are characterised by behavioural and cognitive symptoms resulting from a deficiency of available serotonin or inefficient serotonin from certain regions of the brain, such as the hypothalamus, amygdala, and cortical areas involved in cognition and other higher processes (326). It is thought that the accelerated degradation of TRP via the KYN pathway can lead to decreased serotonin production and likely reduced function of serotonergic pathways (234, 298, 301, 327, 328). This may be compounded by the fact that, as an indoleamine derivative, serotonin is a substrate of IDO, albeit with lower affinity than TRP (302-304). Findings from *in vitro* and *in vivo* studies and from animal model systems support the concept that TRP degradation plays a major role in inflammation-associated neuropsychiatric disorders such as depression and cognitive decline (304, 311, 329). In non-HIV-infected individuals, lower plasma or CSF TRP

concentrations have been shown to be significantly correlated with anxiety, somatisation, agitation, anorexia, suicidal thoughts, depressed mood, neuromuscular symptoms, depersonalisation, obsessions, paranoia and diurnal variation in a number of different studies (330-336). Further evidence comes from a study in which reduced levels of 5-HIAA, a serotonin metabolite, in the CSF were observed in non-HIV-infected, depressed patients (337).

Several studies have investigated TRP metabolism and mood disturbance in HIV+ individuals. In a study by Schroecksnadel *et al*., TRP, KYN and NEO concentrations in plasma and urine were determined in 152 PLWH (338). Subjects also completed the Beck Depression Inventory (BDI). Forty-one subjects scored as having mild, 22 with moderate and 14 with severe depression. Subjects without depression had significantly lower plasma TRP and NEO concentrations than depressed subjects. A significant correlation between the KYN/TRP ratio and BDI scores was observed in subjects not receiving anti-depressant treatment, which was not observed in subjects receiving medication.

In a recent retrospective, cross-sectional analysis of CSF samples from subjects with primary HIV infection (PHI; n=84) and chronic infection (n=235) and HIV- controls (n=22), Grill *et al.* reported untreated HIV-infection to be associated with higher KYN/TRP ratios compared to treated individuals (238). In patients with primary HIV infection (n=54), increased KYN/TRP ratios were associated with increased depressive symptoms as measured by Beck Depression Inventory-II (BDI-II) scores.

In another recent study, Martinez *et al*. measured TRP and KYN concentrations in plasma, dietary diversity and self-reported depression symptom severity using a modified version of the Hopkins Symptom Checklist for Depression (HSCL-D) in a prospective cohort of 504 PLWH initiating their first ARV regimen in rural Uganda (339). Greater depressive symptoms were associated with both lower plasma TRP and higher plasma KYN/TRP ratios over a 12-month follow-up period. Multivariate analysis indicated that declines in the KYN/TRP ratio and increases in plasma TRP concentrations partially explained ART-mediated improvements in depressive symptom severity. The association between KYN/TRP ratios and depression symptom severity was stronger among persions with protein-deficient diets than among those with protein-rich diets.

Other explanations for depression in this population have been addressed. For example, Hammoud *et al.* evaluated the involvement of serotonergic transmission in HIV-associated depression using a radiolabelled serotonin transporter (5-HTT) specific for positron emission tomography (PET), in HIV+ depressed and non-depressed subjects compared with healthy controls (340). They found lower binding in HIV+ subjects compared to healthy controls, possibly reflecting serotonergic neuronal loss as a component of generalised HIV-associated neurodegeneration. HIV+ depressed subjects were found to have a higher mean regional 5-HTT binding potential than HIV+ non-depressed subjects, possibly reflecting an increased density of 5-HTT, leading to increased clearance of serotonin from the synapse, which could account, for symptoms of depression.

Interestingly, peripheral administration of KYN has been shown to induce depressive behaviour in laboratory animals, indicating that TRP and serotonin depletion may not solely be responsible for depressed mood and that KYN and its neuroactive metabolites may have a strong independent effect too (341-343).

1.9.5 Tryptophan Metabolism and Cognitive Impairment in HIV-1

Several studies have demonstrated that TRP depletion results in CI. In healthy controls, diet-induced TRP depletion has been shown to impair learning on visual discrimination and memory retrieval (344), episodic memory (342), stimulus-reward learning (344), and cognitive flexibility (345), among other cognitive processes (295), possibly via serotonergic dysfunction (301, 346).

Fuchs *et al*. first demonstrated an association between lower plasma TRP concentrations and HAD in three PLWH (347). Later, Huengsberg *et al*. explored the relationship TRP and KYN concentrations and the KYN/TRP ratio in plasma with various stages of HIV infection (n=206) compared with an HIV- control group (n=72). Only 53 subjects received AZT therapy during the course of the study, 23 of which also took ddC or ddI at some point. Asymptomatic HIV+ subjects with no signs of HAD (n=82) had significantly higher median KYN/TRP ratios than HIV- controls. Subjects with AIDS with no neurological complications (n=12), as well as subjects with AIDS with either peripheral neuropathy or HAD (n=10) had significantly higher median KYN/TRP ratios than both the HIV- controls and the asymptomatic HIV+ subjects. Changes in

the ratio were driven by both a reduction in TRP concentrations and increases in KYN concentrations. In 15 subjects who were receiving therapy and who had KYN/TRP ratio data available, the median KYN/TRP ratio did not significantly change upon initiation therapy (348).

In a recent retrospective, cross-sectional analysis of CSF samples from subjects with primary HIV infection (PHI; n=84) and chronic infection (n=235) and HIV- controls (n=22), Grill *et al.* reported untreated HIV-infection to be associated with higher KYN/TRP ratios compared to treated individuals (238). Subjects with more severe CI (n=264; from both the PHI and chronic infection groups) displayed markedly elevated phenylalanine-to-tyrosine (PHE/TYR) ratios compared to HIV- controls.

In a related study, Calcagno *et al*. determined plasma and CSF concentrations of NEO, BH_4, di-hydrobiopterin (BH_2), 5-HIAA and HVA in ART-naïve (n=25) or ART-treated (n=24) PLWH (305). A full battery of neuropsychological tests was administered to 26 subjects (normal=11; ANI=10; MND=4; and HAD=1). Plasma BH4 was observed to be significantly lower in subjects with CI and a trend towards lower CSF 5-HIAA concentrations in treated subjects with CI was observed.

Increased CSF QUIN concentrations are correlated with the severity of HIV-related CNS disease. One small study showed that increased levels of QUIN confer an increased risk of HIV-related CNS disease through increased psychomotor slowing (349). Increased concentrations of 3-HK have been found in post-mortem frontal cortex samples of HIV+ subjects compared to HIV- controls, with the increases being greater in subjects with HAD (350). Little is known about the role of 3-HAA in HIV disease.

In a study of post-mortem human brain tissue from 25 subjects with HIV-1, KYNA levels were found to be increased in the frontal cortex and cerebellum compared to HIV- controls (351). In addition, KAT-I enzyme activity was markedly increased in both brain areas. A mild increase in KAT-II activity was observed in the frontal cortex only. However, in a small clinical study, CSF KYNA concentrations from PLWH with psychotic symptoms (n=8) were found to be significantly elevated compared with those from PLWH without psychiatric symptoms (n=14), which may be associated with NMDA receptor hypofunction (352).

1.10 Summary

The available data on the effects of tryptophan metabolism on cognitive performance and mood disorders in PLWH are not conclusive. Studies in subjects who are virologically well-controlled on modern ARV agents are lacking, as are data on the effects of the ARVs themselves. The aim of this PhD is to determine whether chronic immune activation in PLWH leads to alterations in TRP metabolism and whether these are associated with CI and depressed mood.

The hypotheses for these research projects are:

- TRP metabolism is increased in the presence of the HIV-1 virus or ARV agents.

- Increased TRP metabolism is associated with poorer cognitive performance and increased rates of depression in PLWH.

2 LABORATORY MATERIALS AND METHODS

2.1 *In Vitro* Studies

2.1.1 Materials

2.1.1.1 Chemicals and Reagents

Lymphocyte separation medium-1077, Roswell Park Memorial Institute (RPMI) 1640 medium, fetal bovine serum (FBS) 10%, and a combination of penicillin 100 U/ml, streptomycin 0.1 mg/ml and L-glutamine 2mM (Pen-Strep-Glut) were all purchased from PAA GmbH, Pasching, Austria (www.paa.com).

Dulbecco's Modified Eagle's Medium (DMEM) was purchased from Sigma-Aldrich Company Ltd, Dorset, UK (https://www.sigmaaldrich.com/united-kingdom.html). Eagle's Minimum Essential Medium (EMEM) was purchased from LGC Standards, Middlesex, UK (https://www.lgcstandards-atcc.org).

BEGM™ Bronchial Epithelial Cell Growth Medium was purchased from Lonza Sales AG, Warsaw, Poland (https://www.lonza.com). O-phosphorylethanolamine, human epidermal growth factor (hEFG), fibronectin bovine plasma, collagen solution from bovine skin 6 mg/ml and trypsin inhibitor solution were all purchased from Sigma-Aldrich Company Ltd, Dorset, UK (https://www.sigmaaldrich.com/united-kingdom.html). Trypsin-EDTA 0.05% phenol red solution was purchased from Gibco (Fisher Scientific UK Ltd.), Loughborough, UK (https://www.fishersci.co.uk/gb/en/home.html).

Recombinant human IFN-γ protein 100 μg lyophilized powder was purchased from R&D Systems, Minneapolis, MN, USA (www.rndsystems.com).

Dimethyl Sulfoxide (DMSO) ≥99.9% was purchased from Sigma-Aldrich Company Ltd, Dorset, UK (https://www.sigmaaldrich.com/united-kingdom.html).

Pure substance powder forms of abacavir, lamivudine, zidovudine and dolutegravir were provided free of charge under a material transfer agreement by GlaxoSmithKline Research & Development Ltd (https://www.gsk.com). Pure substance powder forms of emtricitabine, tenofovir, darunavir, ritonavir, atazanavir, efavirenz, nevirapine, etravirine, rilpivirine, raltegravir, elvitegravir and maraviroc were purchased from the Health Protection Agency's (HPA) National Institute for Biological Standards and Control (NIBSC), Hertfordshire, UK (http://www.nibsc.org).

2.1.1.2 HIV-1

The HIV-1_{MN} virus (previously known as HTLV-$III_{MN/H9}$) was used for all of the *in vitro* experiments detailed in this chapter. HIV-1_{MN} is a laboratory-adapted, Clade B, CXCR4 tropic virus that is grown in an H9 CL.4 T cell line sourced from the NIH AIDS Research & Reference Reagent Program, Bethesda, MD, USA (https://www.aidsreagent.org). HIV-1_{MN} was added at 1.3 x 10^9 RNA cps/mL at the quantities described in Section 2.2, below.

2.1.1.3 Cells

Whole blood was drawn from healthy donors in 10 mL aliquots from within the Immunology Section at the Chelsea & Westminster Hospital, London, UK. Due to an insufficient number of donors, additional 10 mL cones of whole blood were purchased from the National Health Service (NHS) Blood and Transplant Service, Hertfordshire, UK (https://www.nhsbt.nhs.uk). Peripheral blood mononuclear cells (PBMCs) were then isolated using the methodology described in Section 2.2.1, below.

THLE2 and THLE3 hepatocyte cell lines, U87MG and U373MG astroglioma cell lines, and EOC13.31 and EOC20 microglial cell lines were purchased from ATCC in association with LGC Standards, Middlesex, UK (https://www.lgcstandards-atcc.org).

2.1.2 Methods

2.1.2.1 Determining Changes in Tryptophan Metabolism Following Acute Exposure of Peripheral Blood Mononuclear Cells to Zidovudine and Stavudine

The cell growth medium was prepared by mixing RPMI 1640 medium 500 mL with 50 mL FBS (10%) and 5 mL Pen-Strep-Glut (1%). The DMSO 0.01% control solution was prepared by mixing 10 μL DMSO and 5 mL of medium. AZT and d4T were each solubilised in DMSO 0.01% in medium and then diluted with RPMI 1640 medium and FBS 10% to give the following final concentrations in culture: 200 μM; 20 μM; 2 μM; 0.2 μM; 0.02 μM; and 0.002 μM.

Peripheral blood draws of 10 mL were taken from three healthy donors and collected into BD vacutainer lithium heparin tubes (Becton Dickinson, Oxford, UK, http://www.bd.com/en-uk). Three additional 10 mL component donation leucocyte cones of whole blood were sourced from the NHS Blood & Transplant Service. A minimum of $20x10^6$ PBMCs was isolated from each sample by density gradient centrifugation using lymphocyte separation medium-1077 and resuspended at $4x10^6$ cells/mL in medium consisting of RPMI 1640, 10% FBS, and 1% Pen-Strep-Glut (353, 354).

Four control conditions were prepared. The first control condition was prepared by mixing 750 μL medium solution and 250 μL PBMC solution. The second control condition was prepared by mixing 500 μL DMSO 0.01% solution, 250 μL medium solution and 250 μL of PBMC solution. The third control condition was prepared by mixing 500 μL medium solution, 250 μL PBMC solution and 250 μL of the HIV-1_{MN} 1.3 x 10^9 RNA cps/mL solution. The final control condition was prepared by mixing 500 μL DMSO 0.01% solution, 250 μL PBMC solution and 250 μL of the HIV-1_{MN} 1.3 x 10^9 RNA cps/mL solution. An experimental condition of AZT was prepared as described in Section 2.2.1.1 and mixed with 250 μL PBMC solution to give a final AZT concentration of 200 μM. Additional conditions were prepared by mixing 250 μL PBMC solution and 250 μL HIV-1_{MN} 1.3 x 10^9 RNA cps/mL solution with AZT solution to give final AZT concentrations of 200 μM; 20 μM; 2 μM; 0.2 μM; 0.02 μM; and 0.002 μM. This process was repeated for d4T.

PBMCs were cultured in 96 well plates overnight at 37°C with 5% CO_2. Cell supernatants were collected the next day and frozen at -80°C before being shipped to the Centre for Chemistry

and Biomedicine at Innsbruck Medical University, Innsbruck, Austria (https://biocenter.i-med.ac.at), for analysis. TRP, KYN, NEO and nitrite concentrations were analysed using the methodologies described in Section 2.3. KYN/TRP ratios were also calculated. This was kindly performed by Professor Dietmar Fuchs (Division of Biological Chemistry Biocentre, Innsbruck Medical University, Austria).

2.1.2.2 Determining Changes in Tryptophan Metabolism Following Acute Exposure of Peripheral Blood Mononuclear Cells to Commonly-Used Antiretroviral Agents

In this experiment, the following commonly-used ARVs were investigated: AZT, d4T, 3TC, FTC, ABC, TDF, EFV, RPV, ETV, NVP, DTG, RAL, EVG, MVC, DRV, RTV and ATV. ARVs were solubilized in DMSO 0.01% solution and diluted with RPMI 1640 medium and FBS 10% to give a final concentration in culture of 1mM. Due to solubility issues, DTG, RAL and TDF were diluted to give a final concentration of 0.5mM in culture.

Peripheral blood draws of 10 mL were taken from three healthy donors. Lymphocyte separation was conducted as per Section 2.2.1, above.

Two control conditions were prepared. The first control condition was prepared by mixing 500 μL DMSO 0.01% solution, 250 μL medium solution and 250 μL of PBMC solution. The second control condition was prepared by mixing 500 μL DMSO 0.01% solution, 250 μL PBMC solution and 250 μL of the HIV-1_{MN} 1.3 x 10^9 RNA cps/mL solution. The experimental conditions were prepared by mixing 250 μL PBMC solution and 250 μL HIV-1_{MN} 1.3 x 10^9 RNA cps/mL solution with the ARV solutions described above.

PBMCs were cultured in 96 well plates overnight at 37°C with 5% CO_2. Cell supernatants were collected the next day and frozen at -80°C before being shipped to the Centre for Chemistry and Biomedicine at Innsbruck Medical University, Innsbruck, Austria (https://biocenter.i-med.ac.at), for analysis. TRP and KYN concentrations were analysed using the methodologies described in Section 2.3. KYN/TRP ratios were also calculated. This was kindly performed by Professor Dietmar Fuchs (Division of Biological Chemistry Biocentre, Innsbruck Medical University, Austria).

2.1.2.3 Determining Changes in Tryptophan Metabolism Following Acute Exposure of Peripheral Blood Mononuclear Cells to Commonly-Used Antiretrovirals Individually and in Clinically-Relevant Combinations

The following ARVs were solubilized in DMSO 0.01% solution and diluted with RPMI 1640 medium and FBS 10% to give a final concentration in culture of 1mM: 3TC, FTC, ABC, EFV, RPV and ETV. Due to solubility issues, DTG, RAL and TDF were diluted to give a final concentration of 0.5mM in culture. In addition, for this experiment, combinations of ARVs were mixed so that they matched the ARV regimens used in the SSAT056 and CIIS clinical studies detailed in Chapter 3. These were: ABC+3TC+EFV; TDF+FTC+EFV; ABC+3TC+DTG; TDF+FTC+DTG; ABC+3TC+RAL; and TDF+FTC+RAL. They were diluted to give the same final concentrations in culture as the individual agents described above (i.e. either 1mM or 0.5 mM; see Table 2.1). Additionally, the same ARVs and ARV combinations were also solubilised and diluted to lower, clinically-relevant concentrations so that final culture concentrations approximated their reported C_{max} in plasma (references provide in Table 2.1). Both sets of concentrations are listed in Table 2.1, below. Two additional ARVs, RPV and ETV, were also included. RPV was included on the basis that it was observed to have an effect on KYN concentrations and the KYN/TRP ratio (Chapter 4). ETV was included because it was trending towards a having a significant effect on KYN concentrations and the KYN/TRP ratio (Chapter 4).

Peripheral blood draws of 10 mL were taken from three healthy donors. Lymphocyte separation was conducted as per Section 2.2.1, above.

Two control conditions were prepared. The first control condition was prepared by mixing 500 μL DMSO 0.01% solution, 250 μL medium solution and 250 μL of PBMC solution. The second control condition was prepared by mixing 500 μL DMSO 0.01% solution, 250 μL PBMC solution and 250 μL of the HIV-1_{MN} 1.3 x 10^9 RNA cps/mL solution. The experimental conditions were prepared by mixing 250 μL PBMC solution and 250 μL HIV-1_{MN} 1.3 x 10^9 RNA cps/mL solution with the ARV solutions described above (see Table 2.1).

Table 2.1. Antiretroviral Agent Concentrations Investigated

Antiretroviral Agent	High Concentration (mM)	Low Concentration (µg/mL)	Reference
DTG	0.5	3.67	(355)
ABC	1	4.26	(356)
3TC	1	2	(357)
EFV	1	4.07	(358)
FTC	1	1.8	(359)
RAL	0.5	2.17	(360)
TDF	0.5	0.326	(361)
ETV	1	0.8	(362)
RPV	1	0.2	(363)

Key: DTG, dolutegravir; ABC, abacavir; 3TC, lamivudine; EFV, efavirenz; FTC, emtricitabine; RAL, raltegravir; TDF, tenofovir; ETV, etravirine; RPV, rilpivirine.

PBMCs were cultured in 96 well plates overnight at 37°C with 5% CO_2. Cell supernatants were collected the next day and frozen at -80°C before being shipped to the Centre for Chemistry and Biomedicine at Innsbruck Medical University, Innsbruck, Austria (https://biocenter.i-med.ac.at), for analysis. TRP, KYN, PHE, TYR, and NEO concentrations were analysed using the methodologies described in Section 2.3. KYN/TRP and PHE/TYR ratios were also calculated. This was kindly performed by Professor Dietmar Fuchs (Division of Biological Chemistry Biocentre, Innsbruck Medical University, Austria).

2.1.2.4 Determining the Effects on Tryptophan Metabolism Following Acute Exposure of Hepatocytes, Astrocytes and Microglia to Commonly-Used Antiretrovirals Individually and in Clinically-Relevant Combinations

The THLE2, THLE3, U87, U373, EOC13.31 and EOC20 cells were cultured according to the manufacturers' specifications. These are summarised below.

THLE2 and THLE3 Hepatocyte Culture

A complete growth medium kit (BEGM Bullet Kit, CC3170; BEGM from Lonza/Clonetics Corporation, Walkersville, MD, USA) was supplied with the THLE2 and THLE3 cells. The kit includes 500 mL basal medium and separate frozen additives from which

gentamycin/amphotericin (GA) and epinephrine had been discarded and an extra 5 ng/mL EGF, 70 ng/mL phosphoethanolamine and 10% fetal bovine serum had been added.

Seventy-five cm^2 flasks were precoated with a mixture of 0.01 mg/mL fibronectin, 0.03 mg/mL bovine collagen type I and 0.01 mg/mL bovine serum albumin dissolved in BEBM medium. The culture medium was removed and discarded. The cell layer was briefly rinsed with 0.05% (w/v) Trypsin-0.53% (w/v) EDTA solution to remove all traces of serum containing trypsin inhibitor. Two to 3 mL of Trypsin-EDTA solution was added to the flask and the cells were observed under an inverted microscope until the cell layer dispersed, which took approximately 5 to 15 minutes). 0.1% Soybean Trypsin inhibitor was added and the cells were aspirated by gently pipetting. To remove trypsin-EDTA solution, the cell suspension was transferred to a centrifuge tube and spun at approximately 125 x g for 10 minutes. The supernatant was discarded and the cells were resuspended in fresh growth medium. Cell suspension was added to new coated culture vessels and incubated at 37°C with 5% CO_2. The medium was renewed every two to three days until the cells had grown to 80 to 100% confluence.

U87 and U373 Astroglioma Culture

Eagle's Minimum Essential Medium was used as the base medium with fetal bovine serum added to make a final concentration of 10%.

All culture medium was discarded and the cell layer was briefly rinsed with 0.05% (w/v) Trypsin-0.53% (w/v) EDTA solution to remove all traces of serum containing trypsin inhibitor. Two to 3 mL of Trypsin-EDTA solution was added to the flask and the cells were observed under an inverted microscope until the cell layer dispersed, which took approximately 5 to 15 minutes). Two to 3 mL of complete growth medium was added and the cells were aspirated by gently pipetting. The cell pellet was resuspended in fresh growth medium and the cell suspension was added to new culture vessels and incubated at 37°C with 5% CO_2. The medium was renewed every two to three days until the cells had grown to 80 to 100% confluence.

EOC13.31 and EOC20 Microglial Culture

A complete growth medium kit was supplied containing Dulbecco's modified Eagle's medium with 4 mM L-glutamine adjusted to contain 1.5 g/L sodium bicarbonate, and 4.5 g/L glucose, 70% and 10% fetal bovine serum.

Seventy-five percent of the culture medium was removed. The cells were scraped using the provided cell scraper. The cell suspension was added to new 75 cm^2 culture vessels and incubated at 37°C with 5% CO_2. The medium was renewed every two to three days until the cells had grown to 80 to 100% confluence.

Medium and DMSO control solutions were prepared as previously described (Section 2.2.1). An additional control solution consisting of DMSO and IFN-γ was prepared to use as a positive control to ensure that the cell lines of interest were expressing the KYN pathway. Due to the paucity of information on the use of IFN-γ for the stimulation of IDO in these cell types, three different concentrations of IFN-γ were used to ensure that there was a positive control. Human IFN-γ was used for the human-derived cell lines (i.e. THLE2, THLE3, U87 and U373) and murine IFN-γ was used for the murine cell lines (i.e. EOC13.31 and EOC20). The three final IFN-γ concentrations in cell culture consisting of 500 μL DMSO 0.01% solution, 250 μL PBMC solution and 250 μL of the HIV-1_{MN} 1.3 x 10^9 RNA cps/mL solution were 0.2 μg/mL, 1 μg/mL and 5 μg/mL.

The ARVs TDF, 3TC, FTC, ABC, DTG, RAL, EFV, RPV and ETV were solubilized in DMSO 0.01% solution and diluted with RPMI 1640 medium and FBS 10% to give the final clinically-relevant concentrations in culture that approximate their reported C_{max} in plasma, as described in Table 2.1. In addition, combinations of ARVs (i.e. ABC+3TC+EFV; TDF+FTC+EFV; ABC+3TC+DTG; TDF+FTC+DTG; ABC+3TC+RAL; and TDF+FTC+RAL) were mixed so that they matched the ARV regimens used in the SSAT056 and CIIS clinical studies detailed in Chapter 3. They were diluted to give the same final clinically-relevant concentrations in culture as the individual agents described above (see Table 2.1).

Each of the different cell lines were cultured in the control and ARV solutions in 96 well plates overnight at 37°C with 5% CO_2. Cell supernatants were collected the next day and frozen at -80°C before being shipped to the Centre for Chemistry and Biomedicine at Innsbruck Medical

University, Innsbruck, Austria (https://biocenter.i-med.ac.at), for analysis. TRP, KYN, PHE, TYR, and NEO concentrations were analysed using the methodologies described in Section 3.3. KYN/TRP and PHE/TYR ratios were also calculated. This was kindly performed by Professor Dietmar Fuchs (Division of Biological Chemistry Biocentre, Innsbruck Medical University, Austria).

2.1.3 Analysis of Cell Supernatants

Supernatants were shipped to the Centre for Chemistry and Biomedicine at Innsbruck Medical University, Innsbruck, Austria (https://biocenter.i-med.ac.at), for analysis, as described below. This was kindly performed by Professor Dietmar Fuchs (Division of Biological Chemistry Biocentre, Innsbruck Medical University, Austria). The raw results data were returned for analysis.

Supernatant concentrations of TRP, KYN, PHE and TYR were measured by high performance liquid chromatography (HPLC) by two methods using the Prostar 210 solvent delivery system (Agilent Technologies Inc., Santa Clara, CA) (364). Sample injection was controlled by a Prostar 400 autosampler, a ProStar 360 fluorescence detector and a ProStar 325 ultraviolet detector (Agilent). Separation was accomplished at room temperature using a reversed-phase LiChroCART 55-4 mm cartridge (Merck, Darmstadt, Germany), filled with Purosphere STAR RP18 (3 µm grain size, Merck) together with a reversed-phase C_{18} pre-column (Merck). Before HPLC, serum protein was precipitated with 0.015mM trichloroacetic acid. For both measurements L-nitro-tyrosine is used as an internal standard and monitored at the 360 nm wavelength.

TRP and KYN concentrations were measured in one chromatographic run using dihydrogen-phosphate solution for separation on reversed-phase C_{18} material with mobile phase 0.015 M sodium acetate/acetic acid (pH = 4) + 5% methanol and with the fluorescence detector set at 285 nm excitation and 360 nm emission wavelengths. UV absorption to detect KYN and L-nitrotyrosine concentrations was measured at the 360nm wavelength (364, 365). For PHE and TYR measurements the mobile phase was aqueous 15 mM KH_2PO_4, at a flow rate of 0.9 mL/min, with the fluorescence detector set at 210 nm excitation and 302 emission wavelengths (366). UV absorption to detect L-nitrotyrosine concentrations was measured at

the 360nm wavelength (see above). Within-run and between run coefficients of variance (CVs) are all <5% for all analytes (365).

The ratios of KYN/TRP and PHE/TYR were calculated as indexes of IDO-1 and PAH activity, respectively (174, 303, 347).

Neopterin concentrations were measured by enzyme-linked immunosorbent assay (BRAHMS Diagnostics, Berlin, Germany) following the manufacturers protocol (sensitivity 2 nmol/L).

For an estimate of nitrous oxide (NO) production, the stable NO metabolite nitrite (NO_{2^-}) was determined in the cell-free culture supernatants by the Griess reaction assay (Promega, Madison, Wisconsin) (367, 368) whereby sulfanilamide was quantitatively converted to a diazonium salt by reaction with NO2- in phosphoric acid conditions. The diazonium salt was then coupled to N(1-naphthyl) ethylenediamine dihydrochloride, forming an azo dye that was read at 540nm in a spectrophotometer and calculated by external standardization.

2.1.4 Statistical Analysis

For each of the experiments, all culture conditions were compared with the DMSO reference condition using a non-parametric Friedman test. Due to the low sample numbers and multiple comparisons performed for each experiment, the Friedman test was first performed without applying a correction for multiplicity with the alpha set at 0.05, thus ensuring that associations of interest were not missed. The Friedman's test was then re-run for all comparisons using Dunn's correction for multiplicity to see whether any of the preliminary observations remained statistically significant. Both sets of results are presented in Chapter 4.

2.2 Clinical Studies

2.2.1 Analysis of Cerebrospinal Fluid and Plasma Samples

Plasma and CSF samples were shipped to the Centre for Chemistry and Biomedicine at Innsbruck Medical University, Innsbruck, Austria (https://biocenter.i-med.ac.at), for analysis,

as described below. This was kindly performed by Professor Dietmar Fuchs (Division of Biological Chemistry Biocentre). The raw results data were returned for analysis.

Plasma and CSF concentrations of TRP, KYN, PHE and TYR were measured by high performance liquid chromatography (HPLC) by two methods using the Prostar 210 solvent delivery system (Agilent Technologies Inc., Santa Clara, CA) (364). Sample injection was controlled by a Prostar 400 autosampler, a ProStar 360 fluorescence detector and a ProStar 325 ultraviolet detector (Agilent). Separation was accomplished at room temperature using a reversed-phase LiChroCART 55-4 mm cartridge (Merck, Darmstadt, Germany), filled with Purosphere STAR RP18 (3 µm grain size, Merck) together with a reversed-phase C_{18} pre-column (Merck). Before HPLC, serum protein was precipitated with 0.015mM trichloroacetic acid. For both measurements L-nitro-tyrosine is used as an internal standard and monitored at the 360 nm wavelength.

TRP and KYN concentrations were measured in one chromatographic run using dihydrogen-phosphate solution for separation on reversed-phase C_{18} material with mobile phase 0.015 M sodium acetate/acetic acid (pH = 4) + 5% methanol and with the fluorescence detector set at 285 nm excitation and 360 nm emission wavelengths. UV absorption to detect KYN and L-nitrotyrosine concentrations was measured at the 360nm wavelength (364, 365). For PHE and TYR measurements the mobile phase was aqueous 15 mM KH_2PO_4, at a flow rate of 0.9 mL/min, with the fluorescence detector set at 210 nm excitation and 302 emission wavelengths (366). UV absorption to detect L-nitrotyrosine concentrations was measured at the 360nm wavelength (see above). Within-run and between run coefficients of variance (CVs) are all <5% for all analytes (365).

The ratios of KYN/TRP and PHE/TYR were calculated as indexes of IDO-1 and PAH activity, respectively (174, 303, 347).

Neopterin concentrations were measured by enzyme-linked immunosorbent assay (BRAHMS Diagnostics, Berlin, Germany) following the manufacturers protocol (sensitivity 2 nmol/L).

For an estimate of nitrous oxide (NO) production, the stable NO metabolite nitrite (NO_{2^-}) was determined in the cell-free culture supernatants by the Griess reaction assay (Promega, Madison, Wisconsin) (367, 368) whereby sulfanilamide was quantitatively converted to a

diazonium salt by reaction with NO2- in phosphoric acid conditions. The diazonium salt was then coupled to N(1-naphthyl) ethylenediamine dihydrochloride, forming an azo dye that was read at 540nm in a spectrophotometer and calculated by external standardization.

IFN-γ and TNF-α were quantified using the commercially available Human TNF-alpha Quantikine ELISA Kit (DTA00C; sensitivity 5.5 pg/mL) and the Human IFN-gamma Quantikine ELISA (DIF50; sensitivity 8 pg/mL), respectively (both from R&D Systems, Minneapolis, MN), using the manufacturers protocol. The majority of IFN-γ samples obtained were below the limit of detection and so this parameter was excluded from further analyses.

3 MATERIALS AND METHODS – CLINICAL STUDIES

3.1 A Cross-Sectional, Clinical, Pilot Study To Investigate Tryptophan Metabolism in People Living with HIV from the CHARTER Cohort

3.1.1 Background and Study Design

The CNS HIV Antiretroviral Therapy Effects Research (CHARTER) study was commissioned in 2002 by the National Institute of Mental Health and the National Institute of Neurological Diseases and Stroke to explore the changing presentation of HIV neurological complications and their relationship with emerging antiviral treatments, such as combination ART (https://charternntc.org/about) (95). In order to have a broad representation of participant characteristics, the CHARTER cohort consisted of nearly 1600 PLWH and the study was conducted at six sites nationally whose activities were coordinated by the University of California, San Diego (https://ucsd.edu). The five additional sites participating are: Johns Hopkins University, Baltimore, MD; Icahn School of Medicine at Mount Sinai, New York City, NY; University of Texas Medical Branch, Galveston, TX; University of Washington, Seattle, WA; and Washington University, St. Louis, MO. This afforded the ascertainment of the frequency and severity of HIV-related CNS disease in the US, as well as the specific contributions of HIV vs other factors (e.g. comorbidities, ARV toxicity and genetics) to CI.

In a cross-sectional baseline analysis of the study's participants (N=1555), 52% of the total sample were observed to have CI, with higher rates in groups with greater comorbidity burden. Excluding severely confounded cases, the prevalence estimates for CI diagnoses using the Frascati Criteria (102) were 33% for ANI, 12% for MND, and 2% for HAD (95). At baseline, 15% of subjects were ART-naive, 14% had received prior ART only, and 71% were receiving ART consisting primarily of either PI- or NNRTI-based regimens. Integrase inhibitors and the CCR5 antagonist maraviroc, were not available at this time. In those receiving ART, HIV-1-RNA was detectable in plasma and CSF in 44% and 16% of subjects, respectively, indicating that a large proportion of subjects were not well-controlled on therapy.

Prof Ron Ellis and Prof Scott Letendre designed a cross-sectional analysis of historical case notes and archived CSF and plasma samples collected from HIV+ and HIV- individuals. These samples were analysed as described in Section 3.1.7, below, by Prof Dietmar Fuchs from the Centre for Chemistry and Biomedicine at Innsbruck Medical University, Innsbruck, Austria (https://biocenter.i-med.ac.at). I was invited to join the study and my involvement was to prepare the statistical analysis plan and run and interpret the analysis.

3.1.2 Study Objectives & Endpoints

3.1.3 Patient Selection

Study participant case notes were selected from the University of California, San Diego's (UCSD) HIV Neurobehavioral Research Center-based projects, which had already been reviewed and approved by the UCSD's Human Subjects Protection Program (95, 369).

Eligible participants were adults who had tested positive for HIV-1 antibody, either with or without CI and/or MDD. An HIV- control group with or without CI and/or MDD were also selected. HIV+ individuals and HIV- controls were matched for gender only. Specific exclusion criteria included a history of pre-HIV-1 infection MDD, acute HIV infection, active opportunistic infection, a history of head trauma associated with neurological complications, and those older than 50 years of age (older age is associated with lower TRP levels).

3.1.4 Clinical Examination

All participants had previously received a comprehensive medical examination, which included an assessment of HIV disease consisting of measurement of HIV-1 RNA in CSF and plasma, current and nadir CD4+ cell count, and ART characteristics.

3.1.5 Neuropsychological and Neuropsychiatric Testing

3.1.5.1 Assessment of Depression

All participants had undergone previous comprehensive psychiatric and neuropsychological evaluation. Diagnostic and Statistical Manual-Fourth Edition (DSM-IV) (103) diagnoses for

current and lifetime MDD had been determined using the World Health Organizations (WHO) Composite International Diagnostic Interview (CIDI) (370).

3.1.5.2 Assessment of Cognitive Function

Cognitive performance had been determined using a comprehensive battery of tests covering seven ability domains, including learning, memory, attention/working memory, verbal fluency, processing speed, executive functioning, and motor speed. Raw test scores were converted into demographically-adjusted T-scores and used to derive domain and global deficit scores (GDS), ranging from 0 (no impairment) to 5 (severe impairment) (371). A GDS greater than or equal to 0.5 was used to classify CI (94, 103). All staff administering these tests were certified according to standardized procedures at their entry into the workforce and periodically recertified. No deviations in testing for MDD or CI were detected in the patient notes.

3.1.6 Laboratory Procedures

Plasma and CSF samples were shipped to the Centre for Chemistry and Biomedicine at Innsbruck Medical University, Innsbruck, Austria (https://biocenter.i-med.ac.at), for analysis, as described in Section 2.2.1. This was kindly performed by Professor Dietmar Fuchs (Division of Biological Chemistry Biocentre). The raw results data were returned for analysis.

3.1.7 Statistical Methodology

Statistical analyses were performed with IBM's SPSS Software Version 21. The results were subjected to tests of the normal distribution. Non-parametric tests were selected for use due to skewed distributions in the data.

Univariate analyses were conducted using Mann-Whitney *U* tests and Chi-square tests for independence to look for differences in baseline characteristics between the HIV+ and HIV- groups, and between the HIV+ individuals receiving ART and those not receiving ART. Comparisons of the biochemical and immunological markers in CSF and plasma between the HIV+ and HIV- groups, and between the sub-group of HIV+ individuals who were taking

virologically suppressive ART (n=44) and the HIV- group were made using Mann-Whitney *U* tests. Initially, the alpha for the Mann-Whitney *U* tests was set at 0.05 as these were exploratory analyses. Bonferroni corrections were also applied to account for multiplicity.

Multivariate linear regression analysis exploring the relationship between TNF-α and NEO with the clinically relevant covariates HIV-1 RNA in CSF and plasma (≤ or >50 cps/mL), current CD4+ cell count, and ART-use. In order to understand whether an association exists between the inflammatory biomarkers and TRP metabolism, the relationship between TNF-α and NEO and the KYN/TRP ratio in CSF and plasma from HIV+ individuals was analysed in a second multivariate model.

To explore the relationship between TRP metabolism via the KYN pathway and neuropsychiatric outcomes, logistic regression analyses were performed for the KYN/TRP ratio in both CSF and plasma and either binary MDD or CI status. Due to the number of comparisons performed, Bonferroni were applied to the final multivariate analyses exploring the depressive and cognitive parameters.

To account for the potential confounding effects of the use of antidepressant agents in some patients, Mann-Whitney *U* tests were performed to determine whether there was a correlation between the use of antidepressant medication and TRP, KYN and the KYN/TRP ratio. These were performed for the overall HIV+ group, as well as for patients with either HIV-1-RNA >50 cps/mL or ≤50 cps/mL in both CSF and plasma.

3.2 A Prospective, Open-Label, Clinical Study to Assess the Effects of Switching from Efavirenz to Dolutegravir on Tryptophan Metabolism in Virologically-Suppressed People Living with HIV (The SSAT056 Study)

3.2.1 Background

St Stephen's AIDS Trust (SSAT) is a clinical research organization based at the Chelsea & Westminster Hospital, London (http://www.ssat.org.uk). The SSAT056 study was designed and run by Prof Mark Nelson and the clinical research team at SSAT. Prof Nelson very kindly

agreed to modify the study to include the analysis of TRP and associated biomarkers in plasma. I helped write the study protocol and procured additional funding for shipping, storage and analysis of the samples. The plasma samples were analysed as described in Section 3.2.8, below, by Prof Dietmar Fuchs from the Centre for Chemistry and Biomedicine at Innsbruck Medical University, Innsbruck, Austria (https://biocenter.i-med.ac.at). I also prepared the statistical analysis plan for the TRP analysis and ran and interpreted the statistical analysis.

3.2.2 Study Design

A prospective, randomised, open-label, multi-centre study, in which virologically-suppressed PLWH receiving two NRTIs plus efavirenz for ≥12 weeks who had reported experiencing ongoing CNS drug toxicity with EFV were enrolled, was conducted. Subjects were randomised to switch immediately to DTG 50 mg once daily (n=20) or have their switch delayed for 4 weeks (n=20), without NRTI change. Both groups were followed-up for a further 12 weeks. In this analysis for this PhD, the study arms were pooled and 'Baseline' was defined as the time of ART switch for all subjects.

The study assessments are detailed in the following sections, including a time and events schedule that is summarised in Table 3.2 (Section 3.2.9).

The study team complied with the ethical principles for medical research involving human subjects as defined by the World Medical Associations' Declaration of Helsinki. This study was reviewed and approved by the London Research Ethics Committee (REC reference 14/LO/1493, Date 31/10/2014; EudraCT number 2013-004729-94).

3.2.3 Study Objectives & Endpoints

3.2.3.1 Primary Objective

The primary objective of the study was to investigate whether switching individuals with CNS intolerance to EFV plus two NRTIs to DTG plus two NRTIs was associated with resolution of CNS toxicity at 4 weeks post-switch.

3.2.3.2 Secondary Objectives

Secondary objectives relating to this thesis included:

1. To investigate whether switching individuals with CNS intolerance to EFV plus two NRTIs to DTG plus two NRTIs was associated with resolution of CNS toxicity at 12 weeks post-switch.
2. To investigate the impact of switching from EFV to DTG on anxiety and depression as determined by the Hospital Anxiety and Depression Scale (HAD) over 12 weeks post-switch.
3. To investigate the impact of switching from EFV to DTG on quality of sleep as determined using the Pittsburgh Sleep Quality Index (PSQI) at 4 and 12 weeks post-switch.
4. To investigate the impact of switching from EFV to DTG on changes in neuropsychiatric function as determined by the CogState^{TM} battery of neuropsychological tests over 12 weeks post-switch.
5. To investigate the impact of switching from EFV to DTG on changes in neuropsychiatric function as determined by the International Activities of Daily Living (IADL) questionnaire over 12 weeks post-switch.
6. To investigate the impact of switching from EFV to DTG on plasma concentrations of TRP, KYN, and NEO, and the KYN/TRP ratio.
7. To investigate the relationship between plasma KYN concentrations and measures of CNS toxicity and CI at Baseline and 12 weeks post-switch.
8. To investigate the relationship between plasma KYN/TRP ratios and measures of CNS toxicity and CI at Baseline and 12 weeks post-switch.

3.2.3.3 Primary Endpoint

The primary endpoint of the study was the change in the rate of neuropsychiatric and CNS toxicities as measured using a questionnaire based on the EFV Summary of Product Characteristics (SPC) and graded based on the ACTG adverse events scale from Baseline to 4 weeks of post-switch.

3.2.3.4 Secondary Endpoints

The secondary endpoints related to this thesis included:

1. The change in the rate of neuropsychiatric and CNS toxicities as measured using a questionnaire based on the EFV Summary of Product Characteristics (SPC) and graded based on the ACTG adverse events scale from Baseline to 12 weeks post-switch.
2. The change in anxiety and depression scores as determined using the HAD scale from Baseline to 12 weeks post-switch.
3. The change in quality of sleep score as determined using the PSQI from Baseline to 4 and 12 weeks post-switch.
4. The change in neuropsychiatric function as determined using the CogState^{TM} score from Baseline to 12 weeks post-switch.
5. The change in neuropsychiatric function as determined using the IADL Questionnaire score over 12 weeks post-switch.
6. The change in plasma concentrations of TRP, KYN, and NEO, and the KYN/TRP ratio from Baseline to Weeks 4 and 12.
7. Assessment of the relationship between plasma KYN concentrations and measures of CNS toxicity and CI at Baseline and 12 weeks post-switch.
8. Assessment of the relationship between plasma KYN/TRP ratios and measures of CNS toxicity and CI at Baseline and 12 weeks post-switch.

3.2.4 Patient Selection

Forty HIV+ individuals receiving EFV-containing ART with a viral load <50 copies/mL and a CD4+ cell count >50 cells/mm^3, experiencing EFV-associated CNS-related toxicity after at least 12 weeks of therapy were recruited from four UK centres (Chelsea & Westminster Hospital London, Royal Sussex County Hospital Brighton, St Mary's Hospital London, Mortimer Market Centre London.)

Subjects were required to be of 18 years or older, currently receiving an ARV regimen comprising of at least three ARVs, one of which is EFV for at least 12 weeks, had no prior exposure to integrase inhibitors, and have HIV-1-RNA <50 c/mL.

3.2.5 Clinical Examination

Participants received a comprehensive medical examination, which included an assessment of HIV disease including a complete history and demographics, including ARV and allergy history, hepatitis B and C status, a symptom-directed physical examination, height and weight measurements, vital signs, urinalysis, electrocardiogram (ECG), concomitant medications, adverse events, haematology, biochemistry, current and nadir CD4+ cell count, and plasma HIV-1 RNA.

The time and events schedule for study assessments is summarised in Table 3.2 (Section 3.2.9).

3.2.6 Assessment of Central Nervous System Toxicity

Rates of CNS toxicities were measured at Baseline, Week 4 and Week 12 using a previously used questionnaire based on the EFV label and graded according to the ACTG adverse events scale (372). The questionnaire consisted of 10 sections specifically ascertaining the following symptoms: dizziness, depression, insomnia, anxiety, confusion, impaired concentration, headache, somnolence, aggression, and abnormal dreams. Each score ranged from 0 (none) to 3 (severe) with scores summed, giving a total score ranging from 0 to 30.

3.2.7 Neuropsychological and Neuropsychiatric Testing

3.2.7.1 Assessment of Anxiety and Depression

Anxiety and depression were assessed using the HAD Scale at Baseline, Week 4 and Week 12 (373). The HAD Scale is a short self-assessment scale consisting of 14 questions, seven of which relate to depression and seven of which related to anxiety. Assessment of the overall severity of each condition are rated in each question with scores ranging from 0 (none) to 4 (severe). Scores are summed for each condition with scores ranging from 0 to 7 indicating ‘non-cases’, scores of 8-10 indicating ‘doubtful cases’, and scores of 11 or more indicating ‘definite cases’. The individual subscale scores can then be summed to give an overall anxiety and depression score.

3.2.7.2 Assessment of Quality of Sleep

Quality of sleep was assessed using the PSQI at Baseline, Week 4 and Week 12 (374). The PSQI is a self-rated questionnaire that assesses sleep quality and disturbances over a one month period. It consists of 19 items that generate seven component scores, including subjective sleep quality, sleep latency, sleep duration, habitual sleep efficiency, sleep disturbances, use of sleeping medication, and daytime dysfunction. These scores are summed to provide a global sleep score.

3.2.7.3 Assessment of Cognitive Function

Cognitive function was assessed using both the CogState™ computerised cognitive test battery and the IADL questionnaire.

Cognitive function was assessed at Baseline, Week 4 and Week 12 using the CogState™ computerised cognitive test battery (CogState Ltd., www.cogstate.com, Melbourne, Australia) (375, 376). All tasks within the CogState™ battery are adaptations of standard neuropsychological and experimental psychological tests (Table 3.1), which assess a range of cognitive functions, including attention and psychomotor function (assessed via speed of test), executive function (assessed via the number of errors made on testing), and visual learning and working memory (assessed via accuracy of test). The battery consists of tasks in the form of card games. Therefore, subjects need only to have an understanding of playing cards, thereby minimising language and cultural differences among study subjects. All study participants completed one full practice test prior to undertaking the study examination to obtain optimal performance at baseline.

The Groton Maze Learning Test (GML) consisted of five learning rounds, the scores of which were combined to give a total GML score. The Set Shifting Test (SETS) consisted of six separate tests, the scores of which were combined to give a total SETS score.

Table 3.1. CogState™ Battery of Tests in the SSAT056 Study

Task Name	Cognitive Function Tested	Unit of Measurement	Description and Interpretation of Scores
Identification Task (IDN)	Attention	Log10 milliseconds	Speed of performance; mean of the log10 transformed reaction times for correct responses Lower score = better performance
Detection Task (DET)	Psychomotor function	Log10 milliseconds	Speed of performance; mean of the log10 transformed reaction times for correct responses Lower score = better performance
Groton Maze Learning Test (GML)	Executive function	Total number of errors	Total number of errors made in attempting to learn the same hidden pathway on five consecutive trials at a single session Lower score = better performance
Set Shifting (SETS)	Executive function	Total number of errors	Accuracy of performance; Total number of errors across all rounds (i.e. shifts) Lower score = better performance
One Card Learning (OCL)	Visual learning	Arcsine proportion	Accuracy of performance; arcsine transformation of the proportion of correct responses Higher score = better performance
One Back Memory (ONB)	Working memory - simple	Arcsine proportion	Accuracy of performance; arcsine transformation of the proportion of correct responses Higher score = better performance
Two Back Memory (TWOB)	Working memory - complex	Arcsine proportion	Accuracy of performance; arcsine transformation of the proportion of correct responses Higher score = better performance

The IADL questionnaire was used to assess the subjects ability to perform normal, everyday tasks, including using the phone, grocery shopping, food preparation, housekeeping, doing the laundry, use of transportation, their responsibility for their medications, and their ability to handle their finances at Baseline, Week 4 and Week 12 (377). The subject receives a score of one for each item if their competence is rated at some minimal level or higher. They receive a score of zero for each item that they are unable to perform. The scores are summed to give a total score ranging from 0 – 8. A lower score indicates a higher level of dependence on others.

3.2.8 Laboratory Procedures

Plasma concentrations of TRP, KYN and NEO were measured at Baseline, Week 4 and Week 12 using the same methodology as described in Section 2.2.1. This was kindly performed by Professor Dietmar Fuchs (Division of Biological Chemistry Biocentre). The KYN/TRP ratio was also calculated.

3.2.9 Time and Events Schedule

The time and events schedule for study assessments is summarised in Table 3.2, below. From the baseline visit through to the final study visit, visits may take place +/- 7 days from that specified at the discretion of the investigator. Questionnaires were completed at the beginning of each visit.

Table 3.2. Time and Events Schedule for SSAT056 Study Assessments

Procedure	Screening Up to -28 Days	Baseline Visit Day 1	Week 4 Visit	Week 12 Visit
Informed Consent	X			
Complete history & demographics, including ARV & allergy history	X			
Hepatitis B & C	X			
Physical examination[a]	X	X	X	X
Height	X			
Weight	X			X
Vital signs[b]	X	X	X	X
Urinalysis[c]	X	X	X	X
ECG	X			X
Concomitant medications	X	X	X	X
Non-CNS adverse events		X	X	X
Questionnaires (HAD, IADL, PSQI, CNS Toxicity)		X	X	X
CogState™	X	X	X	X
Haematology[d]	X	X	X	X
Biochemistry[e]	X	X	X	X
CD4+ cell count	X	X	X	X
Plasma HIV-1-RNA	X	X	X	X
Plasma TRP, KYN, NEO concentrations		X	X	X

[a] Symptom-directed; [b] Pulse, blood pressure, temperature; [c] Microanalysis and pregnancy test; [d] Haemoglobin, white cell count and differential and platelets; [e] Sodium, potassium, creatinine, albumin, glucose, alanine aminotransferase (ALT), alkaline phosphatase (ALP), total bilirubin, total cholesterol, HDL, LDL (where feasible), and triglycerides

3.2.10 Statistical Methodology

For the following analyses, the study arms were pooled and 'Baseline' was defined as the time of ART switch for all subjects.

Statistical analyses were performed with IBM's SPSS Software Version 23. The results were subjected to tests of the normal distribution. Parametric tests were selected because the data were normally-distributed.

Paired-samples *t*-tests were conducted to assess changes from baseline to Week 4, Week 4 to Week 12, and baseline to Week 12 for TRP, KYN and NEO concentrations, the KYN/TRP ratio, CNS toxicity scores, IADL scores, HAD scores (Total score, the Anxiety Score and the Depression Score), and PSQI scores.

To investigate the relationship between CNS toxicity scores and KYN concentrations and the KYN/TRP ratio, longitudinal random intercept models were constructed. The models' fixed effects were CNS toxicity (dependent variable) and KYN concentration (independent variable). The random effect, or intercept, was chosen to be the patient (i.e. Patient ID) and the repeated effect was Time (Baseline, and 4 and 12 Weeks). Maximum Likelihood estimation was selected. This model design was utilised again to investigate the relationship between the KYN/TRP relationship and CNS Toxicity. Bonferroni corrections were applied to each group of analyses to adjust the level of significance to account for multiplicity. Only the adjusted *p* values are shown.

Additional, exploratory, models were constructed and analysed to investigate the relationship between plasma KYN concentrations and the KYN/TRP ratio with HAD (Total, Anxiety and Depression) and PSQI scores. Bonferroni corrections were not applied to these analyses and only the unadjusted *p* values are shown.

For the cognitive testing, statistical analysis was conducted according to CogState™ recommendations. Reaction times were $\log^{10}$-transformed because of a positive skew of the distribution, and accuracy measures were transformed using arcsine transformation. Change scores were calculated for each subject, and these scores standardized according to the within-subject standard deviation (SD). Composite scores were calculated overall and for the

speed, accuracy and executive function domains based on the average of standardized scores, and composite changes from Baseline scores to Weeks 4 and 12 were calculated based on the average of standardized reaction time, accuracy and executive function scores. A global composite score (GCS) was calculated. Paired-samples *t*-tests were conducted to assess changes from Baseline to Week 4 and Week 12.

3.3 A Prospective, Open-Label, Clinical Study to Assess the Effects of Switching from Raltegravir to Dolutegravir on Tryptophan Metabolism in Virologically-Suppressed People Living with HIV (The CNS Integrase Inhibitor Study [CIIS])

3.3.1 Background

The Imperial College Clinical Trials Centre is a purpose-built centre in the UK for undertaking clinical trials in sexual health and HIV based at St Mary's Hospital, London (https://www.imperial.nhs.uk/our-services/sexual-health-and-hiv/research-and-clinical-trials). The CIIS study was designed and run by Prof Alan Winston and the clinical research team at the Imperial College Clinical Trials Centre. Prof Winston very kindly agreed to the use of stored plasma and CSF samples from the study to analyse TRP and associated biomarkers. Additional funding for shipping, storage and analysis of the samples was procured from ViiV Healthcare Ltd. The CSF and plasma samples were analysed as described in Section 3.3.8, below, by Prof Dietmar Fuchs from the Centre for Chemistry and Biomedicine at Innsbruck Medical University, Innsbruck, Austria (https://biocenter.i-med.ac.at). I prepared the statistical analysis plan for the TRP analysis and ran and interpreted the statistical analysis.

3.3.2 Study Design

A prospective, randomised, single-centre, clinical study was conducted to assess cerebral function parameters in HIV-infected subjects receiving two different integrase inhibitor-containing ARV regimens. Twenty-one HIV-infected subjects receiving a RAL-containing ARV regimen for at least 4 months were enrolled. Subjects were randomised on a 2:1 basis to switch their ART from RAL to DTG without NRTI backbone change or remain on their current

therapy. Cerebral function parameters were assessed using CogState™, cerebral magnetic resonance imaging and lumbar puncture testing.

The study assessments are detailed in the following sections, including a time and events schedule that is summarised in Table 3.4 (Section 3.3.9).

The study team complied with the ethical principles for medical research involving human subjects as defined by the World Medical Associations' Declaration of Helsinki. This study was reviewed and approved by the London Research Ethics Committee (EudraCT number 2014-003710-84).

3.3.3 Study Objectives & Endpoints

3.3.3.1 Study Objectives

The study objectives relating to this thesis included:

1. To investigate the impact of switching from RAL to DTG on neurocognitive function at 120 days post-switch as determined by the CogState™ battery of neuropsychological tests.
2. To investigate the impact of switching from RAL to DTG on neurocognitive function at 120 days post-switch as determined by the International Activities of Daily Living (IADL) questionnaire.
3. To investigate the impact of switching from RAL to DTG on depression at 120 days post-switch as determined by the Beck Depression Inventory (BDI).
4. To investigate the impact of switching from RAL to DTG on depression at 120 days post-switch as determined by the Patient Health Questionnaire-9 (PHQ-9).
5. To investigate the impact of switching from RAL to DTG on cerebral imaging markers at 120 days post-switch as determined by ^{1}H magnetic resonance spectroscopy (MRS).
6. To investigate the impact of switching from RAL to DTG on plasma and CSF concentrations of TRP, KYN, PHE, TYR, NEO, the KYN/TRP ratio and the PHE/TYR ratio at 120 days post-switch.
7. To investigate the relationship between plasma and CSF concentrations of TRP, KYN, PHE, TYR, NEO, the KYN/TRP ratio and the PHE/TYR ratio and neurocognitive function and MRS metabolite concentrations.

3.3.3.2 Study Endpoints

Study endpoints relating to this thesis included:

1. The change in neuropsychiatric function as determined using the CogState^{TM} score from Baseline to Day 120.
2. The change in neuropsychiatric function as determined using the IADL Questionnaire score from Baseline to Day 120.
3. The change in depression score as determined using the BDI from Baseline to Day 120.
4. The change in depression score as determined using the PHQ-9 from Baseline to Day 120.
5. The change in cerebral imaging markers as determined using MRS from Baseline to Day 120.
6. The change in plasma and CSF concentrations of TRP, KYN, PHE, TYR, NEO, the KYN/TRP ratio and the PHE/TYR ratio from Baseline to 120 days post-switch.
7. Assessment of the between plasma and CSF concentrations of TRP, KYN, PHE, TYR, NEO, the KYN/TRP ratio and the PHE/TYR ratio and neurocognitive function and MRS metabolite concentrations.

3.3.4 Patient Selection

Twenty-one HIV+ individuals receiving RAL-containing ART for at least 4 months, with a viral load <200 copies/mL were recruited from a single UK centre (St Mary's Hospital London). Subjects were required to be of 18 years or older, currently receiving an ARV regimen comprising of TDF/FTC with RAL 400 mg twice daily with no ARV drug switches in the last 3 months and have no prior exposure to DTG.

3.3.5 Clinical Examination

Participants received a comprehensive medical examination, which included an assessment of HIV disease including a complete history and demographics, including ARV history, a symptom-directed physical examination, height and weight measurements, urine test of drugs of abuse, electrocardiogram (ECG), concomitant medications, adverse events, haematology, biochemistry, current and nadir CD4+ cell count, and plasma HIV-1 RNA.

The time and events schedule for study assessments is summarised in Table 3.4 (Section 3.3.9).

3.3.6 Neuropsychological and Neuropsychiatric Testing

3.3.6.1 Assessment of Depression

Depression was assessed using the PHQ-9 questionnaire and BDI scores at Baseline and Day 120 (378-380).

The PHQ is a three-page questionnaire for diagnosing depression and other mental disorders (380). The PHQ-9 is a 9-item sub-module of the full PHQ. Major depression is diagnosed if five or more of the 9 depressive symptom criteria have been present at least more than half the days in the past two weeks and if one of the symptoms is depressed mood or anhedonia. Other depression is diagnosed if 2, 3 or 4 depressive symptoms have been present at least more than half the days in the past two weeks and if one of the symptoms is depressed mood or anhedonia. As a severity measure, the scores for each of the items range from 0 (non) to 3 (nearly every day). Scores are summed and range from 0 to 27 with scores of 0-4 indicating minimal depression, 5-9 indicating mild depression, 10-14 indicating moderate depression, 15-27 indicating severe depression.

The BDI is a 21-item self-reporting questionnaire for evaluating the severity of depression in individuals who have been diagnosed with depression (379). It is able to discriminate between symptoms of depression and anxiety (378). Each item is rated on a 4-point scale from 0 (none) to 3 (severe). Scores are summed for each symptom with scores of 0-13 indicating minimal depression, 14-19 indicating mild depression, 20-28 indicating moderate depression and 29-63 indicating severe depression.

3.3.6.2 Assessment of Cognitive Function

Cognitive function testing was assessed at Screening, Baseline, Day 60 and Day 120 using the CogState™ computerised cognitive test battery (CogState Ltd., www.cogstate.com, Melbourne, Australia) (375, 376). The use of the CogState™ battery was identical to that

described in Section 3.2.7.3, above, with the exception that some of the tests used were different (Table 3.3).

Table 3.3. CogState™ Battery of Tests in the CIIS Study

Task Name	Cognitive Function Tested	Unit of Measurement	Description and Interpretation of Scores
Identification Task (IDN)	Attention	Log10 milliseconds	Speed of performance; mean of the log10 transformed reaction times for correct responses Lower score = better performance
Detection Task (DET)	Psychomotor function	Log10 milliseconds	Speed of performance; mean of the log10 transformed reaction times for correct responses Lower score = better performance
Groton Maze Learning Test (GML)	Executive function	Total number of errors	Total number of errors made in attempting to learn the same hidden pathway on five consecutive trials at a single session Lower score = better performance
Continuous Paired Associate Learning (CPAL)	Delayed visual memory	Total number of errors	Accuracy of performance; Total number of errors across all rounds Lower score = better performance
One Card Learning (OCL)	Visual learning	Arcsine proportion	Accuracy of performance; arcsine transformation of the proportion of correct responses Higher score = better performance
One Back Memory (ONB)	Working memory - simple	Arcsine proportion	Accuracy of performance; arcsine transformation of the proportion of correct responses Higher score = better performance
Groton Maze Chase Test	Speed of visual processing	Moves per second	Accuracy of performance; the total number of correct moves made per second Higher score = better performance

The IADL questionnaire was used to assess subjects' ability to perform normal, everyday tasks as described in Section 3.2.7.3, above.

3.3.7 Magnetic Resonance Imaging

MRS is an non-invasive, *in vivo* technique for the detection, quantitation and anatomical mapping of hydrogen, potassium, carbon, nitrogen and fluorine protons from brain metabolites (292). ^{1}H-MRS has previously been used to investigate changes in cerebral metabolites in PLWH (266, 268, 381).

^{1}H-MRS was performed on a 1.5 Tesla Phillips Achieva scanner (Imperial College, London, UK) in three anatomical locations: right frontal white matter (FWM), mid-frontal grey matter (FGM) and the right basal ganglia (RBG). These were selected based on previous imaging studies describing cerebral metabolite abnormality patterns among PLWH (266, 268, 381). MRS data were acquired by a single voxel examination in each of the 3 locations, using a double-spin-echo sequence in point-resolved spectroscopy with the following settings: an echo time of 36 ms, a repetition time of 3000 ms, 2048 data points, a spectral width of 2500 Hz, and 128 data acquisitions. Spectra from the MR imaging were postprocessed using the manufacturer's software for automated water signal suppression and water shimming. Each examination lasted ~35 min. All spectra were analysed and quantified by a single observer using a Java-based version of the Magnetic Resonance User Interface package (jMRUI VersionNumber: 3.0) incorporating the AMARES algorithm. Metabolites assessed were N-acetylaspartate (NAA), creatine (Cr), choline (Cho), myo-Inositol (mI) and glutamate and glutamine (Glx). All metabolites were expressed as cerebral metabolite ratios with respect to cerebral Cr.

3.3.8 Laboratory Procedures

Plasma and CSF concentrations of TRP, KYN, PHE, TYR and NEO were measured at Baseline and Day 120 using the same methodology as described in Section 2.2.1. The KYN/TRP and PHE/TYR ratios were also calculated.

3.3.9 Time and Events Schedule

The time and events schedule for study assessments is summarised in Table 3.4, below.

Table 3.4. Time and Events Schedule for CIIS Study Assessments

Procedure	Screening Up to -28 Days	Baseline Visit Day 0	Day 21 Visit	Day 60 Visit	Day 120 Visit	Day 150 Visit
Informed Consent	X					
Complete history & demographics, including ARV history	X					
Physical examination[a]	X	X				
Height and weight	X					
Urine drug of abuse screen	X					
Urine pregnancy test	X	X	X	X	X	X
Concomitant medications	X	X	X	X	X	X
Adverse events	X	X	X	X	X	X
Lumbar puncture		X			X	
CogState™	X	X		X	X	
Haematology[b]	X	X	X	X	X	X
Biochemistry[c]	X	X		X	X	X
CD4+ cell count	X	X			X	
Plasma HIV-1-RNA	X	X	X	X	X	X
Plasma and CSF TRP, KYN, NEO concentrations		X			X	

[a] Symptom-directed; [b] Full blood count (+ clotting at Screening and Day 60); [c] LFTs, glucose, lactate, amylase (+ lipids at Baseline and Day 120).

3.3.10 Statistical Methodology

Statistical analyses were performed with IBM's SPSS Software Version 24. The results were subjected to tests of the normal distribution. Data for the biochemical and outcomes variables, with the exception of NEO, were normally distributed. Therefore, parametric tests were selected for the analyses. The results for NEO should, therefore, be interpreted with caution.

Because of the number of statistical tests performed, the alpha for all analyses was set at 0.05 to allow identification of signals of interest. Therefore, caution must be applied when interpreting the results because of the risk of type 1 errors.

For some of the analyses, the study arms were pooled to provide an overall combined group. The individual study arms were also investigated separately and comparisons were made between the arms. Paired-samples *t*-tests were conducted to assess changes in plasma and CSF concentrations for these factors from Baseline to Day 120 for the combined group and for each of the study arms individually. Differences in the changes from Baseline to Week 120 between study arms was assessed using Independent Samples *t*-tests.

Paired-samples *t*-tests were conducted to assess changes in the cerebral metabolite concentrations for NAA/Cr, Cho/Cr, mI/Cr and Glx/Cr in each of the anatomical locations from Baseline to Day 120 for each of the study arms. Differences in the changes from Baseline to Week 120 between study arms was assessed using Independent Samples *t*-tests.

For the cognitive testing, statistical analysis was conducted according to CogState™ recommendations. Reaction times were $\log^{10}$-transformed because of a positive skew of the distribution, and accuracy measures were transformed using arcsine transformation. Change scores were calculated for each subject, and these scores standardized according to the within-subject standard deviation (SD). Paired-samples *t*-tests were conducted to assess changes from Baseline to Day 60 and Day 120. Z scores were calculated for each test score and a Global Composite Score (GCS) was calculated based on the average of the individual Z scores. Differences in the changes from Baseline to Week 120 between study arms was assessed using Independent Samples *t*-tests.

To explore the association between biomarker concentrations and the Global CogState™ score or MRS metabolite concentrations for all subjects at Baseline, Pearson r correlations were conducted.

To investigate the relationship between the changes in TRP concentrations in plasma and CSF and the CogState™ GCS for patients in the DTG arm, mixed models (i.e. longitudinal random intercept models) were constructed. The models' fixed effects were CogState™ GCS (dependent variable) and plasma or CSF TRP concentration (independent variable). The random effect, or intercept, was the patient (i.e. Patient ID) and the repeated effect was Time (Baseline, Day 60 and Day 120). Maximum Likelihood estimation was selected. This approach was also utilised to investigate the relationship between KYN concentrations and the KYN/TRP ratio in plasma and CSF and CogState™ GCS.

4 DETERMINING CHANGES IN TRYPTOPHAN METABOLISM IN INDOLEAMINE 2,3-DIOXYGENASE-EXPRESSING CELLS FOLLOWING ACUTE EXPOSURE TO ANTIRETROVIRAL AGENTS

4.1 Introduction

During HIV-1 infection, IDO is induced via the proinflammatory mediators IFN-γ and TNF-α leading to increased degradation of TRP via the KYN pathway (354, 382). Boasso *et al.* have previously demonstrated that the expression and activity of IDO is further induced in monocyte-derived macrophages and pDC's by exposure to HIV virions and their viral proteins, particularly Nef and Tat. Indeed, productive infection itself does not appear to be necessary (233, 310). A number of other cell types express the TDO and IDO enzymes and have roles in the catabolism of TRP via the KYN pathway (Section 1.9). TDO activity is highest in the liver, whereas IDO is absent from the liver in most mammals but is expressed by antigen-presenting cells both systemically and in intestinal, lung, placenta and brain tissue (234, 283). In the brain, the cellular localisation of the KYN pathway has been shown to be primarily expressed in infiltrating macrophages and resident microglial cells (234, 235). Astrocytes, neurons and BBB epithelial cells also express the KYN pathway to varying degrees (235, 296, 308, 309). Microglia express the KYN pathway in its entirety, though they have been shown to play a lesser role in the catabolism of TRP than infiltrating macrophages due to their threefold lower expression of IFN-γ (234, 235). Astrocytes are able to produce large amounts of the early KYN pathway metabolites, such as KYN and KYNA, but because they do not express KYN(OH)ase they cannot convert KYN into 3-HK and, therefore, are only capable of producing minute amounts of the late metabolites QUIN (only when 3-HAA is added) and PIC. Essentially, the pathway is split in half in astrocytes (235, 308).

Initiation of ART in previously untreated PLWH has been shown to significantly, but incompletely, reduce the degradation of TRP and induce declines in NEO and KYN/TRP ratio levels in-line with decreases in viral loads (321-324). However, there are currently no published data reporting on whether ARV agents have a direct effect on TRP metabolism at a cellular level, independent of HIV-1. Whilst ARVs reduce overall IDO activity by driving down

HIV-1 viral loads, one could postulate that some agents may induce or inhibit IDO either directly or indirectly. Indeed, many agents, such as EFV or PIs, have been shown to directly induce or inhibit CYP450 enzymes and, thus, may have a similar effect on IDO. In addition to this, various inherent toxicities could drive an ongoing induction of IDO either directly or via another mechanism, such as inflammation. For example, thymidine analogues and PIs are known to have distinct toxicities (383, 384) and have been associated with increased plasma levels of TNF-α in individuals experiencing ART-related lipodystrophy and lipoatrophy (385). Given that TNF-α plays a key role in inducing IDO activity, it would be reasonable to hypothesize that these agents could indirectly upregulate TRP degradation via the KYN pathway.

In this Chapter, the aim was to explore the possible effects on TRP metabolism following the acute exposure of IDO-expressing cells with ARVs. This was conducted according to the methodologies described in Chapter 2. To this end, freshly drawn PBMCs and hepatocyte, astrocyte and microglial cell lines were utilized. THLE2 and THLE3 hepatocytes were sourced from established cell lines from non-tumorigenic adult human liver autopsy samples of epithelial cells and immortalised by transfection with the SV40 T antigen (386). They have been shown to express normal hepatocyte phenotypic characteristics, including retaining cytochrome P450 (CYP450) enzyme activity, though no data are available on TDO (or IDO) activity in these cells (387). The U87 (formerly known as U87MG [Uppsala 87 Malignant Glioma]), and U373 cell lines sourced were established from astrocytoma grade III/glioblastomas. Whist they are both known to have highly aberrant genomic structures (388, 389), human glioblastoma tissue has been shown to highly express IDO and this appears to be preserved in glioblastoma cell lines (390), including both U87 and U373 (390, 391). EOC13.31 and EOC20 are spontaneously immortalised rodent microglial cell lines, which have not been genetically modified and maintain the ability to secrete many cytokines and reactive species (392, 393). EOC13.31 cells have been shown to express IDO when induced by IFN-γ and TNF-α (392). No data exist on the expression of IDO in EOC20 cells, though they have been shown to produce large quantities of IFN-γ when stimulated with Toxoplasma *tachyzoite lysate Ags* (394).

Given the broad toxicity profiles of the thymidine analogues d4T and AZT and their previously reported effects on TNF-α (385), it was decided that they would make reasonable initial

candidates for the exploration of the role of ARVs in TRP metabolism in PBMCs (Section 4.2.1). Additional experiments in PBMCs were conducted to explore the effects of a broader panel of ARVs on TRP metabolism, both individually (Sections 4.2.2 and 4.2.3) and in clinically-relevant combinations (Section 4.2.3). This was then repeated in the aforementioned hepatocyte, astrocyte and microglial cell lines (Section 4.2.4).

4.1.1 Aims

To this end, the aim of this chapter was to determine changes in TRP metabolism following acute exposure of PBMCs, hepatocytes, astrocytes and microglia to commonly-used ARVs individually and in clinically-relevant combinations.

4.1.2 Hypothesis

TRP metabolism is increased in the presence of antiretroviral agents in cell types known to express KYN pathway enzymes.

4.2 Results

4.2.1 Tryptophan Metabolism Following Acute Exposure of Peripheral Blood Mononuclear Cells to Zidovudine and Stavudine

The methods employed are detailed in Section 2.2.1. Cell culture supernatant concentrations of TRP, KYN, NEO and nitrite were analysed using the methodologies described in Section 2.3. KYN/TRP ratios were also calculated; a higher KYN/TRP ratio indicates higher levels of IDO activity. All culture conditions were compared with the DMSO reference condition using a non-parametric Friedman test. Due to the low sample numbers and multiple comparisons, the Friedman test was first performed without applying a correction for multiplicity with the alpha set at 0.05, thus ensuring that associations of interest were not missed. The Friedman's test was then re-run for all comparisons using Dunn's correction for multiplicity to see whether any of the preliminary observations remained statistically significant.

The results are detailed in Figures 4.1 and 4.2, below. In the group exposed to AZT, PBMCs acutely exposed to the positive control condition (HIV-1 alone) for a 24-hour period were observed to have significantly lower cell supernatant concentrations of TRP compared with those exposed to DMSO alone (Figure 4.1A; unadjusted *p*=0.030). However, this difference did not remain significant following Dunn's correction for multiplicity. In the d4T group, no difference in TRP concentrations was observed for cells exposed to HIV-1 alone and DMSO alone (Figure 4.1B; unadjusted *p*=0.140). Similarly, no difference was observed between the second positive control condition of DMSO + HIV-1 and DMSO alone in either group (Fig's. 4.1A and B; unadjusted *p* values 0.542 and 0.673, respectively). The cells exposed to HIV-1 in combination with either AZT 200 μM (unadjusted *p*=0.005), AZT 0.2 μM (unadjusted *p*=0.002), AZT 0.002 μM (unadjusted *p*=0.008) or d4T 200 μM (unadjusted *p*=0.027) were all found to have significantly lower cell supernatant concentrations of TRP than those exposed to DMSO alone, but these differences were no longer significant following Dunn's correction. No difference was observed between cells exposed to AZT alone (Fig. 4.1A; unadjusted *p*=0.384) or d4T alone (Fig. 4.1B; unadjusted *p*=0.461) compared with DMSO alone.

PBMCs exposed to DMSO + HIV-1 were found to have significantly higher KYN concentrations than those exposed to DMSO alone (Figures 4.1C and D; unadjusted *p* values 0.006 and 0.007, respectively). All of the conditions combining HIV-1 and AZT were found to have significantly greater concentrations of KYN than DMSO alone and this difference persisted following Dunn's correction, with the exception of AZT 0.002 μM (Figure 4.1C). A similar pattern was observed for d4T (Figure 4.1D), though the lowest two concentrations (0.02 and 0.002 μM) showed no difference. Similar observations were made for the KYN/TRP ratio for both AZT and d4T-exposed cells (Figures 4.1E and F).

Only the HIV-1+d4T 20 μM condition was found to have significantly greater NEO concentrations than DMSO alone (unadjusted *p*=0.023), and this did not survive Dunn's correction. No significant associations were observed for nitrite.

Figure 4.1. Concentrations of TRP, KYN and the KYN/TRP Ratio Following Stimulation of PBMCs with Antiretroviral Agents

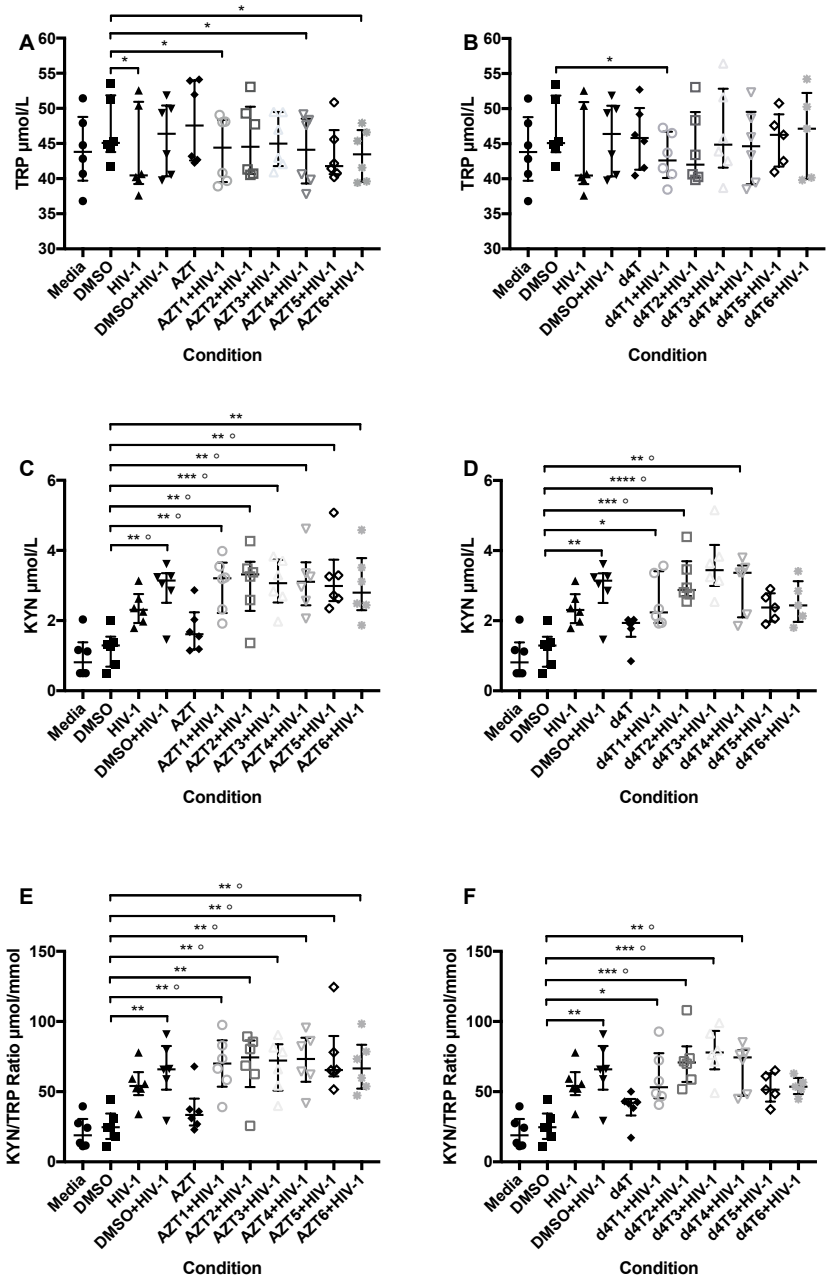

Footnote: Cell supernatant concentrations of TRP, KYN and the KYN/TRP ratio are shown following stimulation with zidovudine (A, C and E, respectively) and stavudine (B, D and F, respectively). Horizontal lines represent median values and vertical lines show the interquartile range (IQR). Each symbol is indicative of one individual donor. Concentrations of AZT and d4T were: AZT1 and d4T1, 200 μM; AZT2 and d4T2, 20 μM; AZT3 and d4T3, 2 μM; AZT4 and d4T4, 0.2 μM; AZT5 and d4T5, 0.02 μM; and AZT6 and d4T6, 0.002 μM. Unadjusted *p* values for the Friedman's test are displayed on the graphs. **p*<0.05; ***p*<0.01; ****p*<0.001; *****p*<0.0001; °Association remains statistically significant following Dunn's correction for multiplicity.

Figure 4.2. Concentrations of NEO and Nitrite Following Stimulation of PBMCs with Antiretroviral Agents.

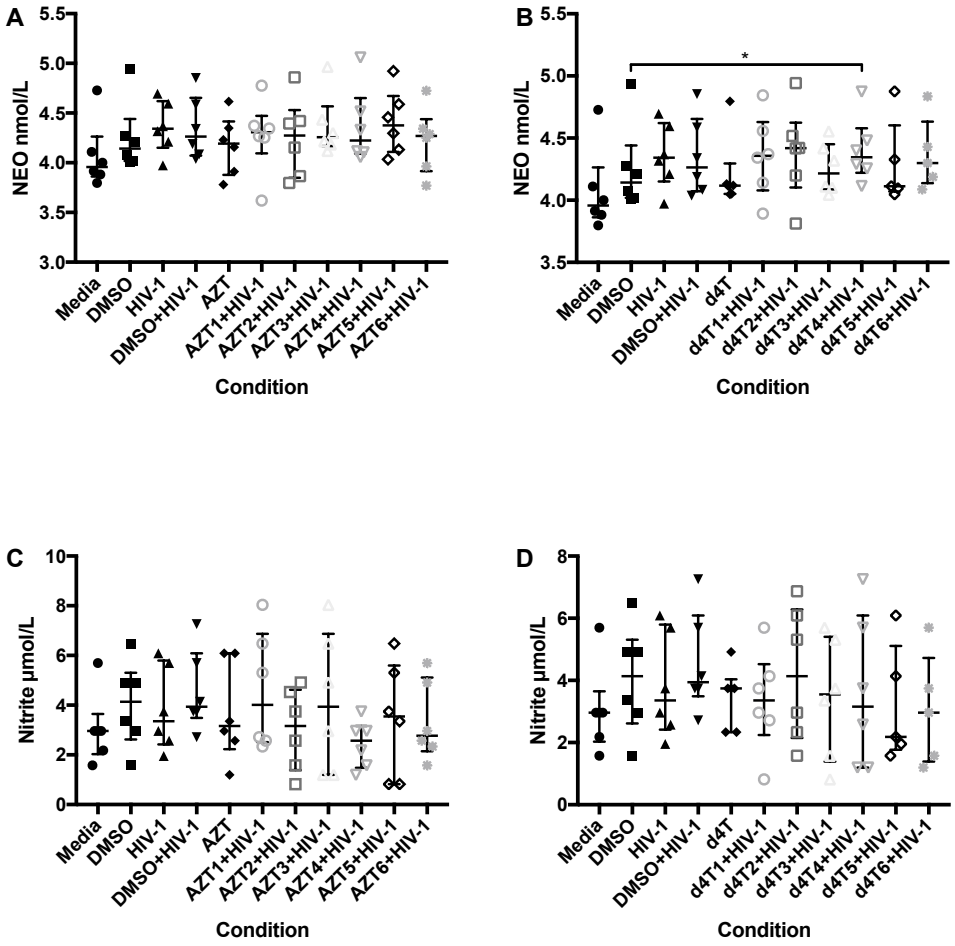

Footnote: Cell supernatant concentrations of TRP, KYN and the KYN/TRP ratio are shown following stimulation with zidovudine (A, C and E, respectively) and stavudine (B, D and F, respectively). Horizontal lines represent median values and vertical lines show the interquartile range (IQR). Each symbol is indicative of one individual donor. Concentrations of AZT and d4T were: AZT1 and d4T1, 200 μM; AZT2 and d4T2, 20 μM; AZT3 and d4T3, 2 μM; AZT4 and d4T4, 0.2 μM; AZT5 and d4T5, 0.02 μM; and AZT6 and d4T6, 0.002 μM. Unadjusted *p* values for the Friedman's test are displayed on the graphs. *$p<0.05$.

In summary, significantly lower TRP concentrations, greater KYN concentrations and greater KYN/TRP ratios in culture supernatants were observed when PBMCs were exposed to combinations of HIV-1 plus either AZT or d4T compared with cells that were exposed to DMSO alone for 24 hours. The majority of the differences for KYN concentrations and the KYN/TRP ratio survived Dunn's correction for multiplicity. DMSO itself was not observed to have significantly different concentrations of TRP and KYN/TRP or the KYN/TRP ratio than media alone. No significant differences were observed in these parameters when either AZT or d4T alone were compared with DMSO alone. No differences were observed for NEO or nitrite concentrations.

4.2.2 Tryptophan Metabolism Following Acute Exposure of Peripheral Blood Mononuclear Cells to Commonly-Used Antiretroviral Agents

An expanded range of ARVs from the NRTI, NNRTI, PI and CCR5 antagonist classes were employed in an attempt to isolate their independent effect, if any, on TRP metabolism in PBMCs. The methods employed are detailed in Section 2.2.2. DMSO alone was used as the control condition and the combination of DMSO and HIV-1 was used as a positive control.

The results are presented in Figure 4.3, below. Overall, very few differences were observed between any of the ARVs and the DMSO control. Cell supernatants from PBMCs exposed to DMSO+HIV-1 were found to have significantly lower TRP concentrations (unadjusted p=0.022) and significantly greater KYN concentrations (unadjusted p=0.006) and KYN/TRP ratios (unadjusted p=0.006) than those exposed to DMSO alone. These observations did not survive Dunn's correction for multiplicity, however. No significant differences in TRP concentrations were observed for cells exposed to any of the ARVs. Rilpivirine was the only ARV that was observed to have a significantly greater KYN concentration than DMSO alone (unadjusted p=0.027). Rilpivirine (unadjusted p=0.032) and FTC (unadjusted p=0.039) were observed to have significantly greater KYN/TRP ratios than DMSO alone. None of these observations survived Dunn's multiplicity correction.

Whilst not being statistically significantly different from the DSMO control, supernatants from cells exposed to EFV and ETV were trending towards having higher KYN concentrations than those exposed to DMSO alone, with unadjusted p values of 0.067 and 0.079, respectively.

However, visual inspection of the data in Figures 4.3D and F indicate that the differences for ETV may be driven by an outlier. Nevirapine, another NNRTI, did not show the same effect (unadjusted p=0.702). Given that RPV was shown to have significantly greater KYN concentrations that the control, and that RPV, ETV and EFV are all ARVs from the NNRTI class an unplanned post-hoc analysis was conducted to investigate whether there was a drug-class effect involved that was being obscured by low sample numbers. Kynurenine concentration and KYN/TRP ratio data for the four NNRTI agents were pooled and a Wilcoxon matched-pairs signed rank test was conducted. The tests were both found to be non-significant (KYN, p=0.250; KYN/TRP ratio, p=0.250), indicating no effect.

Figure 4.3. Concentrations of TRP, KYN and the KYN/TRP Ratio Following Stimulation of PBMCs with Antiretroviral Agents.

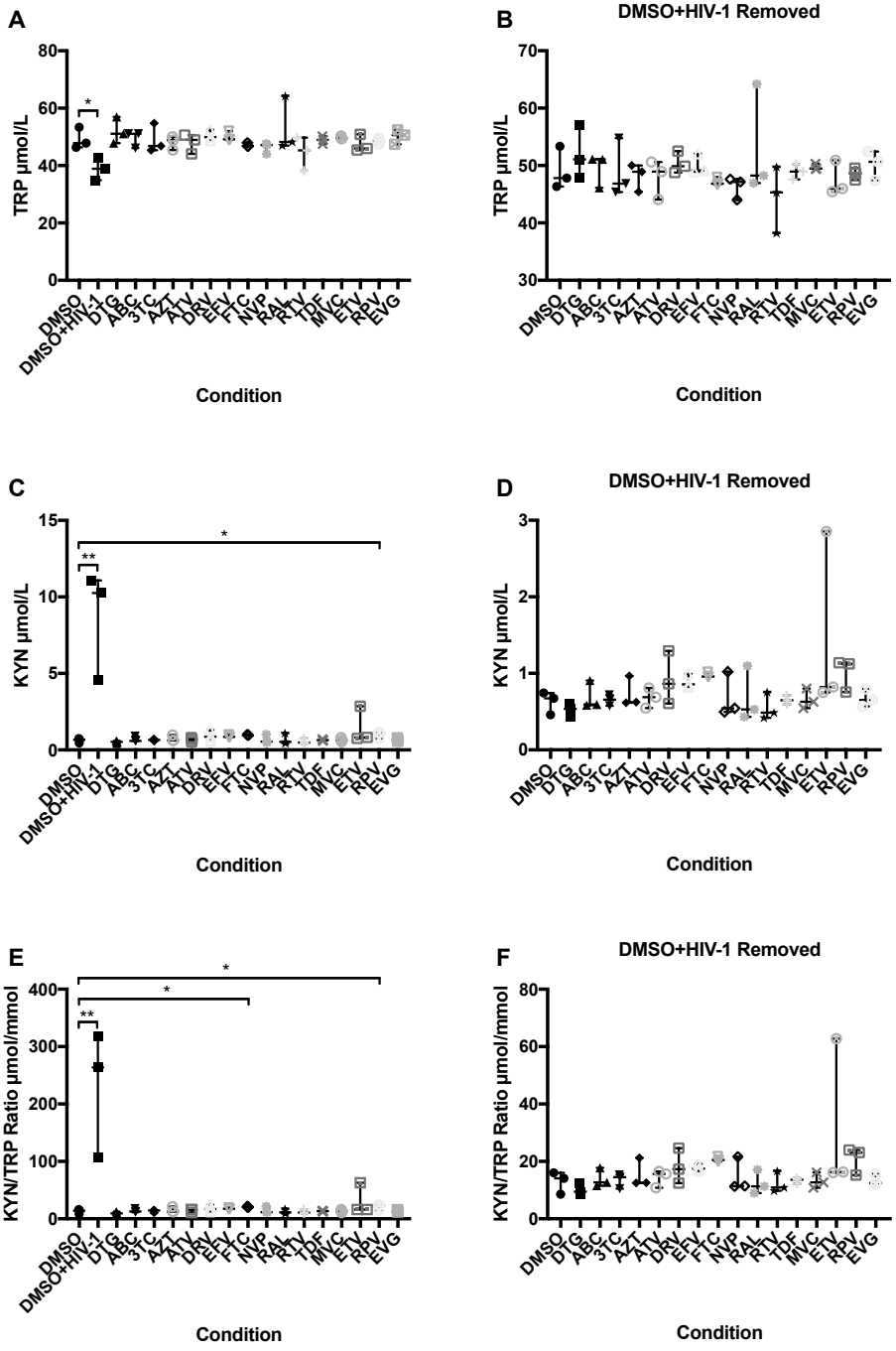

Footnote: Cell supernatant concentrations of TRP, KYN and the KYN/TRP ratio are shown following stimulation with antiretroviral agents (A, C and E, respectively). The DMSO+HIV-1 condition has been removed in B, D and F to allow easier visual comparison of the results for the ARVs. Horizontal lines represent median values and vertical lines show the interquartile range (IQR). Each symbol is indicative of one individual donor. Concentrations of ARVs were 1mM, except for DTG, RAL and TDF, which were 0.5mM. Unadjusted *p* values for the Friedman's test are displayed on the graphs. *p<0.05.

4.2.3 Tryptophan Metabolism Following Acute Exposure of Peripheral Blood Mononuclear Cells to Commonly-Used Antiretrovirals Individually and in Clinically-Relevant Combinations

The previous experiments demonstrated that individual ARVs have no discernible effect on TRP metabolism in PBMCs. In clinical practice multiple ARVs are given in combination. Because of this, clinically-relevant combinations of ARVs were investigated to determine their effect, if any, on TRP metabolism. The ARVs selected (i.e. 3TC, FTC, ABC, TDF, EFV, RPV, ETV, DTG, and RAL) because most of them were used in combination in the SSAT056 and CIIS clinical studies detailed in Chapters 6 and 7 of this thesis (i.e. ABC+3TC+EFV; TDF+FTC+EFV; ABC+3TC+DTG; TDF+FTC+DTG; ABC+3TC+RAL; and TDF+FTC+RAL). Rilpivirine and ETV were also included in this experiment. Rilpivirine was included on the basis that cell supernatants exposed to this agent were observed to have significantly greater KYN concentrations and KYN/TRP ratios than DMSO alone. ETV was included because cells exposed to it were trending towards having significantly greater KYN concentrations compared to those exposed to the control. The methods employed are detailed in Section 2.2.3. DMSO alone was used as the control condition and the combination of DMSO and HIV-1 was used as a positive control. In this experiment, the role of phenylalanine-hydroxylase (PAH) activity (as measured by the phenylalanine-to-tyrosine [PHE/TYR] ratio) was explored. This pathway is analogous to the KYN pathway (Sections 1.9.1 and 1.9.5; Figure 1.11).

The results are presented in Figures 4.4, 4.5 and 4.6. In the high concentration ARV group (i.e. 1 mM [0.5 mM for TDF, DTG and RAL]), cells exposed to the combination of TDF+FTC+RAL were observed to have lower KYN/TRP ratios than those exposed to DMSO alone (unadjusted p=0.036; Figure 4.4E). Cell supernatants from the FTC and ETV conditions were observed to have with lower PHE concentrations than those exposed to DMSO alone (unadjusted p=0.043 and 0.012, respectively; Figure 4.5A). A number of ARV combinations were observed to have statistically significantly lower TYR concentrations than DMSO (Figure 4.5C): TDF+FTC+EFV (unadjusted p=0.043); ABC+3TC+DTG (unadjusted p=0.006); TDF+FTC+DTG (unadjusted p=0.036); ABC+3TC+RAL (unadjusted p=0.024); and TDF+FTC+RAL (unadjusted p=0.012). Etravirine was the only ARV to have a lower PHE/TYR ratio than DMSO (unadjusted p=0.024). The combinations of ABC+3TC+DTG (unadjusted p=0.014), TDF+FTC+DTG (unadjusted p=0.048) and ABC+3TC+RAL (unadjusted p=0.011) were observed to have significantly greater

NEO concentrations than DMSO alone (Figure 4.6A). None of the observations described above survived Dunn's correction for multiplicity.

In the clinically-relevant concentration ARV conditions (i.e. ARV concentrations approximating the clinically-observed C_{max} for each agent), the only statistically significant differences observed were greater KYN and NEO concentrations, and KYN/TRP ratios, for the DMSO+HIV-1 control (unadjusted *p*=0.024, 0.043 and 0.029, respectively), though these did not survive Dunn's correction. No differences were observed for ARVs individually or in combination at the lower, clinically-relevant concentrations.

Figure 4.4. Concentrations of TRP, KYN and the KYN/TRP Ratio Following Stimulation of PBMCs with Antiretroviral Agents.

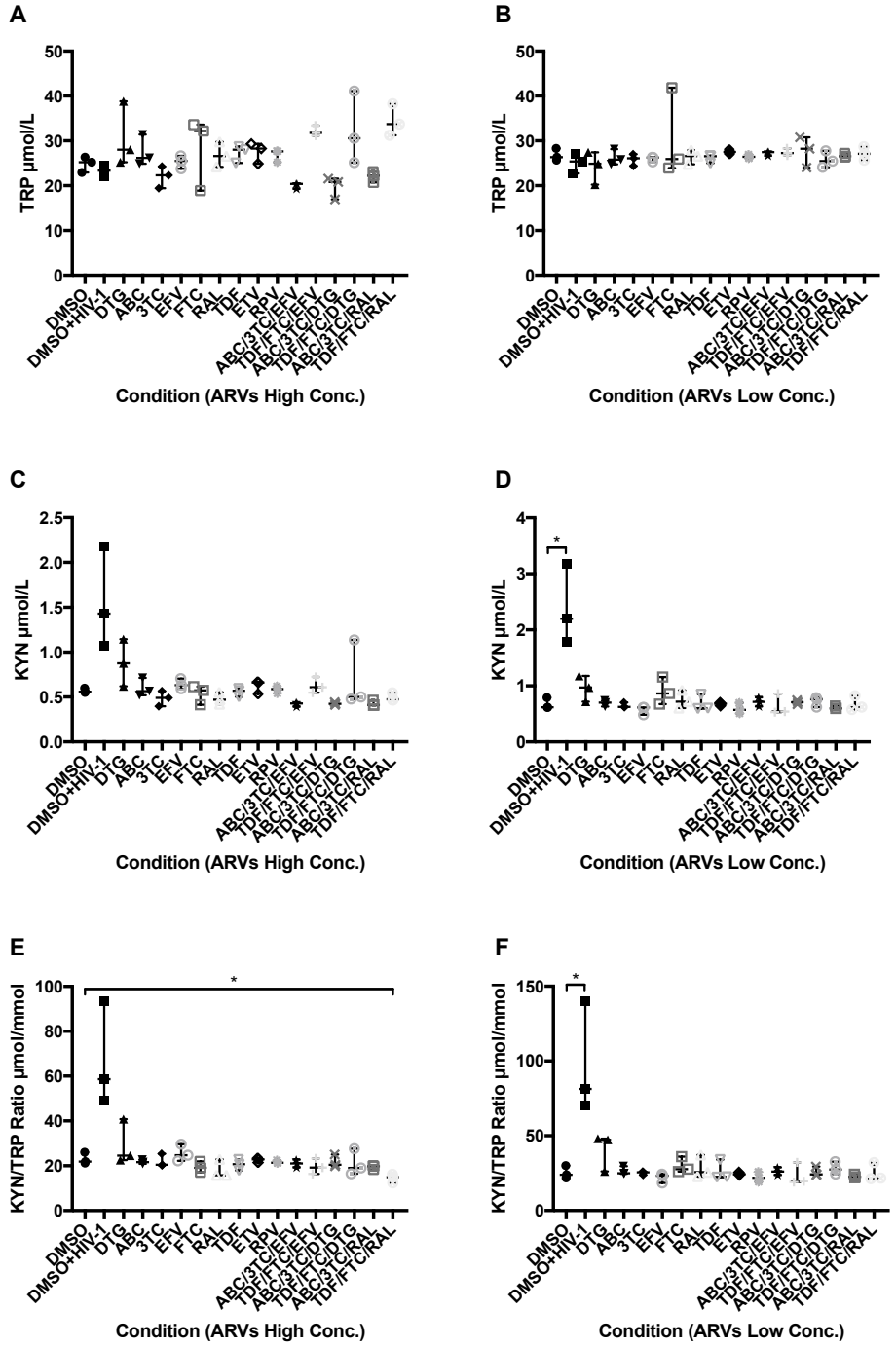

Footnote: Cell supernatant concentrations of TRP, KYN and the KYN/TRP ratio are shown following stimulation with antiretroviral agents at high (A, C and E, respectively) and clinically-relevant concentrations (B, D and F, respectively). Horizontal lines represent median values and vertical lines show the interquartile range (IQR). Each symbol is indicative of one individual donor. Concentrations of ARVs are shown in Sections 2.2.3. Unadjusted *p* values for the Friedman's test are displayed on the graphs. *p<0.05.

Figure 4.5. Concentrations of PHE, TYR and the PHE/TYR Ratio Following Stimulation of PBMCs with Antiretroviral Agents.

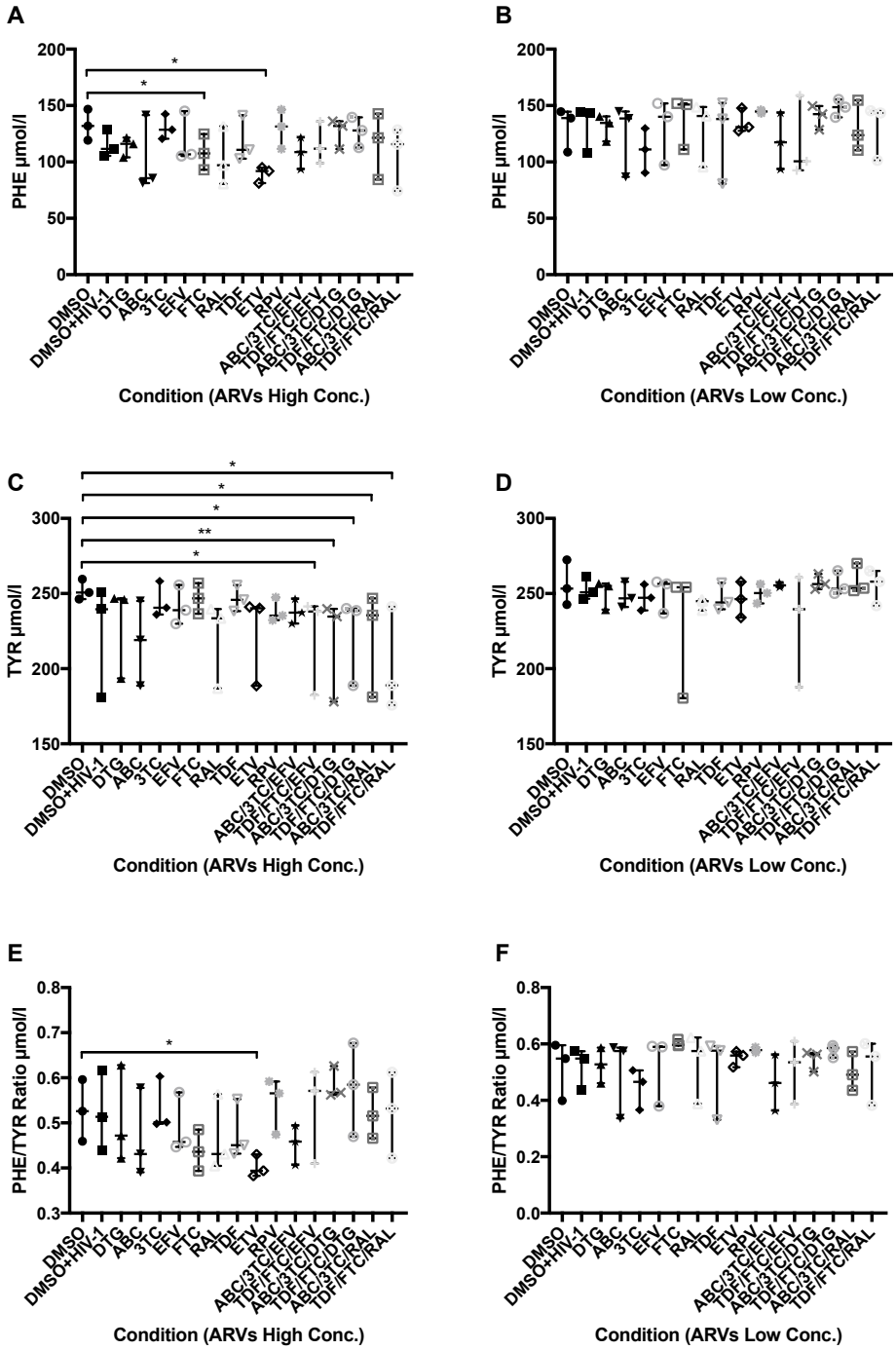

Footnote: Cell supernatant concentrations of PHE, TYR and the PHE/TYR ratio are shown following stimulation with antiretroviral agents at high (A, C and E, respectively) and clinically-relevant concentrations (B, D and F, respectively). Horizontal lines represent median values and vertical lines show the interquartile range (IQR). Each symbol is indicative of one individual donor. Concentrations of ARVs are shown in Sections 2.2.3. Unadjusted *p* values for the Friedman's test are displayed on the graphs. **p*<0.05; ***p*<0.01.

Figure 4.6. Concentrations of NEO Following Stimulation of PBMCs with Antiretroviral Agents.

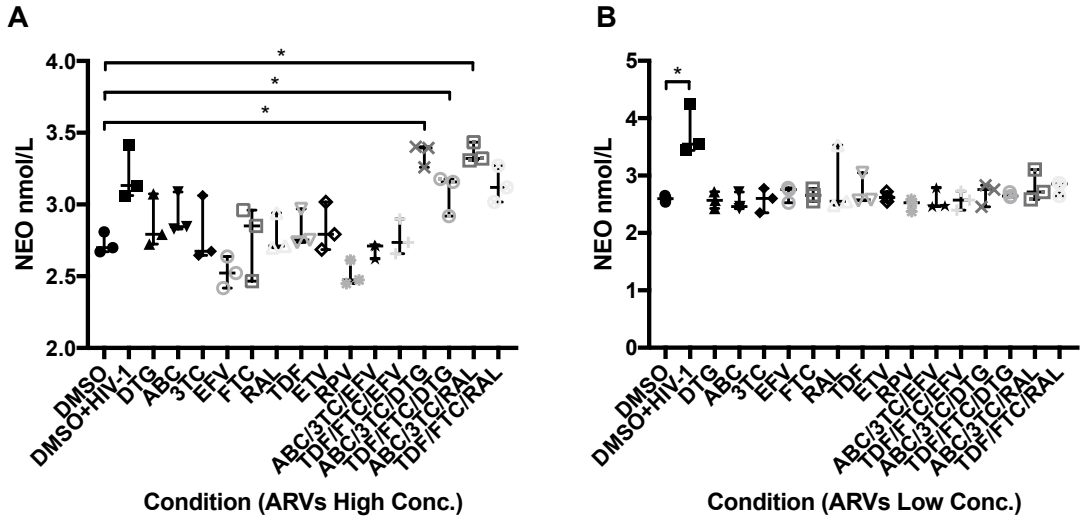

Footnote: Cell supernatant concentrations of NEO are shown following stimulation with antiretroviral agents at high (A, C and E, respectively) and clinically-relevant concentrations (B, D and F, respectively). Horizontal lines represent median values and vertical lines show the interquartile range (IQR). Each symbol is indicative of one individual donor. Concentrations of ARVs are shown in Sections 2.2.3. Unadjusted *p* values for the Friedman's test are displayed on the graphs. *p<0.05.

4.2.4 Tryptophan Metabolism Following Acute Exposure of Hepatocytes, Astrocytes and Microglia to Commonly-Used Antiretrovirals Individually and in Clinically-Relevant Combinations

The methods employed are detailed in Section 2.2.4. The THLE2, THLE3, U87, U373, EOC13.31 and EOC20 cell lines were cultured according to the manufacturers guidelines (Section 2.2.4). When each cell line had grown to approximately 80-100% confluence they were exposed to the experimental conditions described in Section 2.2.4. Digital images of the cells are displayed in Figure 4.7, below, and were taken at 20x optical magnification at when they had grown to approximately 60-100% confluence. DMSO alone was used as the control condition and the combination of DMSO + IFN-γ was used as a positive control.

Figure 4.7. Hepatocyte, Astrocyte and Microglial Cells Grown to Approximately 60-100% Confluence at 20x Optical Magnification.

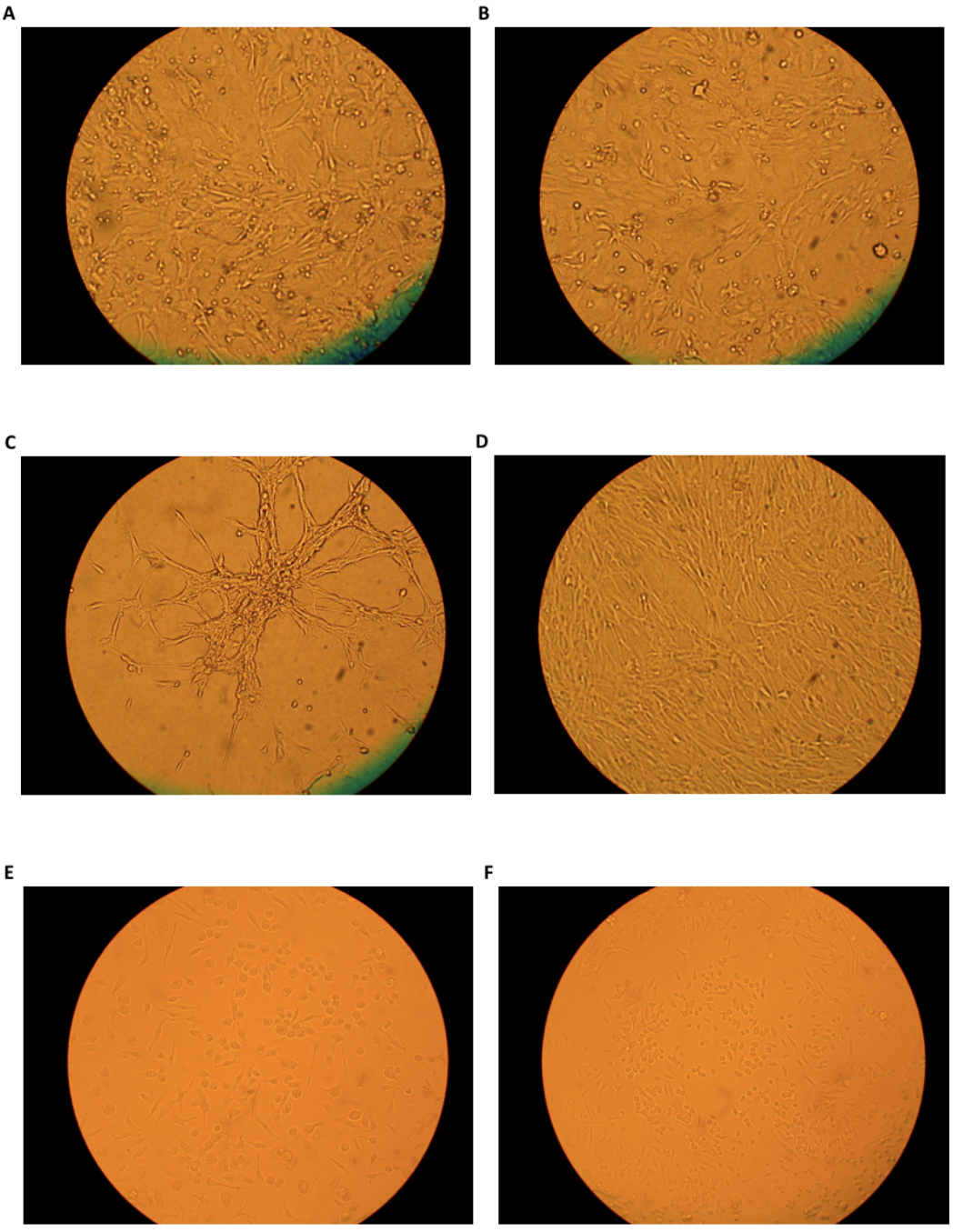

Footnote: Photographs of THLE2 (A), THLE3 (B), U87 (C), U373 (D), EOC13.31 (E) and EOC20 (F) cells are shown.

For the THLE2 cell line (Figures 4.8 and 4.9), the only condition that remained statistically significantly different following multiplicity correction was the DMSO + IFN-γ positive control, which was observed to have lower TRP concentrations than the DMSO control (adjusted *p*=0.017). The combinations of ABC+3TC+DTG (adjusted *p*=0.193), ABC+3TC+DTG (adjusted *p*=0.152) and TDF+FTC+DTG (adjusted *p*=0.594) did not survive Dunn's correction for multiplicity. Of particular note in this cell line were the small increases in the PHE/TYR ratio that were observed for TDF (adjusted *p*=0.387) and the combinations of ABC+3TC+DTG (adjusted *p*=0.387), TDF+FTC+DTG (adjusted *p*=0.152), ABC+3TC+RAL (adjusted *p*=0.254) and TDF+FTC+RAL (adjusted *p*=0.481) compared with the control. Though these did not remain statistically significant following multiplicity correction, the data suggest that there may be a signal of interest for this parameter.

For the THLE3 cell line (Figures 4.10 and 4.11), the only condition that remained statistically significantly different following multiplicity correction was the DMSO + IFN-γ positive control, which was observed to have lower TRP concentrations than the DMSO control (adjusted *p*=0.005). However, the adjusted *p* values for the combinations of ABC+3TC+EFV (adjusted *p*=0.053), TDF+FTC+EFV (adjusted *p*=0.053) and ABC+3TC+RAL (adjusted *p*=0.053) were approaching statistical significance.

Figure 4.8. Concentrations of TRP, KYN and the KYN/TRP Ratio Following Stimulation of THLE2 Cells by Antiretroviral Agents.

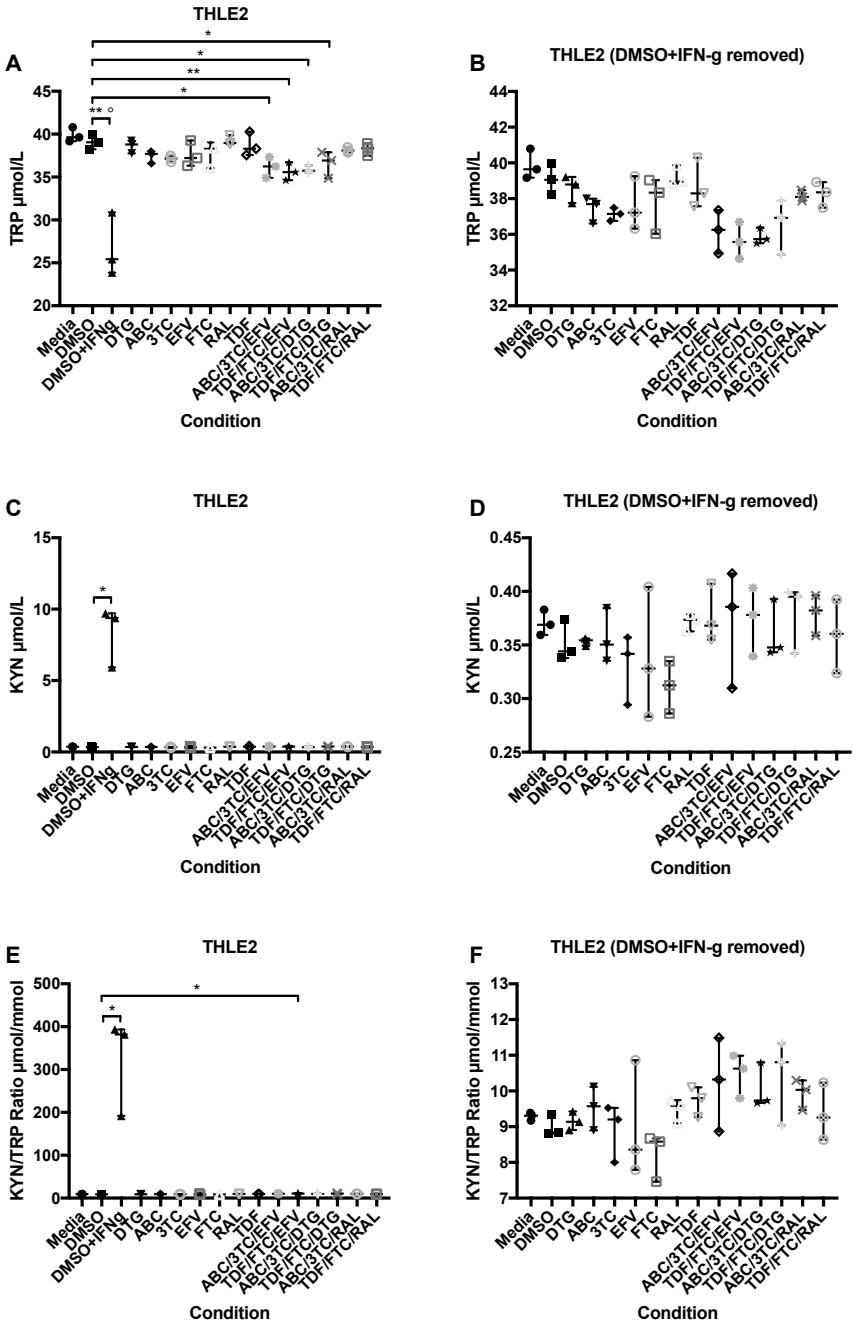

Footnote: Cell supernatant concentrations of TRP, KYN and the KYN/TRP ratio are shown following stimulation with antiretroviral agents individually and in clinically-relevant combinations (A, C and E, respectively). The DMSO + IFN-γ condition has been removed in B, D and F to allow easier visual comparison of the results for the ARVs. Horizontal lines represent median values and vertical lines show the interquartile range (IQR). Each symbol is indicative of one individual donor. Concentrations of ARVs are detailed in Sections 2.2.4. Unadjusted *p* values for the Friedman's test are displayed on the graphs. **p*<0.05; ***p*<0.01.

Figure 4.9. Concentrations of PHE, TYR, the PHE/TYR ratio and NEO Following Stimulation of THLE2 Cells with Antiretroviral Agents.

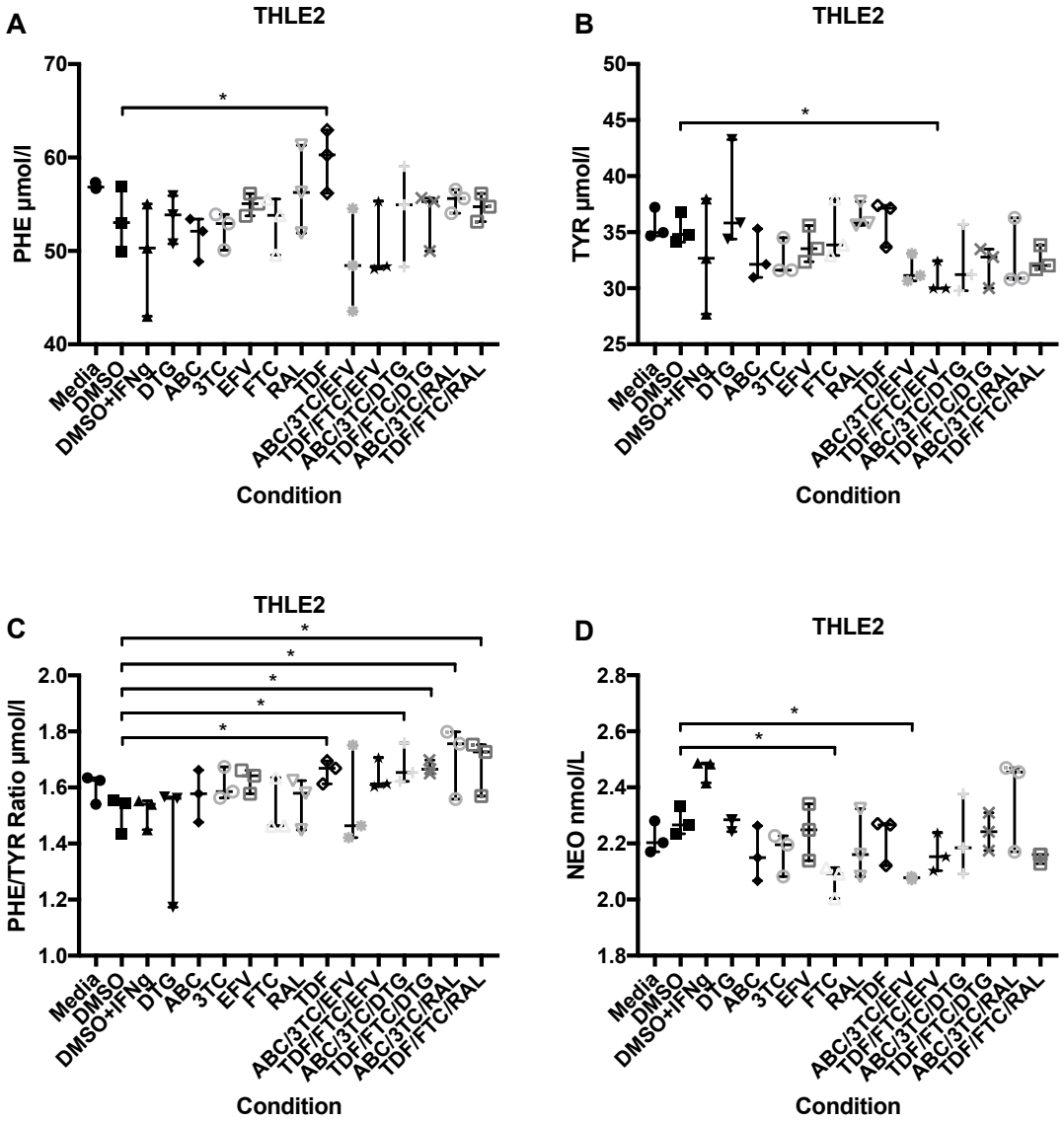

Footnote: Cell supernatant concentrations of PHE, TYR, the PHE/TYR ratio and NEO are shown following stimulation with antiretroviral agents individually and in clinically-relevant combinations (A, C, D and E, respectively). Horizontal lines represent median values and vertical lines show the interquartile range (IQR). Each symbol is indicative of one individual donor. Concentrations of ARVs are detailed in Section 2.2.4. Unadjusted *p* values for the Friedman's test are displayed on the graphs. *p<0.05.

Figure 4.10. Concentrations of TRP, KYN and the KYN/TRP Ratio Following Stimulation of THLE3 Cells with Antiretroviral Agents.

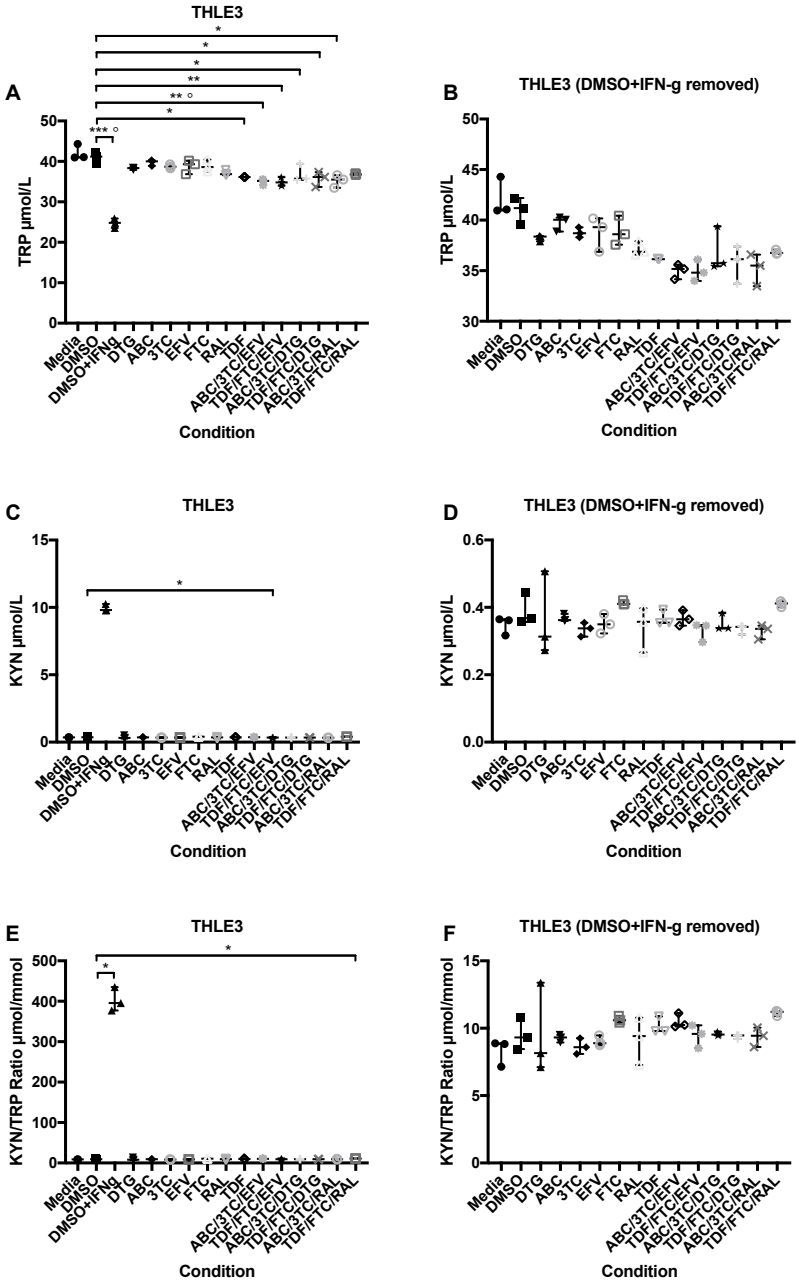

Footnote: Cell supernatant concentrations of TRP, KYN and the KYN/TRP ratio are shown following stimulation with antiretroviral agents individually and in clinically-relevant combinations (A, C and E, respectively). The DMSO+IFN-γ condition has been removed in B, D and F to allow easier visual comparison of the results for the ARVs. Horizontal lines represent median values and vertical lines show the interquartile range (IQR). Each symbol is indicative of one individual donor. Concentrations of ARVs are detailed in Section 2.2.4. Unadjusted *p* values for the Friedman's test are displayed on the graphs. **p*<0.05; ***p*<0.01; ****p*<0.001; °Association remains statistically significant following Dunn's correction for multiplicity.

Figure 4.11. Concentrations of PHE, TYR, the PHE/TYR ratio and NEO Following Stimulation of THLE3 Cells with Antiretroviral Agents.

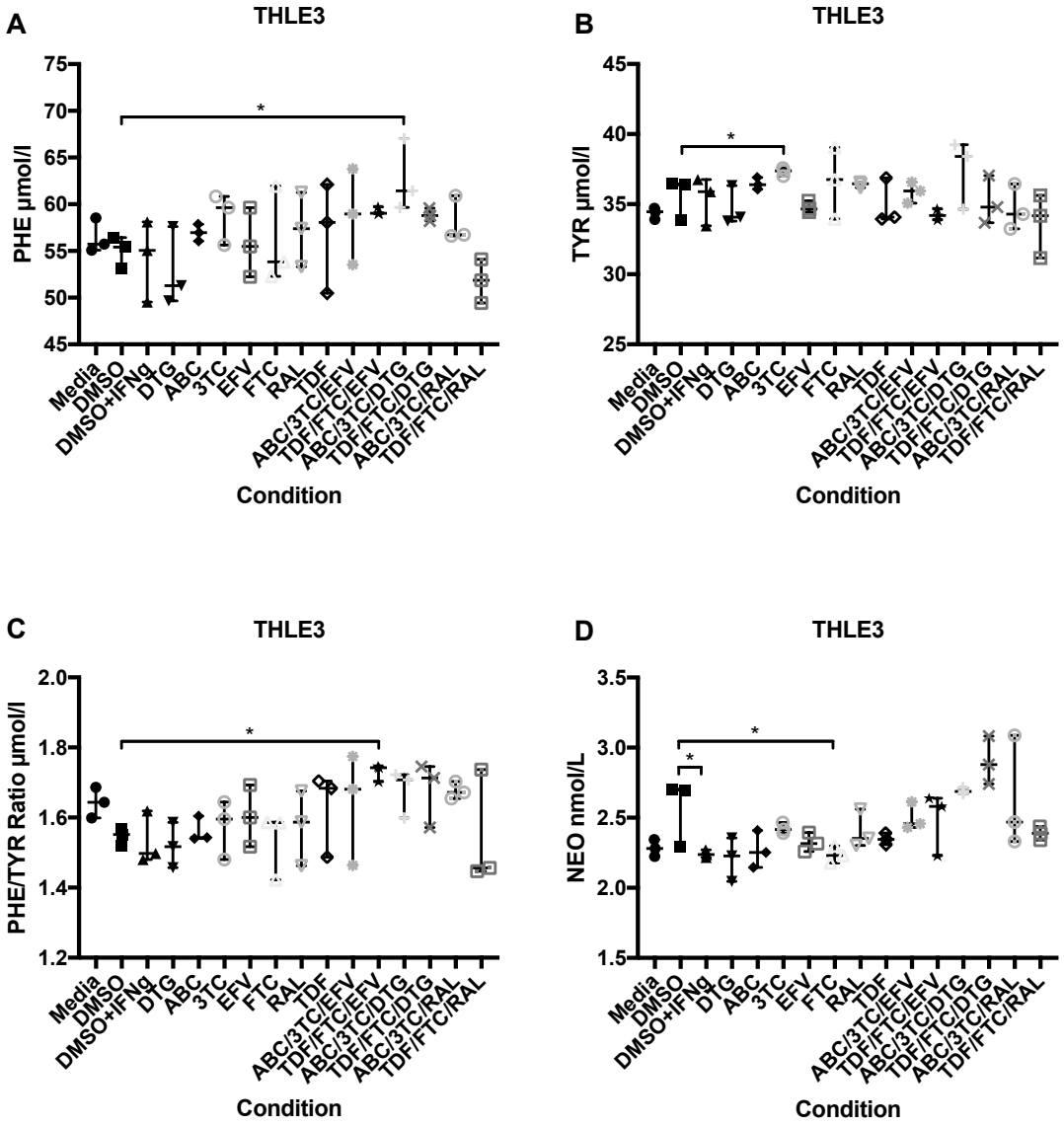

Footnote: Cell supernatant concentrations of PHE, TYR, the PHE/TYR ratio and NEO are shown following stimulation with antiretroviral agents individually and in clinically-relevant combinations (A, C, D and E, respectively). Horizontal lines represent median values and vertical lines show the interquartile range (IQR). Each symbol is indicative of one individual donor. Concentrations of ARVs are detailed in Section 2.2.4. Unadjusted *p* values for the Friedman's test are displayed on the graphs. *p<0.05.

For the U87 cell line (Figures 4.12 and 4.13), TDF (adjusted *p*=0.030) and the ABC+3TC+DTG combination (adjusted *p*=0.030) were both observed to have significantly greater PHE concentrations than DMSO alone (Figure 4.13). In addition to this, RAL (adjusted *p*=0.070) and ABC+3TC+EFV (adjusted *p*=0.091) were both approaching statistical significance post-correction. RAL was also observed to have a significantly greater TYR concentration than control (adjusted *p*=0.007). The EFV and FTC conditions were approaching statistical significance post-correction, both with adjusted *p* values of 0.091. None of the ARVs were shown to have statistically significant differences from the control for the PHE/TYR ratio.

For the U373 cell line (Figures 4.14 and 4.15), the DMSO+IFN-γ positive control was observed to have lower TRP concentrations than the DMSO control post-correction (adjusted *p*=0.020) (Figure 4.14). In addition to this, FTC was observed to have a significantly greater TYR concentration than control (adjusted *p*=0.020) (Figure 4.15). Though it did not survive correction, RAL was observed to have a numerically greater TYR concentration than control that was approaching statistical significance (adjusted *p*=0.065).

Figure 4.12. Concentrations of TRP, KYN and the KYN/TRP Ratio Following Stimulation of U87 Cells with Antiretroviral Agents.

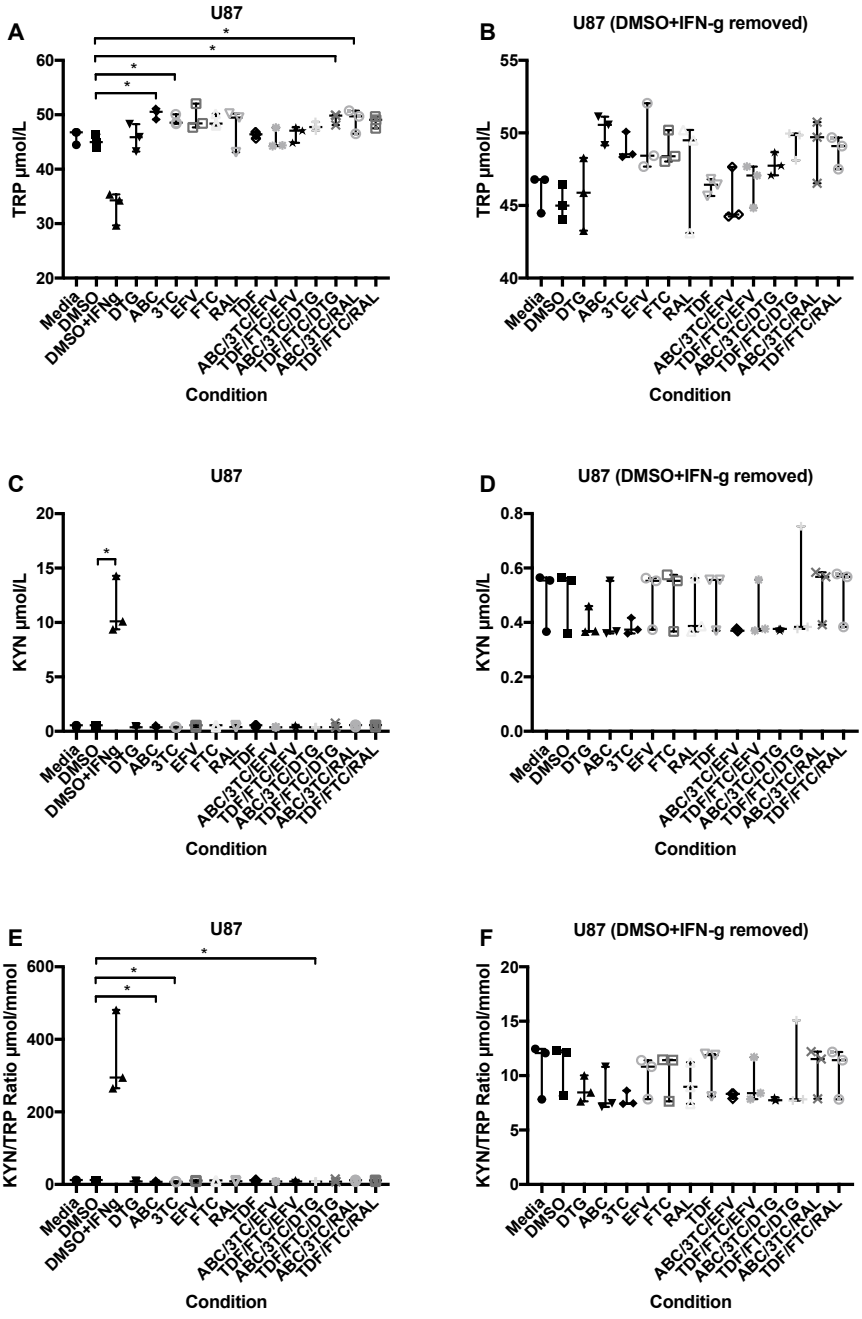

Footnote: Cell supernatant concentrations of TRP, KYN and the KYN/TRP ratio are shown following stimulation with antiretroviral agents individually and in clinically-relevant combinations (A, C and E, respectively). The DMSO+IFN-γ condition has been removed in B, D and F to allow easier visual comparison of the results for the ARVs. Horizontal lines represent median values and vertical lines show the interquartile range (IQR). Each symbol is indicative of one individual donor. Concentrations of ARVs are detailed in Section 2.2.4. Unadjusted *p* values for the Friedman's test are displayed on the graphs. **p*<0.05.

Figure 4.13. Concentrations of PHE, TYR, the PHE/TYR ratio and NEO Following Stimulation of U87 Cells with Antiretroviral Agents.

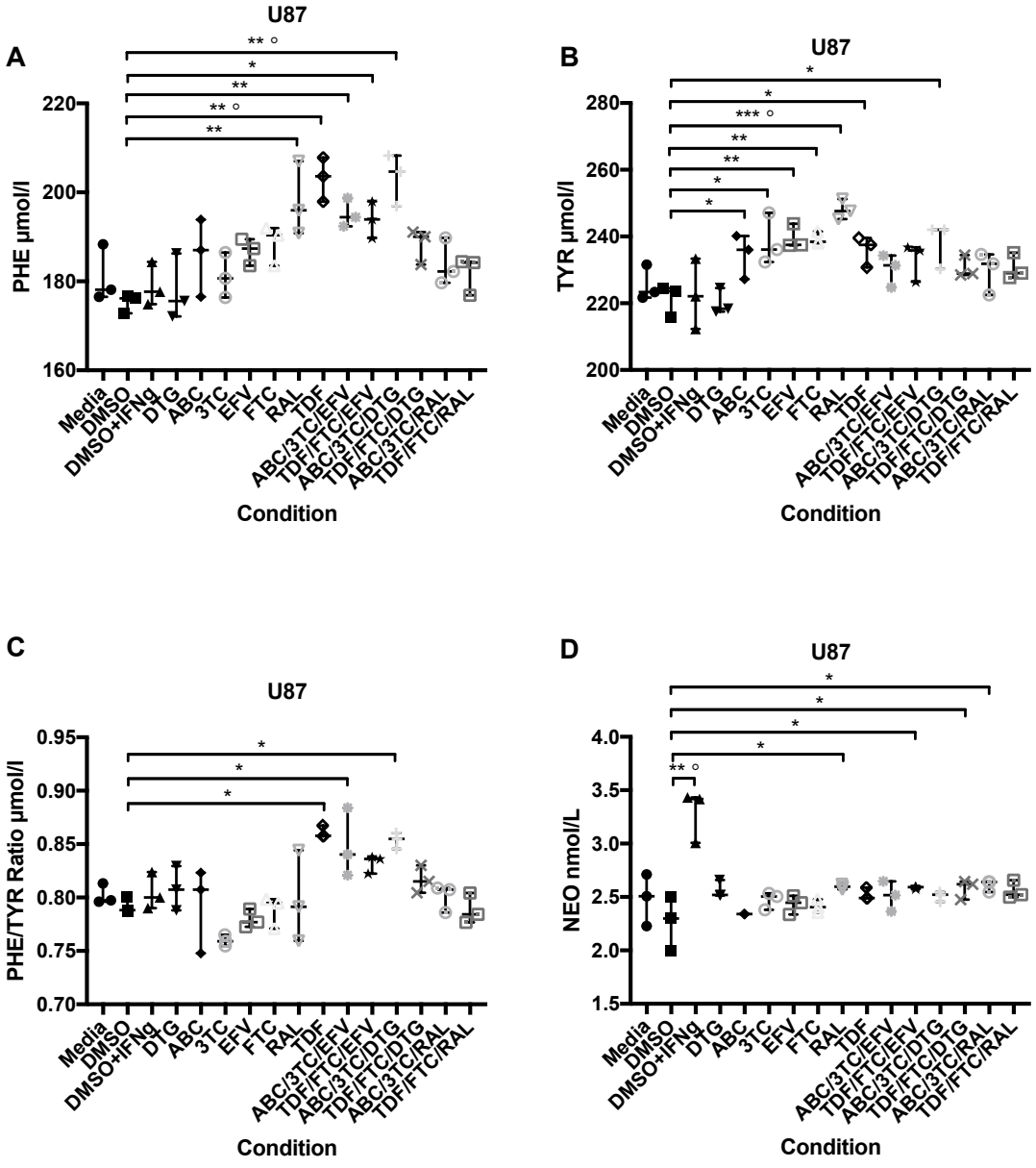

Footnote: Cell supernatant concentrations of PHE, TYR, the PHE/TYR ratio and NEO are shown following stimulation with antiretroviral agents individually and in clinically-relevant combinations (A, C, D and E, respectively). Horizontal lines represent median values and vertical lines show the interquartile range (IQR). Each symbol is indicative of one individual donor. Concentrations of ARVs are detailed in Section 2.2.4. Unadjusted *p* values for the Friedman's test are displayed on the graphs. **p*<0.05; ***p*<0.01; ****p*<0.001; °Association remains statistically significant following Dunn's correction for multiplicity.

Figure 4.14. Concentrations of TRP, KYN and the KYN/TRP Ratio following Stimulation of U373 Cells with Antiretroviral Agents.

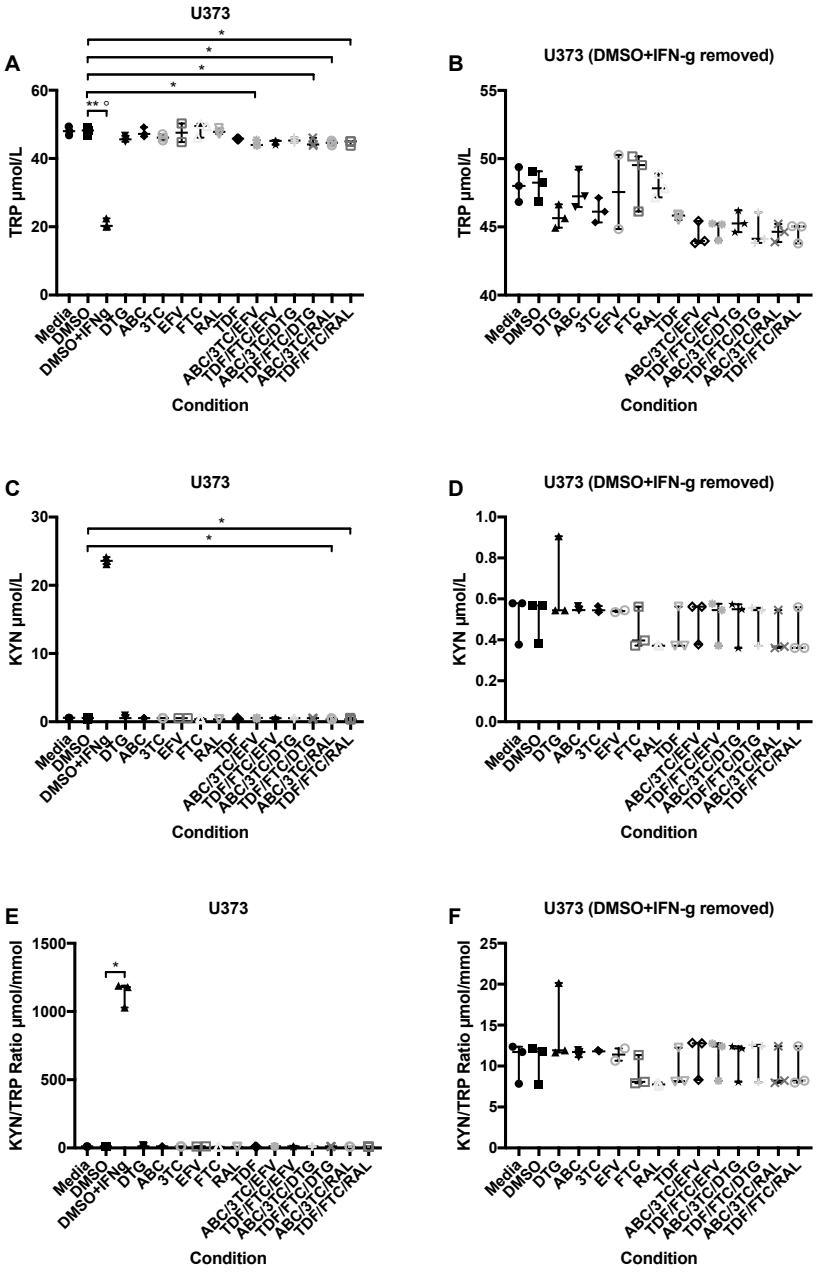

Footnote: Cell supernatant concentrations of TRP, KYN and the KYN/TRP ratio are shown following stimulation with antiretroviral agents individually and in clinically-relevant combinations (A, C and E, respectively). The DMSO+IFN-γ condition has been removed in B, D and F to allow easier visual comparison of the results for the ARVs. Horizontal lines represent median values and vertical lines show the interquartile range (IQR). Each symbol is indicative of one individual donor. Concentrations of ARVs are detailed in Section 2.2.4. Unadjusted *p* values for the Friedman's test are displayed on the graphs. **p*<0.05; ***p*<0.01; °Association remains statistically significant following Dunn's correction for multiplicity.

Figure 4.15. Concentrations of PHE, TYR, the PHE/TYR ratio and NEO Following Stimulation of U373 Cells with Antiretroviral Agents.

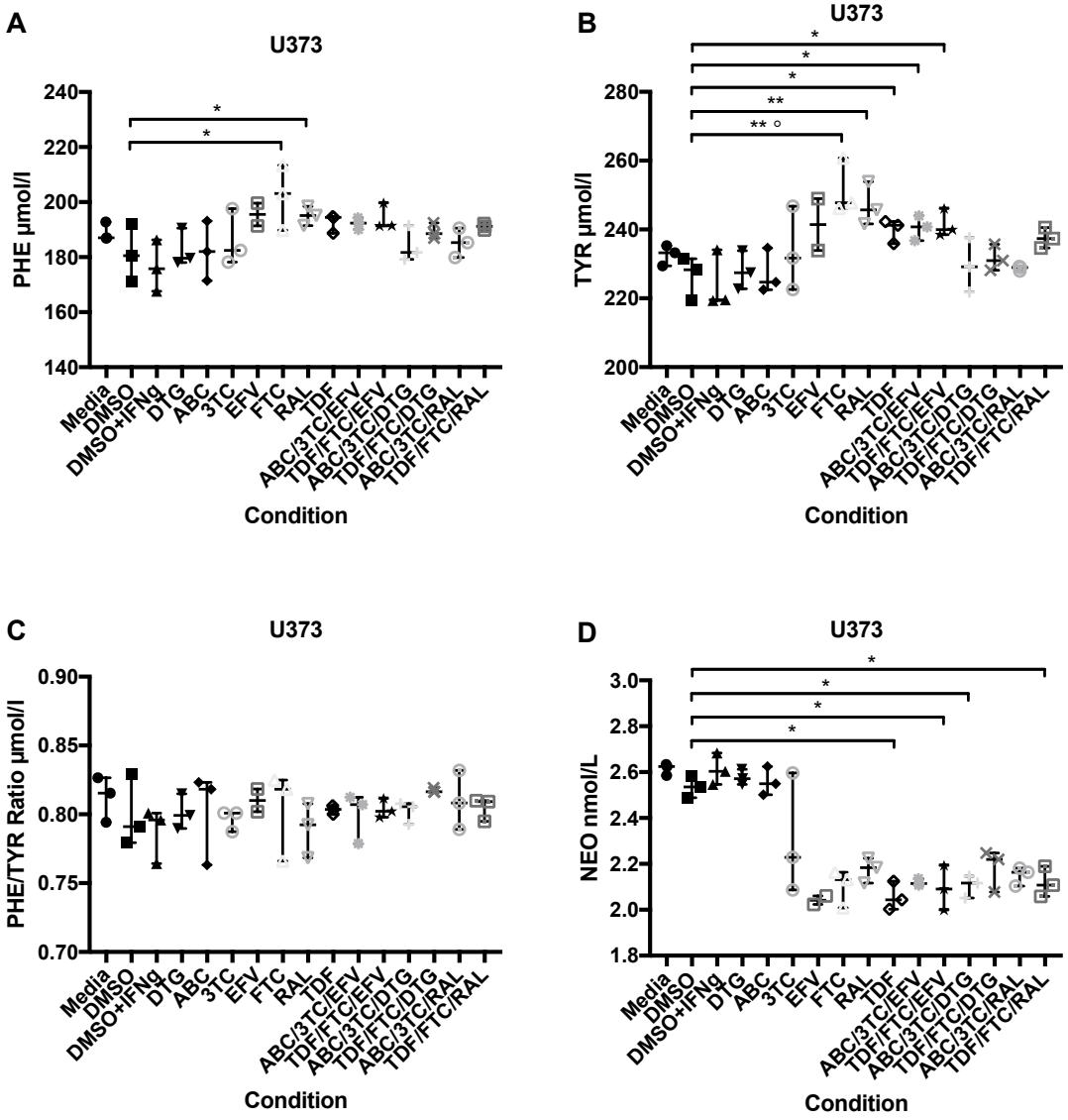

Footnote: Cell supernatant concentrations of PHE, TYR, the PHE/TYR ratio and NEO are shown following stimulation with antiretroviral agents individually and in clinically-relevant combinations (A, C, D and E, respectively). Horizontal lines represent median values and vertical lines show the interquartile range (IQR). Each symbol is indicative of one individual donor. Concentrations of ARVs are detailed in Section 2.2.4. Unadjusted *p* values for the Friedman's test are displayed on the graphs. *$p<0.05$; **$p<0.01$; °Association remains statistically significant following Dunn's correction for multiplicity.

For the EOC13.31 cell line (Figures 4.16 and 4.17), the only condition that remained statistically significantly different following multiplicity correction was RAL, which was observed to have a greater TRP concentration than the DMSO control (adjusted p=0.003) (Figure 4.16).

There were no statistically significant differences for any of the conditions in the EOC20 cell line (Figures 4.18 and 4.19).

Figure 4.16. Concentrations of TRP, KYN and the KYN/TRP Ratio Following Stimulation of EOC13.31 Cells with Antiretroviral Agents.

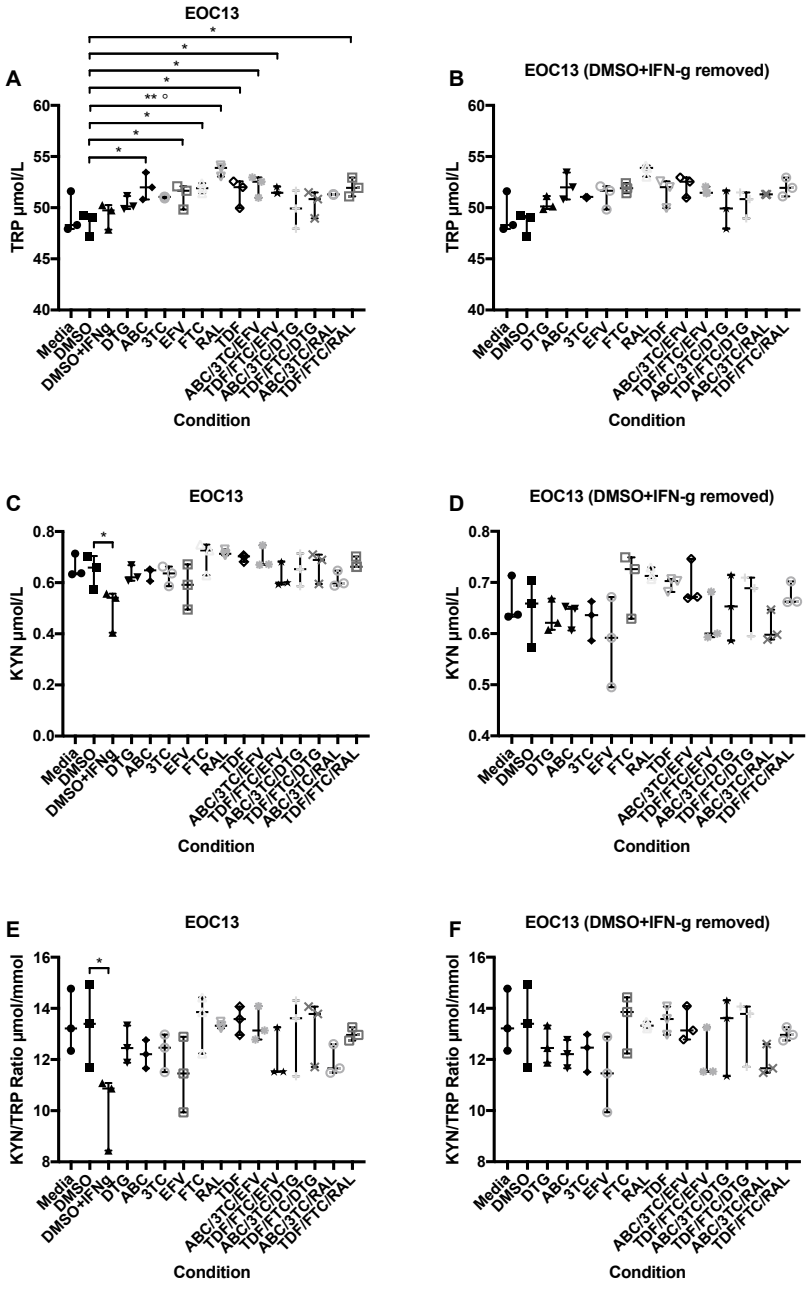

Footnote: Cell supernatant concentrations of TRP, KYN and the KYN/TRP ratio are shown following stimulation with antiretroviral agents individually and in clinically-relevant combinations (A, C and E, respectively). The DMSO+IFN-γ condition has been removed in B, D and F to allow easier visual comparison of the results for the ARVs. Horizontal lines represent median values and vertical lines show the interquartile range (IQR). Each symbol is indicative of one individual donor. Concentrations of ARVs are detailed in Section 2.2.4. Unadjusted *p* values for the Friedman's test are displayed on the graphs. **p*<0.05; ***p*<0.01; °Association remains statistically significant following Dunn's correction for multiplicity.

Figure 4.17. Concentrations of PHE, TYR, the PHE/TYR ratio and NEO Following Stimulation of EOC13.31 Cells with Antiretroviral Agents.

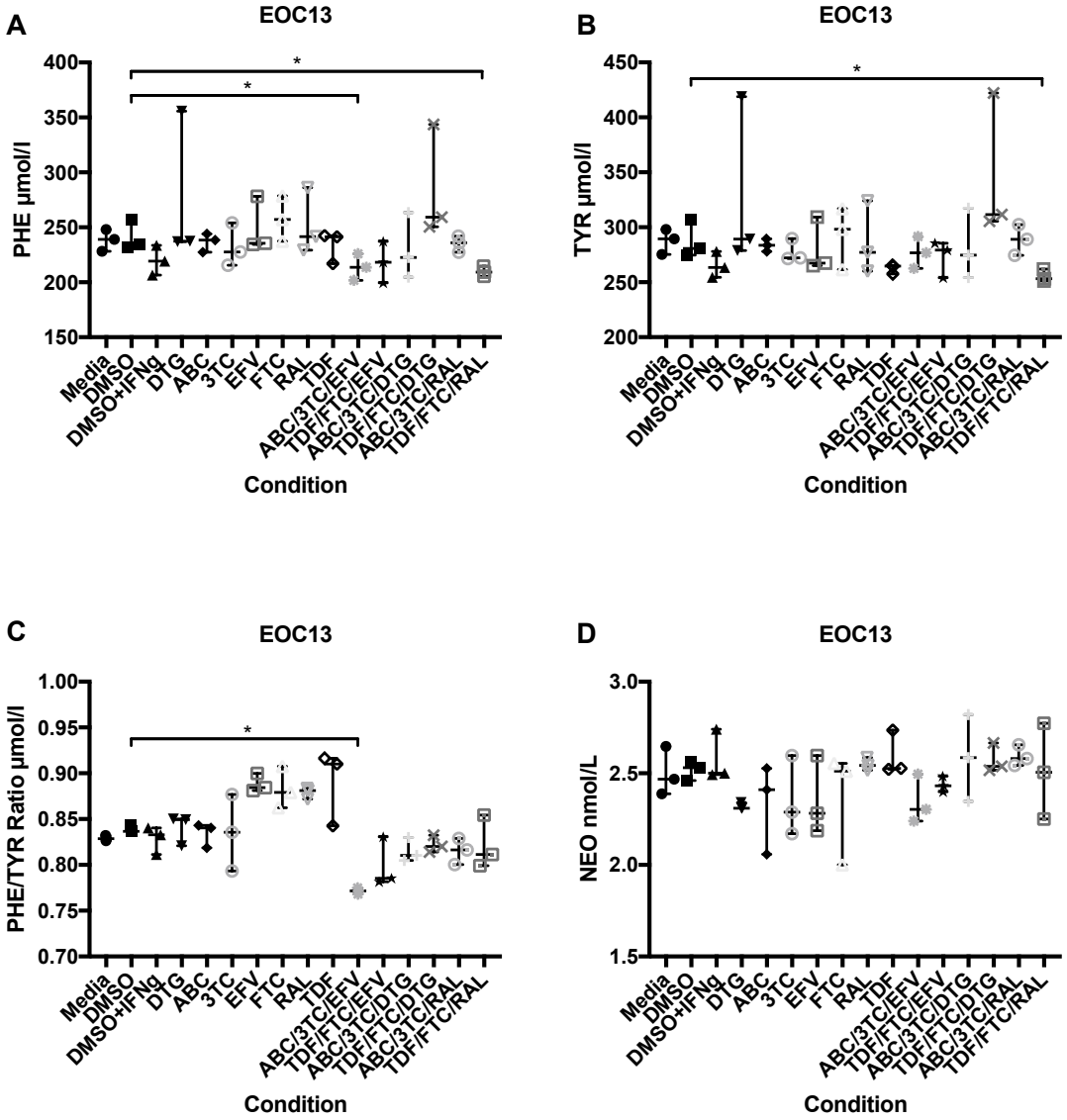

Footnote: Cell supernatant concentrations of PHE, TYR, the PHE/TYR ratio and NEO are shown following stimulation with antiretroviral agents individually and in clinically-relevant combinations (A, C, D and E, respectively). Horizontal lines represent median values and vertical lines show the interquartile range (IQR). Each symbol is indicative of one individual donor. Concentrations of ARVs are detailed in Section 2.2.4. Unadjusted *p* values for the Friedman's test are displayed on the graphs. *p<0.05.

Figure 4.18. Concentrations of TRP, KYN and the KYN/TRP Ratio Following Stimulation of EOC20 Cells with Antiretroviral Agents.

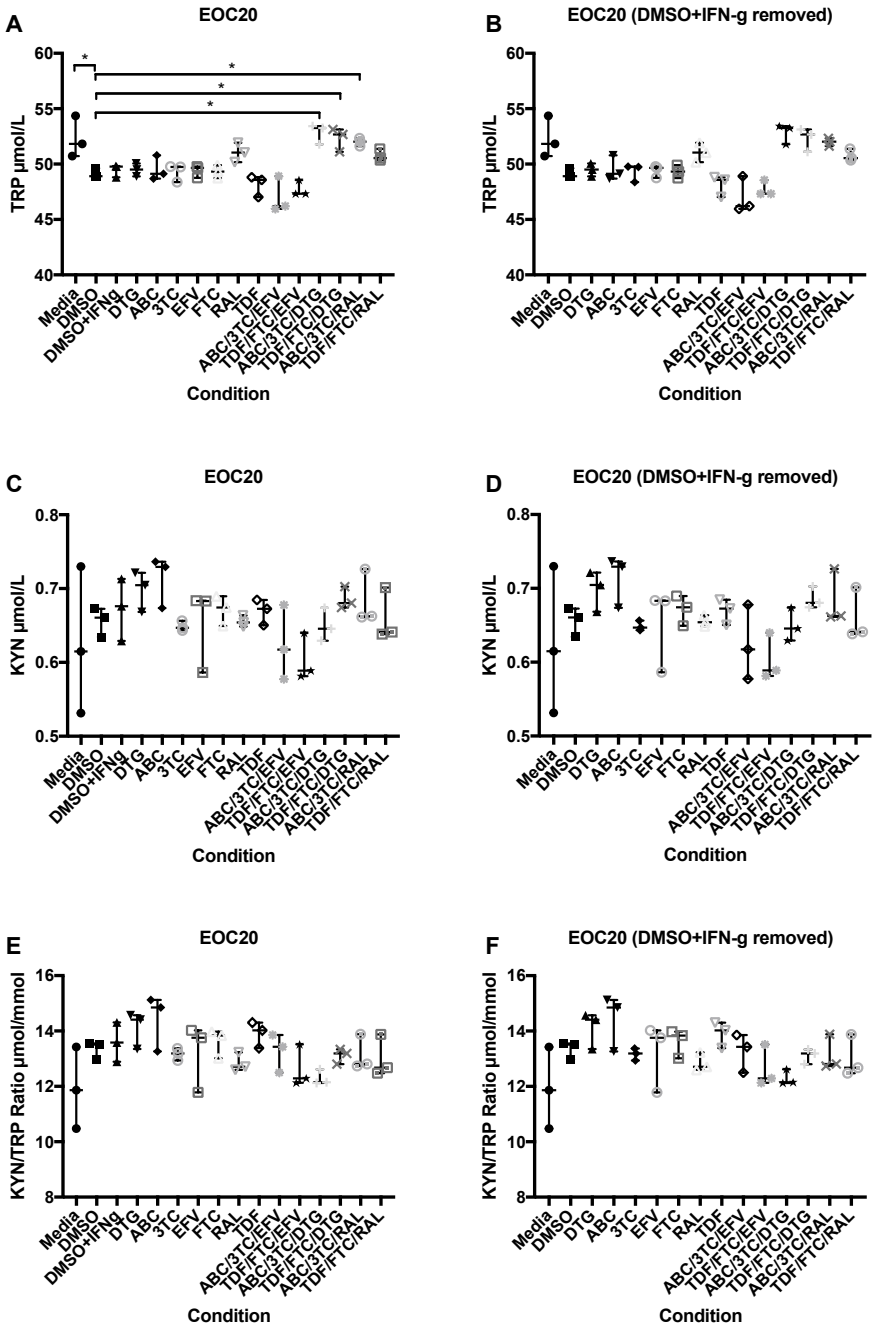

Footnote: Cell supernatant concentrations of TRP, KYN and the KYN/TRP ratio are shown following stimulation with antiretroviral agents individually and in clinically-relevant combinations (A, C and E, respectively). The DMSO+IFN-γ condition has been removed in B, D and F to allow easier visual comparison of the results for the ARVs. Horizontal lines represent median values and vertical lines show the interquartile range (IQR). Each symbol is indicative of one individual donor. Concentrations of ARVs are detailed in Section 2.2.4. Unadjusted *p* values for the Friedman's test are displayed on the graphs. **p*<0.05.

Figure 4.19. Concentrations of PHE, TYR, the PHE/TYR ratio and NEO Following Stimulation of EOC20 Cells with Antiretroviral Agents.

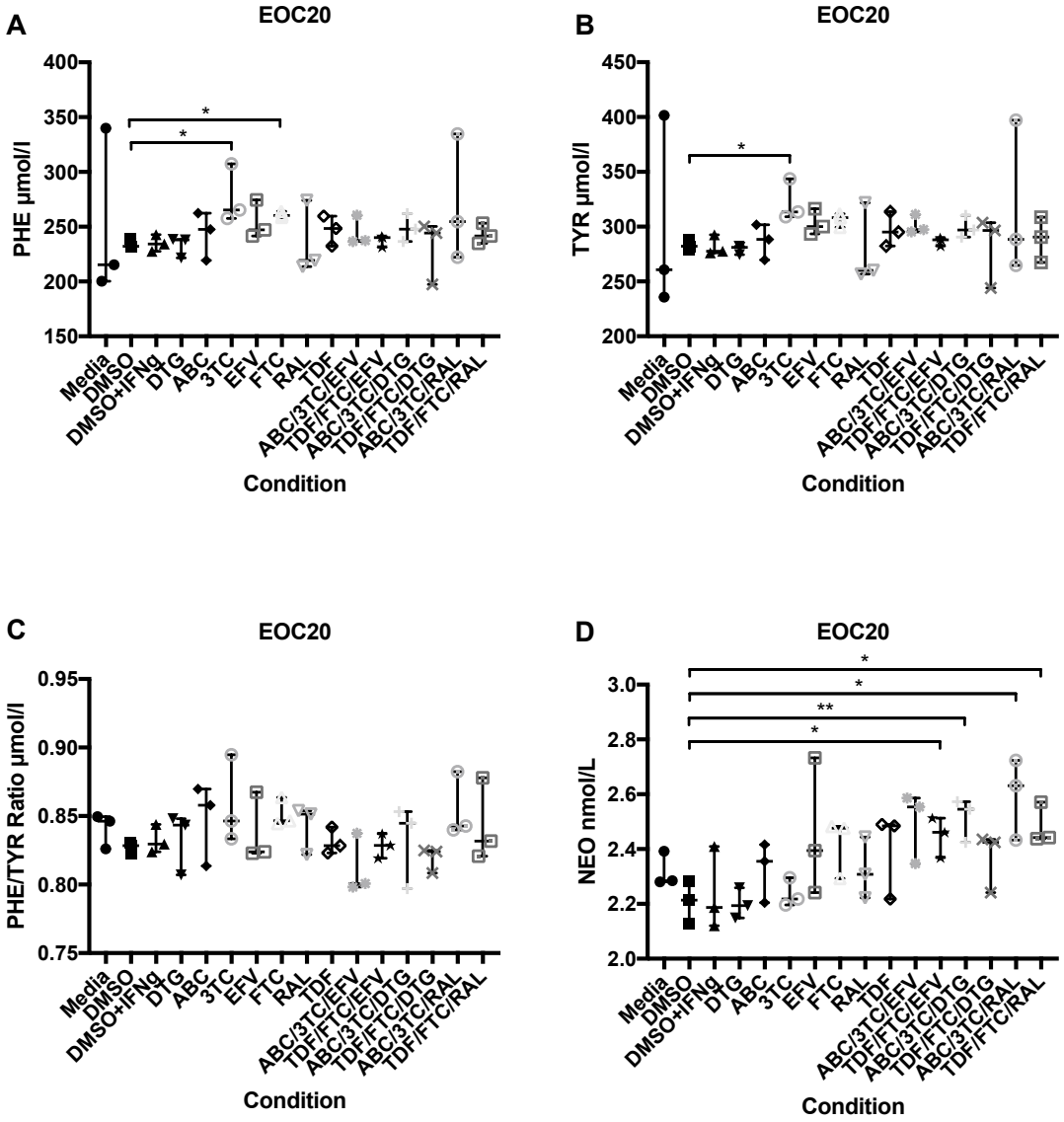

Footnote: Cell supernatant concentrations of PHE, TYR, the PHE/TYR ratio and NEO are shown following stimulation with antiretroviral agents individually and in clinically-relevant combinations (A, C, D and E, respectively). Horizontal lines represent median values and vertical lines show the interquartile range (IQR). Each symbol is indicative of one individual donor. Concentrations of ARVs are detailed in Section 2.2.4. Unadjusted *p* values for the Friedman's test are displayed on the graphs. *p<0.05; **p<0.01.

4.3 Discussion

In this series of experiments, the hypothesis was tested by exposing human PBMCs and hepatocyte, astrocyte and microglial cell lines to ARVs as individual agents or in clinically-relevant combinations. In the first experiment described in Section 4.2.1, the data tentatively suggest an increase in IDO activity in PBMCs when exposed to HIV-1 either alone or in combination with AZT or d4T as evidenced by increased concentrations of KYN in cell supernatant. These observations support the hypothesis that TRP metabolism is increased in their presence. There is no evidence to suggest that AZT or d4T alone contribute to TRP metabolism. These data must, however, be interpreted with caution due to the very low sample numbers and the potential for variability that arises from such low numbers. Interestingly, not all of the positive control conditions (i.e. HIV-1 alone or in combination with DMSO) had statistically significantly different KYN concentrations or KYN/TRP ratios compared to the DMSO control. Indeed, the largest difference was observed when HIV-1 and AZT or d4T were combined. The possibility of this being due to random fluctuations in the data due to low sample numbers cannot be discounted but one could speculate that there may be an additive effect resulting from the combination. These data warranted investigating the effects of other ARVs on TRP metabolism.

In the second experiment (Section 4.2.2) investigating the effect of a broader range of ARVs on TRP metabolism in PBMCs, very few signals of interest were observed. Similarly to the first experiment, AZT alone was not shown to have any effect in either the first experiment or in this one. Low sample numbers (N=6 and N=3, respectively) may have obscured any effect. The differences observed in the KYN concentrations for cells exposed to RPV and DMSO, and the differences in the KYN/TRP ratios for cells exposed to RPV and FTC, did not survive Dunn's correction for multiplicity and may be due to chance due to the low number of samples and the high number of comparisons. If this is a true effect, it is unknown as to whether this is a direct effect exerted on the IDO enzyme or via another mechanism (e.g. an increase TNF-α). These data, therefore, are not supportive of the hypothesis.

In the third experiment described in Section 4.2.3, no evidence was found to suggest that the ARVs investigated, either individually or in combination, at high or clinically-observed concentrations, increase TRP metabolism in PBMCs. In the second experiment (Section 4.2.3), RPV was observed to induce greater KYN concentrations, and RPV and FTC to induce greater

KYN/TRP ratios, than DMSO alone. These observations were not confirmed in this third experiment and so it must be concluded that the observations are either incorrect or that the effect size is sufficiently small to not be obvious in all donors. The observation that cells exposed to TDF+FTC+RAL had lower KYN/TRP ratios than DMSO alone was unexpected and not easily explained. TDF and FTC were also used in combination with DTG and EFV with this effect not being observed. Likewise, RAL was used in combination with ABC and 3TC with no discernible effect. Given the low sample numbers (N=3), the large number of comparisons made and the fact that statistical significance did not survive multiplicity correction, it is possible that is due to chance. In the exploratory analysis looking at the effects of ARVs on PAH activity, a number of ARV combinations were shown to have lower TYR concentrations than DMSO alone. However, visual inspection of the data revealed that this observation was driven by very low TYR concentrations from a single donor and so it must be interpreted with caution. It cannot be discounted that the ARV combinations are somehow interacting with the PAH enzyme, however, and this warrants further exploration, though this is not the focus of this PhD.

In summary, from this series of three small experiments, it must be concluded that there is no evidence to support the hypothesis that ARVs increase TRP metabolism in PBMCs.

In the final experiment described in Section 4.2.4, a number of different cell lines, including hepatocytes, astrocytes and microglia, were acutely exposed to clinically-relevant plasma concentrations of ARVs, both as individual agents and in commonly-used combinations. These data do not support the hypothesis that ARVs increase TRP metabolism in the cell lines used. Overall, very few statistically significant differences were observed for the ARV conditions compared to the DMSO control. In the THLE3 cell line, three ARV combinations (ABC+3TC+EFV, TDF+FTC+EFV and ABC+3TC+RAL) were observed to have lower TRP concentrations than the control, indicating that TRP was perhaps being metabolised, though this observation did not survive multiplicity correction. However, increases in KYN concentrations or KYN/TRP ratios for these combinations were not observed, suggesting that the TRP was not being converted into KYN by TDO. Indeed, the only cell line to show a significant difference between an ARV, in this case FTC, and the control was the microglial cell line, EOC13.31. Interestingly, an increase in TRP concentrations was observed in this case suggesting that TRP was not being metabolised. The reason for this increase is unclear.

Only the U87, U373 and EOC13.31 cell lines have been shown to express IDO in previous studies (390-392). However, even when stimulated with DMSO + IFN-γ, only the U373 cell line showed a significant decrease in TRP concentrations compared to DMSO alone. U87 and EOC13.31 cells showed a non-significant increase in KYN concentrations, suggesting that they may be producing small quantities of this metabolite. There are no prior data on TDO expression for THLE2, THLE3 or IDO expression for EOC20. The DMSO + IFN-γ positive control condition was shown to have lower TRP concentrations than DMSO alone for both THLE2 and THLE3 with corresponding increases in KYN concentrations for THLE2 and increased KYN/TRP ratios for both cell lines, though these did not survive multiplicity corrections. These data suggest that TDO is being upregulated in response to IFN-γ stimulation and that if ARV stimulation of the TDO enzyme was of a similar degree then it would have been observed in the THLE2 and THLE 3 cell lines. It may be that the effect size for the ARVs, if indeed there is one, is too low to detect with such a small sample size. On the basis of these data, however, it must be concluded that there is no effect. No difference was observed in these parameters in the EOC13.31 cell line even for the positive control, suggesting that this cell line may not express IDO to a sufficient degree to be detectable, if at all.

Of interest are the increases observed in PHE and TYR concentrations for some of the ARV conditions compared with controls in the astrocyte cell lines. PAH is primarily expressed in liver and kidney cells and is not thought to be expressed in astrocytes (395, 396). The observed increases are not easily explained. PHE has been shown to induce oxidative stress in rat astrocytes and increases in PHE in the U87 and U373 cells may represent a stress response to ARV-induced toxicity, though this is conjecture (396).

In summary, no evidence was observed to support the hypothesis that ARVs contribute to the metabolism of TRP and so the null hypothesis must be accepted. ARVs have not previously been shown to have any intrinsic effect on the IDO and TDO enzymes. In Section 4.1, it suggested that the enzyme inducing or inhibiting effects seen for agents such as EFV or the PIs could potentially affect the function of IDO or TDO. It was also postulated that ARVs might affect these enzymes due to their inherent toxicities and their effect on cell inflammation. No evidence has been observed to suggest that this is the case.

There are a number of limitations to these experiments. Firstly, the choice of cell types utilised should be challenged. The cells were chosen because previous studies have demonstrated

that they express IDO or, in the case of the cell lines in the final experiment, because they are analogous to cells that express IDO (or TDO for the hepatocytes) in humans. PBMCs are comprised of macrophages, lymphocytes and monocytes. Both macrophages and monocytes express the KYN pathway in its entirety and are potent producers of IDO when exposed to IFN-γ (283, 354, 382). In these experiments, fresh PBMCs from healthy donors were used and, thus, they can reasonably be expected to react normally to IDO stimulation. Liver cells do not express IDO but do express TDO, which is also inducible by proinflammatory cytokines, such as IFN-γ and TNF-α (232, 233, 283). The THLE2 and THLE3 cell lines used in these experiments are derived from a non-tumorigenic adult human liver autopsy sample of epithelial cells and are widely used for experimentation. They have been shown to express normal hepatocyte phenotypic characteristics, including retaining cytochrome P450 (CYP450) enzyme activity, though no previous data were available on TDO activity in these cells (387). THLE cells were exposed to DMSO + IFN-γ and a statistically significant decrease in TRP concentrations and non-significant, numerical increases in KYN concentrations and the KYN/TRP ratios were observed suggesting that these cells are capable of metabolising TRP and are likely to be suitable cell types these experiments. Astrocytes express IDO and are capable of producing large amounts of the early KYN pathway metabolites, such as KYN and KYNA, but because they do not express KYN(OH)ase they cannot convert KYN into 3-HK and, therefore, cannot produce KYN metabolites from later in the pathway without the addition of 3-HAA. Essentially, the pathway is split in half in astrocytes (235, 308). Both the U87 and U373 cell lines have been shown to highly express IDO, making them suitable candidates for this type of experimentation (390-392). Microglia express the KYN pathway in its entirety, though they have been shown to play a lesser role in the catabolism of TRP than macrophages due to their threefold lower expression of IFN-γ (234, 235). The EOC13.31 and EOC20 cells are derived from spontaneously immortalised rodent microglial cell lines, which have not been genetically modified and maintain the ability to secrete many cytokines and reactive species (392, 393). Though they are not of human origin, the EOC13.31 cells have been shown to express IDO when induced by IFN-γ and TNF-α (392). However, no data exist on the expression of IDO in EOC20 cells, though they have been shown to produce large quantities of IFN-γ when stimulated with Toxoplasma *tachyzoite lysate Ags* (394). Neither of the EOC cell lines reacted to the positive control condition, suggesting either that the choice of positive control was not correct – perhaps TNF-α would be more suitable – or that this cell line may not express IDO to a sufficient degree to be detectable, if at all.

Secondly, the sample numbers used throughout these experiments are very low and this is a significant limitation as the any effect size would have to be reasonably large to be observed, meaning that more subtle effects may have been lost. In addition to this, individual variations between donors could heavily skew results. This is highlighted by the fact that not all of the DMSO + HIV-1 or DMSO + IFN-γ positive control conditions were shown to be significantly different from the DMSO alone control. It is possible that a type II error has been made because of low numbers. Ideally, these experiments should have been performed with greater sample numbers but this type of laboratory work is very labour intensive.

The control condition in these experiments was DMSO. DMSO is a solvent that is capable of solubilising pharmacological compounds and is widely used in *in vitro* studies (397). It is considered to be relatively non-toxic to cell cultures at low concentrations but its' physiological and pharmacological effects are not fully understood. A number of recently published studies have sought to establish its' effects on cell cultures and to understand the concentrations at which it is cytotoxic (397-399). In PBMCs, concentrations of 1% and 2% have been shown to reduce the proliferation of lymphocytes, including CD4+ and CD8+ T lymphocytes, and at higher concentrations (5% and 10%) induce cell death. Of particular note is DMSOs ability to reduce PBMC cell inflammation by reducing cell activation and production of IL-2, TNF-α and IFN-γ at concentrations of 5% and 10% (397), and reduction of IL-6 at concentrations of 1% (398). In Mono Mac 6 monocyte cells, concentrations of 0.25% and 0.5% significantly increased IL-6 release (398). In another study, DMSO 1% was shown to potentiate drug toxicity from a variety of different compounds in THLE cell cultures compared with a concentration of 0.2% (399). The concentration of DMSO used in the experiments in this Chapter was 0.01%. Whilst, no specific data exist for the cell lines or drugs used in these experiments, the potential for differential effects on ARV toxicity and the cells reactions to inflammation should not be entirely discounted. An attenuation of inflammatory responses cannot be excluded.

In summary, despite these limitations, it must be concluded that there is no evidence to support the hypothesis that ARVs increase TRP metabolism in the cell lines used in these experiments.

5 A CROSS-SECTIONAL, CLINICAL PILOT STUDY TO INVESTIGATE TRYPTOPHAN METABOLISM IN PEOPLE LIVING WITH HIV IN THE CHARTER COHORT

5.1 Introduction

The available data on the effects of TRP metabolism on cognitive performance and mood disorders in PLWH (Sections 1.9.4 and 1.9.5) are not conclusive. A cross-sectional analysis of historical case notes and archived CSF and plasma samples collected from HIV+ and HIV- individuals, either with or without CI and/or MDD, who were taking part in the CNS HIV Antiretroviral Therapy Effects Research (CHARTER) study (Section 3.1) was conducted. The first hypothesis for this thesis states that TRP metabolism is increased in the presence of the HIV-1 virus or ARV agents (Section 1.1.2). This was tested clinically by determining if chronic immune activation in HIV+ individuals, as estimated by concentrations of inflammatory biomarkers (TNF-α, NEO), is associated with increased TRP metabolism via the KYN pathway (as measured by TRP and KYN concentrations and the KYN/TRP ratio). Firstly, comparisons of the biochemical and immunological markers in CSF and plasma between the HIV+ and HIV- groups were assessed using Mann-Whitney *U* tests. This approach was repeated to compare the biochemical and immunological markers in CSF and plasma from a sub-group of HIV+ individuals who were taking virologically suppressive ART (n=44) with the HIV- group. Multivariate linear regression analyses were then conducted to explore the relationship between TNF-α and NEO concentrations in CSF and plasma with the clinically relevant covariates HIV-1 RNA in CSF and plasma (≤ or >50 cps/mL), current CD4+ cell count, and ART-use. The relationship between TNF-α and NEO and the KYN/TRP ratio in CSF and plasma from HIV+ individuals was analysed in another multivariate model.

The second hypothesis states that increased TRP metabolism is associated with poorer cognitive performance and increased rates of depression in people living with HIV (Section 1.1.2). To test this, logistic regression analyses were performed for the KYN/TRP ratio in both CSF and plasma and either binary MDD or CI status.

To account for the potential confounding effects of the use of antidepressant agents in some patients, Mann-Whitney *U* tests were performed to determine whether there was a correlation between the use of antidepressant medication and TRP, KYN and the KYN/TRP ratio. These were performed for the overall HIV+ group, as well as for subjects with either HIV-1-RNA >50 cps/mL or ≤50 cps/mL in both CSF and plasma.

The role of phenylalanine-hydroxylase (PAH) activity (as measured by the phenylalanine-to-tyrosine [PHE/TYR] ratio) was also explored.

5.2 Results

5.2.1 Baseline Characteristics

Case notes and plasma and CSF samples were identified for 157 subjects (HIV+, n=91; HIV-, n=56). Their demographic and HIV profile are detailed in Table 5.1, below. Of the 91 HIV+ subjects, 65 were receiving ART (information on their ARV regimens was available for 44/65 subjects). Those on ART had lower nadir CD4+ cell counts (144 vs. 330 cells/uL). In the HIV+ group, the median current CD4+ count was 421 cells, reflecting substantial immune recovery on ART. HIV+ subjects had higher rates of CI (39% vs. 14%), MDD (46% vs. 15%) and current antidepressant use (serotonin reuptake inhibitors, including both tricyclic antidepressants and selective serotonin reuptake inhibitors; 30% vs. 3%) compared to HIV- participants. The CSF and plasma samples were collected from subjects taking part in the CHARTER study (95) between 1991 and 2009 and subsequently stored at -80^{o}C.

Table 5.1. Patient Demographics and HIV Profile

	HIV+	HIV-	*P* Value	HIV+ on ART	HIV+ Not on ART	*P* Value
n	91	66	-	65	26	-
Age, yrs, Median (IQR)	40 (34,44)	35 (28,44)	0.027	40 (36,44)	37 (32,42)	0.085
Gender, Male	80 (88%)	61 (92%)	0.512	56 (86%)	24 (92%)	0.647
Ethnicity						
White	47 (52%)	36 (55%)	0.352	33 (51%)	14 (54%)	0.810
Black	21 (23%)	13 (20%)		14 (22%)	7 (27%)	
Asian	1 (1%)	2 (3%)		1 (2%)	0 (0%)	
Hispanic	20 (22%)	10 (15%)		15 (23%)	5 (19%)	
Other	2 (2%)	5 (8%)		2 (3%)	0 (0%)	
Current CD4 cells/uL, Median (IQR) [a]	421 (251,594)	820 (670,989)	<0.001	435 (219,609)	402 (263,510)	0.667
Nadir CD4 cells/uL, Median (IQR)	191 (35,300)	-	-	144 (23,222)	330 (200,450)	<0.001
HCV+ [b]	5 (6%)	9 (17%)	0.102	3 (5%)	2 (3%)	0.979
GDS ≥0.5 [c]	35 (39%)	9 (14%)	0.002	28 (44%)	7 (28%)	0.260
MDD	42 (46%)	10 (15%)	<0.001	27 (42%)	15 (58%)	0.163
Antidepressant Use						
Ever [d]	25 (32%)	12 (21%)	0.240	15 (27%)	10 (43)	0.237
Current [e]	27 (30%)	2 (3%)	<0.001	21 (32%)	6 (23%)	0.537
Current ARV Regimen [f]						
NRTI(s) in regimen				40 (91%)		
NNRTI-based	-	-	-	14 (32%)	-	-
PI-based				20 (45%)		
NRTI-based				5 (11%)		
Other				5 (11%)		

	HIV+	HIV-	*P* Value	HIV+ on ART	HIV+ Not on ART	*P* Value
HIV-1-RNA, Plasma						
Median HIV-1-RNA (IQR)[g]				<50 (0,393)	18,350 (7293,66600)	<0.001
	-	-	-			
HIV-1-RNA [g]						
≤50 cps/mL				n=40	n=0	-
>50 cps/mL				n=22	n=25	
HIV-1-RNA, CSF						
Median HIV-1-RNA (IQR)[h]				<50 (0,6)	315 (73,1220)	<0.001
HIV-1-RNA [h]						
≤50 cps/mL	-	-	-	n=44	n=5	-
>50 cps/mL				n=6	n=16	

Key: GDS, global deficit score; ART, antiretroviral therapy; CSF, cerebrospinal fluid; IQR, interquartile range.

[a] HIV+, n=88; HIV-, n=64; On ART, n=63; Not On ART, n=25

[b] HIV+, n=78; HIV-, n=53; On ART, n=55; Not On ART, n=23

[c] HIV+, n=89; HIV-, n=63; On ART, n=64; Not On ART, n=25

[d] HIV+, n=79; HIV-, n=57; On ART, n=56; Not On ART, n=23

[e] HIV+, n=91; HIV-, n=65; On ART, n=65; Not On ART, n=26

[f] ARV regimen information only available for n=44

[g] On ART, n=62; Not On ART, n=25

[h] On ART, n=50; Not On ART, n=21

5.2.2 Univariate Analysis of Biochemical and Immunological Markers

The concentrations of each of the biochemical and immunological markers in both CSF and plasma are presented in Tables 5.2 and 5.3, respectively.

Significantly higher concentrations of TNF-α were observed in the CSF of both the overall HIV+ group (p<0.001; α=0.0027) and the ART-treated aviraemic (≤50 cps/mL HIV-1-RNA) sub-group (p=0.008; α=0.0027) compared with HIV- controls, though the sub-group comparison did not remain significant post-Bonferroni correction. No differences were observed in plasma concentrations of TNF-α in either group.

Higher concentrations of NEO were observed in both the CSF and plasma of the HIV+ group (p<0.001 and p=0.02, respectively; α=0.0027) and in the CSF of the aviraemic sub-group (p=0.002; α=0.0027) compared with controls. Again, the observed difference in plasma was not statistically significant after Bonferroni correction.

Higher concentrations of nitrite were observed in plasma, but not in CSF, of both the overall HIV+ group (p=0.010; α=0.0027) and the aviraemic sub-group (p=0.036; α=0.0027) compared with controls, though neither observation remained significant following Bonferroni correction.

Lower concentrations of TRP were observed in both the CSF and plasma of the HIV+ group (p=0.012 and p<0.001, respectively; α=0.0027) and in the plasma of the aviraemic sub-group (p=0.004; α=0.0027) compared with controls. No significant differences were observed for KYN. HIV+ participants had greater KYN/TRP ratios in plasma than HIV- controls (p=0.027; α=0.0027). Only the difference in TRP concentration between the HIV+ and HIV- groups in plasma remained significant following the Bonferroni correction.

Concentrations of PHE and TYR did not differ between any of the groups. A significantly elevated PHE/TYR ratio was observed in the CSF of the HIV+ group compared with controls (p=0.038; α=0.0027), though this was not significant following Bonferroni correction. There were no significant differences observed in plasma, or in the CSF and plasma of the aviraemic sub-group.

Table 5.2. Univariate Analysis of Biochemical and Immunological Parameters in CSF, HIV+ Individuals and HIV+ Individuals with HIV-1-RNA <50 cps/mL vs. HIV- Controls

	HIV- (n=66)		HIV+ (n=91)		HIV+ vs HIV- *P* Value	HIV+, <50 cps/mL (n=44)		HIV+, <50 cps/mL vs HIV- *P* Value
	n	median (IQR)	n	median (IQR)		n	median (IQR)	
TNF-α (µmol/mmol)	19	3.84 (3.59,4.47)	33	6.40 (4.92,7.18)	<0.001	21	5.43 (3.85,6.71)	0.008
NEO (µmol/mmol)	43	4.30 (3.77,4.65)	65	5.15 (4.41,9.23)	<0.001	42	4.90 (4.26,6.26)	0.002
TRP (µmol/mmol)	43	1.98 (1.58,2.52)	63	1.66 (1.21,2.05)	0.012	41	1.72 (1.29,2.09)	0.076
KYN (µmol/mmol)	43	0.24 (0.09,0.27)	63	0.13 (0.09,0.27)	0.621	41	0.10 (0.09,0.27)	0.536
KYN/TRP ratio (µmol/mmol / µmol/mmol)	43	76.72 (44.20,151.17)	63	101.77 (54.19,165.21)	0.262	41	90.80 (51.92,151.90)	0.516
TYR (µmol/mmol)	24	9.20 (7.77,13.32)	28	9.05 (6.80,11.14)	0.229	18	9.05 (7.01,11.41)	0.315
PHE (µmol/mmol)	24	8.68 (6.61,10.16)	28	9.17 (7.68,13.08)	0.174	18	9.17 (7.64,13.89)	0.195
PHE/TYR ratio (µmol/mmol / µmol/mmol)	24	0.77 (0.66,1.09)	28	0.96 (0.78,1.29)	0.038	18	0.95 (0.74,1.31)	0.089
Nitrite (µmol/mmol)	13	0.40 (0.10,1.50)	11	1.00 (0.40,1.20)	0.393	7	1.00 (0.40,1.20)	0.420

Key: TNF-α, tumour necrosis factor-alpha; NEO, neopterin; TRP, tryptophan; KYN, kynurenine; TYR, tyrosine; PHE, phenylalanine.

Table 5.3. Univariate Analysis of Biochemical and Immunological Parameters in Plasma, HIV+ Individuals and HIV+ Individuals with HIV-1-RNA <50 cps/mL vs. HIV- Controls

	HIV- (n=66)		HIV+ (n=91)		HIV+ vs HIV- *P* Value	HIV+, <50 cps/mL (n=44)		HIV+, <50 cps/mL vs HIV- *P* Value
	n	median (IQR)	n	median (IQR)		n	median (IQR)	
TNF-α (µmol/mmol)	19	7.77 (6.16,10.41)	28	7.75 (4.72,10.39)	0.948	12	5.40 (3.49,8.13)	0.057
NEO (µmol/mmol)	66	5.65 (4.76,8.60)	84	9.27 (4.98,15.64)	0.020	32	7.60 (4.62,14.30)	0.265
TRP (µmol/mmol)	66	55.39 (46.04,66.08)	84	45.85 (38.38,54.32)	<0.001	32	47.06 (40.41,55.28)	0.004
KYN (µmol/mmol)	66	2.08 (1.52,2.53)	84	2.07 (1.61,2.66)	0.791	32	1.88 (1.32,2.55)	0.625
KYN/TRP ratio (µmol/mmol / µmol/mmol)	66	37.56 (26.36,53.34)	84	47.49 (30.51,61.42)	0.027	32	41.37 (28.24,53.59)	0.413
TYR (µmol/mmol)	47	49.15 (42.76,64.72)	55	46.80 (38.99,58.18)	0.200	20	49.07 (42.56,61.56)	0.902
PHE (µmol/mmol)	47	66.94 (56.42,85.87)	55	65.49 (56.52,88.95)	0.928	20	73.82 (54.11,92.53)	0.468
PHE/TYR ratio (µmol/mmol / µmol/mmol)	47	1.37 (1.05,1.71)	55	1.46 (1.05,1.77)	0.309	20	1.56 (0.92,1.76)	0.476
Nitrite (µmol/mmol)	47	16.86 (12.09,28.24)	55	25.30 (16.68,35.58)	0.010	20	26.49 (20.55,33.89)	0.036

Key: TNF-α, tumour necrosis factor-alpha; NEO, neopterin; TRP, tryptophan; KYN, kynurenine; TYR, tyrosine; PHE, phenylalanine.

5.2.3 Multivariate Analyses

5.2.3.1 Clinical Parameters and Their Association with Immune Activation Markers in CSF and Plasma

In the first model, viraemia and ART-use positively correlated with TNF-α and NEO concentrations in CSF, whilst lower current CD4+ cell counts were associated with higher concentrations of these markers (Table 5.4). Viraemia and current CD4+ cell count were the strongest predictors of TNF-α and NEO. Nadir CD4+ cell count was also included as a covariate in the model but was not significantly correlated with either marker. The models evaluating TNF-α and NEO in plasma were not statistically significant.

Table 5.4. Clinical Parameters and Their Association with Immune Activation Markers in CSF and Plasma

Inflammatory Biomarker	Correlation	*P* Value	R^2	ANOVA Sig.
TNF-α in CSF				
CSF HIV-1 RNA >50 cps/mL	0.487	0.002		
Plasma HIV-1 RNA >50 cps/mL	0.408	0.009	0.354	0.030
Nadir CD4	-0.091	0.307		
Current CD4	-0.417	0.008		
On ART	0.294	0.048		
NEO in CSF				
CSF HIV-1 RNA >50 cps/mL	0.454	<0.001		
Plasma HIV-1 RNA >50 cps/mL	0.456	<0.001	0.364	<0.001
Nadir CD4	-0.162	0.098		
Current CD4	-0.419	<0.001		
On ART	0.305	0.007		
TNF-α in plasma				
CSF HIV-1 RNA >50 cps/mL	0.479	0.005		
Plasma HIV-1 RNA >50 cps/mL	0.407	0.016	0.330	0.095
Nadir CD4	-0.135	0.246		
Current CD4	-0.220	0.130		
On ART	0.323	0.047		
NEO in plasma				
CSF HIV-1 RNA >50 cps/mL	0.321	0.005		
Plasma HIV-1 RNA >50 cps/mL	0.192	0.044	0.122	0.163
Nadir CD4	-0.031	0.390		
Current CD4	-0.175	0.059		
On ART	0.141	0.100		

Key: TNF-α, tumour necrosis factor-alpha; NEO, neopterin; R^2, coefficient of determination.

5.2.3.2 Immune Activation Markers and Their Association with the KYN/TRP and PHE/TYR Ratios in CSF and Plasma

In the second model (Table 5.5), which investigated the relationship between the inflammatory markers and the KYN/TRP ratio, levels of TNF-α and NEO positively correlated with the KYN/TRP ratio in both CSF (R^2=0.277; ANOVA *p*=0.008) and plasma (R^2=0.674; ANOVA *p*<0.001). This analysis was repeated for the PHE/TYR ratio. Due to missing TNF-α values in the data, it was not possible to calculate the correlation between TNF-α and the PHE/TYR ratio and so only the correlation with NEO is shown (Table 5.6). No statistically significant relationships were observed.

Table 5.5. The KYN/TRP Ratio in CSF and Plasma and Its Relationship with Immune Activation Markers

	Correlation	*P* Value	R^2	ANOVA *P* Value
KYN/TRP Ratio in CSF				
TNF-α in CSF	0.487	0.002	0.277	0.008
Neopterin in CSF	0.457	<0.001		
KYN/TRP Ratio in plasma				
TNF-α in plasma	0.741	<0.001	0.674	<0.001
Neopterin in plasma	0.211	0.027		

Key: TNF-α, tumour necrosis factor-alpha; NEO, neopterin; TRP, tryptophan; KYN, kynurenine; R^2, coefficient of determination.

Table 5.6. The PHE/TYR Ratio in CSF and Plasma and Its Relationship with NEO

	Correlation	*P* Value	R^2	ANOVA *P* Value
KYN/TRP Ratio in CSF				
Neopterin in CSF	0.134	0.248	0.018	0.495
KYN/TRP Ratio in plasma				
Neopterin in plasma	0.213	0.059	0.045	0.118

Key: TNF-α, tumour necrosis factor-alpha; NEO, neopterin; TRP, tryptophan; KYN, kynurenine; R^2, coefficient of determination.

5.2.3.3 The KYN/TRP Ratio and its Relationship with Major Depressive Disorder and Cognitive Impairment

In the models evaluating the relationship between the KYN/TRP ratio and cognitive and psychiatric outcomes, there were no significant correlations for any of the groups in CSF for either MDD or CI status (Table 5.7). However, in plasma, a lower KYN/TRP ratio was weakly associated with MDD in the HIV+ group, although this was not statistically significant (χ^2=3.458 [1, n=84], B=-1.643, *p*=0.063; α=0.0031). Stratification by binary viraemia status identified that this trend was driven by the aviraemic sub-group (χ^2=4.874 [1, n=32], B=-4.054, *p*=0.027; α=0.0031), (Table 5.7 and Figure 5.1), though this was not significant following Bonferroni correction. A similar association was observed for the KYN/TRP ratio in plasma and CI. Following Bonferroni correction, non-significant negative correlation trends were observed in both the overall HIV+ group (χ^2=4.312 [1, n=82], B=-1.926, *p*=0.038; α=0.0031), and the aviraemic sub-group (χ^2=3.388 [1, n=32], B=-3.078, *p*=0.066; α=0.0031). Significant correlations were not observed for either the viraemic sub-group or the HIV- controls (Table 5.7 and Figure 5.2).

Table 5.7. The KYN/TRP Ratio in CSF and Plasma and its Relationship with Major Depressive Disorder and Cognitive Impairment

K/T Ratio and Outcome	χ^2	*P* Value
CSF		
KYN/TRP ratio and MDD status in HIV+ Individuals	0.134 (1, n=63)	0.714
KYN/TRP ratio and MDD status in patients with HIV-1-RNA >50 cps/mL	0.006 (1, n=20)	0.936
KYN/TRP ratio and MDD status in patients with HIV-1-RNA <50 cps/mL	0.048 (1, n=41)	0.826
KYN/TRP ratio and MDD status in HIV- individuals	1.240 (1, n=43)	0.265
KYN/TRP ratio and CI in HIV+ Individuals	0.379 (1, n=62)	0.538
KYN/TRP ratio and CI status in patients with HIV-1-RNA >50 cps/mL	3.508 (1, n=20)	0.061
KYN/TRP ratio and CI status in patients with HIV-1-RNA <50 cps/mL	0.159 (1, n=40)	0.690
KYN/TRP ratio and CI status in HIV- individuals	0.379 (1, n=62)	0.538
Plasma		
KYN/TRP ratio and MDD status in HIV+ Individuals	3.458 (1, n=84)	0.063
KYN/TRP ratio and MDD status in patients with HIV-1-RNA >50 cps/mL	0.299 (1, n=44)	0.585
KYN/TRP ratio and MDD status in patients with HIV-1-RNA <50 cps/mL	4.874 (1, n=32)	0.027
KYN/TRP ratio and MDD status in HIV- individuals	0.222 (1, n=66)	0.637
KYN/TRP ratio and NCI in HIV+ Individuals	4.312 (1, n=82)	0.038
KYN/TRP ratio and NCI status in patients with HIV-1-RNA >50 cps/mL	0.000 (1, n=43)	0.986
KYN/TRP ratio and NCI status in patients with HIV-1-RNA <50 cps/mL	3.388 (1, n=32)	0.066
KYN/TRP ratio and CI status in HIV- individuals	0.070 (1, n=63)	0.791

Key: TRP, tryptophan; KYN, kynurenine; MDD, major depressive disorder; CI, cognitive impairment; χ^2, chi square.

Figure 5.1. The KYN/TRP Ratio in Plasma and its Relationship with Major Depressive Disorder

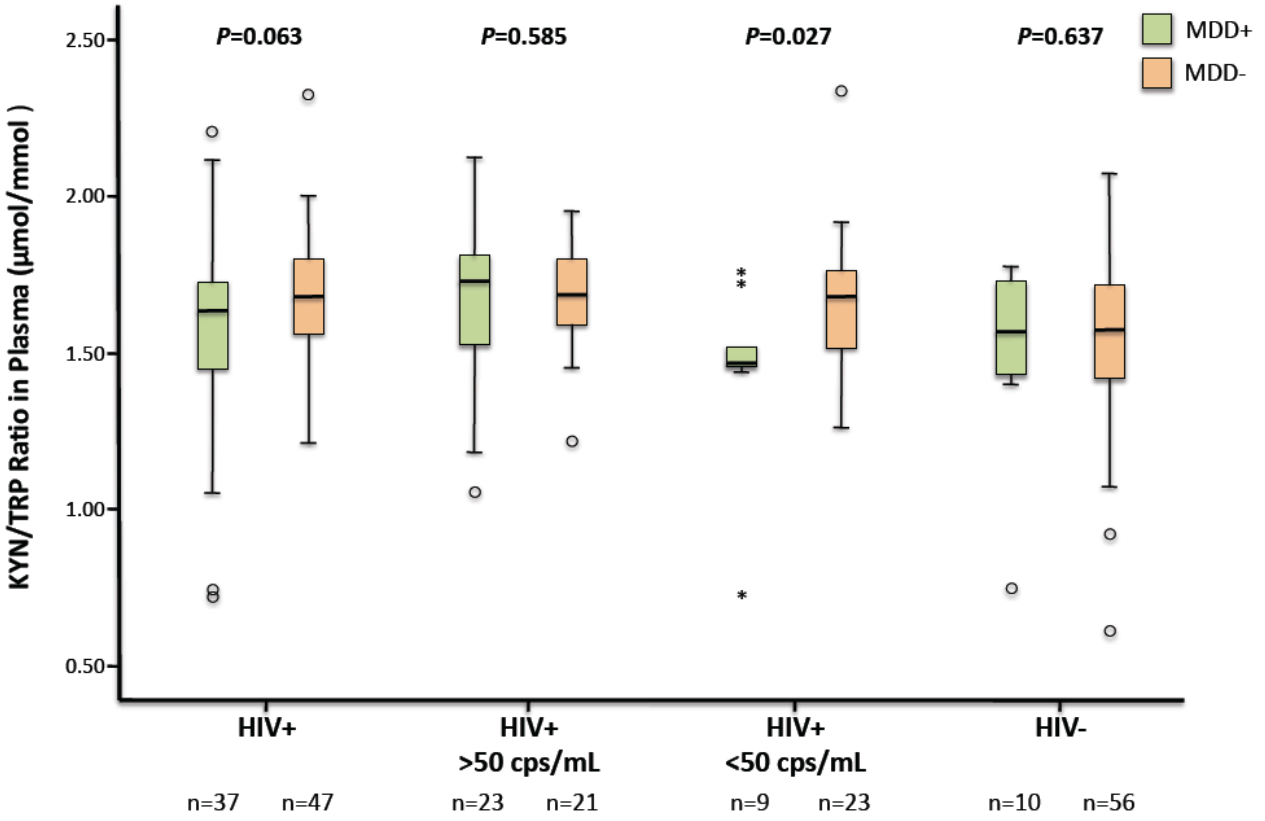

Key: TRP, tryptophan; KYN, kynurenine; MDD, major depressive disorder.

Figure 5.2. The KYN/TRP Ratio in Plasma and its Relationship with Cognitive Impairment

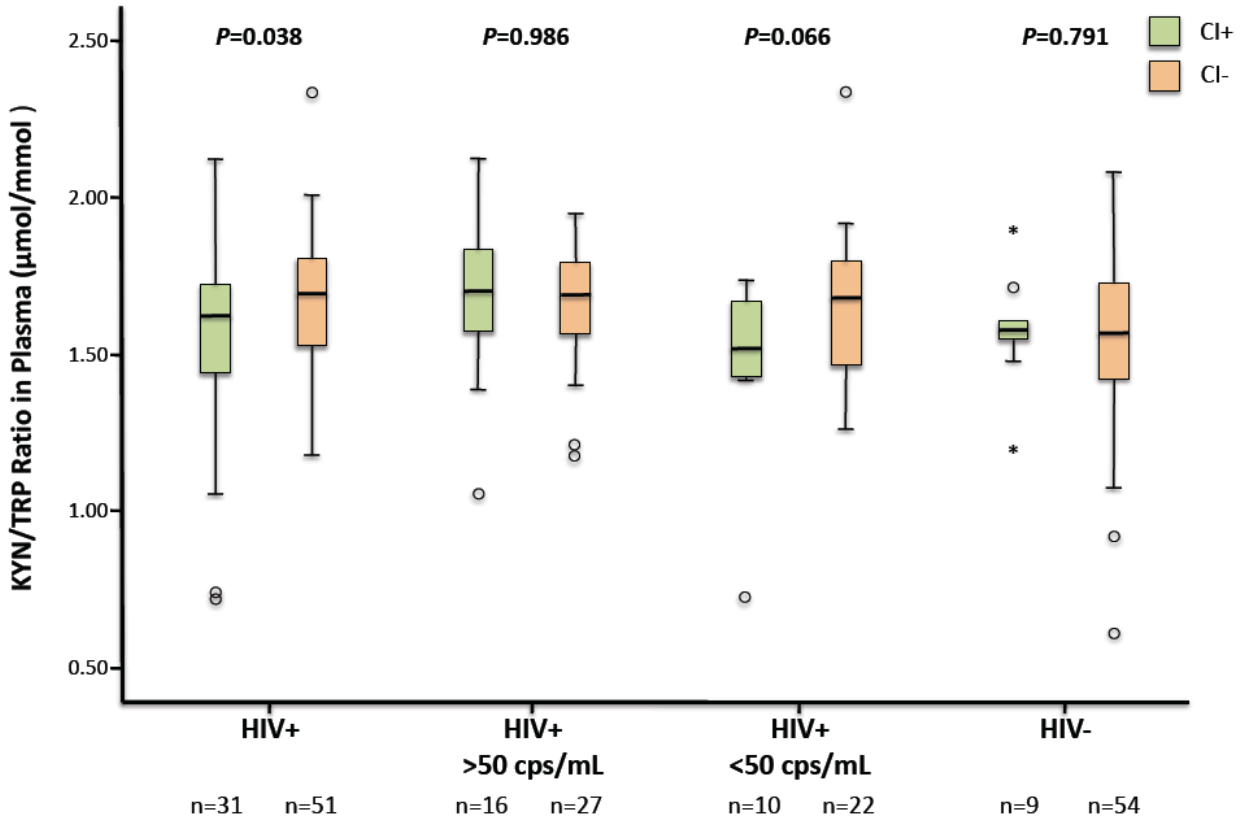

Key: TRP, tryptophan; KYN, kynurenine; CI, cognitive impairment.

5.2.3.4 The PHE/TYR Ratio and its Relationship with Major Depressive Disorder and Cognitive Impairment

The logistic regression analyses described in Section 5.2.3.3 were also performed using the PHE/TYR ratio in CSF and plasma as the predictor variable (Table 5.8). No significant associations were observed (for all comparisons, $p>0.05$ before Bonferroni correction).

5.2.4 The Effect of Antidepressant Drugs on TRP, KYN and the KYN/TRP Ratio

In the models evaluating the effects of antidepressant drugs on TRP, KYN and the KYN/TRP ratios, lower KYN concentrations (Z=-2.645; p=0.008; r=0.289; n=84) and KYN/TRP ratios (Z=1.984; p=0.047; r=0.216; n=84) in plasma were significantly associated with the use of antidepressants in the overall HIV+ group. This association was not observed in either of the sub-groups in plasma or in any of the groups in CSF. Multivariate analyses were also performed to explore the relationship between the KYN/TRP ratio in both CSF and plasma and clinically relevant covariates (viraemia in plasma and CSF, current and nadir CD4 count, ART use and current antidepressant use). Neither of these models were found to be statistically significant overall, though there was a trend towards significance for the model investigating KYN/TRP in plasma (R^2=0.190; ANOVA p=0.058). In this model, antidepressant use was statistically significantly associated with lower KYN/TRP ratios (Correlation=-0.259; p=0.009).

Table 5.8. The PHE/TYR ratio in CSF and Plasma and its Relationship with Major Depressive Disorder and Cognitive Performance

P/T Ratio and Outcome	χ^2	*P* Value
CSF		
PHE/TYR ratio and MDD status in HIV+ Individuals	0.524 (1, n=28)	0.469
PHE/TYR ratio and MDD status in patients with HIV-1-RNA >50 cps/mL	0.479 (1, n=8)	0.489
PHE/TYR ratio and MDD status in patients with HIV-1-RNA <50 cps/mL	0.000 (1, n=18)	0.991
PHE/TYR ratio and MDD status in HIV- individuals	1.388 (1, n=24)	0.239
PHE/TYR ratio and CI status in HIV+ Individuals	0.395 (1, n=27)	0.530
PHE/TYR ratio and CI status in patients with HIV-1-RNA >50 cps/mL	0.015 (1, n=15)	0.904
PHE/TYR ratio and CI status in patients with HIV-1-RNA <50 cps/mL	0.019 (1, n=9)	0.890
PHE/TYR ratio and CI status in HIV- individuals	0.309 (1, n=21)	0.578
Plasma		
PHE/TYR ratio and MDD status in HIV+ Individuals	0.352 (1, n=55)	0.553
PHE/TYR ratio and MDD status in patients with HIV-1-RNA >50 cps/mL	0.889 (1, n=27)	0.346
PHE/TYR ratio and MDD status in patients with HIV-1-RNA <50 cps/mL	0.187 (1, n=20)	0.666
PHE/TYR ratio and MDD status in HIV- individuals	0.494 (1, n=47)	0.482
PHE/TYR ratio and CI status in HIV+ Individuals	0.172 (1, n=53)	0.678
PHE/TYR ratio and CI status in patients with HIV-1-RNA >50 cps/mL	0.944 (1, n=26)	0.331
PHE/TYR ratio and CI status in patients with HIV-1-RNA <50 cps/mL	1.730 (1, n=20)	0.188
PHE/TYR ratio and CI status in HIV- individuals	2.265 (1, n=44)	0.132

Key: TYR, tyrosine; PHE, phenylalanine; MDD, major depressive disorder; CI, cognitive impairment; R^2, coefficient of determination.

5.3 Discussion

In this study, the overall group of PLWH had greater concentrations of TNF-α and NEO in CSF, lower concentrations of TRP in both CSF and plasma, and higher KYN/TRP ratios in plasma compared to HIV- controls. Only the changes observed in TNF-α and NEO in CSF, and TRP in plasma, persisted in virologically-suppressed patients receiving ART. In the first multivariate model, viraemia (i.e. HIV-1-RNA <50 cps/mL) and ART-use positively correlated with TNF-α and NEO concentrations in CSF, whilst lower current CD4+ cell counts were associated with higher concentrations of these markers. In the second model, which investigated the relationship between the inflammatory markers and the KYN/TRP ratio, levels of TNF-α and NEO positively correlated with the KYN/TRP ratio in both CSF and plasma.

These observations provide some support for the first hypothesis that TRP metabolism is increased in the presence of the HIV-1 virus or ARV agents. TRP concentrations were indeed observed to be lower in this heterogeneous group of HIV+ subjects. KYN concentrations were not observed to be increased in either the overall HIV+ group or the sub-group of aviraemic subjects, but the KYN/TRP ratio was observed to be increased in plasma in the overall group only. It is difficult to say what was driving this because of the nature of this heterogeneous group, but it is likely that it was at least in part driven by lower TRP concentrations. In this study, it has not been possible to ascertain whether ARVs themselves play a role in TRP metabolism beyond their ability to reduce virus.

Relating to the second hypothesis that increased TRP metabolism is associated with poorer cognitive performance and increased rates of depression in PLWH, a trend towards lower KYN/TRP ratios in plasma in patients with CI and MDD was observed in both the overall HIV+ group and an aviraemic sub-group, however these findings were not statistically significant. This trend was not observed in HIV+ participants with detectable viral loads. This result was unexpected and has not been observed in previous studies. It does not support the hypothesis that increased TRP metabolism is associated with poorer cognitive performance but does suggest that TRP metabolism is in some way connected to CI and depression.

The increases in TNF-α and NEO were expected and support observations made in previous studies, indicating increased ongoing monocyte, macrophage and microglial activation, and correlating positively with IDO-1 activity (136, 137, 155, 169, 189, 197, 210, 211, 298, 401).

In the study by Grill *et al.*, only untreated acute HIV infection was associated with an increase in the KYN/TRP ratio, which was associated with increased depressive symptoms (238). Treated HIV infection was not associated with an increase in the KYN/TRP ratio, or with CI or MDD. In contrast, these observations do not support this and, instead, suggest that there may be a sub-population of aviraemic ART-treated patients who have low KYN/TRP ratios and are experiencing CI and MDD. These data suggest that the KYN pathway may protect against CI and MDD in aviraemic patients. The reasons for this are, as yet, unclear. Interestingly, differences in the KYN/TRP ratio were not observed in HIV- subjects suffering from MDD or CI compared to those without symptoms, indicating that other factors are involved in psychiatric disease in these subjects.

Tryptophan degradation along the KYN pathway may result in the synthesis of neuroactive metabolites - 3-HK and 3-HAA with neurotoxic, QUIN with excitatory and KYNA and PIC with inhibitory properties (312-314, 351, 402). Greater CSF QUIN concentrations correlate with the severity of CI in PLWH (117, 313, 349, 403). CSF QUIN levels have been shown to fall rapidly with ART (117, 210, 312, 325, 349), probably as a result of a reduction in virus-related immune activation and a reduction in the activity of IDO-1 (321). KYNA is known to be neuroprotective via its ability to block excitotoxic neuronal damage and has been shown to be elevated in the brains of HIV-1 patients (351). In this study, aviraemic patients with CI and MDD had lower KYN/TRP ratios than those not suffering from these conditions, suggesting that higher KYN/TRP ratios may potentially have a protective effect. It is tempting to speculate that this phenomenon is due to an increase in either KYNA concentration or activity.

A trend towards increases in the PHE/TYR ratio in CSF was also observed, indicating a reduction in the production of dopamine and its' downstream catabolites. However, different to the observations made by Grill *et al.*, the differences in the PHE/TRY ratio did not correlate with CI or MDD in the study population.

An important limitation of this study is that it did not account for serotonin production. Serotonin can be unstable and prone to oxidation, which can contribute to pre-analytical errors. However, lowered serotonin concentrations have been described in the blood and CSF of patients with HIV-1 infection (404, 405). In support of this, many HIV+ patients with depression respond well to treatment with SSRIs, indicating that, in some patients, low

serotonin levels may be the primary cause of depression. This is consistent with the hypothesis that low serotonin production could be due to immune-mediated TRP-depletion (406). In this study, antidepressant use was significantly greater in HIV+ patients compared with HIV- controls. Antidepressant use was found to be associated with both lower KYN concentrations and KYN/TRP ratios in plasma in the overall HIV+ group. In contrast to this, in a previous study by Schroecksnadel *et al.* no differences were observed in either TRP or KYN concentrations in depressed HIV+ individuals who were treated with antidepressants compared with those not treated (338). However, in light of the findings from this study, these results should be interpreted with caution as antidepressant use could be a significant confounding factor.

This study has several other important limitations. Firstly, the HIV+ group was heterogeneous in terms of virological and immunological status, as well as ART use and the types of treatment used. ART can induce declines in CSF NEO and KYN/TRP ratio levels (321). However, the impact, if any, of differences between different treatments on TRP metabolism has yet to be explored.

Secondly, the study population is derived from a diverse mix of ethnicities. There are six reported IDO-1 genetic transcript variants, the frequencies of which have been assessed in European, Chinese, Japanese and African cohorts (407). Genetic variations in one or more of these genes, or other genes in the KYN pathway, could account for variable susceptibility to disease or disease outcomes. However, these have not yet been fully examined in the scientific literature and so their effect, if any, is as yet unknown. Also, the potential contribution of dietary differences to TRP levels could not be assessed in this study (408).

The observed results should be interpreted with caution due to the cross-sectional study design. IDO-1 activity is not consistent over time, and so the observed values and associations only provide a snapshot. Additional studies, which include longitudinal follow-up, may be required to further elucidate the role of TRP catabolism and associated metabolic pathways in HIV-1-associated neurological complications.

Given the exploratory nature of this pilot study, corrections for multiple comparisons in the statistical analysis were not initially done so that possible associations were not missed due to conservative multiplicity corrections. However, Bonferroni corrections were then performed resulting in a number of initially significant correlations no longer being significant.

The Bonferroni correction is a conservative method when there are a large number of comparisons to account for, as in this case. Therefore, the possibility of Type II statistical errors must be acknowledged when evaluating these data.

Whilst patients with active opportunistic infections and a history of head trauma associated with neurological complications were excluded, and information on the rates of HCV, MDD and methadone use in our study population was collected, information on other comorbidities, such as metabolic disorders and vascular disease, which are associated with CI was not collected. The results could, therefore, be confounded by the effects of other unknown comorbidities.

The severity of CI amongst HIV+ individuals was mostly mild. As a result, these findings may not generalize to more severely affected patients. Few patients met the criteria for HIV-associated dementia (HAD) in this sample, which is consistent with the current rates of HAND diagnoses.

In summary, trends towards lower KYN/TRP ratios in patients with CI and MDD in plasma in both the overall HIV+ group and an aviraemic sub-group were observed, however these findings were not statistically significant. It may hypothesised that the net result of the KYN/TRP ratio in ART-treated, virologically suppressed patients may be neuroprotective in some cases. The causes of CI and MDD in HIV+ individuals are likely to be multifactorial and these findings warrant further exploration.

Further work is required in less heterogeneous groups with longitudinal follow-up. The effect, if any, of ART drugs on the KYN pathway needs to be characterised in PLWH.

6 A PROSPECTIVE, OPEN-LABEL, CLINICAL STUDY TO ASSESS THE EFFECTS OF SWITCHING FROM EFAVIRENZ TO DOLUTEGRAVIR ON TRYPTOPHAN METABOLISM IN VIROLOGICALLY-SUPPRESSED PEOPLE LIVING WITH HIV (THE SSAT056 STUDY)

6.1 Introduction

The historical studies reporting the role of TRP metabolism in PLWH experiencing MDD and/or CI outlined in Sections 1.9.4 and 1.9.5, and the CHARTER study detailed in Chapter 5, report data from highly heterogeneous populations in terms of their disease and treatment characteristics. Many of these patients are from the pre-HAART era in PLWH who were not receiving therapy or who were receiving sub-optimal therapy, such as AZT monotherapy. These populations do not reflect contemporary PLWH whose virus is well-controlled with potent and, usually, less toxic ART. Studies in this 'modern' population are lacking, as are clinical data on the effects of ARVs themselves. The studies reported in this chapter and in Chapter 7 (the SSAT056 and CIIS studies, respectively) account for these limitations. Both studies are prospective, randomised, longitudinal studies in well-characterised groups of PLWH who are virologically-suppressed (i.e. HIV-1-RNA <50 cps/mL) using guideline recommended (45-48), first-line ART regimens (i.e. 2 NRTI's plus either EFV or an integrase inhibitor). The subjects included (i.e. virologically-suppressed subjects) match the population identified in the pilot study who were found to be experiencing changes in TRP metabolism that were associated with CI and MDD, allowing us the opportunity to confirm these initial findings. In addition to this, the longitudinal follow-up is novel as the majority of the previous studies were of cross-sectional design.

Many ARV agents are associated with CNS toxicities. EFV is a commonly-used agent but is associated with several CNS clinical toxicities including vivid dreams, insomnia, cognitive impairment, suicidal ideation and suicide (75). This has resulted in more recent HIV treatment guidelines moving towards the use of integrase inhibitors. Although overt CNS side effects may be less prevalent with the integrase-inhibitor class, emerging toxicities are being reported (77).

The pathogeneses of CNS toxicities from antiretroviral agents remains elusive (74). One potential mechanism is direct neuronal toxicity. EFV and its major metabolite, 8-hydroxy-efavirenz, have been shown to be toxic in neuron cultures at concentrations found in cerebrospinal fluid (79, 80). Other potential mechanisms may include alterations to TRP metabolism. EFV has been show to inhibit TDO activity in the liver cells of non-HIV-infected rats but it is unclear whether this is associated with neurotoxicity (409).

A prospective, randomised, open-label, multi-centre study was conducted, in which virologically-suppressed PLWH receiving two NRTIs plus efavirenz for ≥12 weeks who had reported experiencing ongoing CNS drug toxicity with EFV were enrolled. Subjects were randomised to switch immediately to DTG 50 mg once daily (n=20) or have their switch delayed for 4 weeks (n=20), without NRTI change. Both groups were followed-up for a further 12 weeks. For the following analyses, the study arms were pooled and 'Baseline' was defined as the time of ART switch for all subjects. The aim was to explore the effects of switching from EFV to DTG on TRP metabolism, CNS toxicity and the relationship between the two in virologically-suppressed PLWH.

The first hypothesis for this thesis states that TRP metabolism is increased in the presence of the HIV-1 virus or ARV agents (Section 1.1.2). This was tested in this study by assessing changes in measures of TRP metabolism in plasma associated with switching from EFV to DTG. Changes in plasma TRP, KYN and NEO concentrations, and the KYN/TRP ratio from Baseline to Week 4, Week 4 to Week 12, and Baseline to Week 12 were assessed using paired-samples *t*-tests.

The second hypothesis states that increased TRP metabolism is associated with poorer cognitive performance and increased rates of depression in people living with HIV (Section 1.1.2). This was assessed by investigating the association between changes in measures of TRP metabolism and changes in measures of CNS toxicity and neuropsychiatric test scores following switch from EFV to DTG. Firstly, paired-samples *t*-tests were used to assess changes from Baseline to Week 4, Week 4 to Week 12, and Baseline to Week 12 for CNS toxicity scores, IADL scores, HAD scores (Total score, the Anxiety Score and the Depression Score), and PSQI scores. Then, to investigate the relationship between CNS toxicity scores and KYN concentrations and the KYN/TRP ratio, longitudinal random intercept models were constructed. In the first model, the fixed effects were CNS toxicity (dependent variable) and

KYN concentration (independent variable). The random effect, or intercept, was chosen to be the patient (i.e. Patient ID) and the repeated effect was Time (Baseline, and 4 and 12 Weeks). Maximum Likelihood estimation was selected. This model design was utilised again to investigate the relationship between the KYN/TRP relationship and CNS Toxicity. This process was repeated for the HAD (Total score, the Anxiety Score and the Depression Score) and PSQI scores. Bonferroni corrections were applied to each group of analyses to adjust the level of significance to account for multiplicity. Only the adjusted *p* values are shown.

For the cognitive testing, statistical analysis was conducted according to CogState™ recommendations (see Sections 3.2.7.3 and 3.2.10 for additional details). Composite scores were calculated for the speed, accuracy and executive function domains and a global composite score (GCS) was calculated. Paired-samples *t*-tests were conducted to assess changes from Baseline to Week 4 and Week 12 for each of the individual test scores and for the domain and GCS scores.

6.2 Results

6.2.1 Baseline Characteristics

Forty patients were recruited. Their demographic and HIV profile are detailed in Table 6.1, below. Most subjects were male (n=38; 95%) and of white ethnicity (n=38; 95%). Mean age was 48 years (standard deviation [SD] 11). All subjects were virologically-suppressed (HIV-1-RNA <50 copies/mL) at baseline and maintained suppression throughout the 12-week follow-up. Mean CD4+ cell count/μL was 604 (SD=201) and 679 (SD=219) at baseline and Week 12, respectively. NRTI backbones were either TDF and FTC (n=39) or AZT and 3TC (n=1).

Table 6.1. Patient Demographics and HIV Profile

	Baseline	Week 4	Week 12
n	40	-	-
Age, Yrs, Mean (SD)	47.8 (11)	-	-
Gender, Male (%)	38 (95%)	-	-
Ethnicity		-	-
British, White	27 (67.5%)		
Irish, White	1 (2.5%)		
White, Other	10 (25.0%)		
Asian, Other	1 (2.5%)		
African, Black	1 (2.5%)		
HBV at Screening (%)	0 (0%)	-	-
HCV at Screening (%)	1 (2.5%)	-	-
HIV-1-RNA in Plasma <50 cps/mL (%)	38 (100%) [a]	40 (100%)	39 (97.5%)
Mean CD4 cell count/mL (SD) [a]	604 (201) [a]	637 (230)	679 (219)
NRTI Backbone		-	-
TDF/FTC	39		
AZT/3TC	1		

[a] n=38

6.2.2 Univariate Analysis of Biochemical and Immunological Markers

The mean plasma concentrations of TRP, KYN, NEO and the KYN/TRP ratio are presented in Table 6.2. The mean plasma concentration of KYN increased significantly from baseline to Week 12 (adjusted *p*=0.041), (Figure 6.1). Numerical increases were observed for the KYN/TRP ratio from baseline to Week 12 (adjusted *p*=0.456) and Week 4 to Week 12 (adjusted *p*=0.276), but these were not statistically significant following Bonferroni correction (Figure 6.2). No significant changes were observed for TRP or NEO at any time point (Table 6.2).

Table 6.2. Changes in TRP, KYN, KYN/TRP Ratio and NEO Concentrations Over a 12-Week Period

Parameter, Mean	n	Baseline	Week 4	Week 12	Mean Change					
					BL to Wk4	Adjusted *P* Value	Wk4 to Wk12	Adjusted *P* Value	BL to Wk12	Adjusted *P* Value
TRP, μmol/L (SD)	36	54.74 (10.59)	57.38 (15.38)	56.42 (11.71)	2.63 (15.76)	1.000	-0.96 (17.48)	1.000	1.67 (13.38)	1.000
KYN, μmol/L (SD)	36	2.15 (0.59)	2.29 (0.67)	2.50 (0.76)	0.14 (0.66)	1.000	0.21 (0.82)	1.000	0.35 (0.66)	0.041
KYN/TRP Ratio, μmol/mmol (SD)	36	40.37 (12.48)	41.08 (10.94)	44.99 (12.41)	0.71 (7.55)	1.000	3.91 (10.91)	0.456	4.62 (11.67)	0.276
NEO, μmol/L (SD)	36	13.76 (9.29)	12.60 (7.42)	12.39 (6.09)	1.16 (7.13)	1.000	-0.21 (6.34)	1.000	-1.36 (6.95)	1.000

Key: TRP, tryptophan; KYN, kynurenine; NEO, neopterin; SD, standard deviation; CI, confidence interval.

Figure 6.1. A: Mean Change in KYN Concentration (µmol/L) from Baseline to Week 12. B: Per Patient Changes in KYN Concentration (µmol/L) from Baseline to Week 12.

A

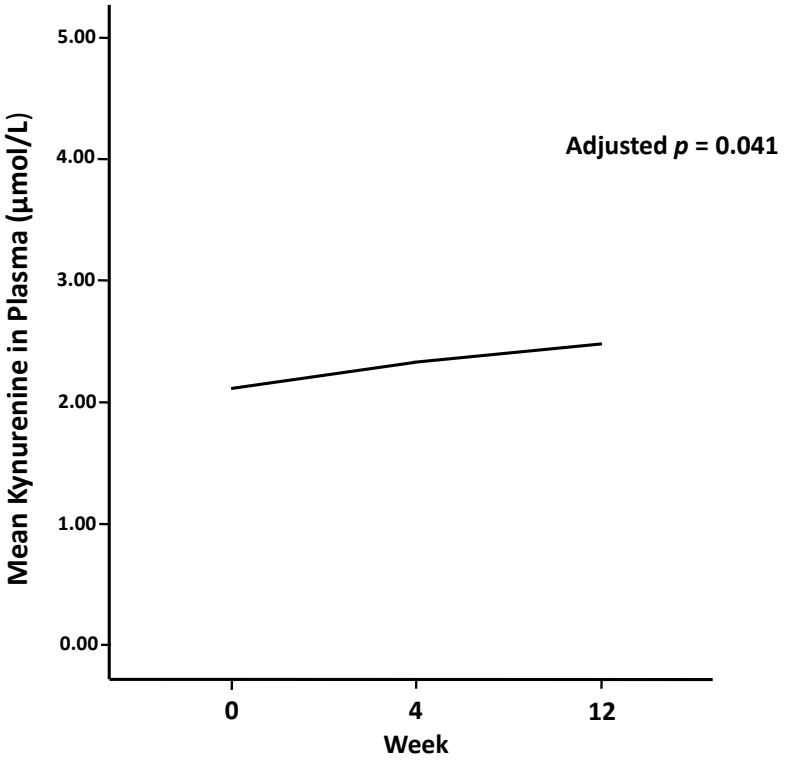

B

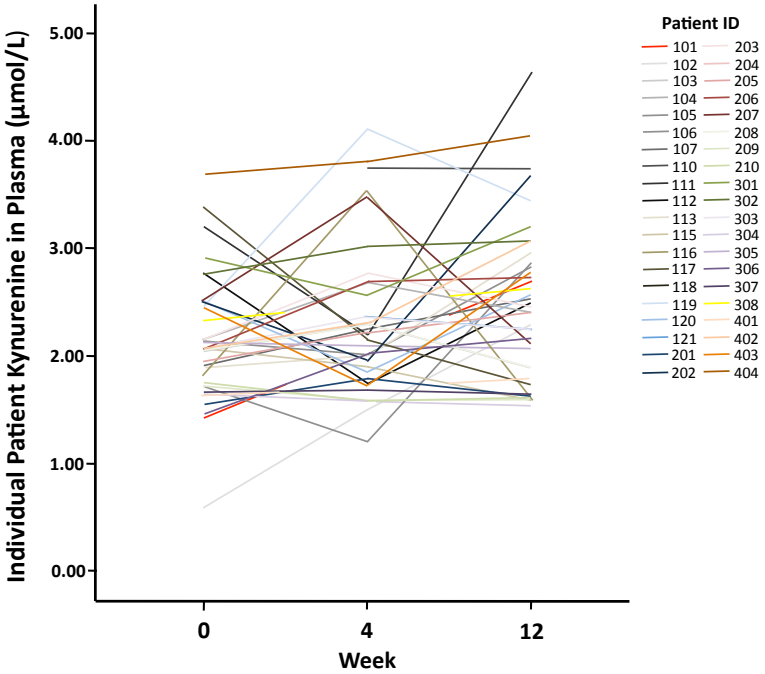

Figure 6.2. A: Mean Change in KYN/TRP Ratio (µmol/mmol) from Baseline to Week 12.

B: Per Patient Changes in KYN/TRP Ratio (µmol/mmol) from Baseline to Week 12.

A

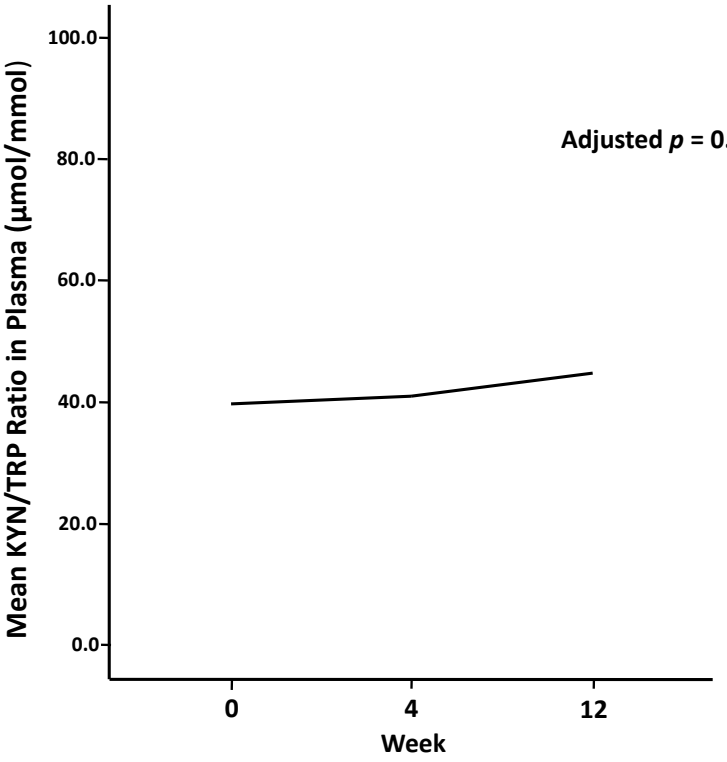

B

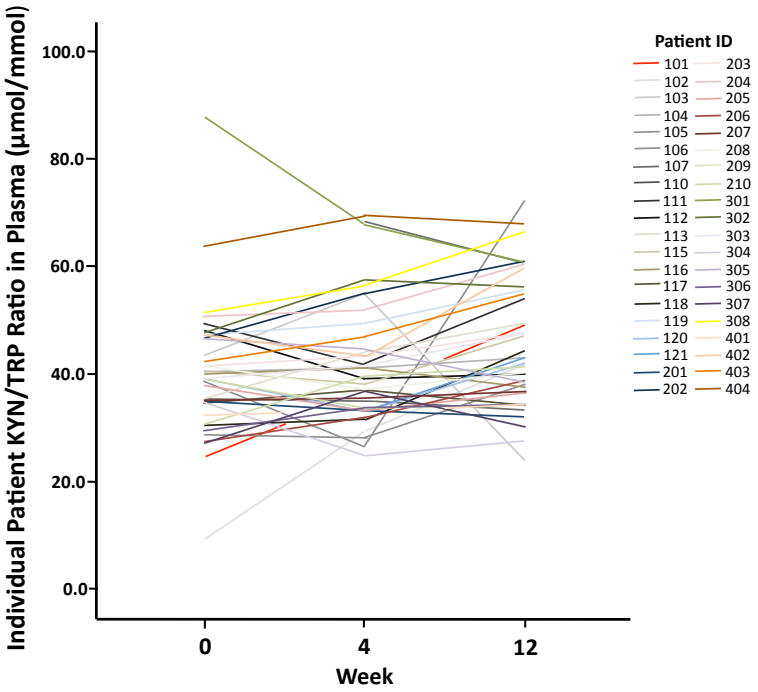

6.2.3 Univariate Analysis of CNS Toxicity, Cognitive Function and Mood Parameters

Statistically significant reductions in mean CNS toxicity (Figure 6.3), HAD (Total, Anxiety and Depression) and PSQI scores were observed from Baseline to Week 4 and Baseline to Week 12 (Table 6.3), indicating improvements in these parameters. There were no significant changes in any score from Weeks 4 to 12. Mean IADL scores did not change significantly at any time point.

The mean scores for each of the CogState™ tests are detailed in Table 6.4, below. None of the changes were found to be statistically significant. Similarly, no statistically significant changes were observed in the individual domain scores of the overall GCS score (Table 6.5). Due to the number of comparisons performed, Bonferroni corrections were not applied and these tests should be considered exploratory. Because significant changes were not observed, the relationship between the CogState™ scores and measures of TRP metabolism was not explored further.

Table 6.3. Changes in CNS Toxicity, Cognitive Function and Mood Parameters

Parameter, Mean (SD)	n	Baseline	Week 4	Week 12	Mean Change (SD)					
					BL to Wk4	Adjusted *P* Value	Wk4 to Wk12	Adjusted *P* Value	BL to Wk12	Adjusted *P* Value
CNS Toxicity	38	10.00 (4.69)	4.79 (4.07)	4.63 (4.24)	-5.21 (4.73)	<0.001	-0.16 (2.38)	1.000	-5.37 (4.73)	<0.001
IADL	39	7.85 (0.49)	7.92 (0.35)	7.90 (0.38)	-0.08 (0.35)	1.000	-0.03 (0.49)	1.000	0.05 (0.56)	1.000
HAD, Total	38	14.24 (6.92)	7.76 (5.27)	8.42 (6.17)	-6.47 (5.21)	<0.001	0.66 (3.42)	1.000	-5.82 (5.32)	<0.001
HAD, Anxiety	38	8.32 (4.27)	5.13 (3.42)	5.39 (3.39)	-3.18 (3.05)	<0.001	0.26 (2.26)	1.000	-2.92 (3.07)	<0.001
HAD, Depression	38	5.92 (3.61)	2.66 (2.59)	3.11 (3.23)	-3.26 (2.98)	<0.001	0.45 (1.97)	1.000	-2.82 (3.10)	<0.001
PSQI	38	3.92 (2.19)	2.39 (1.67)	2.47 (1.80)	-1.53 (2.01)	<0.001	0.08 (1.19)	1.000	-1.51 (2.13)	<0.001

Key: CNS, central nervous system; SD, standard deviation; CI, confidence interval.

Figure 6.3. A: Mean Change in CNS Toxicity Score from Baseline to Week 12. B: Per Patient Changes in CNS Toxicity Scores from Baseline to Week 12.

A

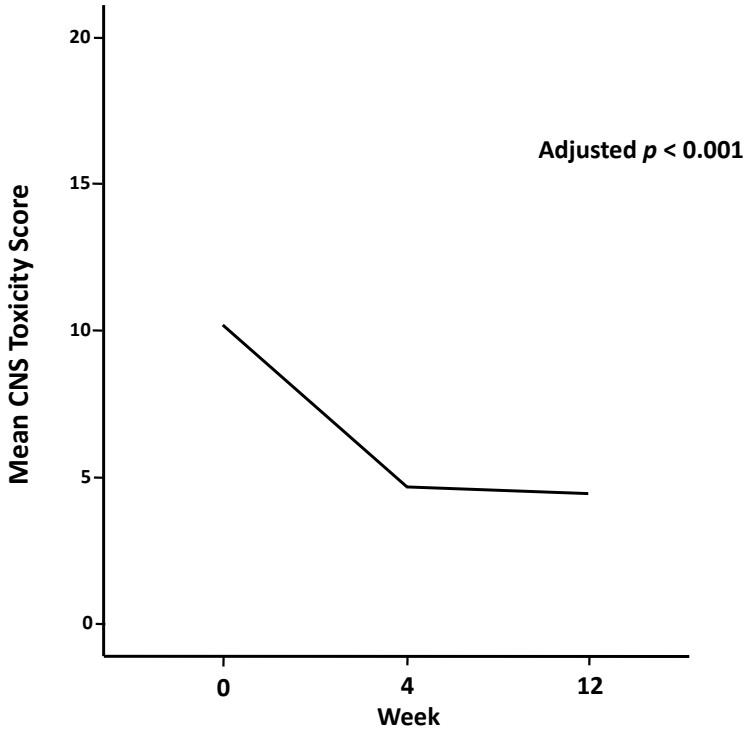

B

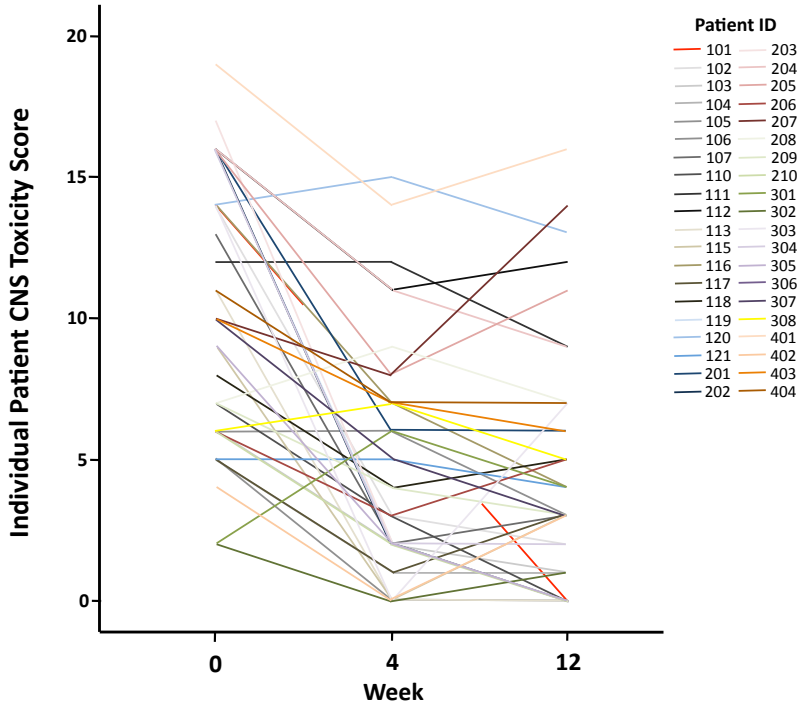

Table 6.4. CogState™ Scores at Baseline, Week 4 and Week 12 and Change Scores from Baseline to Weeks 4 and 12

CogState™ Test Score, Mean (SD)	Baseline	Week 4	Week 12	Mean Change (SD)			
				BL to Wk4	Unadjusted *P* Value	BL to Wk12	Unadjusted *P* Value
Speed							
IDN, Log^{10} ms	2.75 (0.10) [a]	2.77 (0.63) [b]	2.75 (0.07) [c]	0.02 (0.10) [c]	0.352	0.01 (0.06) [g]	0.453
DET, Log^{10} ms	2.59 (0.10) [d]	2.59 (0.08) [e]	2.58 (0.09) [c]	0.00 (0.10) [l]	0.982	-0.00 (0.11) [m]	0.976
Errors							
GML, Total No. Errors	47.67 (24.74) [f]	48.38 (21.34) [g]	43.14 (14.58) [h]	1.13 (23.00) [f]	0.789	-0.19 (14.97) [n]	0.948
SETS, Total No. Errors	37.66 (28.36) [i]	39.68 (28.67) [j]	25.72 (17.96) [i]	4.50 (17.33) [h]	0.181	-9.19 (24.77) [n]	0.070
Accuracy							
OCL, Arcsine proportion	0.97 (0.15) [k]	1.00 (0.16) [b]	0.97 (0.16) [k]	0.02 (0.14) [a]	0.384	0.02 (0.14) [d]	0.534
ONB, Arcsine proportion	1.27 (0.32) [a]	1.34 (0.29) [b]	1.33 (0.29) [a]	0.06 (0.30) [c]	0.234	0.03 (0.38) [l]	0.711
TWOB, Arcsine proportion	1.14 (0.35) [i]	1.16 (0.31) [j]	1.17 (0.30) [i]	0.00 (0.36) [h]	0.952	0.00 (0.25) [n]	0.971

Key: CNS, central nervous system; SD, standard deviation; CI, confidence interval.

[a] n=36; [b] n=39; [c] n=35; [d] n=34; [e] n=38; [f] n=30; [g] n=32; [h] n=28; [i] n=29; [j] n=31; [k] n=37; [l] n=33; [m] n=31; [n] n=26

Table 6.5. CogState™ Domain and Global Composite Scores and Changes from Baseline to Week 12

CogState™ Score, Mean (SD)	Details	Baseline	Week 12	n	Mean Change in Standardised Score from Baseline to Week 12 (SD)	Unadjusted *P* value
Composite Speed Score	Decrease in score = improvement	47.47 (1.29)	47.41 (1.26)	31	0.06 (1.24)	0.780
Composite Executive Function Score	Decrease in score = improvement	2.52 (1.20)	2.21 (0.90)	25	0.31 (0.80)	0.067
Composite Accuracy Score	Increase in score = improvement	6.83 (1.28)	6.80 (1.12)	25	0.03 (1.34)	0.922
Global Composite Score	Increase in score = improvement	18.89 (0.56)	18.92 (0.62)	21	-0.04 (0.73)	0.827

6.2.4 Linear Mixed Model Analyses to Determine Relationships Between KYN and KYN/TRP Ratio Concentrations and CNS Toxicity, HAD and PSQI Scores

In the linear mixed model analyses (Table 6.6), plasma KYN concentrations were found to be negatively correlated with CNS toxicity scores, such that for every 1 μmol/L increase observed in KYN concentration, a 1.7-point decrease was observed in the CNS toxicity score (adjusted *p*=0.038). Likewise, a trend was observed for the KYN/TRP ratio, such that for every 1 μmoL/mmoL increase observed in the KYN/TRP ratio, a 0.1-point decrease was observed in the CNS toxicity score (adjusted *p*=0.054).

Table 6.6. Linear Mixed Model Results for KYN and KYN/TRP Ratio and CNS Toxicity from Baseline to Week 12

Parameter	Estimate (95% CI)	Adjusted *P* value
Model 1: CNS Toxicity and KYN		
Mean CNS Toxicity Score	10.4 (7.0 to 13.9)	<0.001
KYN, μmol/L	-1.7 (-3.1 to -0.3)	0.038
Model 2: CNS Toxicity and KYN/TRP Ratio		
Mean CNS Toxicity Score	10.4 (6.8 to 14.1)	<0.001
KYN/TRP Ratio, μmol/mmol	-0.1 (-0.2 to -0.0)	0.054

Key: TRP, tryptophan; KYN, kynurenine; CNS, central nervous system; CI, confidence interval.

Additional, exploratory, models were constructed and analysed to investigate the relationship between plasma KYN concentrations and the KYN/TRP ratio with HAD (Total, Anxiety and Depression) and PSQI scores (Tables 6.7 to 6.10, below). No significant relationships were observed (unadjusted *P* values only are shown) but trends were observed between KYN concentrations and Total HAD, HAD Anxiety and PSQI scores.

Table 6.7. Linear Mixed Model Results for KYN and KYN/TRP Ratio and Total HAD Scores from Baseline to Week 12

Parameter	Estimate (95% CI)	Unadjusted *P* value
Model 1: Total HAD Score and KYN		
Mean Total HAD Score	13.9 (9.5 to 18.2)	<0.001
KYN, μmol/L	-1.5 (-3.3 to 0.2)	0.075
Model 2: Total HAD Score and KYN/TRP Ratio		
Mean Total HAD Score	12.3 (7.5 to 17.2)	<0.001
KYN/TRP Ratio, μmol/mmol	-0.0 (-0.2 to 0.1)	0.366

Key: TRP, tryptophan; KYN, kynurenine; HAD, Hospital Anxiety and Depression Scale; CI, confidence interval.

Table 6.8. Linear Mixed Model Results for KYN and KYN/TRP Ratio and HAD Anxiety Scores from Baseline to Week 12

Parameter	Estimate (95% CI)	Unadjusted *P* value
Model 1: HAD Anxiety Score and KYN		
Mean HAD Anxiety Score	8.8 (5.9 to 10.9)	<0.001
KYN, μmol/L	-0.9 (-1.8 to 0.1)	0.070
Model 2: HAD Anxiety Score and KYN/TRP Ratio		
Mean HAD Anxiety Score	8.0 (5.3 to 10.8)	<0.001
KYN/TRP Ratio, μmol/mmol	-0.0 (-0.1 to 0.0)	0.194

Key: TRP, tryptophan; KYN, kynurenine; HAD, Hospital Anxiety and Depression Scale; CI, confidence interval.

Table 6.9. Linear Mixed Model Results for KYN and KYN/TRP Ratio and HAD Depression Scores from Baseline to Week 12

Parameter	Estimate (95% CI)	Unadjusted *P* value
Model 1: HAD Depression Score and KYN		
Mean HAD Depression Score	5.3 (3.1 to 7.6)	<0.001
KYN, μmol/L	-0.6 (-1.5 to 0.3)	0.203
Model 2: HAD Depression Score and KYN/TRP Ratio		
Mean HAD Depression Score	4.2 (1.7 to 6.7)	0.001
KYN/TRP Ratio, μmol/mmol	-0.0 (-0.0 to 0.0)	0.851

Key: TRP, tryptophan; KYN, kynurenine; HAD, Hospital Anxiety and Depression Scale; CI, confidence interval.

Table 6.10. Linear Mixed Model Results for KYN and KYN/TRP Ratio and PSQI Scores from Baseline to Week 12

Parameter	Estimate (95% CI)	Unadjusted *P* value
Model 1: PSQI Score and KYN		
Mean PSQI Score	4.2 (2.8 to 5.7)	<0.001
KYN, μmol/L	-0.5 (-1.1 to 0.0)	0.073
Model 2: PSQI Score and KYN/TRP Ratio		
Mean PSQI Score	4.3 (2.8 to 5.9)	<0.001
KYN/TRP Ratio, μmol/mmol	-0.0 (-0.1 to 0.0)	0.082

Key: TRP, tryptophan; KYN, kynurenine; CI, confidence interval.

6.3 Discussion

In this study, virologically-suppressed PLWH experiencing ongoing CNS toxicity with EFV were switched to DTG, resulting in significant improvements in CNS adverse events, anxiety, depression and sleep quality. Following switch, a significant increase was observed in plasma KYN concentrations and a non-significant increase in the KYN/TRP ratio. These changes were negatively correlated with the reduction in CNS toxicities and improvements in neuropsychiatric scores.

These observations provide some support for the first hypothesis. Previous clinical studies have demonstrated that KYN/TRP ratios decline following initiation of ART due to decreases in immune activation resulting from suppression of HIV-1-RNA (321, 410, 411). However, the subjects in this study had HIV-1-RNA <50 cps/mL upon entry and so additional changes were not expected. The increases in plasma KYN concentrations and the KYN/TRP ratio were surprising and suggest that there is a differential effect between ART on TRP metabolism. In this study, NEO was selected as a marker of immune activation based on its correlation with IDO activity (174). The lack of correlation between NEO and KYN concentrations is consistent with the hypothesis that increases in KYN concentrations may be due to changes in hepatic TRP metabolism rather than immune-driven IDO activity. However, only information on one marker of immune activation (NEO) was collected and, therefore, cannot validate this hypothesis by assessing other soluble markers of inflammation. EFV is a potent inhibitor and inducer of cytochrome P450 enzymes in the liver (412). Unpublished data by Zheve showed that efavirenz inhibits TDO activity in the liver cells of non-HIV-infected rats (409). If this effect translates to human subjects, then removal of EFV would result in an increase in TDO activity and a corresponding increase in KYN production, which is what was observed. Whilst this is a plausible

explanation, I cannot exclude other immunologic or virologic factors that may have influenced TRP metabolism and KYN production and remain undetected in this study. Indeed, I did not observe an increase in IDO activity in the THLE2 and THLE3 cell lines detailed in Chapter 4, so this explanation must be considered with caution. These data support the first hypothesis that states that TRP metabolism is increased in the presence of ARV agents but also suggest that there may be multiple factors at play, including a differential effect of ARV agents, namely EFV and DTG.

These data do not support the second hypothesis that increased TRP metabolism is associated with poorer cognitive performance and increased rates of depression in PLWH, however. The improvements in clinical parameters are not unexpected in patients switching from EFV. Several clinical studies have demonstrated similar results when switching from EFV to other antiretroviral agents, such as ETV, RAL and RPV (372, 413, 414). The results of the mixed model analyses suggest that the improvements in CNS toxicity scores are associated with the increases observed in KYN concentrations and the KYN/TRP ratio, which is the opposite of what was predicted. Similar relationships were not observed in the exploratory models looking at KYN concentrations and the KYN/TRP ratio and HAD and PSQI scores. The reasons for this are unclear and it is important to acknowledge that other mechanisms could also be contributing. For example, the direct neurotoxic effects of the 8-hydroxy-efavirenz metabolite were not measured in this study and it is possible that they may be confounding the observations. The effect of increases in KYN concentrations may be drowned out by the removal of 8-hydroxy-efavirenz. This would appear to be the most likely explanation.

Other alternative explanations could include the activity of KYNA, a downstream catabolite of KYN, which is known to be neuroprotective due to its ability to block excitotoxic neuronal damage (415, 416) and has been shown to be elevated in the brains of PLWH (351). Whilst changes in this compound were not measured, it is interesting to speculate that increases in KYNA concentration or activity following the removal of EFV could be attenuating neuronal damage and contributing to the improvements in CNS toxicity. These data should, therefore, be interpreted with caution.

There are some important limitations to this study. Firstly, only TRP and KYN concentrations in plasma were measured. Cerebrospinal fluid analysis would be useful to help determine whether there are similar changes occurring in the CNS compartment. In addition to this, analysis of other KYN pathway catabolites, such as KYNA and QUIN, as well as additional markers of immune activation, would be

useful to help explain the observations. Measurement of serotonin concentrations, which are known to be lower in the blood and cerebrospinal fluid of PLWH, would also be helpful (404, 405).

Given that most of the subjects were white males, these findings may not be extrapolatable to other ethnicities or females. Differences in TDO activity have been reported in men and women of various ethnicities (417) There are also six reported IDO-1 genetic transcript variants, the effects of which are currently unknown (407).

Lastly, the potential contribution of dietary differences to tryptophan concentration was not assessed in this study (408).

In summary, I have switching from EFV to DTG resulted in changes in TRP metabolism and improvements in measures of CNS toxicity, anxiety, depression and sleep quality. The data are potentially confounded, however, by the possible neurotoxic effects of 8-hydroxy-efavirenz. The CIIS study, presented in Chapter 7, excludes the use of EFV and focusses instead on two integrase inhibitors, RAL and DTG, thus removing this confounding factor.

7 A PROSPECTIVE, OPEN-LABEL, CLINICAL STUDY TO ASSESS THE EFFECTS OF SWITCHING FROM RALTEGRAVIR TO DOLUTEGRAVIR ON TRYPTOPHAN METABOLISM IN VIROLOGICALLY-SUPPRESSED PEOPLE LIVING WITH HIV (The CNS Integrase Inhibitor Study [CIIS])

7.1 Introduction

In the SSAT056 study (Chapter 6), virologically-suppressed PLWH experiencing ongoing CNS toxicity with EFV were switched to DTG, resulting in significant improvements in CNS adverse events, anxiety, depression and sleep quality. Following switch, a significant increase was observed in plasma KYN concentrations and a non-significant increase in the KYN/TRP ratio. These changes were negatively correlated with the reduction in CNS toxicities and improvements in neuropsychiatric scores. These data support the first hypothesis that states that TRP metabolism is increased in the presence of ARV agents but they also suggest that there may be multiple factors at play, including a differential effect between different ARV agents, namely EFV and DTG. No evidence was found to support the second hypothesis that increased TRP metabolism is associated with poorer cognitive performance and increased rates of depression in PLWH. In fact, the opposite was observed – that increased plasma KYN concentrations and KYN/TRP ratios were associated with improvements in CNS toxicity scores, though this improvement is more likely to be explained by the removal of EFV, which is strongly associated with these events due to its inherent neurotoxicity (74-77, 79-83, 372, 413, 414). The changes in KYN concentrations are not as easily explained. Evidence exists to suggest that it may be due to EFV-mediated TDO-induction in the liver (409), though the data in human THLE2 and THLE3 cell lines presented in Section 4.2.4 of this thesis do not support this previous finding.

The CNS Integrase Inhibitor study (CIIS) excludes the use of EFV and focusses instead on two integrase inhibitors, RAL and DTG, thus removing this confounding factor. Integrase inhibitors are potent ARV agents that have demonstrated favourable safety and tolerability (77). RAL and DTG have shown similar rates of adverse events, the most commonly reported being mild to moderate nausea, diarrhoea and headache. Psychiatric adverse events, such as insomnia, anxiety, depression and suicidality, have also been reported. In a recent review of five randomised clinical trials, a cohort study, and cases of spontaneously psychiatric adverse events reported to ViiV Healthcare Ltd., DTG was

compared with RAL, ATV, DRV and EFV. Overall, DTG was shown to have a low incidence of psychiatric adverse events, with lower clinical study withdrawal rates (0% to 0.6%) compared with RAL (0% to 2.5%) (77).

The CIIS study is a prospective, randomised, single centre, clinical study, in which neurologically-asymptomatic, virologically-suppressed PLWH (plasma HIV-1 RNA <20 copies/mL for at least 3 months) receiving two NRTIs (N=21) plus RAL for at least 4 months underwent assessment at baseline of their cerebral function parameters as measured by neurocognitive testing, cerebral magnetic resonance (MRS) imaging and lumbar puncture examination before being randomised on a 2:1 basis to either switch from RAL to a DTG-containing regimen (n=14) without NRTI change or remain on their current therapy (n=7). After 120 days, cerebral parameter assessments were repeated. The aim was to explore the effects of switching from RAL to DTG on TRP metabolism and investigate its' relationship with cerebral function parameters in virologically-suppressed PLWH.

The first hypothesis for this thesis states that TRP metabolism is increased in the presence of the HIV-1 virus or ARV agents (Section 1.1.2). This was tested in this study by assessing changes in measures of TRP metabolism in CSF and plasma associated with switching from RAL to DTG. Plasma and CSF concentrations of TRP, KYN, PHE, TYR and NEO were measured at Baseline and Day 120 using the same methodology as described in Section 3.1.6. The KYN/TRP and PHE/TYR ratios were also calculated. For some of the analyses, the study arms were pooled to provide an overall combined group. The individual study arms were also investigated separately and comparisons were made between the arms. Paired-samples *t*-tests were conducted to assess changes in plasma and CSF concentrations for these factors from Baseline to Day 120 for the combined group and for each of the study arms individually. Differences in the changes from Baseline to Week 120 between study arms was assessed using Independent Samples *t*-tests.

In an effort to explore the association between TRP metabolism and markers of CNS cell integrity, ^{1}H-MRS was employed to quantify the cerebral metabolites NAA, Cho, mI, Glx and Cr. NAA is a sensitive marker of neuronal integrity *in vivo*, with reductions in its concentrations being indicative of damage and, possibly, a reduction in neuronal density (117, 265, 292). Cho is a water-soluble vitamin-like essential nutrient, whilst mI is a simple sugar-alcohol that is believed to be a marker of astrocyte integrity and, possibly, a breakdown product of myelin (292, 293). Cho and mI are indicators of glial proliferation and cellular injury and, as such, their levels increase with neuroinflammation. Cr is a marker of intracellular energy stores and is used as a reference for metabolite levels (292, 294). Glx is

a combination of glutamate, an excitatory neurotransmitter found primarily in glutamatergic neurons, and its stored form, glutamine, which is found within astrocytes. Since glutamate is required for aspartate synthesis within the neuronal mitochondria, decreased levels of Glx may be an early indicator of neuronal metabolism changes (265). Paired-samples *t*-tests were conducted to assess changes in the cerebral metabolite concentrations for NAA/Cr, Cho/Cr, mI/Cr and Glx/Cr in each of the anatomical locations from Baseline to Day 120 for each of the study arms. Differences in the changes from Baseline to Week 120 between study arms was assessed using Independent Samples *t*-tests. To explore the association between biomarker concentrations and MRS metabolite concentrations for all subjects at Baseline, Pearson r correlations were conducted.

The second hypothesis states that increased TRP metabolism is associated with poorer cognitive performance and increased rates of depression in people living with HIV (Section 1.1.2). This was assessed by investigating the association between changes in measures of TRP metabolism and changes in measures of cognitive function and neuropsychiatric test scores following switch from RAL to DTG. For the cognitive testing, statistical analysis was conducted according to CogState™ recommendations (See Sections 4.2.6.3 and 4.2.9 for additional details). Paired-samples *t*-tests were conducted to assess changes from Baseline to Day 60 and Day 120. Z scores were calculated for each test score and a Global Composite Score (GCS) was calculated based on the average of the individual Z scores. Differences in the changes from Baseline to Week 120 between study arms was assessed using Independent Samples *t*-tests. To explore the association between biomarker concentrations and the Global CogState™ score for all subjects at Baseline, Pearson r correlations were conducted. To investigate the relationship between the changes in TRP concentrations in plasma and CSF and the CogState™ GCS for patients in the DTG arm, mixed models (i.e. longitudinal random intercept models) were constructed. The models' fixed effects were CogState™ GCS (dependent variable) and plasma or CSF TRP concentration (independent variable). The random effect, or intercept, was the patient (i.e. Patient ID) and the repeated effect was Time (Baseline, Day 60 and Day 120). Maximum Likelihood estimation was selected. This approach was also utilised to investigate the relationship between KYN concentrations and the KYN/TRP ratio in plasma and CSF and CogState™ GCS.

7.2 Results

7.2.1 Baseline Characteristics

Twenty-one patients were recruited. Their demographic and HIV profiles are detailed in Table 7.1, below. All but one subject was male (n=20, 95.2%) and most were of white ethnicity (n=14; 66.7%). Mean age was 55 (SD=9.3). All subjects were virologically-suppressed in both plasma (HIV-1-RNA <20 copies/mL) and CSF (HIV-1 RNA <5 copies/mL) at Baseline and maintained suppression throughout the 120-day follow-up. Mean CD4+ cell count/uL was 760 (SD=230) and 688 (SD=395) at Baseline for the DTG and RAL arms, respectively. One patient from the DTG arm did not complete all study procedures. No treatment-related adverse events were observed.

Table 7.1. Patient Demographics and HIV Profile

Parameter	Overall	Study Arm	
		DTG	RAL
n	21	13	8
Age, years (SD)	44 (9.3)	46 (9.7)	40 (7.9)
Male, n (%)	20 (95.2)	13 (100)	7 (87.5)
Ethnicity (%)			
White	14 (66.7)	9 (69.2)	5 (62.5)
Black	2 (9.5)	1 (7.7)	1 (12.5)
Other	5 (23.8)	3 (23)	2 (25)
BMI	26.1 (3.2)	25.4 (2.9)	27.4 (3.4)
Baseline absolute CD4+ count (cells/µL)	731 (299)	760 (230)	688 (395)
Number completing all study procedures	20	12	8
Plasma HIV RNA <20 copies/mL, n (%)	20 (100)	12 (100)	8 (100)
CSF HIV RNA <5 copies/mL, n (%)	20 (100)	12 (100)	8 (100)
Absolute CD4+ count (cells/uL)	768 (389)	742 (277)	808 (536)
Remained on randomised therapy	20	12	8

Key: SD, standard deviation; CSF, cerebrospinal fluid.

7.2.2 Univariate Analysis of Biochemical and Immunological Markers

The change from Baseline to Day 120 for the mean plasma and CSF concentrations for TRP, KYN, the KYN/TRP ratio, PHE, TYR, the PHE/TYR ratio and NEO for the overall population and the individual study arms are presented in Tables 7.2 to 7.4, below. Multiplicity corrections have not been applied and unadjusted *P* values are shown. No significant changes were observed in any of the biomarkers in the overall population. In the DTG arm, the mean plasma concentration of TRP increased significantly from Baseline to Day 120 (mean increase, 4.84 μmol/L; *p*=0.038; 95% CI, -0.32 to 9.37) (Table 7.3). No other significant changes were observed in either arm. Whilst not statistically significant, subjects in the RAL arm experienced a numerical decrease in mean CSF NEO concentrations (mean decrease, 1.93 μmol/L; *p*=0.069; 95% CI, -4.06 to 0.20), perhaps indicating a reduction in intrathecal inflammation despite CSF viral loads being consistently undetectable (i.e. HIV-1 RNA >5 copies/mL) during the course of the 120-day follow-up.

Table 7.2. Changes in TRP, KYN, KYN/TRP Ratio, PHE, TYR, PHE/TYR Ratio and NEO Concentrations in Plasma and CSF from Baseline to Day 120 in the Overall Population

Overall, N=20	Baseline, Mean (SD)	Day 120, Mean (SD)	*t* (df)	Unadjusted *P* Value	Mean Change (95% CI)	Eta^2
Plasma						
TRP, µmol/L	50.55 (8.87)	51.83 (10.07)	0.710 (19)	0.487	1.28 (-2.50 to 5.07)	0.026
KYN, µmol/L	2.04 (0.71)	2.07 (0.56)	0.277 (19)	0.785	0.03 (-0.22 to 0.29)	0.004
KYN/TRP Ratio, µmol/mmol	40.22 (10.72)	41.18 (13.63)	0.358 (19)	0.724	0.97 (-4.68 to 6.61)	0.007
PHE, µmol/L	59.69 (8.43)	60.45 (10.71)	0.327 (19)	0.747	0.76 (-4.11 to 5.63)	0.006
TYR, µmol/L	65.40 (12.52)	67.12 (17.66)	0.617 (19)	0.545	1.72 (-4.10 to 7.53)	0.020
PHE/TYR Ratio, µmol/mmol	0.93 (0.16)	0.93 (0.16)	-0.209 (19)	0.837	-0.01 (-0.08 to 0.63)	0.002
NEO, nmol/L	12.11 (6.84)	16.70 (12.53)	1.498 (19)	0.151	4.59 (-1.82 to 10.00)	0.106
CSF						
TRP, µmol/L	1.64 (0.46)	1.75 (0.55)	1.274 (19)	0.218	0.11 (-0.07 to 0.29)	0.081
KYN, µmol/L [a]	0.06 (0.03)	0.06 (0.03)	0.138 (9)	0.893	0.00 (-0.01 to 0.01)	0.002
KYN/TRP Ratio, µmol/mmol [a]	40.62 (20.68)	38.22 (24.48)	-0.721 (9)	0.489	-2.40 (-9.93 to 5.13)	0.055
PHE, µmol/L	11.96 (2.15)	11.96 (2.31)	0.000 (19)	1.000	0.000 (-0.90 to 0.90)	0.000
TYR, µmol/L	12.05 (2.83)	12.48 (3.24)	0.843 (19)	0.410	0.44 (-0.64 to 1.51)	0.036
PHE/TYR Ratio, µmol/mmol	1.01 (0.14)	0.99 (0.18)	-0.732 (19)	0.473	-0.03 (-0.10 to 0.05)	0.027
NEO, nmol/L	8.30 (5.99)	7.66 (4.84)	-1.169 (19)	0.257	-0.64 (-1.78 to 0.50)	0.067

Key: SD, standard deviation

Table 7.3. Changes in TRP, KYN, KYN/TRP Ratio, PHE, TYR, PHE/TYR Ratio and NEO Concentrations in Plasma and CSF from Baseline to Day 120 in the DTG Arm

DTG Arm, n=12	Baseline, Mean (SD)	Day 120, Mean (SD)	*t* (df)	Unadjusted *P* Value	Mean Change (95% CI)	Eta^2
Plasma						
TRP, μmol/L	50.15 (8.03)	54.99 (10.32)	2.357 (11)	0.038	4.84 (-0.32 to 9.37)	0.336
KYN, μmol/L	2.07 (0.69)	2.17 (0.46)	0.528 (11)	0.608	0.10 (-0.31 to 0.50)	0.025
KYN/TRP Ratio, μmol/mmol	41.15 (9.49)	40.59 (10.61)	-0.151 (11)	0.882	-0.55 (-8.56 to 7.46)	0.002
PHE, μmol/L	58.38 (9.05)	62.19 (12.66)	1.487 (11)	0.165	3.82 (-1.83 to 9.47)	0.167
TYR, μmol/L	65.44 (15.00)	69.22 (19.17)	1.215 (11)	0.250	3.78 (-3.06 to 10.61)	0.118
PHE/TYR Ratio, μmol/mmol	0.92 (0.18)	0.93 (0.17)	0.201 (11)	0.844	0.01 (-0.08 to 0.10)	0.004
NEO, nmol/L	12.30 (5.89)	17.54 (12.95)	1.176 (11)	0.264	5.23 (-4.56 to 15.03)	0.112
CSF						
TRP, μmol/L	1.67 (0.26)	1.85 (0.49)	1.394 (11)	0.191	0.17 (-0.10 to 0.44)	0.150
KYN, μmol/L [a]	0.06 (0.03)	0.07 (0.03)	1.205 (5)	0.282	0.01 (-0.01 to 0.02)	0.225
KYN/TRP Ratio, μmol/mmol [a]	38.77 (15.78)	38.29 (18.59)	-0.109 (5)	0.917	-0.48 (-11.81 to 10.84)	0.002
PHE, μmol/L	11.73 (2.02)	11.94 (1.98)	0.347 (11)	0.735	0.22 (-1.16 to 1.60)	0.011
TYR, μmol/L	11.83 (2.61)	12.64 (3.01)	1.457 (11)	0.173	0.82 (-0.42 to 2.05)	0.162
PHE/TYR Ratio, μmol/mmol	1.01 (0.16)	0.97 (0.16)	-1.039 (11)	0.321	-0.04 (-0.13 to 0.05)	0.089
NEO, nmol/L	7.70 (4.26)	7.92 (4.15)	0.385 (11)	0.707	0.23 (-1.06 to 1.51)	0.013

Key: SD, standard deviation; [a] n=6.

Table 7.4. Changes in TRP, KYN, KYN/TRP Ratio, PHE, TYR, PHE/TYR Ratio and NEO Concentrations in Plasma and CSF from Baseline to Day 120 in the RAL Arm

RAL Arm, n=8	Baseline, Mean (SD)	Day 120, Mean (SD)	*t* (df)	Unadjusted *P* Value	Mean Change (95% CI)	Eta^2
Plasma						
TRP, μmol/L	51.15 (10.56)	47.09 (8.06)	-1.735 (7)	0.126	-4.06 (-9.58 to 1.47)	0.301
KYN, μmol/L	1.98 (0.78)	1.92 (0.68)	-0.436 (7)	0.676	-0.06 (-0.39 to 0.27)	0.026
KYN/TRP Ratio, μmol/mmol	38.82 (12.90)	42.06 (18.05)	0.788 (7)	0.456	3.24 (-6.48 to 12.96)	0.081
PHE, μmol/L	61.65 (7.55)	57.83 (6.83)	-0.952 (7)	0.373	-3.83 (-13.32 to 5.67)	0.115
TYR, μmol/L	65.34 (8.49)	63.96 (15.82)	-0.262 (7)	0.800	-1.38 (-13.76 to 11.01)	0.009
PHE/TYR Ratio, μmol/mmol	0.96 (0.15)	0.93 (0.16)	-0.512 (7)	0.625	-0.03 (-0.17 to 0.11)	0.036
NEO, nmol/L	11.83 (8.50)	15.44 (12.64)	0.885 (7)	0.405	3.61 (-6.04 to 13.27)	0.101
CSF						
TRP, μmol/L	1.58 (0.68)	1.60 (0.63)	0.168 (7)	0.872	0.02 (-0.27 to 0.30)	0.004
KYN, μmol/L [a]	0.07 (0.03)	0.06 (0.03)	-1.175 (3)	0.325	-0.01 (-0.03 to 0.01)	0.315
KYN/TRP Ratio, μmol/mmol [a]	43.39 (29.17)	38.12 (34.95)	-0.963 (3)	0.406	-5.27 (-22.69 to 12.15)	0.236
PHE, μmol/L	12.31 (2.43)	11.99 (12.15)	-0.575 (7)	0.584	-0.33 (-1.66 to 1.01)	0.045
TYR, μmol/L	12.38 (3.28)	12.24 (3.76)	-0.138 (7)	0.894	-0.14 (-2.49 to 2.21)	0.003
PHE/TYR Ratio, μmol/mmol	1.01 (0.10)	1.01 (0.21)	0.000 (7)	1.000	0.000 (-0.15 to 0.15)	0.000
NEO, nmol/L	9.19 (8.20)	7.26 (6.01)	-2.146 (7)	0.069	-1.93 (-4.06 to 0.20)	0.397

Key: SD, standard deviation; [a] n=4.

Table 7.5 details the differences in changes in biomarkers between the two arms. The mean difference between the arms in plasma TRP concentrations (unadjusted *p*=0.011) and CSF NEO concentrations (unadjusted *p*=0.049) were observed to be statistically significant. The difference in mean plasma TRP concentrations is driven by increases in the DTG arm and decreases in the RAL arm. Corresponding changes in KYN concentrations or the KYN/TRP ratio were not observed, indicating that the IDO enzyme is likely not involved in the observed changes in TRP concentrations. The difference in mean CSF NEO concentrations is primarily driven by decreases in the RAL arm. No other changes were observed for any parameter in either CSF or plasma.

Table 7.5. Differences in Changes in TRP, KYN, KYN/TRP Ratio, PHE, TYR, PHE/TYR Ratio and NEO Concentrations in Plasma and CSF from Baseline to Day 120 between the DTG and RAL Arms

	Absolute change over 120 days, Mean (SD)		*t* (df)	Unadjusted *P* Value	Mean Difference (95% CI)	Eta^2
	DTG Arm n=12	RAL Arm n=8				
Plasma						
TRP, μmol/L	4.84 (7.12)	-4.06 (6.61)	2.815 (18)	0.011	8.90 (2.26 to 15.54)	0.306
KYN, μmol/L	0.10 (0.64)	-0.06 (0.40)	0.624 (18)	0.541	0.16 (-0.38 to 0.69)	0.021
KYN/TRP Ratio, μmol/mmol	-0.55 (12.60)	3.24 (11.63)	-0.679 (18)	0.506	-3.79 (-15.52 to 7.94)	0.025
PHE, μmol/L	3.82 (8.90)	-3.83 (11.36)	1.687 (18)	0.109	7.64 (-1.88 to 17.16)	0.137
TYR, μmol/L	3.78 (10.76)	-1.38 (14.82)	0.903 (18)	0.378	5.15 (-6.83 to 17.13)	0.043
PHE/TYR Ratio, μmol/mmol	0.01 (0.14)	-0.03 (0.17)	0.550 (18)	0.589	0.04 (-0.11 to 0.18)	0.017
NEO, nmol/L	5.23 (15.42)	3.61 (11.55)	0.253 (18)	0.803	1.62 (-11.84 to 15.08)	0.004
CSF						
TRP, μmol/L	0.17 (0.43)	0.02 (0.33)	0.850 (18)	0.406	0.15 (-0.22 to 0.53)	0.039
KYN, μmol/L	0.01 [a] (0.01)	-0.01 [b] (0.01)	1.686 (8)	0.130	0.01 (-0.00 to 0.03)	0.262
KYN/TRP Ratio, μmol/mmol	-0.48 [a] (10.79)	-5.27 [b] (10.95)	0.684 (8)	0.513	4.79 (-11.36 to 20.94)	0.055
PHE, μmol/L	0.22 (2.17)	-0.33 (1.60)	0.604 (18)	0.553	0.54 (-1.34 to 2.43)	0.020
TYR, μmol/L	0.82 (1.94)	-0.14 (2.81)	0.902 (18)	0.379	0.95 (-1.27 to 3.18)	0.043
PHE/TYR Ratio, μmol/mmol	-0.04 (0.14)	0.00 (0.18)	-0.587 (18)	0.565	-0.04 (-0.19 to 0.11)	0.019
NEO, nmol/L	0.23 (2.03)	-1.93 (2.54)	2.11 (18)	0.049	2.15 (0.01 to 4.31)	0.198

Key: SD, standard deviation; [a] n=6; [b] n=4.

Tables 7.6 to 7.8 detail the changes in mean cerebral metabolite levels from Baseline to Day 120 for the overall population and for the DTG and RAL arms. Statistically significant increases in the mean mI/Cr ratio in frontal grey matter (unadjusted *p*=0.019) and decreases in the Cho/Cr ratio in right basal ganglia (unadjusted *p*=0.018) were observed in patients in the RAL arm (Table 7.8). Whilst not statistically significant, subjects in the DTG arm experienced a small numerical increase in mean NAA/Cr concentrations in frontal grey matter (mean increase, 0.08; *p*=0.082; 95% CI, -0.01 to 0.16). No other changes were observed in either arm, or in the overall combined group, during the 120-day period.

No statistically significant differences were observed in cerebral metabolite changes between the DTG and RAL Arms from Baseline to Day 120 (Table 7.9). Whilst not statistically significant, there was a small numerical difference in mean NAA/Cr concentrations between the two arms (mean difference, 0.13; *p*=0.078; 95% CI, -0.02 to 0.28).

Table 7.6. Changes in Mean Cerebral Metabolite Levels from Baseline to Day 120 in the Overall Population

Overall, N=19	Baseline, Mean (SD)	Day 120, Mean (SD)	*t* (df)	Unadjusted *P* Value	Mean Change (95% CI)	Eta^2
Frontal Grey Matter						
NAA/Cr	1.01 (0.09)	1.04 (0.12)	0.748 (18)	0.464	0.03 (-0.05 to 0.10)	0.012
Cho/Cr	0.23 (0.03)	0.23 (0.03)	-0.344 (18)	0.735	-0.00 (-0.02 to 0.02)	0.006
mI/Cr	0.58 (0.09)	0.64 (0.29)	0.797 (18)	0.436	0.06 (-0.10 to 0.22)	0.034
Glx/Cr	1.26 (0.14)	1.28 (0.22)	0.500 (18)	0.623	0.02 (-0.08 to 0.13)	0.014
Frontal White Matter						
NAA/Cr	1.23 (0.28)	1.19 (0.15)	-0.816 (18)	0.425	-0.04 (-0.16 to 0.07)	0.036
Cho/Cr	0.31 (0.04)	0.32 (0.04)	0.552 (18)	0.588	0.01 (-0.02 to 0.03)	0.017
mI/Cr	0.68 (0.15)	0.68 (0.13)	0.401 (18)	0.693	0.01 (-0.04 to 0.05)	0.008
Glx/Cr	0.93 (0.54)	0.90 (0.39)	-0.438 (18)	0.666	-0.03 (-0.19 to 0.12)	0.012
Right Basal Ganglia						
NAA/Cr	0.95 (0.19)	0.90 (0.20)	-0.635 (18)	0.533	-0.04 (-0.19 to 0.10)	0.022
Cho/Cr	0.24 (0.02)	0.22 (0.04)	-1.496 (18)	0.152	-0.01 (-0.03 to 0.01)	0.111
mI/Cr	0.42 (0.16)	0.45 (0.10)	0.732 (18)	0.473	0.03 (-0.73 to 0.05)	0.029
Glx/Cr	1.24 (0.53)	1.16 (0.91)	-0.278 (18)	0.784	-0.08 (-0.71 to 0.55)	0.004

Key: SD, standard deviation; NAA, N-acetyl aspartate; Cr, creatinine; Cho, choline; mI, myoinositol; Glx, glutamate and glutamine.

Table 7.7. Changes in Mean Cerebral Metabolite Levels from Baseline to Day 120 in the DTG Arm

DTG Arm, n=12	Baseline, Mean (SD)	Day 120, Mean (SD)	*t* (df)	Unadjusted *P* Value	Mean Change (95% CI)	Eta^2
Frontal Grey Matter						
NAA/Cr	1.00 (0.09)	1.08 (0.11)	1.916 (11)	0.082	0.08 (-0.01 to 0.16)	0.250
Cho/Cr	0.24 (0.03)	0.23 (0.04)	-0.889 (11)	0.383	-0.01 (-0.04 to 0.02)	0.067
mI/Cr	0.58 (0.11)	0.65 (0.12)	0.590 (11)	0.567	0.07 (-0.19 to 0.34)	0.031
Glx/Cr	1.28 (0.12)	1.34 (0.21)	1.024 (11)	0.328	0.05 (-0.06 to 0.17)	0.087
Frontal White Matter						
NAA/Cr	1.16 (0.15)	1.18 (0.14)	0.284 (11)	0.781	0.01 (-0.07 to 0.09)	0.007
Cho/Cr [a]	0.31 (0.04)	0.32 (0.03)	0.506 (10)	0.624	0.01 (-0.03 to 0.04)	0.025
mI/Cr	0.63 (0.12)	0.64 (0.09)	0.181 (11)	0.860	0.01 (-0.06 to 0.08)	0.002
Glx/Cr	0.82 (0.13)	0.86 (0.19)	0.083 (11)	0.621	0.04 (-0.12 to 0.19)	0.001
Right Basal Ganglia						
NAA/Cr	0.92 (0.20)	0.93 (0.25)	0.065 (11)	0.949	0.01 (-0.20 to 0.21)	0.000
Cho/Cr	0.23 (0.02)	0.22 (0.04)	-0.378 (11)	0.712	-0.01 (-0.04 to 0.02)	0.013
mI/Cr	0.38 (0.17)	0.45 (0.10)	1.266 (11)	0.232	0.07 (-0.05 to 0.19)	0.127
Glx/Cr	1.22 (0.63)	1.26 (1.13)	0.083 (11)	0.935	0.04 (-0.99 to 1.07)	0.001

Key: SD, standard deviation; NAA, N-acetyl aspartate; Cr, creatinine; Cho, choline; mI, myoinositol; Glx, glutamate and glutamine. [a] n=11

Table 7.8. Changes in Mean Cerebral Metabolite Levels from Baseline to Day 120 in the RAL Arm

RAL Arm, n=7	Baseline, Mean (SD)	Day 120, Mean (SD)	*t* (df)	Unadjusted *P* Value	Mean Change (95% CI)	Eta^2
Frontal Grey Matter						
NAA/Cr	1.02 (0.11)	0.96 (0.09)	-0.896 (6)	0.405	-0.06 (-0.21 to 0.98)	0.118
Cho/Cr	0.22 (0.02)	0.23 (0.02)	1.654 (6)	0.149	0.01 (-0.01 to 0.03)	0.313
mI/Cr	0.58 (0.04)	0.62 (0.06)	3.194 (6)	0.019	0.04 (-0.01 to 0.07)	0.630
Glx/Cr	1.21 (0.17)	1.19 (0.22)	-0.273 (6)	0.794	-0.03 (-0.27 to 0.21)	0.012
Frontal White Matter						
NAA/Cr	1.34 (0.40)	1.21 (0.18)	-1.057 (6)	0.331	-0.14 (-0.45 to 0.18)	0.157
Cho/Cr	0.32 (0.04)	0.32 (0.04)	0.071 (6)	0.945	0.00 (-0.05 to 0.05)	0.001
mI/Cr	0.75 (0.17)	0.76 (0.15)	0.693 (6)	0.514	0.01 (-0.03 to 0.06)	0.074
Glx/Cr	1.13 (0.87)	0.98 (0.62)	-0.907 (6)	0.399	-0.15 (-0.55 to 0.25)	0.121
Right Basal Ganglia						
NAA/Cr	0.99 (0.17)	0.87 (0.11)	-1.423 (6)	0.205	-0.13 (-0.35 to 0.09)	0.252
Cho/Cr	0.25 (0.03)	0.22 (0.01)	-3.338 (6)	0.018	-0.03 (-0.05 to 0.01)	0.650
mI/Cr	0.49 (0.10)	0.45 (0.10)	-1.116 (6)	0.307	-0.04 (-0.14 to 0.05)	0.172
Glx/Cr	1.29 (0.32)	1.00 (0.32)	1.860 (6)	0.112	-0.30 (-0.68 to 0.09)	0.366

Key: SD, standard deviation; NAA, N-acetyl aspartate; Cr, creatinine; Cho, choline; mI, myoinositol; Glx, glutamate and glutamine.

Table 7.9. Differences in Changes in Cerebral Metabolites from Baseline to Day 120 Between the DTG and RAL Arms

	Absolute change over 120 days, Mean (SD)		*t* (df)	Unadjusted *P* Value	Mean Difference (95% CI)	Eta^2
	DTG Arm n=12	DTG Arm n=7				
Frontal Grey Matter						
NAA/Cr	0.08 (0.04)	-0.06	1.876 (17)	0.078	0.13 (-0.02 to 0.28)	0.172
Cho/Cr	-0.01 (0.04)	0.01 (0.02)	-1.284 (17)	0.216	-0.02 (-0.06 to 0.01)	0.088
mI/Cr	0.07 (0.42)	0.04 (0.03)	0.192 (17)	0.850	0.03 (-0.31 to 0.38)	0.002
Glx/Cr	0.05 (0.18)	-0.03 (0.26)	0.797 (17)	0.437	0.08 (-0.13 to 0.29)	0.036
Frontal White Matter						
NAA/Cr	0.01 (0.13)	0.14 (0.34)	1.357 (17)	0.192	0.15 (-0.08 to 0.38)	0.098
Cho/Cr	0.01 (0.05)	0.00 (0.05)	0.323 (17)	0.751	-0.01 (-0.04 to 0.06)	0.006
mI/Cr	0.01 (0.11)	0.01 (0.05)	-0.159 (17)	0.876	-0.01 (-0.10 to 0.09)	0.001
Glx/Cr	0.03 (0.24)	-0.15 (0.44)	1.203 (17)	0.246	0.19 (-0.14 to 0.51)	0.078
Right Basal Ganglia						
NAA/Cr	0.01 (0.32)	0.13 (0.24)	0.947 (17)	0.357	0.13 (-0.16 to 0.43)	0.050
Cho/Cr	0.01 (0.05)	0.03 (0.02)	1.267 (17)	0.222	0.02 (-0.02 to 0.07)	0.086
mI/Cr	0.07 (0.19)	-0.04 (0.10)	1.431 (17)	0.170	0.11 (-0.05 to 0.28)	0.108
Glx/Cr	0.04 (1.63)	0.29 (0.42)	0.524 (17)	0.607	0.33 (-1.01 to 1.67)	0.016

Key: SD, standard deviation; NAA, N-acetyl aspartate; Cr, creatinine; Cho, choline; mI, myoinositol; Glx, glutamate and glutamine.

7.2.3 Univariate Analysis of Cognitive Function and Mood Parameters

The results of the Patient Health Questionnaire-9 (PHQ-9) and Beck Depression Inventory (BDI) measures of depression both indicated that subjects were experiencing minimal depression during the study with no statistically significant changes in either measure for the overall group or the separate study arms from Baseline to D120 (Tables 7.10 to 7.12, below). No significant differences were observed between the two arms for changes in PHQ-9 and BDI scores from Baseline to Day 120 (Table 7.13). The result of the Lawton's instrumental activities of daily living scale (IADL) questionnaire was a score of 8 for all patients at all time points indicating high function/independence (data not in tables). Because significant changes were not observed, the relationship between the PHQI-9, BDI and IADL scores and measures of TRP metabolism was not explored further.

Table 7.10. Change in Mean Questionnaire Scores at Baseline and Day 120 for the Overall Group

Overall, N=20	Baseline, Mean (SD)	Day 120, Mean (SD)	Mean Change from Baseline to Day 120			
			t (df)	Unadjusted *P* Value	Mean Change (95% CI)	Eta^2
PHQ-9	2.85 (2.98)	1.95 (1.96)	1.851 (19)	0.080	-0.90 (-1.9 to 0.1)	0.153
BDI	4.60 (5.73)	2.90 (4.15)	1.491 (19)	0.152	-1.70 (-4.1 to 0.7)	0.105

Key: SD, standard deviation; PHQ-9, Patient Health Questionnaire-9; BDI, Beck Depression Inventory.

Table 7.11. Change in Mean Questionnaire Scores at Baseline and Day 120 for the DTG Arm

DTG Arm, n=12	Baseline, Mean (SD)	Day 120, Mean (SD)	Mean Change from Baseline to Day 120			
			t (df)	Unadjusted *P* Value	Mean Change (95% CI)	Eta^2
PHQ-9	3.17 (3.46)	2.08 (2.23)	1.545 (11)	0.151	-1.08 (-0.5 to 2.6)	0.178
BDI	3.00 (5.82)	3.25 (5.03)	-0.220 (11)	0.830	0.25 (-2.2 to 2.7)	0.004

Key: SD, standard deviation; PHQ-9, Patient Health Questionnaire-9; BDI, Beck Depression Inventory.

Table 7.12. Change in Mean Questionnaire Scores at Baseline and Day 120 for the RAL Arm

RAL ARM, n=8	Baseline, Mean (SD)	Day 120, Mean (SD)	Mean Change from Baseline to Day 120			
			t (df)	Unadjusted *P* Value	Mean Change (95% CI)	Eta^2
PHQ-9	2.38 (2.20)	1.75 (1.58)	0.957 (7)	0.370	-0.63 (-2.2 to 0.9)	0.116
BDI	5.00 (4.47)	2.38 (2.56)	1.966 (7)	0.090	-2.63 (-5.8 to 0.5)	0.356

Key: SD, standard deviation; PHQ-9, Patient Health Questionnaire-9; BDI, Beck Depression Inventory.

Table 7.13. Differences in Changes in Mean Questionnaire Scores from Baseline to Day 120 between the DTG and RAL Arms

Parameter	Change over 120 days, Mean (SD)		*t* (df)	Unadjusted *P* Value	Mean Difference (95% CI)	Eta^2
	DTG Arm n=12	RAL Arm n=8				
PHQ-9	1.08 (2.43)	0.63 (1.85)	0.452 (18)	0.657	-0.46 (-1.0 to 0.5)	0.011
BDI	1.08 (5.90)	2.63 (3.78)	-0.652 (18)	0.523	1.54 (-3.4 to 6.5)	0.023

Key: SD, standard deviation; PHQ-9, Patient Health Questionnaire-9; BDI, Beck Depression Inventory.

Tables 7.14 to 7.16, below, present the changes in the mean CogState™ scores from Baseline to Day 120 for the overall population and for the individual study arms. A statistically significant reduction in the mean total number of errors for the Groton Maze Learning Task (GML; unadjusted p=0.033) and a significant increase in the mean number of moves per second for the Groton Maze Chase Test (GMCT; unadjusted p=0.041) were observed in the overall population from Baseline to Day 120, indicating improvements in these parameters (Table 7.14). These changes appear to be primarily driven by changes in the performance of patients in the DTG arm (Table 7.15).

Table 7.14. Changes in Mean CogState™ Scores from Baseline to Day 120 for the Overall Population

Overall, N=20	Baseline, Mean (SD)	Day 60, Mean (SD)	Day 120, Mean (SD)	Mean Change from Baseline to Day 120			
				t (df)	Unadjusted *P* Value	Mean Change (95% CI)	Eta^2
IDN, Log^{10} ms	2.67 (0.05)	2.67 (0.07)	2.66 (0.07)	-0.350 (19)	0.730	-0.00 (-0.03 to 0.02)	0.006
DET, Log^{10} ms	2.52 (0.10)	2.50 (0.10)	2.48 (0.09)	-1.802 (19)	0.087	-0.03 (-0.07 to 0.01)	0.146
GML, Total No. Errors	46.10 (14.44)	42.15 (13.10)	38.95 (13.62)	-2.304 (19)	0.033	-6.10 (-11.64 to 0.56)	0.218
CPAL, Total No. Errors	60.00 (50.00)	58.30 (54.26)	57.85 (50.67)	0.487 (19)	0.632	4.25 (-14.01 to 22.51)	0.012
OCL, Arcsine proportion	0.75 (0.07)	0.74 (0.07)	0.74 (0.09)	-1.436 (19)	0.167	-0.02 (-0.06 to 0.01)	0.098
ONB, Log^{10} ms	2.85 (0.07)	2.84 (0.07)	2.82 (0.07)	-1.671 (19)	0.111	-0.02 (-0.05 to 0.01)	0.023
GMCT, mps	1.56 (0.33)	1.61 (34)	1.69 (0.33)	2.188 (19)	0.041	0.10 (-0.00 to 0.20)	0.201

Key: SD, standard deviation; IDN, identification task; DET, detection task; GML, Groton maze learning task; CPAL, continuous paired associate learning; OCL, one card learning; ONB, one back memory; GMCT, Groton maze chase test.

Table 7.15. Changes in Mean CogState™ Scores from Baseline to Day 120 for the DTG Arm

DTG Arm, n=12	Baseline, Mean (SD)	Day 60, Mean (SD)	Day 120, Mean (SD)	Mean Change from Baseline to Day 120			
				t (df)	Unadjusted *P* Value	Mean Change (95% CI)	Eta^2
IDN, Log^{10} ms	2.68 (0.05)	2.67 (0.07)	2.66 (0.07)	-0.763 (11)	0.461	-0.01 (-0.05 to 0.05)	0.050
DET, Log^{10} ms	2.52 (0.10)	2.51 (0.10)	2.50 (0.10)	-1.468 (11)	0.170	-0.02 (-0.06 to 0.01)	0.164
GML, Total No. Errors	46.42 (13.91)	41.42 (11.44)	39.25 (14.94)	-1.817 (11)	0.097	-7.17 (-15.85 to 1.51)	0.231
CPAL, Total No. Errors	58.75 (41.91)	48.59 (52.31)	64.58 (52.12)	0.510 (11)	0.620	5.83 (-19.33 to 31.00)	0.023
OCL, Arcsine proportion	0.76 (0.07)	0.73 (0.08)	0.73 (0.09)	-1.474 (11)	0.169	-0.03 (-0.08 to 0.02)	0.165
ONB, Log^{10} ms	2.84 (0.06)	2.83 (0.07)	2.82 (0.08)	-1.234 (11)	0.243	-0.02 (-0.06 to 0.02)	0.122
GMCT, mps	1.48 (0.31)	1.58 (0.33)	1.63 (0.33)	2.182 (11)	0.052	0.14 (-0.00 to 0.29)	0.302

Key: SD, standard deviation; IDN, identification task; DET, detection task; GML, Groton maze learning task; CPAL, continuous paired associate learning; OCL, one card learning; ONB, one back memory; GMCT, Groton maze chase test.

Table 7.16. Changes in Mean CogState™ Scores from Baseline to Day 120 for the RAL Arm

RAL Arm, n=8	Baseline, Mean (SD)	Day 60, Mean (SD)	Day 120, Mean (SD)	Mean Change from Baseline to Day 120			
				t (df)	Unadjusted *P* Value	Mean Change (95% CI)	Eta^2
IDN, Log^{10} ms	2.64 (0.04)	2.66 (0.07)	2.65 (0.06)	0.731 (7)	0.489	0.01 (-0.02 to 0.04)	0.071
DET, Log^{10} ms	2.49 (0.10)	2.46 (0.07)	2.45 (0.06)	-1.161 (7)	0.284	-0.05 (-0.14 to 0.05)	0.161
GML, Total No. Errors	43.00 (14.76)	43.25 (16.07)	38.50 (12.35)	-1.403 (7)	0.203	-4.50 (-12.08 to 3.08)	0.219
CPAL, Total No. Errors	45.88 (42.45)	72.88. (57.32)	47.75. (50.07)	0.130 (7)	0.900	1.88 (-32.13 to 35.88)	0.002
OCL, Arcsine proportion	0.75 (0.06)	0.74 (0.04)	0.75 (0.09)	-0.348 (7)	0.738	-0.01 (0.06 to 0.04)	0.017
ONB, Log^{10} ms	2.86 (0.08)	2.86 (0.07)	2.83 (0.05)	-1.068 (7)	0.321	-0.03 (-1.07 to 0.09)	0.140
GMCT, mps	1.76 (0.23)	1.66 (0.42)	1.80 (0.33)	0.649 (7)	0.537	0.04 (-0.10 to 0.17)	0.057

Key: SD, standard deviation; IDN, identification task; DET, detection task; GML, Groton maze learning task; CPAL, continuous paired associate learning; OCL, one card learning; ONB, one back memory; GMCT, Groton maze chase test.

The differences in changes from Baseline to Day 60 in individual CogState™ test Z scores and the GCS Z score between the two study arms are displayed in Table 7.17, below. A statistically significant difference between arms was observed in the Z score for the continuous paired associate learning (CPAL) test (unadjusted p=0.004), which appears to be driven by improvement in this parameter in the RAL arm. No other differences were observed. The differences in changes in CogState™ Z score, including the GCS, from Baseline to Day 120 between arms are displayed in Table 7.18 below. No statistically significant differences were observed, indicating that the difference between arms in performance on the CPAL test at Day 60 did not persist out to Day 120.

Table 7.17. Differences in Changes in CogState™ Z Score from Baseline to Day 60 Between the DTG and RAL Arms

Z Score	Change over 60 days, Mean Z Score (SD)		*t* (df)	Unadjusted *P* Value	Mean Difference (95% CI)	Eta^2
	DTG Arm n=12	RAL Arm n=8				
GCS	0.12 (0.39)	-0.17 (0.41)	1.573 (18)	0.133	0.29 (-0.10 to 0.67)	0.121
IDN	0.13 (0.72)	-0.44 (1.09)	1.394 (18)	0.180	0.56 (-0.29 to 1.41)	0.097
DET	0.12 (0.73)	0.31 (1.05)	-0.472 (18)	0.643	-0.19 (-1.02 to 0.65)	0.012
GML	0.35 (0.77)	-0.01 (0.77)	1.023 (18)	0.320	0.36 (-0.38 to 1.10)	0.055
CPAL	0.20 (0.49)	-0.54 (0.51)	3.248 (18)	0.004	0.74 (0.26 to 1.22)	0.370
OCL	-0.46 (1.11)	-0.19 (0.66)	-0.599 (18)	0.557	-0.26 (-1.18 to 0.66)	0.020
ONB	0.21 (0.73)	0.02 (0.71)	0.579 (18)	0.570	0.19 (-0.50 to 0.88)	0.018
GMCT	0.30 (0.91)	-0.30 (1.28)	1.226 (18)	0.236	0.60 (-0.43 to 1.62)	0.077

Key: SD, standard deviation; IDN, identification task; DET, detection task; GML, Groton maze learning task; CPAL, continuous paired associate learning; OCL, one card learning; ONB, one back memory; GMCT, Groton maze chase test.

Table 7.18. Differences in Changes in CogState™ Z Score from Baseline to Day 120 Between the DTG and RAL Arms

Z Score	Change over 120 days, Mean Z Score (SD)		*t* (df)	Unadjusted *P* Value	Mean Difference (95% CI)	Eta^2
	DTG Arm n=12	RAL Arm n=8				
GCS	0.14 (0.41)	0.14 (0.37)	-0.014 (18)	0.989	-0.00 (-0.38 to 0.37)	0.000
IDN	0.18 (1.02)	-0.18 (1.02)	0.895 (18)	0.383	0.36 (-0.49 to 1.21)	0.043
DET	0.22 (0.51)	0.48 (1.11)	-0.705 (18)	0.490	-0.26 (-1.02 to 0.51)	0.027
GML	0.50 (0.95)	0.31 (0.63)	0.476 (18)	0.640	0.18 (-0.62 to 0.99)	0.012
CPAL	-0.12 (0.79)	-0.04 (0.81)	-0.217 (18)	0.831	-0.08 (-0.85 to 0.69)	0.002
OCL	-0.48 (1.12)	-0.11 (0.90)	-0.770 (18)	0.451	-0.37 (-1.36 to 0.63)	0.032
ONB	0.25 (0.74)	0.44 (1.07)	-0.468 (18)	0.645	-0.19 (-1.04 to 0.66)	0.012
GMCT	0.43 (0.68)	0.11 (0.49)	1.136 (18)	0.271	0.32 (-0.27 to 0.91)	0.067

Key: SD, standard deviation; GCS, global composite score; IDN, identification task; DET, detection task; GML, Groton maze learning task; CPAL, continuous paired associate learning; OCL, one card learning; ONB, one back memory; GMCT, Groton maze chase test.

7.2.4 Multivariate Analysis to Determine Relationships Between Plasma and CSF Biomarkers and CogState™ Global Composite Scores

The associations between plasma and CSF biomarker concentrations and the CogState™ GCS (Tables 7.19 and 7.20, respectively) for all subjects at Baseline were explored using Pearson r correlations. All subjects were receiving RAL at this time point and had not received their first dose of DTG.

No statistically significant associations were observed between plasma biomarkers and the GCS Z score at Baseline (Table 7.19). However, CSF PHE concentrations positively correlated with the GCS Z score (r=0.489, unadjusted *p*=0.024), as did CSF PHE/TYR ratios (r=0.567, unadjusted *p*=0.007) (Table 7.20). Plasma and CSF concentrations of NEO positively correlated with KYN concentrations (r=0.503, unadjusted *p*=0.020; and r=0.563; unadjusted *p*=0.023, respectively) and the KYN/TRP ratio (r=0.774, unadjusted *p*<0.001; and r=0.845; unadjusted *p*<0.001, respectively), (Tables 7.19 and 7.20).

Table 7.19. Correlations Between Plasma Biomarker Concentrations and CogState™ Global Composite Score for the Overall Population at Baseline

		GCS	TRP	KYN	KYN/TRP	PHE	TYR	PHE/TYR	NEO
GCS, Z Score	N	21							
	P Value	-	-	-	-	-	-	-	-
	r	1							
TRP, µmol/L	N	21	21						
	P Value	0.077	-	-	-	-	-	-	-
	r	0.394	1						
KYN, µmol/L	N	21	21	21					
	P Value	0.627	0.030	-	-	-	-	-	-
	r	0.114	0.474	1					
KYN/TRP Ratio,	N	21	21	21	21				
µmol/mmol	*P* Value	0.535	0.798	<0.001	-	-	-	-	-
	r	-0.143	-0.059	0.843	1				
PHE, µmol/L	N	21	21	21	21	21			
	P Value	0.467	0.034	0.033	0.182	-	-	-	-
	r	0.168	0.434	0.467	0.303	1			
TYR, µmol/L	N	21	21	21	21	21	21		
	P Value	0.781	0.037	0.026	0.201	0.006	-	-	-
	r	-0.064	0.457	0.484	0.291	0.580	1		
PHE/TYR Ratio,	N	21	21	21	21	21	21	21	
µmol/mmol	*P* Value	0.224	0.525	0.486	0.738	0.372	0.01	-	-
	r	0.277	-0.147	-0.161	-0.078	0.205	-0.660	1	
NEO, nmol/L	N	21	21	21	21	21	21	21	21
	P Value	0.175	0.209	0.020	<0.001	0.153	0.576	0.453	-
	r	-0.308	-0.286	0.503	0.774	0.324	0.129	0.173	1

Key: GCS, global composite score.

Table 7.20. Correlations Between CSF Biomarker Concentrations and CogState™ Global Composite Score for the Overall Population at Baseline

		GCS	TRP	KYN	KYN/TRP	PHE	TYR	PHE/TYR	NEO
GCS, Z Score	N	21							
	P Value	-	-	-	-	-	-	-	-
	r	1							
TRP, μmol/L	N	21	21						
	P Value	0.289	-	-	-	-	-	-	-
	r	-0.243	1						
KYN, μmol/L	N	21	21	21					
	P Value	0.066	0.682	-	-	-	-	-	-
	r	-0.471	0.111	1					
KYN/TRP Ratio,	N	21	21	21	21				
μmol/mmol	*P* Value	0.876	0.329	0.005	-	-	-	-	-
	r	-0.042	-0.261	0.667	1				
PHE, μmol/L	N	21	21	21	21	21			
	P Value	0.024	0.421	0.440	0.919	-	-	-	-
	r	0.489	0.186	-0.208	0.028	1			
TYR, μmol/L	N	21	21	21	21	21	21		
	P Value	0.878	0.051	0.551	0.634	0.006	-	-	-
	r	-0.036	0.432	0.161	0.129	0.580	1		
PHE/TYR Ratio,	N	21	21	21	21	21	21	21	
μmol/mmol	*P* Value	0.007	0.233	0.096	0.581	0.056	0.028	-	-
	r	0.567	-0.272	-0.430	-0.149	0.423	-0.480	1	
NEO, nmol/L	N	21	21	21	21	21	21	21	21
	P Value	0.475	0.174	0.023	<0.001	0.993	0.801	0.852	-
	r	0.165	-0.308	0.563	0.845	-0.002	-0.059	0.043	1

Key: GCS, global composite score.

7.2.5 Multivariate Analysis to Determine Relationships Between Plasma and CSF Biomarkers and Magnetic Resonsance Imaging Cerebral Metabolite Concentrations

The associations between plasma and CSF biomarker concentrations and MRS metabolite concentrations (Tables 7.21 and 7.22, respectively) for all subjects at Baseline were explored using Pearson r correlations. All subjects were receiving RAL at this time point and had not received their first dose of DTG.

In plasma, mean TRP concentrations positively correlated with mean frontal white matter Naa/Cr (r=0.626; p<0.002) and Glx/Cr (r=0.603; p<0.004) concentrations (Table 7.21). Mean plasma TRP (r=-0.576; p<0.006), KYN (r=-0.451; p<0.04), PHE (r=-0.561; p<0.008) and TYR (r=-0.544; p<0.011) concentrations all negatively correlated with mean frontal grey matter Cho/Cr concentrations at Baseline. In CSF, the mean PHE/TYR ratio was observed to be negatively correlated with mean right basal ganglia Cho/Cr concentrations (r=-0.439; p<0.047) and positively correlated with mean frontal grey matter Glx/Cr concentrations (r=0.441; p<0.045) (Table 7.22).

Table 7.21. Correlations Between Plasma Biomarker Concentrations and MRS Cerebral Metabolite Concentrations for the Overall Population at Baseline

		FGM NaaCr Baseline	FWM NaaCr Baseline	RBG NaaCr Baseline	FGM ChoCr Baseline	FWM ChoCr Baseline	RBG ChoCr Baseline	FGM mICr Baseline	FWM mICr Baseline	RBG mICr Baseline	FGM GlxCr Baseline	FWM GlxCr Baseline	RBG GlxCr Baseline
TRP, μmol/L	N	21	21	21	21	21	21	21	21	21	21	21	21
	P Value	0.605	0.002	0.909	0.006	0.223	0.753	0.211	0.105	0.563	0.136	0.004	0.732
	r	-0.120	0.626	-0.027	-0.576	0.272	-0.073	-0.285	0.363	0.134	0.337	0.603	0.079
KYN, μmol/L	N	21	21	21	21	21	21	21	21	21	21	21	21
	P Value	0.299	0.655	0.801	0.040	0.894	0.674	0.344	0.568	0.107	0.453	0.649	0.885
	r	-0.238	0.103	-0.058	-0.451	-0.031	0.098	-0.217	0.132	0.362	-0.173	0.106	0.034
KYN/TRP	N	21	21	21	21	21	21	21	21	21	21	21	21
Ratio,	*P* Value	0.326	0.318	0.738	0.441	0.428	0.424	0.830	0.880	0.082	0.078	0.326	0.912
μmol/mmol	r	-0.225	-0.229	-0.078	-0.178	-0.183	0.184	-0.050	-0.035	0.389	-0.393	-0.225	-0.026
PHE, μmol/L	N	21	21	21	21	21	21	21	21	21	21	21	21
	P Value	0.168	0.164	0.340	0.008	0.700	0.642	0.546	0.321	0.146	0.503	0.143	0.333
	r	-0.313	0.315	-0.219	-0.561	-0.089	-0.108	-0.140	0.227	0.329	0.155	0.331	-0.222
TYR, μmol/L	N	21	21	21	21	21	21	21	21	21	21	21	21
	P Value	0.437	0.685	0.774	0.011	0.204	0.785	0.744	0.219	0.302	0.857	0.928	0.656
	r	-0.179	0.094	-0.067	-0.544	-0.289	0.063	-0.076	0.280	0.236	0.042	-0.021	0.103
PHE/TYR	N	21	21	21	21	21	21	21	21	21	21	21	21
Ratio,	*P* Value	0.668	0.595	0.702	0.495	0.495	0.260	0.968	0.422	0.816	0.673	0.186	0.114
μmol/mmol	r	-0.100	0.123	-0.089	0.158	0.158	-0.257	-0.009	-0.185	-0.054	0.098	0.300	-0.355
NEO, nmol/L	N	21	21	21	21	21	21	21	21	21	21	21	21
	P Value	0.174	0.184	0.721	0.903	0.058	0.420	0.382	0.709	0.162	0.094	0.213	0.386
	r	-0.308	-0.302	-0.083	-0.028	-0.420	0.186	0.201	-0.086	0.317	-0.375	-0.284	-0.200

Key: FGM, frontal grey matter; FWM, frontal white matter; RBG, right basal ganglia; NaaCr, N-acetylaspartate/creatinine ratio; ChoCr, choline/creatinine ratio; mICr, myo-inositol/creatinine ratio; GlxCr, glutamate/creatinine ratio.

Table 7.22. Correlations Between CSF Biomarker Concentrations and MRS Cerebral Metabolite Concentrations for the Overall Population at Baseline

		FGM NaaCr Baseline	FWM NaaCr Baseline	RBG NaaCr Baseline	FGM ChoCr Baseline	FWM ChoCr Baseline	RBG ChoCr Baseline	FGM mICr Baseline	FWM mICr Baseline	RBG mICr Baseline	FGM GlxCr Baseline	FWM GlxCr Baseline	RBG GlxCr Baseline
TRP, μmol/L	N	21	21	21	21	21	21	21	21	21	21	21	21
	P Value	0.756	0.443	0.899	0.447	0.523	0.425	0.858	0.980	0.354	0.797	0.335	0.571
	r	0.072	0.177	-0.030	-0.175	0.148	0.184	-0.042	0.006	0.213	0.060	0.221	-0.131
KYN, μmol/L	N	16	16	16	16	16	16	16	16	16	16	16	16
	P Value	0.220	0.341	0.987	0.735	0.595	0.181	0.887	0.739	0.137	0.479	0.303	0.550
	r	-0.324	-0.255	0.005	-0.092	-0.144	0.352	0.039	0.090	0.388	-0.191	-0.275	-0.161
KYN/TRP Ratio, μmol/mmol	N	16	16	16	16	16	16	16	16	16	16	16	16
	P Value	0.697	0.193	0.475	0.287	0.325	0.338	0.632	0.911	0.272	0.221	0.334	0.945
	r	-0.106	-0.343	0.193	-0.284	-0.263	0.256	-0.130	0.030	0.292	-0.324	-0.259	0.019
PHE, μmol/L	N	21	21	21	21	21	21	21	21	21	21	21	21
	P Value	0.575	0.550	0.194	0.239	0.956	0.177	0.476	0.703	0.505	0.251	0.217	0.763
	r	0.130	0.138	0.295	-0.269	-0.013	-0.306	-0.164	0.089	-0.154	0.262	0.281	-0.070
TYR, μmol/L	N	21	21	21	21	21	21	21	21	21	21	21	21
	P Value	0.723	0.956	0.671	0.114	0.243	0.808	0.531	0.763	0.375	0.529	0.734	0.975
	r	-0.082	-0.013	0.098	-0.355	-0.267	0.056	-0.145	0.070	0.204	-0.145	0.079	-0.007
PHE/TYR Ratio, μmol/mmol	N	21	21	21	21	21	21	21	21	21	21	21	21
	P Value	0.370	0.495	0.434	0.563	0.348	0.047	0.764	0.997	0.064	0.045	0.340	0.684
	r	0.206	0.158	0.180	0.134	0.216	-0.439	0.070	0.001	-0.411	0.441	0.219	-0.094
NEO, nmol/L	N	21	21	21	21	21	21	21	21	21	21	21	21
	P Value	0.771	0.262	0.658	0.534	0.267	0.649	0.521	0.747	0.502	0.289	0.232	0.896
	r	-0.068	-0.257	0.103	-0.144	-0.254	0.105	-0.148	-0.075	0.155	-0.243	-0.273	0.030

Key: FGM, frontal grey matter; FWM, frontal white matter; RBG, right basal ganglia; NaaCr, N-acetylaspartate/creatinine ratio; ChoCr, choline/creatinine ratio; mICr, myo-inositol/creatinine ratio; GlxCr, glutamate/creatinine ratio; Sig., significance 2-tailed.

7.2.6 Linear Mixed Model Analyses to Determine Relationships Between Plasma and CSF TRP, KYN and KYN/TRP Ratio Concentrations and Cogstate™ Global Composite Scores

The relationship between the changes in TRP and KYN concentrations and KYN/TRP ratios in plasma and CSF and the CogState™ GCS for patients in the DTG arm were explored using linear mixed models, the results of each are detailed in Tables 7.23 and 7.24, below. The plasma KYN/TRP ratio was found to be negatively correlated with CogState™ GCS, such that for every 1 μmol/L increase observed in KYN/TRP ratio, a 0.019-point decrease was observed in the CogState™ GCS (unadjusted *p*=0.021), indicating a small decline in cognitive function as the KYN/TRP ratio increases. No other significant associations were found, though trends were observed for both plasma KYN (estimate=-0.287, unadjusted *p*=0.084) and CSF TRP (estimate=0.396, unadjusted *p*=0.091) and the CogState™ GCS.

Table 7.23. Regression Coefficients for Random Intercept Model for TRP, KYN and KYN/TRP Ratio in Plasma and CogState™ GCS from Baseline to Day 120

Parameter	Estimate (95% CI)	Unadjusted *P* value
Model 1: GCS Z Score and TRP		
GCS Z Score	-0.897 (-2.26 to 0.47)	0.186
TRP, μmol/L	0.016 (-0.01 to 0.04)	0.207
Model 2: GCS Z Score and KYN		
GCS Z Score	-0.544 (-2.77 to 1.37)	0.184
KYN, μmol/L	-0.287 (-0.62 to 0.04)	0.084
Model 3: GCS Z Score and KYN/TRP Ratio		
GCS Z Score	0.750 (-0.03 to 1.53)	0.059
KYN/TRP Ratio, μmol/mmol	-0.019 (-0.04 to 0.00)	0.021

Key: TRP, tryptophan; KYN, kynurenine; CNS, central nervous system; CI, confidence interval.

Table 7.24. Regression Coefficients for Random Intercept Model for TRP, KYN and KYN/TRP Ratio in CSF and CogState™ GCS from Baseline to Day 120

Parameter	Estimate (95% CI)	Unadjusted *P* value
Model 1: GCS Z Score and TRP		
GCS Z Score	-0.797 (-1.73 to 0.13)	0.089
TRP, μmol/L	0.396 (-0.07 to 0.86)	0.091
Model 2: GCS Z Score and KYN		
GCS Z Score	0.679 (-0.40 to 1.75)	0.198
KYN, μmol/L	-9.361 (-23.66 to 4.94)	0.184
Model 3: GCS Z Score and KYN/TRP Ratio		
GCS Z Score	0.502 (-0.52 to 1.52)	0.315
KYN/TRP Ratio, μmol/mmol	-0.014 (-0.04 to 0.01)	0.289

Key: TRP, tryptophan; KYN, kynurenine; CNS, central nervous system; CI, confidence interval.

7.3 Discussion

In this study, neurologically-asymptomatic, virologically-suppressed PLWH receiving a RAL-based regimen were either switched to DTG or remained on RAL. Whilst some subtle changes in biomarker concentrations and cognitive test results were observed, there appears to be very little difference between the two integrase inhibitors in terms of their effect on TRP metabolism and CNS function. These observations do not support the first hypothesis that TRP metabolism is increased in the presence of ARVs. Mean plasma TRP concentrations were observed to increase in patients receiving DTG over 120 days, with a statistically significant difference in changes between the DTG and RAL arms over this period. However, no significant changes were observed in either KYN concentrations or the KYN/TRP ratio for either of the two agents, suggesting that switching from RAL to DTG does not influence TDO or IDO activity in this population. Previous clinical studies have demonstrated that KYN/TRP ratios decline following initiation of ART due to decreases in immune activation resulting from suppression of HIV-1-RNA (321, 410, 411), However, in the SSAT056 study reported in Chapter 6, KYN concentrations and the KYN/TRP ratio were observed to increase following switch from EFV. It is possible that EFV is attenuating TDO or IDO activity, which is in-line with the effects reported by Zheve (409) but in contrast with the lack of effect seen in THLE2 and THLE3 in the *in vitro* studies reported in Chapter 4 of this thesis. The increases in plasma KYN concentrations and the KYN/TRP ratio were unexpected and suggest that there is a differential effect between ARVs on TRP metabolism *in vivo*, one that was not supported by the *in vitro*

data. The CIIS study data suggest that a similar effect is not evident when switching from one integrase inhibitor to another.

Subjects receiving RAL were observed to have declines in CSF NEO concentrations over the 120-day follow-up period suggesting a progressive decline in CSF immune activation in patients already virologically-stable on a RAL-based regimen. This was not seen in the DTG arm. As with the SSAT056 study (Chapter 6), NEO was included as a marker of immune activation based on its correlation with IDO activity (174). Whilst CSF NEO levels have been shown to decrease after initiating ARV therapy, they do not appear to return to normal in all subjects even following up to a decade of suppressive therapy, indicating a persistent low-level intrathecal immune activation (136, 137, 211). In a previous study by Dahl *et al*., in which the effect of treatment intensification with RAL in PLWH with virological-suppression in both plasma and CSF was investigated, NEO concentrations were not observed to change significantly over a 12-week follow-up period (418). However, it is difficult to make direct comparisons with this study because RAL was added to an existing virologically-suppressive triple ARV regimen that may already be maximally suppressing NEO levels. In the CIIS study reported in this chapter, coinciding changes in KYN concentrations or the KYN/TRP ratio in the RAL arm were not observed, perhaps suggesting that the observed decline in NEO is not sufficient to affect IDO activity or that other, potentially competing, factors are involved.

Very few changes were observed in MRS cerebral metabolite concentrations, with no significant differences between study arms. In the RAL arm (Table 7.8), statistically significant increases were observed in mI/Cr concentrations in frontal grey matter and decreases were observed in Cho/Cr concentrations in right basal ganglia. Cho and mI are indicators of glial proliferation and cellular injury and, as such, their levels increase with neuroinflammation (292, 294). These data may indicate that there are localised pockets of increased and decreased inflammation in different anatomical locations in the brain. No other significant changes were observed in either arm or in the combined group. In the baseline cross-sectional analysis, statistically significant positive correlations were observed between plasma TRP and Naa/Cr and Glx/Cr in frontal white matter. NAA is used as a sensitive marker of neuronal integrity *in vivo*, with reductions in its concentrations being indicative of damage and, possibly, a reduction in neuronal density (117, 265, 292). Glx is a combination of glutamate, an excitatory neurotransmitter found primarily in glutamatergic neurons, and its stored form, glutamine, which is found within astrocytes. Decreased levels of Glx are suspected to be an

early indicator of neuronal metabolism changes (265). These data indicate that greater TRP concentrations in plasma are associated with greater frontal white matter integrity. Plasma TRP concentrations were also observed to be negatively correlated with the Cho/Cr ratio in frontal grey matter, as were KYN, PHE and TYR concentrations. In addition to this, the PHE/TYR ratio in CSF was negatively correlated with Cho/Cr in right basal ganglia and positively correlated with Glx/Cr in frontal grey matter. These are interesting observations and, again, possibly indicate localised pockets of increased or decreased immune activation. Further research is needed to understand these complex inflammatory relationships and whether there are causal mechanistic effects between each marker.

Despite the lack of changes in KYN production, this study does provide evidence to support the second hypothesis that increased TRP metabolism is associated with poorer cognitive performance. In the linear mixed model analysis, the plasma KYN/TRP ratio was found to be negatively correlated with CogState^{TM} GCS, such that for every 1 µmol/L increase observed in the KYN/TRP ratio, a 0.019-point decrease was observed in the CogState^{TM} GCS (unadjusted p=0.021), indicating a modest decline in cognitive function as the KYN/TRP ratio increases. Linear mixed models account for data for all subjects at all time points and, whilst statistically significant changes were not observed in the KYN/TRP ratio separately, the mixed model did detect a significant relationship between the KYN/TRP ratio and GCS scores. It must be noted that these data were not subjected to multiplicity correction and that the relationship would no longer be significant if this had been applied. No other significant associations were found, though trends were observed for both plasma KYN (estimate=-0.287, unadjusted p=0.084) and CSF TRP (estimate=0.396, unadjusted p=0.091) and the CogState^{TM} GCS score.

There are a several differences between this study and the SSAT056 study. In SSAT056, CSF was not analysed making it difficult to extrapolate observations in plasma to the CNS compartment. In the CIIS study, the CSF data provided additional information about the CNS micro-environment. In addition to this, most of the subjects in SSAT056 were white males (95%). The CIIS study was slightly more diverse in terms of ethnicity (67% white males) but not gender, though absolute numbers were low. Given that differences in TDO activity have been reported in men and women of various ethnicities (417), and that there are also six reported IDO-1 genetic transcript variants, the effects of which are currently unknown (407), additional work is required to elucidate whether there are differences in other populations. Compared with SSAT056, the population size was small. Given the intensity and time-

consuming nature of the various procedures, however, it was not feasible to explore this in a larger population.

Analysis of other KYN pathway catabolites, such as KYNA and QUIN, as well as additional markers of immune activation, would be useful to help explain the observations. Measurement of serotonin concentrations, which are known to be lower in the blood and cerebrospinal fluid of PLWH, would also be helpful (404, 405).

In summary, it was observed that switching from RAL to DTG did not result in significant changes in TRP metabolism. However, a modest relationship was detected between increased KYN/TRP ratios and decreased CogState^{TM} GCS scores.

8 DISCUSSION AND CONCLUSIONS

8.1 Discussion and Conclusions

HIV-1 enters the CNS during the early stages of HIV-infection (54, 55) and has been associated with neurological and neuropsychiatric effects, including MDD and CI. The pathogenesis of HIV-related CNS disease is multifactorial and is characterised by neuronal loss, reactive astrogliosis, activated microglia, and leukocyte infiltration. In the brain, perivascular monocyte-derived macrophages and microglial cells are the main producers of HIV-1 (61-63), with astrocytes, oligodendrocytes and neurons possibly playing additional roles as viral reservoirs or producers of virus (55, 60). Indirect pathways for neuronal injury and death are implicated, including the inherent toxicity of secreted viral proteins, the release of inflammatory mediators and neurotoxins by infected macrophages and microglia, and the loss of integrity of compromised blood-brain and blood-CSF barriers that allow toxins into the CNS from plasma (56, 64-67). A significant number of additional pathological mechanisms are thought to contribute to cognitive impairment in PLWH (68-70).

The role of TRP and the effects exerted by its catabolites on neural tissue, mood and cognition in individuals with immune-related diseases such as HIV-infection has been an area of interest for the last 30 years and is characterised to some extent in PLWH who are not receiving ART or who are receiving on non-suppressive ART, such as AZT monotherapy (232, 238, 305, 338-340, 347-352). IDO is induced via the proinflammatory mediators IFN-γ and TNF-α during HIV infection, resulting in disturbed TRP metabolism throughout the course of the disease (234). The expression and/or activity of IDO is further induced in monocyte-derived macrophages and pDCs by HIV virions and their viral proteins (233). The resulting chronic depletion of TRP leads to the suppression of CD4+ T cell, CD8+ T cell, NK cell and B cell proliferation (233, 299, 310), decreased TRP concentrations, increased KYN and QUIN concentrations, and decreased serotonin and intracellular NAD+ concentrations (173, 232, 233, 237, 307). The decrease in serotonin production and increase in neurotoxin production has been thought to be of particular importance in the pathogenesis of depression and CI in PLWH (311).

Initiation of ART significantly but incompletely reduces the degradation of TRP (197, 313, 321-325). However, residual immune activation and its relationship with TRP metabolism and CNS disease has not been well-described in patients who are stable on virologically-suppressive

therapy. Mood and cognitive disorders, whilst clearly attenuated compared to the early days of HIV treatment, are still prevalent despite the availability of new, more potent ART. It has been shown that CSF NEO concentrations, a marker of immune activation that correlates highly with IDO activity (174), do not return to baseline levels in all subjects, even following a decade of suppressive therapy, indicating a persistent low-level intrathecal immune activation in many PLWH (136, 137, 211). There is clear potential for TRP metabolism to continue to be disturbed, albeit at a lower level, in this population. In addition, there are currently no published data reporting whether ARV agents have a direct effect on TRP metabolism at a cellular level, independent of the effects of HIV. Whilst ARVs reduce overall IDO activity by driving down HIV-1 viral loads, it could be postulated that some agents may induce or inhibit IDO either directly or indirectly. Indeed, many agents, such as EFV and PIs, directly induce or inhibit CYP450 enzymes. In addition, various inherent toxicities could drive an ongoing induction of IDO either directly or via another mechanism, such as inflammation.

The aim of this PhD was to determine whether chronic immune activation in PLWH leads to alterations in TRP metabolism and whether these are associated with CI and depressed mood. The hypotheses focused on whether TRP metabolism is increased in the presence of HIV-1 or ARV agents and whether increased TRP metabolism is associated with poorer cognitive performance and increased rates of depression in PLWH. This was done in two ways: the first was to investigate the effects of acute exposure of HIV-1 and ARV agents to cells that have a role in TRP metabolism. The second was to investigate TRP metabolism in PLWH receiving virologically-suppressive ART.

Boasso *et al.* had previously demonstrated that the expression and activity of IDO is induced in monocyte-derived macrophages and pDC's by exposure to HIV virions and their viral proteins, particularly Nef and Tat without the need for productive infection itself (233, 310). However, there are no published data reporting on whether ARV agents have a direct effect on TRP metabolism at a cellular level, independent of the effects of HIV-1. In what became a series of *in vitro* experiments, the hypothesis that TRP metabolism is increased in the presence of ARVs was tested by exposing human PBMCs and hepatocyte, astrocyte and microglial cell lines to a range of different ARVs as individual agents or in clinically-relevant combinations at both supratherapeutic and clinically-relevant concentrations. Over the course of the four experiments, no evidence was observed to support the hypothesis that ARVs contribute to the metabolism of TRP and so, instead, the null hypothesis was accepted. ARVs have not

previously been shown to have any intrinsic effect on the IDO and TDO enzymes but the enzyme inducing or inhibiting effects seen for agents such as EFV or the PIs could potentially affect the function of IDO or TDO. It was postulated that ARVs might also affect these enzymes due to their inherent toxicities and their effect on cell inflammation. However, there was no evidence to suggest that this is the case.

The CHARTER study was a cross-sectional analysis of historical case notes and archived CSF and plasma samples collected from HIV+ and HIV- individuals, either with or without CI and/or MDD. The first hypothesis was tested in a clinical setting by determining if chronic immune activation in HIV+ individuals, as estimated by concentrations of inflammatory biomarkers (TNF-α, NEO), is associated with increased TRP metabolism via the KYN pathway. The overall group of PLWH, which consisted of subjects with detectable viral loads and those that were undetectable receiving suppressive ART, were observed to have greater concentrations of TNF-α and NEO in CSF, lower concentrations of TRP in both CSF and plasma, and higher KYN/TRP ratios in plasma compared to HIV- controls. This is supported by a multivariate model that found that levels of TNF-α and NEO positively correlated with the KYN/TRP ratio in both CSF and plasma. The increases in TNF-α and NEO in CSF and decreases in TRP in plasma were observed to persist in virologically-suppressed patients receiving ART, suggesting an ongoing immune activation in both the CNS compartment and the periphery. These observations support the first hypothesis that TRP metabolism is increased in the presence of HIV or ARV agents.

With respect to the second hypothesis that increased TRP metabolism is associated with poorer cognitive performance and increased rates of depression in PLWH, a trend towards lower KYN/TRP ratios in plasma in patients who were experiencing CI and MDD in both the overall HIV+ group and an aviraemic sub-group was observed, however these findings were not statistically significant when multiplicity corrections were applied. The effect in the overall HIV+ group appeared to be driven by the aviraemic sub-group and was not observed in HIV+ subjects with detectable viral loads. This result was unexpected and has not been observed in previous studies. It does not support the hypothesis that TRP metabolism is increased but does suggest that disturbed TRP metabolism is in some way connected to CI and depression. The reasons for this are unclear but may suggest that the net result of the KYN pathway may somehow protect against CI and depression in aviraemic patients.

The CHARTER study enrolled a highly heterogeneous population in terms of their disease and treatment characteristics, making it difficult to draw clear conclusions. Many of the samples and case notes included were taken from subjects in the pre-HAART era who were not receiving therapy or who were receiving sub-optimal therapy, such as AZT monotherapy. These populations do not reflect contemporary PLWH whose virus is well-controlled with potent and, usually, less toxic ART. In an effort to account for this and to investigate TRP metabolism in more homogenous populations, the SSAT056 and CIIS studies were conducted. Both studies were prospective, randomised, longitudinal studies in well-characterised groups of PLWH who were virologically-suppressed using guideline recommended (45-48), first-line ART regimens (i.e. 2 NRTI's plus either EFV or an integrase inhibitor). The subjects included (i.e. virologically-suppressed subjects) match the population identified in the pilot study who were found to be experiencing changes in TRP metabolism that were associated with CI and MDD, allowing us the opportunity to confirm these initial findings. In addition to this, the longitudinal follow-up in this population was novel.

In the SSAT056 study, virologically-suppressed PLWH experiencing ongoing CNS toxicity with EFV were switched to DTG, resulting in significant improvements in CNS adverse events, anxiety, depression and sleep quality. Following switch, a significant increase was observed in plasma KYN concentrations and a non-significant increase in the KYN/TRP ratio. These changes were negatively correlated with the reduction in CNS toxicities and improvements in neuropsychiatric scores. Previous clinical studies have demonstrated that KYN/TRP ratios decline following initiation of ART due to decreases in immune activation resulting from suppression of HIV-1-RNA (321, 410, 411). In the CHARTER study, the cross-sectional analysis indicated that lower KYN concentrations and KYN/TRP ratios were associated with CI and depression. The SSAT056 study supports this observation with increases in KYN and KYN/TRP ratios being associated with decreases in measures of CNS toxicity and depression. However, the results of the SSAT056 study may be confounded by contributions from other mechanisms. EFV is known to be directly neurotoxic via its 8-hydroxy-efavirenz metabolite, and several studies have demonstrated that switching away from EFV to less toxic agents, such as ETV, RAL and RPV, results in significant improvements in CNS adverse events (372, 413, 414). In addition to this, Zheve has shown that that EFV inhibits TDO activity in the liver cells of non-HIV-infected rats (409). If this effect translates to HIV+ human subjects, then a combination of the removal of EFV-related neurotoxicity and its suspected inhibitory effects on TDO would neatly explain the observed effect. However, whilst this is a plausible

explanation, the contradictory data from the *in vitro* analysis of THLE2 and THLE3 cells detailed in this thesis, casts some suspicion on EFVs effect on the TDO enzyme. The effect of increases in KYN concentrations and its associated metabolites on CNS parameters cannot be excluded and a combination of neurotoxic effects from both the 8-hydroxy-efavirenz metabolite and KYN metabolites may play a part in the observed phenomena. For example, KYN metabolism could be attenuated by EFVs inhibition of IDO activity, resulting in reduced neurotoxicity from this pathway, but this is masked by the greater neurotoxicity of 8-hydroxy-efavirenz. As subjects switch from EFV and 8-hydroxy-efavirenz neurotoxicity declines, it could be replaced by toxicity from increases KYN and KYN pathway metabolites, but the net result appears to be improvements in CNS parameters. Unfortunately, this cannot be determined from the current data-set. What can be concluded from this study is that switching from EFV to DTG in stable, virologically-suppressed subjects results in changes in TRP metabolism that correspond with improvements in CNS parameters. These data do not support the hypothesis that increased TRP metabolism is associated with CI and depression, quite the opposite in fact, but do suggest that TRP metabolism is disturbed in this population.

The CIIS study excluded the use of EFV and focused instead on the integrase inhibitors RAL and DTG, thus removing the potential confounding effects of EFV on TRP metabolism and CNS parameters. In this study, virologically-suppressed PLWH receiving a RAL-based regimen were either switched to DTG or remained on RAL. Whilst some subtle changes in biomarker concentrations and cognitive test results were observed, there appears to be very little difference between the two integrase inhibitors in terms of their effect on TRP metabolism and CNS function. Mean plasma TRP concentrations were observed to increase in patients receiving DTG over 120 days, with a statistically significant difference in changes between the DTG and RAL arms over this period. However, no significant changes were observed in either KYN concentrations or the KYN/TRP ratio between the two agents. In the SSAT056 study, KYN concentrations and the KYN/TRP ratio were observed to increase following switch from EFV. The CIIS study data suggest that a similar effect is not evident when switching from one integrase inhibitor to another.

Despite the lack of changes in KYN production, this study does provide evidence to support the second hypothesis that increased TRP metabolism is associated with poorer cognitive performance. In the linear mixed model analysis, the plasma KYN/TRP ratio was found to be negatively correlated with CogState^{TM} GCS, such that for every 1 µmol/L increase observed in

KYN/TRP ratio, a 0.019-point decrease was observed in the CogState^{TM} GCS, indicating a modest decline in cognitive function as the KYN/TRP ratio increases. No other significant associations were found, though similar trends were observed for both plasma KYN and CSF TRP and the CogState^{TM} GCS score. These observations are in-line with what was predicted from historical studies in the literature and support the second hypothesis. However, the results of the CHARTER and SSAT056 studies appear to be contradictory. Potential confounding factors were identified for both the CHARTER and SSAT056 studies that make it difficult to draw firm conclusions (as previously discussed). Because of this, the CIIS study may present a more faithful representation of the role of TRP metabolism and its relationship with CNS parameters in a virologically-suppressed population.

The results of the *in vitro* experiments and the clinical studies present a complex, at times seemingly contradictory, picture of the relationship between TRP metabolism and CNS parameters in virologically-suppressed PLWH. Drawing firm conclusions is difficult given the potential confounding factors that have been identified. When placed in the context of HIV-related CNS disease as a whole, which has a profoundly multifactorial neuropathogenesis, this is not surprising as many potential confounding factors exist that could be contributing to the observations. Central nervous system injury is not a universal complication of HIV infection and HIV-infected individuals differ in their likelihood of experiencing CI according to several fundamental factors, including ongoing – possibly localised – viral replication, CD4+ cell count, inter-individual differences in immune response, legacy effects, cognitive reserve, and possibly disease duration (117). Differences in the integrity of the blood-brain and blood-CSF barriers could result in differing competencies in the exclusion of, potentially toxic, plasma proteins (118, 119) and other factors, such as co-morbidities, duration of ARV therapy, inter-drug variability in CNS penetration, distribution, toxicity and neurologic effectiveness in lowering HIV viral loads, are common factors that can confound the evaluation of biomarkers (117). Sampling a handful of biomarkers and trying to find associations with global cognitive ability and mood is difficult and cannot capture the full extent of the complex interplay that is occurring. These data represent the first analysis of the direct effects of ARVs on TRP metabolism in human PBMCs and hepatic, microglial and astrocyte cell lines. The SSAT056 and CIIS studies also represent the first longitudinal studies in homogenous, well-characterised subjects with undetectable viral loads who are stable on ART. Further work is needed to elucidate the other factors that are contributing to TRP metabolism in this population. Some suggestions of what this work could look like are made in Section 8.2, below.

In conclusion, these data demonstrate an ongoing disturbance in TRP metabolism in virologically-suppressed PLWH that is mediated by residual immune activation and choice of antiretroviral agents.

8.2 Further Work

There are opportunities for further work in this area. Two important questions to ask are detailed below.

Does IDO have a cyclic biological rhythm in PLWH?

It would be important to understand the biological rhythm, if any, of the IDO enzyme in PLWH. If IDO activity varies over the period of a day (or week or month), then only a limited picture of TRP metabolism will be available when sampling every few weeks or months, as was the case in the SSAT056 and CIIS studies in this thesis. A small study akin to a pharmacokinetic study with multiple sample collections made over a 24-hour period (or longer) would likely suffice. This may enable us to collect samples more accurately based on the cycle.

What does the profile of the KYN pathway metabolites look like in virologically-suppressed PLWH?

Targeted analysis of KYNA, QUIN and the other neurologically-active KYN metabolites would be useful to describe the KYN pathway in its entirety in virologically-suppressed PLWH. In a recent study by Lim et al., aberrant concentrations of KYNA and QUIN were observed in people suffering from multiple sclerosis (419). The QUIN/KYNA ratio was found to be a useful marker of the overall excitotoxic activity at the N-methyl-D-Aspartate (NMDA) receptor. This could be a more accurate way of assessing the neurotoxic potential of the KYN pathway in PLWH.

REFERENCES

1. (CDC) CfDCaP. Pneumocystis pneumonia - Los Angeles. MMWR. 1981;30(21):1-3.
2. Gottlieb MS, Schroff R, Schanker HM, Weisman JD, Fan PT, Wolf RA, et al. Pneumocystis carinii pneumonia and mucosal candidiasis in previously healthy homosexual men: Evidence of a new acquired cellular immunodeficiency. N Engl J Med. 1981;305(24):1425-31.
3. (CDC) CfDCaP. Kaposi's Sarcoma and Pneumocystis Pneumonia Among Homosexual Men - New York City and California. MMRW. 1981;30:305-8.
4. (CDC) CfDCaP. Current Trends Update on Acquired Immune Deficiency Syndrome (AIDS) - United States. MMWR. 1982;31(37):507-8,13-14.
5. Barre-Sinoussi F, Chermann J, Rey F, Nugeyre M, Chamaret S, Gruest J, et al. Isolation of a T-lymphotropic retrovirus from a patient at risk for acquired immune deficiency syndrome (AIDS). Science. 1983;220(4599):868-71.
6. Gallo R, Sarin P, Gelmann E, Robert-Guroff M, Richardson E, Kalyanaraman V, et al. Isolation of human T-cell leukemia virus in acquired immune deficiency syndrome (AIDS). Science. 1983;220(4599):865-7.
7. Coffin J, Haase A, Levy JA, Montagnier L, Oroszlan S, Teich N, et al. What to call the AIDS virus? Nature. 1986;321(6065):10.
8. Daniel M, Letvin N, King N, Kannagi M, Sehgal P, Hunt R, et al. Isolation of T-cell tropic HTLV-III-like retrovirus from macaques. Science. 1985;228(4704):1201-4.
9. Reeves JD, Doms RW. Human immunodeficiency virus type 2. Journal of General Virology. 2002;83:1253-65.
10. Hu WS, Hughes SH. HIV-1 reverse transcription. Cold Spring Harb Perspect Med. 2012;2(10).
11. Pepin J. The Origin of AIDS. Cambridge University Press. 2011.
12. Wertheim JO. Dating the age of the SIV lineages that gave rise to HIV-1 and HIV-2. PLOS Computational Biology. 2009;5(5):e1000377.
13. Hoy JF, Lewin SR, Post JJ, Street AC. HIV Management in Australasia: A Guide for Clinical Care. (2009 ed.). Darlinghurst, NSW, Australia: Australasian Society for HIV Medicine. 2009.
14. Hu Y, Wan Z, Zhou YH, Smith D, Zheng YT, Zhang C. Identification of Two New HIV-1 Circulating Recombinant Forms (CRF87_cpx and CRF88_BC) from Reported Unique Recombinant Forms in Asia. AIDS Res Hum Retroviruses. 2017;33(4):353-8.
15. (WHO) WHO. Global Health Observatory Data - HIV/AIDS 2015. http://wwwwhoint/gho/hiv/en/. 2017;Accessed 26/04/2017.
16. Barmania F, Pepper MS. C-C chemokine receptor type five (CCR5): An emerging target for the control of HIV infection. Appl Transl Genom. 2013;2:3-16.
17. Korber B, Gaschen B, Yusim K, Thakallapally R, Kesmir C, Detours V. Evolutionary and immunological implications of contemporary HIV-1 variation. British Medical Bulletin. 2001;58:19-42.
18. Moore MD, Hu W-S. HIV-1 RNA dimerization: it takes two to tango. AiDS Rev. 2009;11(2):91-102.
19. Ganor Y, Zhou Z, Tudor D, Schmitt A, Vacher-Lavenu MC, Gibault L, et al. Within 1 h, HIV-1 uses viral synapses to enter efficiently the inner, but not outer, foreskin mucosa and engages Langerhans-T cell conjugates. Mucosal Immunol. 2010;3(5):506-22.
20. McMichael AJ, Borrow P, Tomaras GD, Goonetilleke N, Haynes BF. The immune response during acute HIV-1 infection: clues for vaccine development. Nat Rev Immunol. 2010;10(1):11-23.

21. Kariuki SM, Selhorst P, Arien KK, Dorfman JR. The HIV-1 transmission bottleneck. Retrovirology. 2017;14(1):22.
22. Mulampaka SN, Dixit NM. Estimating the threshold surface density of Gp120-CCR5 complexes necessary for HIV-1 envelope-mediated cell-cell fusion. PLoS One. 2011;6(5):e19941.
23. Engelman A, Cherepanov P. The structural biology of HIV-1: mechanistic and therapeutic insights. Nat Rev Microbiol. 2012;10(4):279-90.
24. <neopterin_dietmar summary.pdf>.
25. Barre-Sinoussi F, Ross AL, Delfraissy JF. Past, present and future: 30 years of HIV research. Nat Rev Microbiol. 2013;11(12):877-83.
26. Bartlett JG, Gallant JE, Pham PA. Medical management of HIV infection. 2012;Knowledge Source Solutions; Mill City Press, USA(www.mmhiv.com).
27. Stacey AR, Norris PJ, Qin L, Haygreen EA, Taylor E, Heitman J, et al. Induction of a striking systemic cytokine cascade prior to peak viremia in acute human immunodeficiency virus type 1 infection, in contrast to more modest and delayed responses in acute hepatitis B and C virus infections. J Virol. 2009;83(8):3719-33.
28. Haase AT. Early events in sexual transmission of HIV and SIV and opportunities for interventions. Annu Rev Med. 2011;62:127-39.
29. Marchetti G, Tincati C, Silvestri G. Microbial translocation in the pathogenesis of HIV infection and AIDS. Clin Microbiol Rev. 2013;26(1):2-18.
30. Moir S, Fauci AS. B cells in HIV infection and disease. Nat Rev Immunol. 2009;9(4):235-45.
31. Bacchetti P, Moss AR. Incubation period of AIDS in San Francisco. Nature. 1989;338:251-3.
32. Ballana E, Este JA. HIV-1 infection and CCR5Δ32 homozygosis. Future Virol. 2012;7(7):653-8.
33. Galvani AP, Novembre J. The evolutionary history of the CCR5-Delta32 HIV-resistance mutation. Microbes Infect. 2005;7(2):302-9.
34. Hanson DL, Chu SY, Farizo KM, Ward JW. Distribution of CD4+ T Lymphocytes at Diagnosis of Acquired Immunodeficiency Syndrome—Defining and Other Human Immunodeficiency Virus—Related Illnesses. Archives of Internal Medicine. 1995;155(14):1537-42.
35. Hileman CO, Funderburg NT. Inflammation, immune activation, and antiretroviral therapy in HIV. Curr HIV/AIDS Rep. 2017;14:93-100.
36. Group ISS, Lundgren JD, Babiker AG, Gordin F, Emery S, Grund B, et al. Initiation of Antiretroviral Therapy in Early Asymptomatic HIV Infection. N Engl J Med. 2015;373(9):795-807.
37. Group TAS, Danel C, Moh R, Gabillard D, Badje A, Le Carrou J, et al. A Trial of Early Antiretrovirals and Isoniazid Preventive Therapy in Africa. N Engl J Med. 2015;373(9):808-22.
38. (CDC) CfDCaP. 1993 Revised classification system for HIV infection and expanded surveillance case definition for AIDS among adolescents and adults. MMRW. 1992;41(RR-17).
39. (CDC) CfDCaP. Revised surveillance case definitions for HIV infection among adults, adolescents and children ages <18 months and for HIV infection and AIDS among children 18 months to <13 years - United States, 2008. MMRW. 2008;57(RR-10):1-9.
40. Nelson M, Manji H, Wilkins E. Central nervous system opportunistic infections. HIV Medicine. 2011;12((Suppl. 2)):8-24.
41. Anthony IC, Bell JE. The Neuropathology of HIV/AIDS. Int Rev Psychiatry. 2008;20(1):15-24.
42. Arts EJ, Hazuda DJ. HIV-1 antiretroviral drug therapy. Cold Spring Harb Perspect Med. 2012;2(4):a007161.

43. Hurwitz SJ, Schinazi RF. Practical considerations for developing nucleoside reverse transcriptase inhibitors. Drug Discovery Today: Technologies. 2012;9(3):e183-e93.
44. Seckler JM, Barkley MD, Wintrode PL. Allosteric suppression of HIV-1 reverse transcriptase structural dynamics upon inhibitor binding. Biophys J. 2011;100(1):144-53.
45. Waters L, Ahmed N, Angus B, Boffito M, Bower M, Churchill D, et al. BHIVA guidelines for the treatment of HIV-1-positive adults with antiretroviral therapy 2015 (2016 interim update). British HIV Association. 2016.
46. (EACS) EACS. EACS Guidelines V8.2. 2017.
47. Adolescents. PoAGfAa. Guidelines for the use of antiretroviral agents in HIV-1-infected adults and adolescents. Department of Health and Human Services. http://wwwaidsinfonihgov/ContentFiles/AdultandAdolescentGLpdf. 2016:Accessed 14/5/2017.
48. Gunthard HF, Saag MS, Benson CA, del Rio C, Eron JJ, Gallant JE, et al. Antiretroviral Drugs for Treatment and Prevention of HIV Infection in Adults: 2016 Recommendations of the International Antiviral Society-USA Panel. JAMA. 2016;316(2):191-210.
49. Abbott RealTime HIV-1 Viral Load Assay, Technical Specifications Webpage: https://www.molecular.abbott/int/en/products/infectious-disease/realtime-hiv-1-viral-load Accessed on 19/9/2017.
50. Murray JS, Elashoff MR, Iacono-Connors LC, Cvetkovich TA, Struble KA. The use of plasma HIV RNA as a study endpoint in efficacy trials of antiretroviral drugs. AIDS. 1999;13(7):797-804.
51. Marschner IC, Collier AC, Coombs RW, D'Aquila RT, DeGruttola V, Fischl M, et al. Use of changes in plasma levels of human immunodeficiency virus type 1 RNA to assess the clinical benefit of antiretroviral therapy. J Infect Dis. 1998;177(1):40-7.
52. Thiebaut R, Morlat P, Jacqmin-Gadda H, Neau D, Mercie P, Dabis F, et al. Clinical progression of HIV-1 infection according to the viral response during the first year of antiretroviral treatment. Groupe d'Epidemiologie du SIDA en Aquitaine (GECSA). AIDS. 2000;14(8):971-8.
53. World Health Organization: Laboratory guide enumerating CD4 T lymphocytes in the context of HIV/AIDS (2007), http://www.who.int/hiv/amds/LaboratoryGuideEnumeratingCD4TLymphocytes.pdf. Accessed 19/9/2017.
54. Williams DW, Eugenin EA, Calderon TM, Berman JW. Monocyte maturation, HIV susceptibility, and transmigration across the blood brain barrier are critical in HIV neuropathogenesis. J Leukoc Biol. 2012;91(3):401-15.
55. Kramer-Hammerle S, Rothenaigner I, Wolff H, Bell JE, Brack-Werner R. Cells of the central nervous system as targets and reservoirs of the human immunodeficiency virus. Virus Res. 2005;111(2):194-213.
56. Valcour V, Sithinamsuwan P, Letendre S, Ances B. Pathogenesis of HIV in the central nervous system. Curr HIV/AIDS Rep. 2011;8(1):54-61.
57. D'Mello C, Le T, Swain MG. Cerebral microglia recruit monocytes into the brain in response to tumor necrosis factoralpha signaling during peripheral organ inflammation. J Neurosci. 2009;29(7):2089-102.
58. Williams DW, Veenstra M, Gaskill PJ, Morgello S, Calderon TM, Berman JW. Monocytes mediate HIV neuropathogenesis: mechanisms that contribute to HIV associated neurocognitive disorders. Curr HIV Res. 2014;12(2):85-96.
59. Williams DW, Calderon TM, Lopez L, Carvallo-Torres L, Gaskill PJ, Eugenin EA, et al. Mechanisms of HIV entry into the CNS: increased sensitivity of HIV infected CD14+CD16+ monocytes to CCL2 and key roles of CCR2, JAM-A, and ALCAM in diapedesis. PLOS ONE. 2013;8(7):e69270.

60. Farhadian S, Patel P, Spudich S. Neurological Complications of HIV Infection. Curr Infect Dis Rep. 2017;19(12):50.
61. Burdo TH, Lackner A, Williams KC. Monocyte/macrophages and their role in HIV neuropathogenesis. Immunological Reviews. 2013;254:102-13.
62. Schnell G, Joseph S, Spudich S, Price RW, Swanstrom R. HIV-1 replication in the central nervous system occurs in two distinct cell types. PLoS Pathog. 2011;7(10):e1002286.
63. Rock RB, Gekker G, Hu S, Sheng WS, Cheeran M, Lokensgard JR, et al. Role of microglia in central nervous system infections. Clin Microbiol Rev. 2004;17(4):942-64.
64. Minagar A, Commins D, Alexander JS, Hoque R, Chiappelli F, Singer EJ, et al. NeuroAIDS: Characteristics and diagnosis of the neurological complications of AIDS. Mol Diag Ther. 2008;12(1):25-43.
65. Schmitz G, Leuthauser-Jaschinski K, Orso E. Are circulating monocytes as microglia orthologues appropriate biomarker targets for neuronal diseases? Central Nervous System Agents in Medicinal Chemistry. 2009;9:307-30.
66. Vazquez-Santiago FJ, Noel RJ, Jr., Porter JT, Rivera-Amill V. Glutamate metabolism and HIV-associated neurocognitive disorders. J Neurovirol. 2014;20(4):315-31.
67. Letendre SL. HIV-associated neurocognitive disorders in the era of potent antiretroviral therapy: risk factors/prevalence, CSF HIV-RNA, ART PK/penetration, assessment tools. 49th Interscience Conference on Antimicrobial Agents and Chemotherapy Complications Workshop San Francisco, CA. 2009;Oral Presentation.
68. Aquaro S, Calio R, Balzarini J, Bellocchi MC, Garaci E, Perno CF. Macrophages and HIV infection: therapeutical approaches toward this strategic virus reservoir. Antiviral Res. 2002;55(2):209-25.
69. McArthur JC, Steiner J, Sacktor N, Nath A. Human immunodeficiency virus-associated neurocognitive disorders: Mind the gap. Ann Neurol. 2010;67(6):699-714.
70. Nightingale S, Winston A, Letendre S, Michael BD, McArthur JC, Khoo S, et al. Controversies in HIV-associated neurocognitive disorders. Lancet Neurol. 2014;13:1139-51.
71. Joska JA, Gouse H, Paul RH, Stein DJ, Flisher AJ. Does highly active antiretroviral therapy improve neurocognitive function? A systematic review. J Neurovirol. 2010;16(2):101-14.
72. Letendre S, Marquie-Beck J, Capparelli E, Best B, Clifford D, Collier AC, et al. Validation of the CNS penetration-effectiveness rank for quantifying antiretroviral penetration into the central nervous system. Arch Neurol. 2008;65(1):65-70.
73. Varatharajan L, Thomas SA. The transport of anti-HIV drugs across blood-CNS interfaces: summary of current knowledge and recommendations for further research. Antiviral Res. 2009;82(2):A99-109.
74. Underwood J, Robertson KR, Winston A. Could antiretroviral neurotoxicity play a role in the pathogenesis of cognitive impairment in treated HIV disease? AIDS. 2015;29(3):253-61.
75. Cavalcante GI, Capistrano VL, Cavalcante FS, Vasconcelos SM, Macedo DS, Sousa FC, et al. Implications of efavirenz for neuropsychiatry: a review. Int J Neurosci. 2010;120(12):739-45.
76. Perez-Valero I, Bailon L, Gozalez A, Alejos B, Melero H, Malpica N, et al. Brain volume changes after ABC/3TC + EFV or TDF/FTC + ATV/r as first-line ART. 25th Conference on Retroviruses and Opportunistic Infections (CROI), 4-7 March 2018, Boston, MA. 2018:Poster 425.
77. Fettiplace A, Stainsby C, Winston A, Givens N, Puccini S, Vannappagari V, et al. Psychiatric symptoms in patients receiving dolutegravir. J Acquir Immune Defic Syndr. 2017;74:423-31.
78. Hoffmann C, Wolf E, Schewe K, Sabranski M, Stellbrink H-J, Adam A, et al. CNS toxicity of dolutegravir is not associated with psychiatric conditions or higher plasma exposure. 25th

Conference on Retroviruses and Opportunistic Infections (CROI), 4-7 March 2018, Boston, MA. 2018:Poster 424.
79. Robertson K, Liner J, Meeker RB. Antiretroviral neurotoxicity. J Neurovirol. 2012;18(5):388-99.
80. Tovar-y-Romo LB, Bumpus NN, Pomerantz D, Avery LB, Sacktor N, McArthur JC, et al. Dendritic spine injury induced by the 8-hydroxy metabolite of efavirenz. J Pharmacol Exp Ther. 2012;343(3):696-703.
81. Grilo NM, Batalha VL, Lopes LV, Marques MM, Monteiro EC, Antunes AMM, et al. An animal model to explore efavirenz toxicokinetics and its relation to neurological phenotype. Toxicology Letters. 2014;229:S244.
82. Grilo NM, Correia MJ, Sequeira C, Harjivan SG, Caixas U, Diogo LN, et al. Efavirenz biotransformation as an up-stream event of mood changes in HIV-infected patients. Toxicol Lett. 2016;260:28-35.
83. Grilo NM, Joao Correia M, Miranda JP, Cipriano M, Serpa J, Matilde Marques M, et al. Unmasking efavirenz neurotoxicity: Time matters to the underlying mechanisms. Eur J Pharm Sci. 2017;105:47-54.
84. Berger-Greenstein JA, Cuevas CA, Brady SM, Trezza G, Richardson MA, Keane TM. Major depression in patients with HIV/AIDS and substance abuse. AIDS Patient Care STDS. 2007;21(12):942-55.
85. Sherr L, Clucas C, Harding R, Sibley E, Catalan J. HIV and depression - a systematic review of interventions. Psychology, Health & Medicine. 2011;16(5):493-527.
86. Ghafouri M, Amini S, Khalili K, Sawaya BE. HIV-1 associated dementia: symptoms and causes. Retrovirology. 2006;3:28.
87. Cespedes MS, Aberg JA. Neuropsychiatric complications of antiretroviral therapy. Drug Safety. 2006;29(10):865-74.
88. Lichtenstein B, Laska MK, Clair JM. Chronic sorrow in the HIV-positive patient: issues of race, gender, and social support. AIDS Patient Care STDS. 2002;16(1):27-38.
89. Nott KH, Vedhara K. Nature and consequences of stressful life events in homosexual HIV-positive men: a review. AIDS Care. 1999;11(2):235-43.
90. DiMatteo MR, Lepper HS, Croghan TW. Depression is a risk factor for noncompliance with medical treatment. Arch Intern Med. 2000;160:2101-7.
91. De Francesco D, Underwood J, Boffito M, Post F, Mallon PWG, Vera JH, et al. Cognitive function and depression in HIV-positive individuals and matched controls. International Congress of Drug Therapy in HIV Infection, 23-26 October 2016, Glasgow, UK. 2016:O215.
92. Elliott AJ, Russo J, Roy-Byrne PP. The effect of changes in depression on health related quality of life (HRQoL) in HIV infection. General Hospital Psychiatry. 2002;24:43-7.
93. Lima VD, Geller J, Bangsberg DR, Patterson TL, Daniel M, Kerr T, et al. The effect of adherence on the association between depressive symptoms and mortality among HIV-infected individuals first initiating HAART. AIDS. 2007;21:1175-83.
94. Heaton RK, Grant I, Butters N, White DA, Kirson D, Atkinson JHM, J.A. Taylor, M.J., et al. The HNRC 500—Neuropsychology of HIV infection at different disease stages. Journal of the International Neuropsychological Society. 1995;1:231-51.
95. Heaton RK, Clifford DB, Franklin DR, Woods SP, Ake C, Vaida F, et al. HIV-associated neurocognitive disorders persist in the era of potent antiretroviral therapy. Neurology. 2010;75:2087-96.
96. Garvey L, Surendrakumar V, Winston A. Low rates of neurocognitive impairment are observed in neuro-asymptomatic HIV-infected subjects on effective antiretroviral therapy. HIV Clin Trials. 2011;12(6):333-8.
97. Robertson KR, Smurzynski M, Parsons TD, Wu K, Bosch RJ, Wu J, et al. The prevalence and incidence of neurocognitive impaurment in the HAART era. AIDS. 2007;21:1915-21.

98. Simioni S, Cavassini M, Annoni JM, Rimbault Abraham A, Bourquin I, Schiffer V, et al. Cognitive dysfunction in HIV patients despite long-standing suppression of viremia. AIDS. 2010;24:1243-50.
99. Heaton RK, Franklin DR, Ellis RJ, McCutchan JA, Letendre SL, Leblanc S, et al. HIV-associated neurocognitive disorders before and during the era of combination antiretroviral therapy: differences in rates, nature, and predictors. Journal of Neurovirology. 2011;17:3-16.
100. Woods SP, Moore DJ, Weber E, Grant I. Cognitive neuropsychology of HIV-associated neurocognitive disorders. Neuropsychol Rev. 2009;19(2):152-68.
101. Spudich S. HIV and neurocognitive dysfunction. Curr HIV/AIDS Rep. 2013;10(3):235-43.
102. Antinori A, Arendt G, Becker JT, Brew BJ, Byrd DA, Cherner M, et al. Updated research nosology for HIV-associated neurocognitive disorders. Neurology. 2007;69:1789-99.
103. Carey CL, Woods SP, Gonzalez R, Conover E, Marcotte TD, Grant I, et al. Predictive validity of global deficit scores in detecting neuropsychological impairment in HIV infection. J Clin Exp Neuropsychol. 2004;26(3):307-19.
104. Huizenga HM, Smeding H, Grasman RP, Schmand B. Multivariate normative comparisons. Neuropsychologia. 2007;45(11):2534-42.
105. Su T, Schouten J, Geurtsen GJ, Wit FW, Stolte IG, Prins M, et al. Multivariate normative comparison, a novel method for more reliably detecting cognitive impairment in HIV infection. AIDS. 2015;29(5):547-57.
106. De Francesco D, Underwood J, Post FA, Vera JH, Williams I, Boffito M, et al. Defining cognitive impairment in people-living-with-HIV: the POPPY study. BMC Infect Dis. 2016;16(1):617.
107. Group BDW. Biomarkers and surrogate endpoints: preferred definitions and conceptual framework. Clin Pharmacol Ther. 2001;69:89-95.
108. Safety WIPoC. Biomarkers in risk assessment: validity and validation. http://wwwinchemorg/documents/ehc/ehc/ehc222htm. 2001.
109. Mallal S, Phillips E, Carosi G, Molina J-M, Workman C, Tomazic J, et al. HLA-B*5701 Screening for Hypersensitivity to Abacavir. N Engl J Med. 2008;358:568-79.
110. Hughes S, Hughes A, Brothers C, Spreen W, Thorborn D, Team CNAS. PREDICT-1 (CNA106030): the first powered, prospective trial of pharmacogenetic screening to reduce drug adverse events. Pharm Stat. 2008;7(2):121-9.
111. Strimbu K, Tavel JA. What are biomarkers? Curr Opin HIV AIDS. 2010;5(6):463-6.
112. Stoop MP, Coulier L, Rosenling T, Shi S, Smolinska AM, Buydens L, et al. Quantitative proteomics and metabolomics analysis of normal human cerobrospinal fluid samples. Molecular & Cellular Proteomics. 2010;9:2063-75.
113. . !!! INVALID CITATION !!! (55-59).
114. Wishart DS, Lewis MJ, Morrissey JA, Flegel MD, Jeroncic K, Xiong Y, et al. The human cerebrospinal fluid metabolome. J Chromatogr B Analyt Technol Biomed Life Sci. 2008;871(2):164-73.
115. Schutzer SE, Liu T, Natelson BH, Angel TE, Schepmoes AA, Purvine SO, et al. Establishing the proteome of normal human cerebrospinal fluid. PLoS One. 2010;5(6):e10980.
116. Mandal R, Guo AC, Chaudhary KK, Liu P, Yallou FS, Dong E, et al. Multi-platform characterization of the human cerebrospinal fluid metabolome: a comprehensive and quantitative update. Genome Medicine. 2012;4:38.
117. Brew BJ, Letendre SL. Biomarkers of HIV related central nervous system disease. Int Rev Psychiatry. 2008;20(1):73-88.
118. Cibrorowski P. Biomarkers of HIV-1-associated neurocognitive disorders: challenges of proteomic approaches. Biomarkers Med. 2009;3(6):771-85.
119. Ivey NS, MacLean AG, Lackner AA. Acquired immunodeficiency syndrome and the blood-brain barrier. J Neurovirol. 2009;15(2):111-22.

120. McGuire D. CSF biomarkers in HIV dementia. Neurology. 2009;73:1942-4.
121. Schouten J, Cinque P, Gisslen M, Reiss P, Portegies P. HIV-1 infection and cognitive impairment in the cART-era: a review. AIDS. 2011;25(5):561-75.
122. Vissers M, Stelma FF, Koopmans PP. Could differential virological characteristics account for ongoing viral replication and insidious damage of the brain during HIV 1 infection of the central nervous system? J Clin Virol. 2010;49(4):231-8.
123. Di Carlofelice M, Everitt A, Muir D, Winston A. Cerebrospinal fluid HIV RNA in persons living with HIV. HIV Med. 2018.
124. Ellis R, Hsia K, Spector SA, Nelson JA, Heaton RK, Wallace MR, et al. Cerebrospinal fluid human immunodeficiency virus type 1 RNA levels are elevated in neurocognitively impaired individuals with acquired immunodeficiency syndrome. Ann Neurol. 1997;42:679-88.
125. Sacktor N, McDermott MP, Marder K, Schifitto G, Selnes OA, McArthur JC, et al. HIV-associated cognitive impairment before and after the advent of combination therapy. J Neurovirol. 2002;8(2):136-42.
126. Lyons JL, Uno H, Ancuta P, Kamat A, Moore DJ, Singer EJ, et al. Plasma sCD14 is a biomarker associated with impaired neurocognitive test performance in attention and learning domains in HIV infection. J Acquir Immune Defic Syndr. 2011;57:371-9.
127. Shiramizu B, Gartner S, Williams A, Shikuma C, Ratto-Kim S, Watters M, et al. Circulating proviral HIV DNA and HIV-associated dementia. AIDS. 2005;19:45-52.
128. Burdo TH, Weiffenbach A, Woods SP, Letendre S, Ellis RJ, Williams KC. Elevated sCD163 in plasma but not cerebrospinal fluid is a marker of neurocognitive impairment in HIV infection. AIDS. 2013;27(9):1387-95.
129. Canestri A, Lescure FX, Jaureguiberry S, Moulignier A, Amiel C, Marcelin AG, et al. Discordance between cerebral spinal fluid and plasma HIV replication in patients with neurological symptoms who are receiving suppressive antiretroviral therapy. Clin Infect Dis. 2010;50(5):773-8.
130. McArthur JC, McClernon DR, Cronin MF, Nance-Sproson TE, Saah AJ, St Clair M, et al. Relationship between human immunodeficiency virus-associated dementia and viral load in cerebrospinal fluid and brain. Ann Neurol. 1997;42:689-98.
131. Brew BJ, Pemberton L, Cunningham P, Law MG. Levels of human immunodeficiency virus type 1 RNA in cerebrospinal fluid correlate with AIDS dementia stage. The Journal of Infectious Diseases. 1997;175:963-6.
132. Perez-Valero I, Gonzalez-Baeza A, Estebanez M, Monge S, Montes-Ramirez ML, Bayon C, et al. A prospective cohort study of neurocognitive function in aviremic HIV-infected patients treated with 1 or 3 antiretrovirals. Clin Infect Dis. 2014;59(11):1627-34.
133. Spudich S, Gisslen M, Hagberg L, Lee E, Liegler T, Brew B, et al. Central nervous system immune activation characterizes primary human immunodeficiency virus 1 infection even in participants with minimal cerebrospinal fluid viral burden. J Infect Dis. 2011;204(5):753-60.
134. Sevigny JJ, Albert SM, McDermott MP, McArthur JC, Sacktor N, Conant K, et al. Evaluation of HIV RNA and markers of immune activation as predictors of HIV-associated dementia. Neurology. 2004;63:2084-90.
135. Ellis RJ, Moore DJ, Childers ME, Letendre S, McCutchan JA, Wolfson T, et al. Progression to neuropsychological impairment in human immunodeficiency virus infection predicted by elevated cerebrospinal fluid levels of human immunodeficiency virus RNA. Arch Neurol. 2002;59:923-8.
136. Abdulle S, Hagberg L, Svennerholm B, Fuchs D, Gisslen M. Continuing intrathecal immunoactivation despite two years of effective antiretroviral therapy against HIV-1 infection. AIDS. 2002;16:2145-9.
137. Dahl V, Peterson J, Fuchs D, Gisslen M, Palmer S, Price RW. Low levels of HIV-1 RNA detected in the cerebrospinal fluid after up to 10 years of suppressive therapy are associated with local immune activation. AIDS. 2014;28(15):2251-8.

138. de Oliveira MF, Murrell B, Perez-Santiago J, Vargas M, Ellis RJ, Letendre S, et al. Circulating HIV DNA Correlates With Neurocognitive Impairment in Older HIV-infected Adults on Suppressive ART. Sci Rep. 2015;5:17094.
139. Cysique LA, Maruff P, Brew BJ. Variable benefit in neuropsychological function in HIV-infected HAART-treated patients. Neurology. 2006;66:1447-50.
140. Valcour VG, Ananworanich J, Agsalda M, Sailasuta N, Chalermchai T, Schuetz A, et al. HIV DNA reservoir increases risk for cognitive disorders in cART-naive patients. PLoS One. 2013;8(7):e70164.
141. Shiramizu B, Lau E, Tamamoto A, Uniatowski J, Troelstrup D. Feasibility assessment of cerebrospinal fluid from HIV-1-infected children for HIV proviral DNA and monocyte chemoattractant protein 1 alleles. J Investig Med. 2006;54(8):468-72.
142. Chen MF, Gill AJ, Kolson DL. Neuropathogenesis of HIV-associated neurocognitive disorders: roles for immune activation, HIV blipping and viral tropism. Curr Opin HIV AIDS. 2014;9(6):559-64.
143. Rao VR, Ruiz AP, Prasad VR. Viral and cellular factors underlying neuropathogenesis in HIV associated neurocognitive disorders (HAND). AIDS Research and Therapy. 2014;11:13.
144. Rao VR, Sas AR, Eugenin EA, Siddappa NB, Bimonte-Nelson H, Berman JW, et al. HIV-1 clade-specific differences in the induction of neuropathogenesis. J Neurosci. 2008;28(40):10010-6.
145. Gandhi N, Saiyed Z, Thangavel S, Rodriguez J, Rao KVK, Nair MPN. Differential effects of HIV type 1 clade B and clade C tat protein on expression of proinflammatory and antiinflammatory cytokines by primary monocytes. AIDS Res Hum Retroviruses. 2009;25(7):691-9.
146. Gandhi N, Saiyed ZM, Napuri J, Samikkannu T, Reddy PV, Agudelo M, et al. Interactive role of human immunodeficiency virus type 1 (HIV-1) clade-specific Tat protein and cocaine in blood-brain barrier dysfunction: implications for HIV-1-associated neurocognitive disorder. J Neurovirol. 2010;16(4):294-305.
147. Tungaturthi PK, Sawaya BE, Singh SP, Tomkowicz B, Ayyavoo V, Khalili K, et al. Role of HIV-1 Vpr in AIDS pathogenesis: relevance and implications of intravirion, intracellular and free Vpr. Biomedicine & Pharmacotherapy. 2003;57:20-4.
148. Almeida SM. Cognitive impairment and major depressive disorder in HIV infection and cerebrospinal fluid biomarkers. Arq Neuropsiquiatr. 2013;71(9B):689-92.
149. Nakamuta S, Endo H, Higashi Y, Kousaka A, Yamada H, Yano M, et al. Human immunodeficiency virus type 1 gp120-mediated disruption of tight junction proteins by induction of proteasome-mediated degradation of zonula occludens-1 and -2 in human brain microvascular endothelial cells. J Neurovirol. 2008;14(3):186-95.
150. Hu S, Sheng WS, Lokensgard JR, Peterson PK, Rock RB. Preferential sensitivity of human dopaminergic neurons to gp120-induced oxidative damage. J Neurovirol. 2009;15(5-6):401-10.
151. Giunta B, Figueroa KP, Town T, Tan J. Soluble CD40 ligand in dementia. Drugs of the Future. 2009;34(4):333-9.
152. Yao H, Allen JE, Zhu X, Callen S, Buch S. Cocaine and human immunodeficiency virus type 1 gp120 mediate neurotoxicity through overlapping signaling pathways. J Neurovirol. 2009;15(2):164-75.
153. Wagner GA, Chaillon A, Liu S, Franklin DR, Jr., Caballero G, Kosakovsky Pond SL, et al. HIV-associated neurocognitive disorder is associated with HIV-1 dual infection. AIDS. 2016;30(17):2591-7.
154. Dore GJ, McDonald A, Li Y, Kaldor JM, Brew BJ, National HIVSC. Marked improvement in survival following AIDS dementia complex in the era of highly active antiretroviral therapy. AIDS. 2003;17(10):1539-45.

155. Brew BJ, Dunbar N, Pemberton L, Kaldor J. Predictive markers of AIDS dementia complex: CD4 cell count and cerebrospinal fluid concentrations of beta2-microglobulin and neopterin. The Journal of Infectious Diseases. 1996;174:294-98.
156. Sun B, Abadjian L, Rempel H, Calosing C, Rothlind J, Pulliam L. Peripheral biomarkers do not correlate with cognitive impairment in highly active antiretroviral therapy-treated subjects with human immunodeficiency virus type 1 infection. J Neurovirol. 2010;16(2):115-24.
157. Svatonova J, Borecka K, Adam P, Lanska V. Beta2-microglobulin as a diagnostic marker in cerebrospinal fluid: a follow-up study. Dis Markers. 2014;2014:495402.
158. Brew BJ, Pemberton L, Blennow K, Wallin A, Hagberg L. CSF amyloid beta42 and tau levels correlate with AIDS dementia complex. Neurology. 2005;65(9):1490-2.
159. Cysique LA, Brew BJ, Halman M, Catalan J, Sacktor N, Price RW, et al. Undetectable cerebrospinal fluid HIV RNA and β-2 microglobulin do not indicate inactive AIDS dementia complex in highly active antiretroviral therapy–treated patients. J Acquir Immune Defic Syndr. 2005;39:426-9.
160. Brew BJ, Bhalla RB, Paul M, Sidtis JJ, Keilp JJ, Sadler AE, et al. Cerebrospinal fluid beta2-microglobulin in patients with AIDS dementia complex: an expanded series including response to zidovudine treatment. AIDS. 1992;6:461-5.
161. Enting RH, Foudraine NA, Lange JMA, Jurriaans S, van der Poll T, Weverling G-J, et al. Cerebrospinal fluid β2-microglobulin, monocyte chemotactic protein-1, and soluble tumour necrosis factor α receptors before and after treatment with lamivudine plus zidovudine or stavudine. J Neuroimmunol. 2000;102:216-21.
162. Lien E, Aukrust P, Sundan A, Muller F, Froland SS, Espevik T. Elevated levels of serum-soluble CD14 in human immunodeficiency virus type 1 (HIV-1) infection: correlation to disease progression and clinical events. Blood. 1998;92(6):2084-92.
163. Ryan LA, Zheng J, Brester M, Bohac D, Hahn F, Anderson J, et al. Plasma levels of soluble CD14 and tumor necrosis factor-α type II receptor correlate with cognitive dysfunction during human immunodeficiency virus type 1 infection. J Infect Dis. 2001;184:699-706.
164. Kamat A, Lyons JL, Misra V, Uno H, Morgello S, Singer EJ, et al. Monocyte activation markers in cerebrospinal fluid associated with impaired neurocognitive testing in advanced HIV infection. J Acquir Immune Defic Syndr. 2012;60:234-43.
165. Tippett E, Cheng WJ, Westhorpe C, Cameron PU, Brew BJ, Lewin SR, et al. Differential expression of CD163 on monocyte subsets in healthy and HIV-1 infected individuals. PLoS One. 2011;6(5):e19968.
166. Chawla-Sarkar M, Lindner DJ, Liu Y-F, Williams BR, Sen GC, Silverman RH, et al. Apoptosis and interferons: role of interferon-stimulated genes as mediators of apoptosis. Apoptosis. 2003;8:237-49.
167. Silva K, Hope-Lucas C, White T, Hairston TK, Rameau T, Brown A. Cortical neurons are a prominent source of the proinflammatory cytokine osteopontin in HIV-associated neurocognitive disorders. J Neurovirol. 2015;21(2):174-85.
168. Vera JH, Guo Q, Cole JH, Boasso A, Greathead L, Kelleher P, et al. Neuroinflammation in treated HIV-positive individuals: A TSPO PET study. Neurology. 2016;86:1425-32.
169. Perrella O, Carrieri PB, Guarnaccia D, Soscia M. Cerebrospinal fluid cytokines in AIDS dementia complex. J Neurol. 1992;239:387-8.
170. Perrella O, Carreiri PB, Perrella A, Sbreglia C, Gorga F, Guanaccia D, et al. Transforming growth factor beta-1 and interferon-alpha in the AIDS dementia complex (ADC): a possible relationship with cerebral viral load? Eur Cytokine Netw. 2001;12(1):51-5.
171. Rho MB, Wesselingh S, Glass JD, McArthur JC, Choi S, Griffin J, et al. A potential role for interferon-α in the pathogenesis of HIV-associated dementia. Brain, Behavior and Immunity. 1995;9:366-77.

172. Yuan L, Qiao L, Wei F, Yin J, Liu L, Ji Y, et al. Cytokines in CSF correlate with HIV-associated neurocognitive disorders in the post-HAART era in China. J Neurovirol. 2013;19(2):144-9.
173. Griffin DE, McArthur JC, Cornblath DR. Neopterin and interferon-gamma in serum and cerebrospinal fluid patients with HIV-associated neurologic disease. Neurology. 1991;41(1):69-74.
174. Fuchs D, Moller AA, Reibnegger G, Werner ER, Werner-Felmayer G, Dierich MP, et al. Increased endogenous interferon-gamma and neopterin correlate with increased degradation of tryptophan in human immunodeficiency virus type 1 infection. Immunology Letters. 1991;28:207-12.
175. Dhillon N, Zhu X, Peng F, Yao H, Williams R, Qiu J, et al. Molecular mechanism(s) involved in the synergistic induction of CXCL10 by human immunodeficiency virus type 1 Tat and interferon-γ in macrophages. J Neurovirol. 2008;14(3):196-204.
176. Cinque P, Bestetti A, Marenzi R, Sala S, Gisslen M, Hagberg L, et al. Cerebrospinal fluid interferon-γ-inducible protein 10 (IP-10, CXCL10) in HIV-1 infection. J Neuroimmunol. 2005;168:154-63.
177. Shacklett BL, Cox CA, Wilkens DT, Karlsson RK, Nilsson A, Nixon DF, et al. Increased adhesion molecule and chemokine receptor expression on CD8+ T cells trafficking to cerebrospinal fluid in HIV-1 infection. J Infect Dis. 2004;189:2202-12.
178. Kolb SA, Sporer B, Lahrtz F, Koedel U, Pfister HW, Fontana A. Indenfication of a T cell chemotactic factor in the cerebrospinal fluid of HIV-1-infected individuals as interferon-γ inducible protein 10. J Neuroimmunol. 1999;93:172-81.
179. van Marle G, Henry S, Todoruk T, Sullivan A, Silva C, Rourke SB, et al. Human immunodeficiency virus type 1 Nef protein mediates neural cell death: a neurotoxic role for IP-10. Virology. 2004;329(2):302-18.
180. Gallo P, Frei K, Rordorf C, Lazdins J, Tavolato B, Fontana A. Human immunodeficiency virus type 1 (HIV-1) infection of the central nervous system: an evaluation of cytokines in cerebrospinal fluid. J Neuroimmunol. 1989;23:109-16.
181. Nolting T, Arendt G. Cytokine findings in the CSF of HIV-positive patients. Future HIV Ther. 2008;2(1):59-67.
182. Nolting T, Lindecke A, Koutsilieri E, Maschke M, Husstedt IW, Sopper S, et al. Measurement of soluble inflammatory mediators in cerebrospinal fluid of human immunodeficiency virus-positive patients at distinct stages of infection by solid-phase protein array. J Neurovirol. 2009;15(5-6):390-400.
183. Tyor WR, Glass JD, Griffin JW, Becker PS, McArthur JC, Bezman L, et al. Cytokine expression in the brain during the acquired immunodeficiency syndrom. Ann Neurol. 1992;31:349-60.
184. Correia S, Cohen R, Gongvatana A, Ross S, Olchowski J, Devlin K, et al. Relationship of plasma cytokines and clinical biomarkers to memory performance in HIV. J Neuroimmunol. 2013;265(1-2):117-23.
185. Kallianpur K, Sakoda M, Umaki T, Norris P, Keating S, Barbour J, et al. High ratios of circulating pro-inflammatory cytokines to anti-inflammatory IL-10 correlate with regional brain atrophy in chronic suppressed HIV infection. 20th International AIDS Conference, Melbourne Australia. July 20-25, 2014:THAB0104.
186. Gongvatana A, Correia S, Dunsiger S, Gauthier L, Devlin KN, Ross S, et al. Plasma cytokine levels are related to brain volumes in HIV-infected individuals. J Neuroimmune Pharmacol. 2014;9(5):740-50.
187. Griffin DE, McArthur JC, Cornblath DR. Soluble interleukin-2 receptor and soluble CD8 in serum and cerebrospinal fluid during human immunodeficiency virus-associated neurologic disease. J Neuroimmunol. 1990;28:97-109.

188. Kelder W, McArthur JC, Nance-Sproson T, McClernon D, Griffin DE. β-chemokines MCP-1 and RANTES are selectively increased in cerebrospinal fluid of patients with human immunodeficiency virus-assocated dementia. Ann Neurol. 1998;44:831-5.
189. Mastroianni CM, Paoletti F, Valenti C, Vullo V, Jirillo E, D'elia SA, A. Tumour necrosis factor (TNF-α) and neurological disorders in HIV infection. Journal of Neurology, Neurosurgery, and Psychiatry. 1992;55:219-21.
190. Wesselingh SL, Glass J, McArthur JC, Griffin JW, Griffin DE. Cytokine dysregulation in HIV-associated neurological disease. Adv Neuroimmunol. 1994;4:199-206.
191. Gisolf EH, van Praag RME, Jurriaans S, Portegies P, Goudsmit J, Danner SA, et al. Increasing cerebrospinal fluid chemokine concentrations despite undetectable cerebrospinal fluid HIV RNA in HIV-1-infected patients receiving antiretroviral therapy. J Acquir Immune Defic Syndr. 2000;25:426-33.
192. Portegies P, Godfried MH, Hintzen RQ, Stam J, van der Poll T, Bakker M, et al. Low levels of specific T cell activation marker CD27 accompanied by elevated levels of markers for non-specific immune activation in the cerebrospinal fluid of patients with AIDS dementia complex. J Neuroimmunol. 1993;48:241-8.
193. Vullo V, Mastroianni CM, Lichtner M, Mengoni F, Delia S. Increased cerobrospinal fluid levels of soluble receptors for tumour necrosis factor in HIV-infected patients with neurological diseases. AIDS. 1995;9:1099-112.
194. Sabri F, De Milito A, Pirskanen R, Elovaara I, Hagberg L, Cinque P, et al. Elevated levels of soluble fas and fas ligand in cerebrospinal fluid of patients with AIDS dementia complex. J Neuroimmunol. 2001;114:197-206.
195. Sporer B, Koedel U, Goebel FD, Pfister HW. Increased levels of soluble Fas receptor and Fas ligand in the cerebrospinal fluid of HIV-infected patients. AIDS Res Hum Retroviruses. 2000;16(3):221-6.
196. Towfighi A, Skolasky RL, St. Hillaire C, Conant K, McArthur JC. CSF soluble Fas correlates with the severity of HIV-infected dementia. Neurology. 2004;62:654-6.
197. Gendelman HE, Zheng J, Coulter CL, Ghorpade A, Che M, Thylin M, et al. Suppression of inflammatory neurotoxins by highly active antiretroviral therapy in human immunideficiency virus-associated dementia. J Infect Dis. 1998;178:1000-7.
198. Conant K, Garzino-Demo A, Nath A, McArthur JC, Halliday W, Power C, et al. Induction of monocyte chemoattractant protein-1 in HIV-1 Tat-stimulated astrocytes and elevation in AIDS dementia. Proc Natl Acad Sci USA. 1998;95:3117-21.
199. Schmidtmayerova H, Nottet HSLM, Nuovo G, Raabe T, Flanagan CR, Dubrovsky L, et al. Human immunodeficiency virus type 1 infection alters chemokine β peptide expression in human monocytes: Implications for recruitment of leukocytes into brain and lymph nodes. Proc Natl Acad Sci U S A. 1996;93:700-4.
200. Bernasconi S, Cinque P, Giuseppe P, Sozzani S, Crociati A, Torri W, et al. Selective elevation of monocyte chemotactic protein-1 in the cerebrospinal fluid of AIDS patients with cytomegalovirus encephalitis. The Journal of Infectious Diseases. 1996;174:1098-101.
201. Cinque P, Vago L, Mengozzi M, Torri V, Ceresa D, Vicenzi E, et al. Elevated cerebrospinal fluid levels of monocyte chemotactic protein-1 correlate with HIV-1 encephalitis and local viral replication. AIDS. 1998;12(11):1327-32.
202. Monteiro de Almeida S, Letendre S, Zimmerman J, Lazzaretto D, McCutchan A, Ellis R. Dynamics of monocyte chemoattractant protein type one (MCP-1) and HIV viral load in human cerebrospinal fluid and plasma. J Neuroimmunol. 2005;169(1-2):144-52.
203. Sozzani S, Introna M, Bernasconi S, Polentarutti N, Cinque P, Poli G, et al. MCP-1 and CCR2 in HIV infection: regulation of agonist and receptor expresssion. J Leukoc Biol. 1997;62:30-3.

204. Letendre SL, Zheng JC, Kaul M, Yiannoutsos CT, Ellis RJ, Taylor MJ, et al. Chemokines in cerebrospinal fluid correlate with cerebral metabolite patterns in HIV-infected individuals. J Neurovirol. 2011;17(1):63-9.
205. Letendre SL, Lanier ER, McCutchan JA. Cerebrospinal fluid β chemokine concentrations in neurocognitively impaired individuals with human immunodeficiency virus type 1. J Infect Dis. 1999;180:310-9.
206. Erichsen D, Lopez AL, Peng H, Niemann D, Williams C, Bauer M, et al. Neuronal injury regulates fractalkine: relevance for HIV-1 associated dementia. Journal of Neuroimmunology. 2003;138(1-2):144-55.
207. Sporer B, Kastenbauer S, Koedel U, Arendt G, Pfister HW. Increased intrathecal release of soluble fractalkine in HIV-infected patients. AIDS Res Hum Retroviruses. 2003;19(2):111-6.
208. Johnson MD, Kim P, Tourtellotte W, Federspiel CF. Transforming growth factor beta and monocyte chemotactic protein-1 are elevated in cerebrospinal fluid of immunocompromised patients with HIV-1 infection. J NeuroAIDS. 2004;2(4):33-43.
209. Scorziello A, Florio T, Bajetto A, Thellung S, Schettini G. TGF-β1 prevents gp120-induced impairment of Ca2+ homeostasis and rescues cortical neurons from apoptotic death. J Neurosci Res. 1997;49:600-7.
210. Brew BJ, Bhalla RB, Paul M, Gallardo H, McArthur JC, Schwartz MK, et al. Cerebrospinal fluid neopterin in human immunodeficiency virus type 1 infection. Ann Neurol. 1990;28:556-60.
211. Hagberg L, Cinque P, Gisslen M, Brew BJ, Spudich S, Bestetti A, et al. Cerebrospinal fluid neopterin: an informative biomarker of central nervous system immune activation in HIV-1 infection. AIDS Res Ther. 2010;7:15.
212. Huang S-H, Jong AY. Cellular mechanisms of microbial proteins contributing to invasion of the blood-brain barrier. Cellular Microbiology. 2001;3(5):277-87.
213. Rieckmann P, Nunke K, Burchhardt M, Albrecht M, Wiltfang J, Ulrich M, et al. Soluble intercellular adhesion molecule-1 in cerebrospinal fluid: an indicator for the inflammatory impairment of the blood-cerebrospinal fluid barrier. J Neuroimmunol. 1993;47:133-40.
214. Heidenreich F, Arendt G, Jander S, Jablonowski H, Stoll G. Serum and cerebrospinal fluid levels of soluble intercellular adhesion molecule 1 (sICAM-1) in patients with HIV-1 associated neurological diseases. J Neuroimmunol. 1994;52:117-26.
215. Roberts TK, Eugenin EA, Morgello S, Clements JE, Zink MC, Berman JW. PrPC, the cellular isoform of the human prion protein, is a novel biomarker of HIV-associated neurocognitive impairment and mediates neuroinflammation. Am J Pathol. 2010;177(4):1848-60.
216. Li S, Wu Y, Keating SM, Du H, Sammet CL, Zadikoff C, et al. Matrix metalloproteinase levels in early HIV infection and relation to in vivo brain status. J Neurovirol. 2013;19(5):452-60.
217. Rumbaugh J, Turchan-Cholewo J, Galey D, St Hillaire C, Anderson C, Conant K, et al. Interaction of HIV Tat and matrix metalloproteinase in HIV neuropathogenesis: a new host defense mechanism. FASEB J. 2006;20(10):1736-8.
218. Rosenberg GA. Matrix metalloproteinases in neuroinflammation. Glia. 2002;39(3):279-91.
219. Ragin AB, Wu Y, Ochs R, Scheidegger R, Cohen BA, McArthur JC, et al. Serum matrix metalloproteinase levels correlate with brain injury in human immunodeficiency virus infection. J Neurovirol. 2009;15(3):275-81.
220. Sporer B, Paul R, Koedel U, Grimm R, Wick M, Goebel FD, et al. Presence of matrix metalloproteinase-9 activity in the cerebrospinal fluid of human immunodeficiency virus-infected patients. J Infect Dis. 1998;178:854-7.

221. Conant K, McArthur JC, Griffin DE, Sjulson L, Wahl LM, Irani DN. Cerebrospinal fluid levels of MMP-2, 7, and 9 are elevated in association with human immunodeficiency virus dementia. Ann Neurol. 1999;46:391-8.
222. Cantres-Rosario Y, Plaud-Valentin M, Gerena Y, Skolasky RL, Wojna V, Melendez LM. Cathepsin B and cystatin B in HIV-seropositive women are associated with infection and HIV-1-associated neurocognitive disorders. AIDS. 2013;27(3):347-56.
223. Graziano F, Elia C, Laudanna C, Poli G, Alfano M. Urokinase plasminogen activator inhibits HIV virion release from macrophage-differentiated chronically infected cells via activation of RhoA and PKCepsilon. PLoS One. 2011;6(8):e23674.
224. Cinque P, Nebuloni M, Santovito ML, Price RW, Gisslen M, Hagberg L, et al. The urokinase receptor is overexpressed in the AIDS dementia complex and other neurological manifestations. Ann Neurol. 2004;55(5):687-94.
225. Nebuloni M, Cinque P, Sidenius N, Ferri A, Lauri E, Omodeo-Zorini E, et al. Expression of the urokinase plasminogen activator receptor (uPAR) and its ligand (uPA) in brain tissues of human immunodeficiency virus patients with opportunistic cerebral diseases. J Neurovirol. 2009;15(1):99-107.
226. Asahchop EL, Branton WG, Broadhurst D, Reinke S, Gill J, Power C. HIV-associated neurocognitive disorder displays a distinct microRNA profile in plasma. 21st Conference on Retroviruses and Opportunistic Infections (CROI), 3-6 March 2014, Boston. 2014:Poster 460.
227. Sporer B. Vascular endothelial growth factor (VEGF) is increased in serum, but not in cerebrospinal fluid in HIV associated CNS diseases. Journal of Neurology, Neurosurgery & Psychiatry. 2004;75(2):298-300.
228. Sporer B, Missler U, Magerkurth O, Koedel U, Wiesmann M, Pfister HW. Evaluation of CSF glial fibrillary acidic protein (GFAP) as a putative marker for HIV-associated dementia. Infection. 2004;32(1):20-3.
229. Mielke MM, Bandaru VV, McArthur JC, Chu M, Haughey NJ. Disturbance in cerebral spinal fluid sphingolipid content is associated with memory impairment in subjects infected with the human immunodeficiency virus. J Neurovirol. 2010;16(6):445-56.
230. Sacktor N, Haughey N, Cutler R, Tamara A, Turchan J, Pardo C, et al. Novel markers of oxidative stress in actively progressive HIV dementia. J Neuroimmunol. 2004;157(1-2):176-84.
231. Zhou D, Masliah E, Spector SA. Autophagy is increased in postmortem brains of persons with HIV-1-associated encephalitis. J Infect Dis. 2011;203(11):1647-57.
232. Fuchs D, Forsman A, Hagberg L, Larsson M, Norkrans G, Reibnegger G, et al. Immune activation and decreased tryptophan in patients with HIV-1 infection. J Interferon Research. 1990;10:599-603.
233. Boasso A, Shearer GM. How does indoleamine 2,3-dioxygenase contribute to HIV-mediated immune dysregulation. Current Drug Metabolism. 2007;8:217-23.
234. Guillemin GJ, Smith DG, Smythe GA, Armati PJ, Brew BJ. Expression of the kynurenine pathway enzymes in human microglia and macrophages. Adv Exp Med Biol. 2003;527:105-12.
235. Guillemin GJ, Smythe G, Takikawa O, Brew BJ. Expression of indoleamine 2,3-dioxygenase and production of quinolinic acid by human microglia, astrocytes, and neurons. Glia. 2004;49(1):15-23.
236. Davies NWS, Guillemin G, Brew BJ. Tryptophan, neurodegeneration and HIV-associated neurocognitive disorder. Int J Tryptophan Res. 2010;3:121-40.
237. Heyes MP, Brew BJ, Saito K, Quearry BJ, Price RW, Lee K, et al. Inter-relationships between quinolinic acid, neuroactive kynurenines, neopterin and β2-microglobulin in cerebrospinal fluid and serum of HIV-1-infected patients. J Neuroimmunol. 1992;40:71-80.
238. Grill M, Gisslen M, Cinque P, Peterson J, Lee E, Spudich S, et al. Kynurenine-tryptophan and phenylalanine-tyrosine levels in cerebrospinal fluid in HIV infection. 19th Conference on Retroviruses and Opportunistic Infections (CROI), 5-8 March 2012, Seattle, WA. 2012:P463.

239. Letendre S, Croteau D, Ellis RJ, Rosario D, Potter M, Woods SP. HIgher levels of phosphorylated tau in CSF are associated with HIV infection, older age, antiretroviral use, and worse prospective memory. 18th Conference on Retroviruses and Opportunistic Infections (CROI), 27 February–-3 March 2011, Boston. 2011:P406.
240. Aprea S, Del Valle L, Mameli G, Sawaya BE, Khalili K, Peruzzi F. Tubulin-mediated binding of human immunodeficiency virus-1 Tat to the cytoskeleton causes proteasomal-dependent degradation of microtubule-associated protein 2 and neuronal damage. J Neurosci. 2006;26(15):4054-62.
241. Krut JJ, Price RW, Zetterberg H, Hagberg L, Cinque P, Nilsson S, et al. Hyperphosphorylated tau in cerebrospinal fluid: A biomarker for neurological aging in HIV-1? 21st Conference on Retroviruses and Opportunistic Infections (CROI), 3-6 March 2014, Boston.P453.
242. Green AJE. Cerebrospinal fluid tau concentrations in HIV infected patients with suspected neurological disease. Sexually Transmitted Infections. 2000;76(6):443-6.
243. Clifford DB, Fagan AM, Holtzman DM, Morris JC, Teshome M, Shah AR, et al. CSF biomarkers of Alzheimer disease in HIV-associated neurologic disease. Neurology. 2009;73:1982-7.
244. Gisslen M, Krut J, Andreasson U, Blennow K, Cinque P, Brew BJ, et al. Amyloid and tau cerebrospinal fluid biomarkers in HIV infection. BMC Neurol. 2009;9:63.
245. Steinbrink F, Evers S, Buerke B, Young P, Arendt G, Koutsilieri E, et al. Cognitive impairment in HIV infection is associated with MRI and CSF pattern of neurodegeneration. Eur J Neurol. 2013;20(3):420-8.
246. Smith DB, Simmonds P, Bell JE. Brain viral burden, neuroinflammation and neurodegeneration in HAART-treated HIV positive injecting drug users. J Neurovirol. 2014;20(1):28-38.
247. Anthony IC, Ramage SN, Carnie FW, Simmonds P, Bell JE. Accelerated Tau deposition in the brains of individuals infected with human immunodeficiency virus-1 before and after the advent of highly active anti-retroviral therapy. Acta Neuropathol. 2006;111(6):529-38.
248. Patrick C, Crews L, Desplats P, Dumaop W, Rockenstein E, Achim CL, et al. Increased CDK5 expression in HIV encephalitis contributes to neurodegeneration via tau phosphorylation and is reversed with Roscovitine. Am J Pathol. 2011;178(4):1646-61.
249. Brown AM, Scarola J, Smith AJ, Sanberg PR, Tan J, Giunta B. The role of tau protein in HIV-associated neurocognitive disorders. Molecular Neurodegeneration. 2014;9:40.
250. Brew BJ, Pemberton L, Blennow K, Wallin A, Hagberg L. CSF amyloid beta42 and tau levels correlate with AIDS dementia complex. Neurology. 2005;65:1490-2.
251. Rempel HC, Pulliam L. HIV-1 Tat inhibits neprilysin and elevated amyloid beta. AIDS. 2005;19(2):127-35.
252. Giunta B, Ehrhart J, Obregon DF, Lam L, Le L, Jin J, et al. Antiretroviral medications disrupt microglial phagocytosis of β-amyloid and increase its production by neurons: implications for HIV-associated neurocognitive disorders. Molecular Brain. 2011;4:23.
253. Ances BM, Christensen JJ, Teshome M, Taylor J, Xiong C, Aldea P, et al. Cognitively unimpaired HIV-positive subjects do not have increased 11C-PiB: a case control study. Neurology. 2010;75:111-5.
254. Ances BM, Benzinger TL, Christensen JJ, Thomas J, Venkat R, Teshome M, et al. 11C-PiB Imaging of Human Immunodeficiency Virus–Associated Neurocognitive Disorder. Arch Neurol. 2012;69(1):72-7.
255. Esiri MM, Biddolph SC, Morris CS. Alzheimer plaques in AIDS. J Neurol Neurosurg Psychiatry. 1998;65(1):29-33.
256. Peluso MJ, Meyerhoff DJ, Price RW, Peterson J, Lee E, Young AC, et al. Cerebrospinal fluid and neuroimaging biomarker abnormalities suggest early neurological injury in a subset of individuals during primary HIV infection. J Infect Dis. 2013;207(11):1703-12.

257. Abdulle S, Mellgren A, Brew BJ, Cinque P, Hagberg L, Price RW, et al. CSF neurofilament protein (NFL) - a marker of active HIV-related neurodegeneration. J Neurol. 2007;254(8):1026-32.
258. Gisslen M, Rosengren L, Hagberg L, Deeks SG, Price RW. Cerebrospinal fluid signs of neuronal damage after antiretroviral treatment interruption in HIV-1 infection. AIDS Res Ther. 2005;2:6.
259. Gisslen M, Hagberg L, Brew BJ, Cinque P, Price RW, Rosengren L. Elevated cerebrospinal fluid neurofilament light protein concentrations predict the development of AIDS dementia complex. J Infect Dis. 2007;195(12):1774-8.
260. Mellgren A, Price RW, Hagberg L, Rosengren L, Brew BJ, Gisslen M. Antiretroviral treatment reduces increased CSF neurofilament protein (NFL) in HIV-1 infection. Neurology. 2007;69:1536-41.
261. Anderson C, Sacktor N, McArthur JC, Nath A. Significant neuronal injury in asymptomatic HIV infection. 18th Conference on Retroviruses and Opportunistic Infections (CROI), 27 February-3 March 2011, Boston. 2011:Poster 407.
262. Morales D, Skoulakis EC, Acevedo SF. 14-3-3s are potential biomarkers for HIV-related neurodegeneration. J Neurovirol. 2012;18(5):341-53.
263. Morales D, Hechavarria R, Wojna V, Acevedo SF. YWHAE/14-3-3epsilon: a potential novel genetic risk factor and CSF biomarker for HIV neurocognitive impairment. J Neurovirol. 2013;19(5):471-8.
264. Rearden A, Hurford R, Luu N, Kieu E, Sandoval M, Perez-Liz G, et al. Novel expression of PINCH in the central nervous system and its potential as a biomarker for human immunodeficiency virus-associated neurodegeneration. J Neurosci Res. 2008;86(11):2535-42.
265. Lentz MR, Kim WK, Lee V, Bazner S, Halpern EF, Venna N, et al. Changes in MRS neuronal markers and T cell phenotypes observed during early HIV infection. Neurology. 2009;72:1465-72.
266. Winston A, Duncombe C, Li PC, Gill JM, Kerr SJ, Puls R, et al. Does choice of combination antiretroviral therapy (cART) alter changes in cerebral function testing after 48 weeks in treatment-naive, HIV-1-infected individuals commencing cART? A randomized, controlled study. Clin Infect Dis. 2010;50(6):920-9.
267. Winston A, Puls R, Kerr SJ, Duncombe C, Li PC, Gill JM, et al. Dynamics of cognitive change in HIV-infected individuals commencing three different initial antiretroviral regimens: a randomized, controlled study. HIV Med. 2012;13(4):245-51.
268. Winston A, Puls R, Kerr SJ, Duncombe C, Li P, Gill JM, et al. Differences in the direction of change of cerebral function parameters are evident over three years in HIV-infected individuals electively commencing initial cART. PLoS One. 2015;10(2):e0118608.
269. Pemberton LA, Brew BJ. Cerebrospinal fluid S-100β and its relationship with AIDS dementia complex. J Clin Virol. 2001;22:249-53.
270. Hu J, Ferreira A, Van Eldik LJ. S100β induces neuronal cell death through nitiric oxide release from astrocytes. J Neurochem. 1997;69:2294-301.
271. Du Pasquier RA, Jilek S, Kalubi M, Yerly S, Fux CA, Gutmann C, et al. Marked increase of the astrocytic marker S100B in the cerebrospinal fluid of HIV-infected patients on LPV/r-monotherapy. AIDS. 2013;27(2):203-10.
272. Singer EJ, Syndulko K, Fahy-Chandon B, Schmid P, Conrad A, Tourtellotte WW. Intrathecal IgG synthesis and albumin leakage are increased in subjects with HIV-1 neurologic disease. J Acquir Immune Defic Syndr. 1994;7:265-71.
273. Cauwels A, Frei K, Sansano S, Fearns C, Ulevitch R, Zimmerli W, et al. The origin and function of soluble CD14 in experimental bacterial meningitis. J Immunol. 1999;162:4762-72.
274. Landmann R, Muller B, Zimmerli W. CD14, new aspects of ligand and signal diversity. Microbes and Infection. 2000;2:295-304.

275. Lund SA, Giachelli CM, Scatena M. The role of osteopontin in inflammatory processes. J Cell Commun Signal. 2009;3(3-4):311-22.
276. Cruse JM, Lewis RE. Atlas of Immunology. 3rd ed. Boca Raton, FL: CRC Press, Taylor & Francis Group; 2010.
277. Ware CF, VanArsdale S, VanArsdale TL. Apoptosis mediated by the TNF-related cytokine and receptor families. J Cellular Biochem. 1996;60:47-55.
278. Re DB, Przedborski S. Fractalkine: moving from chemotaxis to neuroprotection. Nature Neuroscience. 2006;9(7):859-61.
279. Shorter J, Lindquist S. Prions as adaptive conduits of memory and inheritance. Nat Rev Genet. 2005;6(6):435-50.
280. Maglio LE, Perez MF, Martins VR, Brentani RR, Ramirez OA. Hippocampal synaptic plasticity in mice devoid of cellular prion protein. Brain Res Mol Brain Res. 2004;131(1-2):58-64.
281. Neitzel JJ. Enzyme Catalysis: The Serine Proteases. Nature Education. 2010;3(9):21.
282. Lopez-Otin C, Bond JS. Proteases: multifunctional enzymes in life and disease. J Biol Chem. 2008;283(45):30433-7.
283. Stone TW. Neuropharmacology of quinolinic and kynurenic acids. Pharmacological Reviews. 1993;45(3):309-79.
284. Tumani H, Teunissen C, Sussmuth S, Otto M, Ludolph AC, Brettscheider J. Cerebrospinal fluid biomarkers of neurodegeneration in chronic neurological diseases. Expert Rev Mol Diagn. 2008;8(4):479-94.
285. Kirkpatrick LL, Brady ST. Molecular Components of the Neuronal Cytoskeleton. In: Siegel GJ, Agranoff BW, Albers RW, et al., editors. Basic Neurochemistry: Molecular, Cellular and Medical Aspects. 6th edition. Philadelphia: Lippincott-Raven; 1999. Available from: https://www.ncbi.nlm.nih.gov/books/NBK28122/. 1999.
286. Hoe HS, Lee HK, Pak DT. The upside of APP at synapses. CNS Neurosci Ther. 2012;18(1):47-56.
287. Nussbaum JM, Seward ME, Bloom GS. Alzheimer disease: a tale of two prions. Prion. 2013;7(1):14-9.
288. Diniz BS, Pinto Junior JA, Forlenza OV. Do CSF total tau, phosphorylated tau, and beta-amyloid 42 help to predict progression of mild cognitive impairment to Alzheimer's disease? A systematic review and meta-analysis of the literature. World J Biol Psychiatry. 2008;9(3):172-82.
289. Spies PE, Verbeek MM, van Groen T, Claassen JA. Reviewing reasons for the decreased CSF Abeta42 concentration in Alzheimer disease. Front Biosci (Landmark Ed). 2012;17:2024-34.
290. Hersh LB, Rodgers DW. Neprilysin and amyloid beta peptide degradation. Curr Alzheimer Res. 2008;5(2):225-31.
291. Shimada T, Fournier AE, Yamagata K. Neuroprotective function of 14-3-3 proteins in neurodegeneration. Biomed Res Int. 2013;2013:564534.
292. Ross B, Bluml S. Magnetic resonance spectroscopy of the human brain. The Anatomical Record. 2001;265:54-84.
293. Scheau C, Preda EM, Popa GA, Ghergas AE, Capsa RA, Lupesca IG. Magnetic resonance spectroscopy - a non-invasive methods in evaluating focal and diffuse central nervous system disease. Journal of Medicine and Life. 2012;5(4):423-7.
294. Winston A, Garvey L. Effects of different antiretroviral agents on cerebral function in HIV-infected individuals. Future Virol. 2011;6(9):1129-36.
295. Richard DM, Dawes MA, Mathias CW, Acheson A, Hill-Kapturczak N, Dougherty DM. L-tryptophan: basic metabolic functions, behavioral research and therapeutic functions. Int J Tryptophan Res. 2009;2:45-60.

296. Guillemin GJ, Cullen KM, Lim CK, Smythe GA, Garner B, Kapoor V, et al. Characterization of the kynurenine pathway in human neurons. J Neurosci. 2007;27(47):12884-92.
297. Walker AK, Budac DP, Bisulco S, Lee AW, Smith RA, Beenders B, et al. NMDA receptor blockade by ketamine abrogates lipopolysaccharide-induced depressive-like behavior in C57BL/6J mice. Neuropsychopharmacology. 2013;38(9):1609-16.
298. Kwidzinski E, Bechmann I. IDO expression in the brain: a double-edged sword. J Mol Med (Berl). 2007;85(12):1351-9.
299. Boasso A. Wounding the immune system with its own blade: HIV-induced tryptophan catabolism and pathogenesis. Current Medicinal Chemistry. 2011;18:2247-56.
300. Routy JP, Mehraj V, Vyboh K, Cao W, Kema I, Jenabian MA. Clinical relevance of kynurenine pathway in HIV/AIDS: an immune checkpoint at the crossraods of metabolism and inflammation. AIDS Rev. 2015;17:96-106.
301. van Donkelaar EL, Blokland A, Ferrington L, Kelly PA, Steinbusch HW, Prickaerts J. Mechanism of acute tryptophan depletion: is it only serotonin? Mol Psychiatry. 2011;16(7):695-713.
302. Schroecksnadel S, Kurz K, Weiss G, Fuchs D. Immune activation and neuropsychiatric symptoms in human immunodeficiency virus type 1 infection. Neurobehavioral HIV Medicine. 2012;4:1-13.
303. Schrocksnadel K, Wirleitner B, Winkler C, Fuchs D. Monitoring tryptophan metabolism in chronic immune activation. Clin Chim Acta. 2006;364(1-2):82-90.
304. Fuchs D, Werner ER, Dierich MP, Wachter H. Cellular immune activation in the brain and human immunodeficiency virus infection. Annals of Neurology. 1988;24(2):289-.
305. Calcagno A, Lo A, Vai D, Imperiale D, Atzori C, Romito A, et al. Pterin and neurotransmitter status in HIV-positive patients with neurocognitive disorders. European AIDS Clinical Society (EACS) Conference 2017, MIlan, Italy, Poster BPD2/4. 2017.
306. Capuron L, Schroecksnadel S, Feart C, Aubert A, Higueret D, Barberger-Gateau P, et al. Chronic low-grade inflammation in elderly persons is associated with altered tryptophan and tyrosine metabolism: role in neuropsychiatric symptoms. Biol Psychiatry. 2011;70(2):175-82.
307. Murray MF. Tryptophan depletion and HIV infection: a metabolic link to pathogenesis. The Lancet Infectious Diseases. 2003;3(10):644-52.
308. Guillemin GJ, Kerr SJ, Smythe GA, Smith DG, Kapoor V, Armati PJ, et al. Kynurenine pathway metabolism in human astrocytes: a paradox for neuronal protection. J Neurochem. 2001;78:842-53.
309. Owe-Young R, Webster NL, Mukhtar M, Pomerantz RJ, Smythe G, Walker D, et al. Kynurenine pathway metabolism in human blood-brain-barrier cells: implications for immune tolerance and neurotoxicity. J Neurochem. 2008;105(4):1346-57.
310. Boasso A, Herbeuval J-P, Hardy AW, Anderson SA, Dolan MJ, Fuchs D, et al. HIV inhibits CD4 T-cell proliferation by inducing indoleamine 2,3-dioxygenase in plasmacytoid dendritic cells. Blood. 2007;109(8):3351-9.
311. Widner B, Laich A, Sperner-Unterweger B, Ledochowski M, Fuchs D. Neopterin production, tryptophan degradation, and mental depression - What is the link? Brain, Behavior and Immunity. 2002;16:590-5.
312. Braidy N, Grant R, Adams S, Brew BJ, Guillemin GJ. Mechanism for quinolinic acid cytotoxicity in human astrocytes and neurons. Neurotox Res. 2009;16(1):77-86.
313. Huang Y, Zhao L, Jia B, Wu L, Li Y, Curthoys N, et al. Glutaminase dysregulation in HIV-1-infected human microglia mediates neurotoxicity: relevant to HIV-1-associated neurocognitive disorders. J Neurosci. 2011;31(42):15195-204.
314. Murray MF. Insights into therapy: tryptophan oxidation and HIV infection. Science Translational Medicine. 2010;2(32):32ps23.

315. Okuda S, Nishiyama N, Saito H, Katsuki H. 3-hydroxykynurenine, an endogenous oxidative stress generator, causes neuronal cell death with apoptotic features and region selectivity. J Neurochem. 1998;70:299-307.
316. Grant RS, Coggan SE, Smythe GA. The physiological action of picolinic acid in the human brain. Int J Tryptophan Res. 2009;2:71-9.
317. Fernandez-Pol JA, Klos DJ, Hamilton PD. Antiviral, cytotoxic and apoptotic activities of picolinic acid on human immunodeficiency virus-1 and human herpes simplex virus-2 infected cells. Anticancer Research. 2001;21:3773-6.
318. Taylor EW. The oxidative stress-induced niacin sink (OSINS) model for HIV pathogenesis. Toxicology. 2010;278(1):124-30.
319. Murray MF. Nicotinamide: an oral antimicrobial agent with activity against both Mycobacterium tuberculosis and human immunodeficiency virus. Clin Infect Dis. 2003;36:453-60.
320. Murray MF. Increased plasma tryptophan in HIV-infected patients treated with pharmacologic doses of nicotinamide. Nutrition. 2001;17:654-6.
321. Zangerle R, Widner B, Quirchmair G, Neurauter G, Sarcletti M, Fuchs D. Effective Antiretroviral Therapy Reduces Degradation of Tryptophan in Patients with HIV-1 Infection. Clinical Immunology. 2002;104(3):242-7.
322. Gisslen M, Larsson M, Norkrans G, Fuchs D, Wachter H, Hagberg L. Tryptophan concentrations increase in cerebrospinal fluid and blood after zidovudine treatment in patients with HIV type 1 infection. AIDS Res Hum Retroviruses. 1994;10(8):947-51.
323. Fuchs D, Gisslen M, Larsson M, Norkrans G, Hagberg L, Wachter H. Increase of Tryptophan in Serum and in Cerebrospinal Fluid of Patients with HIV Infection During Zidovudine Therapy. In: Filippini GA, Costa CVL, Bertazzo A (eds) Recent Advances in Tryptophan Research Advances in Experimental Medicine and Biology Springer, Boston, MA. 1996;398.
324. Neurauter G, Zangerle R, Widner B, Quirchmair G, Sarcletti M, Fuchs D. Effective Antiretroviral Therapy Reduces Degradation of Tryptophan in Patients with HIV-1 Infection. In: Allegri G, Costa CVL, Ragazzi E, Steinhart H, Varesio L (eds) Developments in Tryptophan and Serotonin Metabolism Advances in Experimental Medicine and Biology, Springer, Boston, MA. 2003;527.
325. Valle M, Price RW, Nilsson A, Heyes M, Verotta D. CSF quinolinic acid levels are determined by local HIV infection: cross-sectional analysis and modelling of dynamics following antiretroviral therapy. Brain. 2004;127(Pt 5):1047-60.
326. Doris A, Ebmeier K, Shajahan P. Depressive illness. Lancet. 1999;354:1369-75.
327. Maes M. Depression is an inflammatory disease, but cell-mediated immune activation is the key component of depression. Prog Neuropsychopharmacol Biol Psychiatry. 2011;35(3):664-75.
328. Maes M, Leonard BE, Myint AM, Kubera M, Verkerk R. The new '5-HT' hypothesis of depression: cell-mediated immune activation induces indoleamine 2,3-dioxygenase, which leads to lower plasma tryptophan and an increased synthesis of detrimental tryptophan catabolites (TRYCATs), both of which contribute to the onset of depression. Prog Neuropsychopharmacol Biol Psychiatry. 2011;35(3):702-21.
329. Konsman JP, Parnet P, Dantzer R. Cytokine-induced sickness behaviour: mechanisms and implications. Trends Neurosci. 2002;25:154-9.
330. Look MP, Altfeld M, Kreuzer KA, Riezler R, Stabler SP, Allen RH, et al. Parallel decrease in neurotoxin quinolinic acid and soluble tumor necrosis factor receptor p75 in serum during highly active antiretroviral therapy of HIV Type 1 disease. AIDS Res Hum Retroviruses. 2000;16(13):1215-21.

331. Benkelfat C, Ellenbogen MA, Dean P, Palmour RM, Young SN. Mood-lowering effect of tryptophan depletion. Enhanced susceptibility in young men at genetic risk for major affective disorders. Arch Gen Psychiatry. 1994;51:687-97.
332. Ricaurte GA, Finnegan KT, Irwin I, Langston JW. Aminergic metabolites in cerebrospinal fluid of humans previously exposed to MDMA: preliminary observations. Ann N Y Acad Sci. 1990;600:699-708.
333. Joseph MS, Brewerton TD, Reus VI, Stebbins GT. Plasma L-tryptophan/neutral amino acid ratio and dexamethasone suppression in depression. Psychiatry Res. 1984;11(3):185-92.
334. Curzon G. Study of disturbed tryptophan metabolism in depressive illness. Ann Biol Clin (Paris). 1979;37(1):27-33.
335. Banki CM, Molnar G, Fekete I. Correlation of individual symptoms and other clinical variables with cerebrospinal fluid amine metabolites and tryptophan in depression. Arch Psychiatr Nervenkr. 1981;229(4):345-53.
336. Lehmann J. Mental and neuromuscular symptoms in tryptophan deficiency: a review with special reference to mental symptoms in a selected material of carcinoid patients. Acta Psychiatr Scand Suppl. 1972;237.
337. Maes M, Maes L, Suy E. Symptom profiles of biological markers in depression: a multivariate study. Psychoneuroendocrinology. 1990;15(1):29-37.
338. Schroecksnadel K, Sarcletti M, Winkler C, Mumelter B, Weiss G, Fuchs D, et al. Quality of life and immune activation in patients with HIV-infection. Brain Behav Immun. 2008;22(6):881-9.
339. Martinez P, Tsai AC, Muzoora C, Kembabazi A, Weiser SD, Huang Y, et al. Reversal of kynurenine pathway of tryptophan catabolism may improve depression in ART-treated HIV-infected Ugandans. J Acquir Immune Defic Syndr. 2014;65:456-62.
340. Hammoud DA, Endres CJ, Hammond E, Uzuner O, Brown A, Nath A, et al. Imaging serotonergic transmission with [11C]DASB-PET in depressed and non-depressed patients infected with HIV. NeuroImage. 2010;49:2588-95.
341. Suh HS, Zhao ML, Rivieccio M, Choi S, Connolly E, Zhao Y, et al. Astrocyte indoleamine 2,3-dioxygenase is induced by the TLR3 ligand poly(I:C): mechanism of induction and role in antiviral response. J Virol. 2007;81(18):9838-50.
342. McAllister-Williams RH, Massey AE, Rugg MD. Effects of tryptophan depletion on brain potential correlates of episodic memory retrieval. Psychopharmacology (Berl). 2002;160(4):434-42.
343. Muller N, Schwarz MJ. The immune-mediated alteration of serotonin and glutamate: towards an integrated view of depression. Mol Psychiatry. 2007;12:988-1000.
344. Park SB, Coull JT, McShane RH, Young AH, Sahakian BJ, Robbins TW, et al. Tryptophan depletion in normal volunteers producers selective impairments in learning and memory. Neuropharmacology. 1994;33(3-4):575-88.
345. Rogers RD, Blackshaw AJ, Middleton HC, Matthews K, Hawtin K, Crowley C, et al. Tryptophan depletion impairs stimulus-reward learning while methylphenidate disrupts attentional control in healthy young adults: implications for the monoaminergic basis of impulsive behaviour. Psychopharmacology (Berl). 1999;146(4):482-91.
346. Gallagher P, Massey AE, Young AH, McAllister-Williams RH. Effects of acute tryptophan depletion on executive function in healthy male volunteers. BMC Psychiatry. 2003;3:10.
347. Fuchs D, Moller AA, Reibnegger G, Stockle E, Werner ER, Wachter H. Decreased serum tryptophan in patients with HIV-1 infection correlates with increased serum neopterin and with neurologic/psychiatric symptoms. J Acquir Immune Defic Syndr. 1990;3(9):873-6.
348. Huengsberg M, Winer JB, Gompels M, Round R, Ross J, Shahmanesh M. Serum kynurenine-to-tryptophan ratio increases with progressive disease in HIV-infected patients. Clinical Chemistry. 1998;44(4):858-62.

349. Martin A, Heyes MP, Salazar AM, Kampen DL, Williams J, Law WA, et al. Progressive slowing of reaction time and increasing cerebrospinal fluid concentrations of quinolinic acid in HIV-infected individuals. J Neuropsychiatry Clin Neurosci. 1992;4:270-9.
350. Sardar AM, Bell JE, Reynolds GP. Increased concentrations of the neurotoxin 3-hydroxykynurenine in the frontal cortex of HIV-1-positive patients. Journal of Neurochemistry. 1995;64(2):932-5.
351. Baran H, Hainfellner JA, Kepplinger B, Mazal PR, Schmid H, Budka H. Kynurenic acid metabolism in the brain of HIV-1 infected patients. J Neural Transm. 2000;107:1127-38.
352. Atlas A, Gisslen M, Nordin C, Lindstrom L, Schwieler L. Acute psychotic symptoms in HIV-1 infected patients are associated with increased levels of kynurenic acid in cerebrospinal fluid. Brain Behav Immun. 2007;21(1):86-91.
353. Royle CM, Tsai MH, Tabarrini O, Massari S, Graham DR, Aquino VN, et al. Modulation of HIV-1-induced activation of plasmacytoid dendritic cells by 6-desfluoroquinolones. AIDS Res Hum Retroviruses. 2014;30(4):345-54.
354. Royle CM, Graham DR, Sharma S, Fuchs D, Boasso A. HIV-1 and HIV-2 differentially mature plasmacytoid dendritic cells into IFN-producing cells or APCs. J Immunol. 2014;193(7):3538-48.
355. Liverpool Uo. Dolutegravir PK Fact Sheet. wwwhiv-druginteractionsorg. 2013.
356. Liverpool Uo. Abacavir PK Fact Sheet. wwwhiv-druginteractionsorg. 2011.
357. Liverpool Uo. Lamivudine PK Fact Sheet. wwwhiv-druginteractionsorg. 2011.
358. Liverpool Uo. Efavirenz PK Fact Sheet. wwwhiv-druginteractionsorg. 2011.
359. Liverpool Uo. Emtricitabine PK Fact Sheet. wwwhiv-druginteractionsorg. 2011.
360. Liverpool Uo. Raltegravir PK Fact Sheet. wwwhiv-druginteractionsorg. 2011.
361. Liverpool Uo. Tenofovir PK Factsheet. wwwhiv-druginteractionsorg. 2011.
362. Liverpool Uo. Etravirine PK Fact Sheet. wwwhiv-druginteractionsorg. 2011.
363. Liverpool Uo. Rilpivirine PK Fact Sheet. wwwhiv-druginteractionsorg. 2011.
364. Laich A, Neurauter G, Widner B, Fuchs D. More rapid method for simultaneous measurement of tryptophan and kynurenine by HPLC. Clin Chemistry. 2002;48(3):579-81.
365. Widner B, Werner ER, Schennach H, Wachter H, Fuchs D. Simultaneous Measurement of Serum Tryptophan and Kynurenine by HPLC. Clin Chemistry. 1997;43(12):2424-6.
366. Neurauter G, Scholl-Bürgi S, Haara A, Geisler S, Mayersbach P, Schennach H, et al. Simultaneous measurement of phenylalanine and tyrosine by high performance liquid chromatography (HPLC) with fluorescence detection. Clin Biochem. 2013;46:1848-51.
367. Griess P. Bemerkungen zu der Abhandlung der HH. Weselky und Benedikt "Ueber einige Azoverbindungen". Chem Ber. 1879;12:426-8.
368. Giustarini D, Dalle-Donne I, Colombo R, Milzani A, Rossi R. Adaptation of the Griess reaction for detection of nitrite in human plasma. Free Radic Res. 2004;38:1235-40.
369. Marquine MJ, Umlauf A, Rooney AS, Fazeli PL, Gouaux BD, Paul Woods S, et al. The veterans aging cohort study index is associated with concurrent risk for neurocognitive impairment. J Acquir Immune Defic Syndr. 2014;65(2):190-7.
370. Kessler RC, Andrews G, Mroczek D, Ustun TB, Wittchen H-U. The World Health Organization composite international diagnostic interview short form (CID-SF). Int J Methods Psychiatr Res. 1998;7(4):171-85.
371. Heaton RK, Miller SW, Taylor MJ, Grant I. Revised Comprehensive Norms for an Expanded Halstead Reitan Battery: Demographically Adjusted Neuropsychological Norms for African American and Caucasian Adults. Lutz: Psychological Assessment Resources, Inc; 2004 Website last accessed 12th April 2018: https://wwwparinccom/Products/Pkey/357. 2004.
372. Yapa HM, Waters L, Rowlands J, Jackson A, Mandalia S, Higgs C, et al. The feasibility of switching efavirenz (EFV)-based highly active antiretroviral therapy to raltegravir (RAL)-based thereapy in HIV-infected individuals with central nervous system (CNS) toxicity: a Phase

IV open label pilot study. British HIV Association (BHIVA) Conference, Manchester, UK, 16-19 April 2013 Oral Presentation. 2013.
373. Zigmond AS, Snaith RP. The Hospital Anxiety and Depression Scale. Acta Psychiatr Scand. 1983;67:361-70.
374. Buysse DJ, Reynolds III CF, Monk TH, R. BS, Kupfer DJ. The Pittsburgh Sleep Quality Index: A new instrument for psychiatric practice and research. Psychiatry Res. 1989;28:193-213.
375. Overton ET, Kauwe JS, Paul R, Tashima K, Tate DF, Patel P, et al. Performances on the CogState and standard neuropsychological batteries among HIV patients without dementia. AIDS Behav. 2011;15(8):1902-9.
376. Cysique LA, Maruff P, Darby D, Brew BJ. The assessment of cognitive function in advanced HIV-1 infection and AIDS dementia complex using a new computerised cognitive test battery. Arch Clin Neuropsychol. 2006;21(2):185-94.
377. Lawton MP, Brody EM. Assessment of older people: self-maintaining and instrumental activities of daily living. Gerontologist. 1969;9(3):179-86.
378. Beck AT, Steer RA, Carbin MG. Psychometric properties of the Beck Depression Inventory: Twenty-five Years of Evaluation. Clinical Psychology Review. 1988;8(1):77-100.
379. Jackson-Koku G. Beck Depression Inventory. Occup Med (Lond). 2016;66(2):174-5.
380. Kroenke K, Spitzer RL, Williams JBW. The PHQ-9: Validity of a Brief Depression Severity Measure. J Gen Intern Med 2001. 2001;16:606-13.
381. Garvey L, Higgs C, Mohammed P, Hill A, Allsop JM, Taylor-Robinson SD, et al. Changes in cerebral function parameters in HIV type 1-infected subjects switching to darunavir/ritonavir either as monotherapy or with nucleoside analogues. AIDS Res Hum Retroviruses. 2011;27(7):701-3.
382. Jones SP, Franco NF, Varney B, Sundaram G, Brown DA, de Bie J, et al. Expression of the Kynurenine Pathway in Human Peripheral Blood Mononuclear Cells: Implications for Inflammatory and Neurodegenerative Disease. PLoS One. 2015;10(6):e0131389.
383. Moyle G. Toxicity of antiretroviral nucleoside and nucleotide analogues. Drug Safety. 2000;23(6):467-81.
384. Wang Y, Lv Z, Chu Y. HIV protease inhibitors: a review of molecular selectivity and toxicity. HIV/AIDS - Research and Palliative Care. 2015.
385. Vigouroux C, Maachi M, Nguyen TH, Coussieu C, Gharakhanian S, Funahashi T, et al. Serum adipocytokines are related to lipodystrophy and metabolic disorders in HIV-infected men under antiretroviral therapy. AIDS. 2003;17(10):1503-11.
386. Shiraha H, Yamamoto K, Namba M. Human hepatocyte carcinogenesis (review). Int J Oncol. 2013;42(4):1133-8.
387. Pfeifer AMA, Cole KE, Smoot DT, Weston A, Groopman JD, Shields PG, et al. Simian virus 40 large tumor antigen-immortalized normal human liver epithelial cells express hepatocyte characteristics and metabolize chemical carcinogens. Proc Natl Acad Sci U S A. 1993;90:5123-7.
388. Clark MJ, Homer N, O'Connor BD, Chen Z, Eskin A, Lee H, et al. U87MG decoded: the genomic sequence of a cytogenetically aberrant human cancer cell line. PLoS Genet. 2010;6(1):e1000832.
389. Iacopino F, Angelucci C, Piacentini R, Biamonte F, Mangiola A, Maira G, et al. Isolation of cancer stem cells from three human glioblastoma cell lines: characterization of two selected clones. PLoS One. 2014;9(8):e105166.
390. Hanihara M, Kawataki T, Oh-Oka K, Mitsuka K, Nakao A, Kinouchi H. Synergistic antitumor effect with indoleamine 2,3-dioxygenase inhibition and temozolomide in a murine glioma model. J Neurosurg. 2016;124(6):1594-601.

391. Obojes K, Andres O, Kim KS, Daubener W, Schneider-Schaulies J. Indoleamine 2,3-dioxygenase mediates cell type-specific anti-measles virus activity of gamma interferon. J Virol. 2005;79(12):7768-76.
392. Yadav MC, Burudi EME, Alirezaei M, Flynn CC, Watry DD, Lanigan CM, et al. IFN-γ induced IDO and WRS expression in microglia is differentially regulated by IL-4. Glia. 2007;55(13):1385-96.
393. Stansley B, Post J, Hensley K. A comparative review of cell culture systems for the study of microglial biology in Alzheimer's disease. J Neuroinflammation. 2012;9:115.
394. Sa Q, Ochiai E, Tiwari A, Perkins S, Mullins J, Gehman M, et al. Cutting Edge: IFN-gamma Produced by Brain-Resident Cells Is Crucial To Control Cerebral Infection with Toxoplasma gondii. J Immunol. 2015;195(3):796-800.
395. Rycerz K, Jaworska-Adamu JE. Effects of aspartame metabolites on astrocytes and neurons. Folia Neuropathologica. 2013;1:10-7.
396. Preissler T, Bristot IJ, Costa BM, Fernandes EK, Rieger E, Bortoluzzi VT, et al. Phenylalanine induces oxidative stress and decreases the viability of rat astrocytes: possible relevance for the pathophysiology of neurodegeneration in phenylketonuria. Metab Brain Dis. 2016;31(3):529-37.
397. de Abreu Costa L, Henrique Fernandes Ottoni M, Dos Santos MG, Meireles AB, Gomes de Almeida V, de Fatima Pereira W, et al. Dimethyl Sulfoxide (DMSO) Decreases Cell Proliferation and TNF-alpha, IFN-gamma, and IL-2 Cytokines Production in Cultures of Peripheral Blood Lymphocytes. Molecules. 2017;22(11).
398. Timm M, Saaby L, Moesby L, Hansen EW. Considerations regarding use of solvents in in vitro cell based assays. Cytotechnology. 2013;65(5):887-94.
399. Gustafsson F, Foster AJ, Sarda S, Bridgland-Taylor MH, Kenna JG. A correlation between the in vitro drug toxicity of drugs to cell lines that express human P450s and their propensity to cause liver injury in humans. Toxicol Sci. 2014;137(1):189-211.
400. Keegan MR, Chittiprol S, Letendre SL, Winston A, Fuchs D, Boasso A, et al. Tryptophan Metabolism and Its Relationship with Depression and Cognitive Impairment among HIV-infected Individuals. International Journal of Tryptophan Research. 2016;9.
401. Lafeuillade A, Poggi C, Pellegrino P, Corti K, Profizi N, Sayada C. HIV-1 replication in the plasma and cerebropinal fluid. Infection. 1996;24(5):367-71.
402. Tavares RG, I. TC, Santos CES, Alves LB, Porciuncula LO, Emanuelli T, et al. Quinolinic acid stimulates synaptosomal glutamate release and inhibits glutamate uptake into astrocytes. Neurochem Int. 2002;40:621-7.
403. Heyes MP, Lackner A, Kaufman S, Milstien S. Cerebrospinal fluid and serum neopterin and biopterin in D-retrovirus-infected rhesus macaques (Macaca mulatta): relationship to clinical and viral status. AIDS. 1991;5:555-60.
404. Launay JM, Copel L, Callebert J, Corvaia N, Lepage E, Bricaire F, et al. Decreased whole blood 5-hydroxytryptamine (serotonin) in AIDS patients. J Acquir Immune Defic Syndr. 1988;1(4):324-5.
405. Larsson M, Hagberg L, Norkrans G, A. F. Indoleamine deficiency in blood and cerebrospinal fluid from patients with human immunodeficiency virus infection. J Neurosci Res. 1989;23(4):441-6.
406. Caballero J, Nahata MC. Use of selective serotonin-reuptake inhibitors in the treatment of depression in adults with HIV. Annals of Pharmacotherapy. 2005;39(1):141-5.
407. Murray MF. The human indoleamine 2,3-dioxygenase gene and related human genes. Curr Drug Metabol. 2007;8:197-200.
408. Strasser B, Gostner JM, Fuchs D. Mood, food, and cognition: role of tryptophan and serotonin. Curr Opin Clin Nutr Metab Care. 2016;19(1):55-61.
409. Zheve GT. Neuroprotective mechanisms of nevirapine and efavirenz in a model of neurodegeneration. Rhodes, Greece: Rhodes University 2007. 2007.

410. Byakwaga H, Hunt PW, Laker-Oketta M, Glidden DV, Huang Y, Bwana BM, et al. The kynurenine pathway of tryptophan catabolism and AIDS-associated Kaposi sarcoma in Africa. J Acquir Immune Defic Syndr. 2015;70:296-303.
411. Chen J, Shao J, Cai R, Shen Y, Zhang R, Liu L, et al. Anti-retroviral therapy decreases but does not normalize indoleamine 2,3-dioxygenase activity in HIV-infected patients. PLoS One. 2014;9(7):e100446.
412. McDonagh EM, Lau JL, Alvarellos ML, Altman RB, Klein TE. PharmGKB summary: Efavirenz pathway, pharmacokinetics. Pharmacogenet Genomics. 2015;25(7):363-76.
413. Waters L, Fisher M, Winston A, Higgs C, Hadley W, Garvey L, et al. A phase IV, double-blind, multicentre, randomized, placebo-controlled, pilot study to assess the feasibility of switching individuals receiving efavirenz with continuing central nervous system adverse events to etravirine. AIDS. 2011;25:65-71.
414. Rowlands J, Higgs C, De Esteban N, McKenna S, Perry N, Winston A, et al. Multicenter open-label study of switching from Atripla to Eviplera for CNS toxicity. 54th Interscience Conference on Antimicrobial Agents and Chemotherapy, September 5-9, 2014 Washington, DC Abstract H-1005. 2014.
415. Foster AC, Vexxani A, Frencg ED, Schwarz R. Kynurenic acid blocks neurotox¬icity and seizures induced in rats by the related brain metabolite quinolinic acid. Neuroscience Letters. 1984;48:273-8.
416. Andine P, Lehmann A, Ellren K, al. e. The excitatory amino acid antagonist kynurenic acid administered after hypoxic-ischemia in neonatal rats offers neu¬roprotection. Neuroscience Letters. 1988;90(208-212).
417. Badawy AA, Dougherty DM. Assessment of the Human Kynurenine Pathway: Comparisons and Clinical Implications of Ethnic and Gender Differences in Plasma Tryptophan, Kynurenine Metabolites, and Enzyme Expressions at Baseline and After Acute Tryptophan Loading and Depletion. Int J Tryptophan Res. 2016;9:31-49.
418. Dahl V, Lee E, Peterson J, Spudich SS, Leppla I, Sinclair E, et al. Raltegravir treatment intensification does not alter cerebrospinal fluid HIV-1 infection or immunoactivation in subjects on suppressive therapy. J Infect Dis. 2011;204(12):1936-45.
419. Lim CK, Bilgin A, Lovejoy DB, Tan V, Bustamante S, Taylor BV, et al. Kynurenine pathway metabolomics predicts and provides mechanistic insight into multiple sclerosis progression. Scientific Reports. 2017;7:41473.